ISSN 0021-9673

VOL. 647 NO. 1 SEPTEMBER 10, 1993

9th Montreux Symp. on LC–MS, SFC–MS, CZE–MS and MS–MS Montreux, November 4–6, 1992 Part I

JOURNAL OF

CHROMATOGRAPHY

INCLUDING ELECTROPHORESIS AND OTHER SEPARATION METHODS

SYMPOSIUM VOLUMES

ELSEVIER

JOURNAL OF CHROMATOGRAPHY

INCLUDING ELECTROPHORESIS AND OTHER SEPARATION METHODS

Scope. The *Journal of Chromatography* publishes papers on all aspects of **chromatography, electrophoresis** and related methods. Contributions consist mainly of research papers dealing with chromatographic theory, instrumental developments and their applications. The section *Biomedical Applications*, which is under separate editorship, deals with the following aspects: developments in and applications of chromatographic and electrophoretic techniques related to clinical diagnosis or alterations during medical treatment; screening and profiling of body fluids or tissues related to the analysis of active substances and to metabolic disorders; drug level monitoring and pharmacokinetic studies; clinical toxicology; forensic medicine; veterinary medicine; occupational medicine; results from basic medical research with direct consequences in clinical practice. In *Symposium volumes*, which are under separate editorship, proceedings of symposia on chromatography, electrophoresis and related methods are published.

Submission of Papers. The preferred medium of submission is on disk with accompanying manuscript (see *Electronic manuscripts* in the Instructions to Authors, which can be obtained from the publisher, Elsevier Science Publishers B.V., P.O. Box 330, 1000 AH Amsterdam, Netherlands). Manuscripts (in English; *four* copies are required) should be submitted to: Editorial Office of *Journal of Chromatography*, P.O. Box 681, 1000 AR Amsterdam, Netherlands, Telefax (+31-20) 5862 304, or to: The Editor of *Journal of Chromatography, Biomedical Applications*, P.O. Box 681, 1000 AR Amsterdam, Netherlands. Review articles are invited or proposed in writing to the Editors who welcome suggestions for subjects. An outline of the proposed review should first be forwarded to the Editors for preliminary discussion prior to preparation. Submission of an article is understood to imply that the article is original and unpublished and is not being considered for publication elsewhere. For copyright regulations, see below.

Publication. The *Journal of Chromatography* (incl. *Biomedical Applications*) has 40 volumes in 1993. The subscription prices for 1993 are:

J. Chromatogr. (incl. *Cum. Indexes, Vols. 601–650*) + *Biomed. Appl.* (Vols. 612–651):
Dfl. 8520.00 plus Dfl. 1320.00 (p.p.h.) (total *ca.* US$ 5466.75)

J. Chromatogr. (incl. *Cum Indexes, Vols. 601–650*) only (Vols. 623–651):
Dfl. 7047.00 plus Dfl. 957.00 (p.p.h.) (total *ca.* US$ 4446.75)

Biomed. Appl. only (Vols. 612–622):
Dfl. 2783.00 plus Dfl. 363.00 (p.p.h.) (total *ca.* US$ 1747.75).

Subscription Orders. The Dutch guilder price is definitive. The US$ price is subject to exchange-rate fluctuations and is given as a guide. Subscriptions are accepted on a prepaid basis only, unless different terms have been previously agreed upon. Subscriptions orders can be entered only by calender year (Jan.–Dec.) and should be sent to Elsevier Science Publishers, Journal Department, P.O. Box 211, 1000 AE Amsterdam, Netherlands, Tel. (+31-20) 5803 642, Telefax (+31-20) 5803 598, or to your usual subscription agent. Postage and handling charges include surface delivery except to the following countries where air delivery via SAL (Surface Air Lift) mail is ensured: Argentina, Australia, Brazil, Canada, China, Hong Kong, India, Israel, Japan*, Malaysia, Mexico, New Zealand, Pakistan, Singapore, South Africa, South Korea, Taiwan, Thailand, USA. *For Japan air delivery (SAL) requires 25% additional charge of the normal postage and handling charge. For all other countries airmail rates are available upon request. Claims for missing issues must be made within six months of our publication (mailing) date, otherwise such claims cannot be honoured free of charge. Back volumes of the *Journal of Chromatography* (Vols. 1–611) are available at Dfl. 230.00 (plus postage). Customers in the USA and Canada wishing information on this and other Elsevier journals, please contact Journal Information Center, Elsevier Science Publishing Co. Inc., 655 Avenue of the Americas, New York, NY 10010, USA, Tel. (+1-212) 633 3750, Telefax (+1-212) 633 3764.

Abstracts/Contents Lists published in Analytical Abstracts, Biochemical Abstracts, Biological Abstracts, Chemical Abstracts, Chemical Titles, Chromatography Abstracts, Current Awareness in Biological Sciences (CABS), Current Contents/Life Sciences, Current Contents/Physical, Chemical & Earth Sciences, Deep-Sea Research/Part B: Oceanographic Literature Review, Excerpta Medica, Index Medicus, Mass Spectrometry Bulletin, PASCAL-CNRS, Referativnyi Zhurnal, Research Alert and Science Citation Index.

US Mailing Notice. *Journal of Chromatography* (ISSN 0021-9673) is published weekly (total 52 issues) by Elsevier Science Publishers (Sara Burgerhartstraat 25, P.O. Box 211, 1000 AE Amsterdam, Netherlands). Annual subscription price in the USA US$ 4446.75 (subject to change), including air speed delivery. Second class postage paid at Jamaica, NY 11431. **USA POSTMASTERS:** Send address changes to *Journal of Chromatography*, Publications Expediting, Inc., 200 Meacham Avenue, Elmont, NY 11003. Airfreight and mailing in the USA by Publications Expediting.

See inside back cover for Publication Schedule, Information for Authors and information on Advertisements.

0021-9673/93/$06.00

Printed in the Netherlands

For Contents see p. VII.

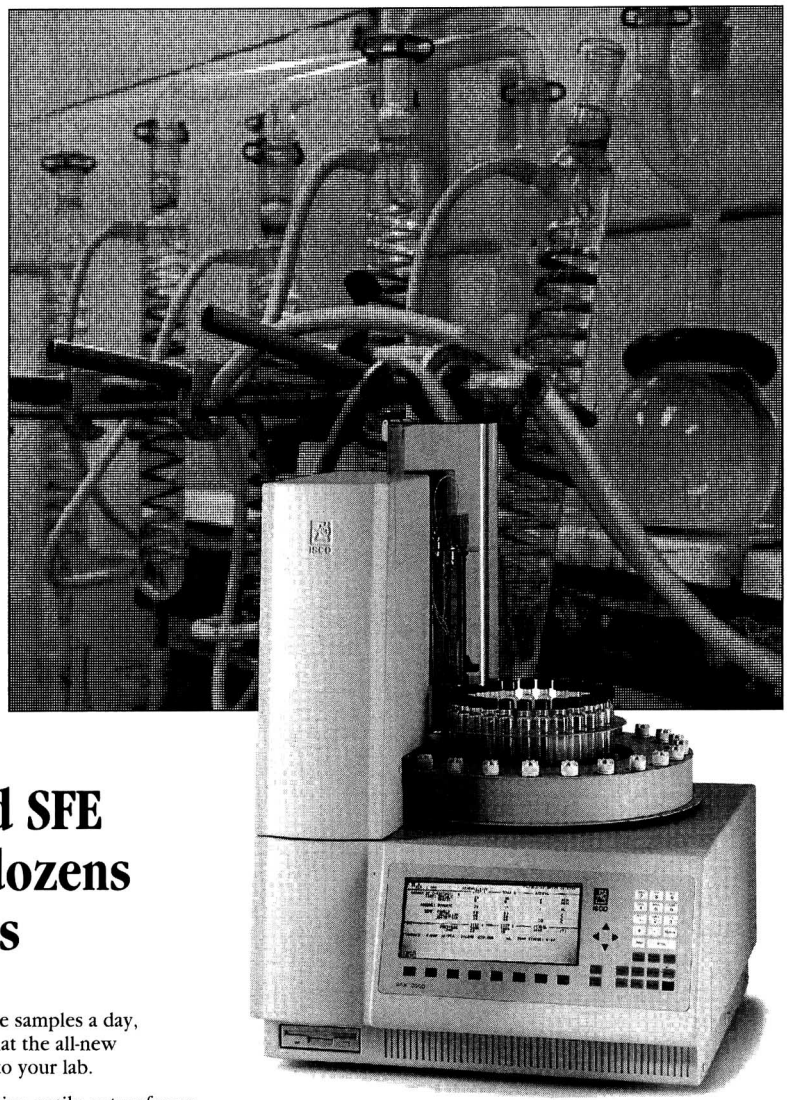

Automated SFE replaces dozens of Soxhlets

If you extract 20 or more samples a day, take a close look at what the all-new Isco SFX® 3560 can add to your lab.

Supercritical fluid extraction easily outperforms traditional Soxhlet and sonication methods. You can expect extraction cycles of minutes instead of hours or days, and cleaner analytes due to better selectivity. And CO_2 extraction eliminates regulated solvent purchase and disposal costs, along with fire and health hazards.

The SFX 3560 gives you walkaway automation to cut labor and speed results. A big, interactive display helps you quickly set up all extraction parameters for method development or routine sample prep.

Load twenty-four samples in disposable, barcoded cartridges, extract overnight, and get a printed report, with only an hour's labor!

Superior extraction conditions mean superior results. Up to 10,000 psi, 40 ml/min, 150 °C, and precision modifier addition assure fast and clean extraction.

Find out how an Isco SFX 3560 can revolutionize your sample prep. Phone or fax now for answers and literature.

Isco, Inc., Separation Instruments Division
P.O. Box 5347 • Lincoln, NE 68505 • USA

ISCO

Phone: USA **(800)228-4250; (402)464-0231**
Fax: (402)464-0318

Australia: Australian Chromatography Co. • **Austria:** Neuber • **Benelux:** Beun-de Ronde, B.V. • **Canada:** Canberra Packard Canada, Ltd. • **Denmark:** Mikrolab Aarhus • **Finland:** ORDIOR ANALYTICAL OY • **France:** Ets. Roucaire, S.A. • **Germany:** Colora Messtechnik GmbH • **Italy:** Analytical Control Italia S.p.A. • **Japan:** Astech Corporation • **Korea:** IWOO Scientific Corp. • **Norway:** Dipl. Ing. Houm A.S. • **Portugal:** CAMPOS & Ca., Lda. • **Spain:** VARIAN IBERICA, S.L. • **Sweden:** SpectroChrom AB • **Switzerland:** Instrumenten-Gesellschaft AG • **UK:** Jones Chromatography Ltd. •

New Developments in Ion Exchange

Materials, Fundamentals and Applications

Proceedings of the International Conference on Ion Exchange, ICIE '91, Tokyo, Japan, October 2-4, 1991

edited by **M. Abe**, Tokyo Institute of Technology, Tokyo, Japan,
T. Kataoka, University of Osaka Prefecture, Osaka, Japan and
T. Suzuki, Yamanashi University, Yamanashi, Japan

This volume contains the papers presented at the International Conference on Ion Exchange (ICIE '91). Included are reviews and original papers reflecting recent progress in new branches of science and technology based on novel ion-exchange materials and ion-exchange theory.

Topics covered include: Fundamentals (Ion exchange theory and process), Synthesis of New Materials, Chromatography (Ion and liquid chromatography, and associated techniques), Water Purification, Environmental, Membranes, Hydrometallurgy, Separation Science and Technology (Food, pharmaceutical, biological and others).

Contents:

1991 xlii + 636 pages
Price: US $ 218.00 / Dfl. 425.00
ISBN 0-444-98688-X

Co-edition with and distributed in Japan by Kodansha Scientific Ltd.

Elsevier Science Publishers

P.O. Box 211, 1000 AE Amsterdam, The Netherlands
P.O. Box 882, Madison Square Station, New York, NY 10159, USA

JOURNAL OF CHROMATOGRAPHY

VOL. 647 (1993)

JOURNAL of CHROMATOGRAPHY

INCLUDING ELECTROPHORESIS AND OTHER SEPARATION METHODS

SYMPOSIUM VOLUMES

ELSEVIER
AMSTERDAM — LONDON — NEW YORK — TOKYO

Chateau Chillon

0021-9673/93/$06.00

Printed in the Netherlands

SYMPOSIUM VOLUME

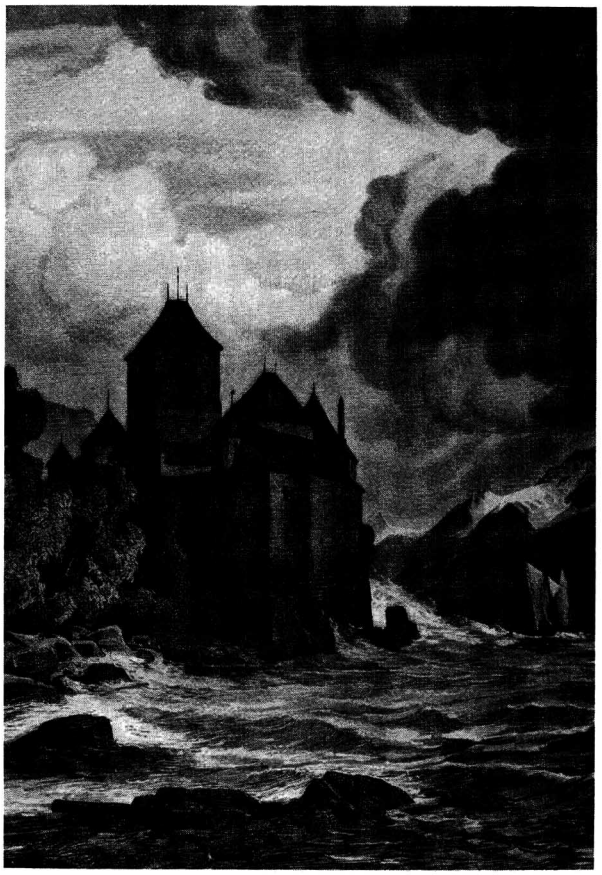

9TH MONTREUX SYMPOSIUM ON LIQUID CHROMATOGRAPHY–MASS SPECTROMETRY,

SUPERCRITICAL FLUID CHROMATOGRAPHY–MASS SPECTROMETRY, CAPILLARY ZONE ELECTROPHORESIS–MASS SPECTROMETRY AND TANDEM MASS SPECTROMETRY

Montreux (Switzerland), November 4–6, 1992

Guest Editor

J. VAN DER GREEF
(Leiden)

VOL. 647, NOS. 1 + 2 JOURNAL OF CHROMATOGRAPHY SEPTEMBER 10, 1993

CONTENTS

9TH MONTREUX SYMPOSIUM ON LIQUID CHROMATOGRAPHY–MASS SPECTROMETRY, SUPERCRITICAL FLUID CHROMATOGRAPHY–MASS SPECTROMETRY, CAPILLARY ZONE ELECTROPHORESIS–MASS SPECTROMETRY AND TANDEM MASS SPECTROMETRY, MONTREUX, NOVEMBER 4–6, 1992

Journal of Chromatography, 647 (1993) 1
Elsevier Science Publishers B.V., Amsterdam

CHROM. 25 311

Foreword

The *9th Montreux Symposium on LC–MS, SFC–MS, CZE–MS and MS–MS* was held in Montreux, Switzerland, from November 4 to 6, 1992. Again, an increased number of scientists from all over the world gathered to exchange knowledge in this research field.

Liquid chromatography coupled to mass spectrometry has become a routine method for many laboratories working in the pharmaceutical, biotechnological, environmental and food areas. This was clearly reflected by the large number of presentations dealing with quantitative and qualitative LC–MS analysis, often automated. Especially the analytical challenges in the pharmaceutical industry have given a major impulse to the development of robust methods for the determination of compounds at low levels, often in the pg/ml (ppt) range.

In recent years, biotechnology and biochemical research have stimulated the development of the detection of macromolecules by mass spectrometry. The new ionization techniques that became available are now being investigated in the on-line LC–MS or CE–MS mode. Several contributions dealing with this subject were presented and results obtained in qualitative analysis, often by using tandem mass spectrometry, have been very impressive.

The ongoing developments in interface technology are spawning new commercial instruments, based on the successful atmospheric pressure design. A new approach, based on surface-ionization interfacing, was also presented, and several contributions were aimed at optimizing strategies for the various interfaces. Other instrumental developments have been achieved in interfacing of LC with an ion trap, magnetic-sector instruments in the LC–MS mode with array detection and dual-beam thermospray. The number of contributions to chromatography, especially with miniaturized separation systems, showed an increase compared with the previous symposium.

Continued interest in SFC–MS was also evident, and new source designs, based on electrospray, were presented. Capillary electrophoresis–mass spectrometry for trace analysis is taking important strides towards the development of on-line preconcentration techniques based on isotachophoretic principles.

In conclusion, LC–MS and related techniques are well established in many laboratories. A modern laboratory can hardly afford to be without them.

The next American meeting was held in Ithaca, NY, July 19–20th, 1993, and the next European meeting will be held in Montreux, Switzerland, November 7–11th, 1994.

Leiden (Netherlands) Jan van der Greef

Journal of Chromatography, 647 (1993) 3–12
Elsevier Science Publishers B.V., Amsterdam

CHROMSYMP. 2804

Peptide mapping of recombinant human interferon-γ by reversed-phase liquid chromatography with on-line identification by thermospray mass spectrometry and UV absorption spectrometry

Raymond Legrand, Jean-Bernard Falconnet☆, Daniele Prevost, Bernard Schoot and Philippe Devaux*

Physics Department, Roussel Uclaf Research Centre, 102 Route de Noisy, F-93230 Romainville (France)

ABSTRACT

The detection and identification of minor peaks in a complex peptide map of recombinant human interferon-γ was realized by on-line analysis of the eluted peptides using thermospray mass spectrometry and UV absorbance spectrometry. By this procedure the time-consuming process of collection, purification and chemical sequence analysis is avoided. Owing to the formation of multiply charged ions, the domain of the covered masses is extended. Fragmentation of the peptides in the thermospray source was observed resulting from, amongst others, cleavage by acid hydrolysis of peptide bonds involving an aspartic acid. This was of great use for the identification of peptides in a digest of recombinant human interferon-γ by *Staphylococcus aureus* strain V8 endoprotease.

INTRODUCTION

Peptide mapping is a widely used technique in the identification of proteins. It allows the identification and localization of a single amino acid substitution or its deletion in a protein and, therefore, it is a powerful method for checking the integrity of the molecule [1,2]. Changes in the structure of the molecule may be detected by the appearance of new peaks in RP-HPLC of the protein digest. After separation, the peptides have to be identified, in general, by an N-terminal sequence determination. Mass spectrometry and UV absorbance spectrometry are also of interest. Submicrogram amounts of material eluted from the LC column can be analysed by both methods. Mass spectrometry has become a valuable tool for peptide and protein analysis as it can provide accurate molecular mass and sequence information below the nanomole level [3].

To avoid lengthy sample clean-up procedures, on-line coupling of HPLC to mass spectrometry has been investigated for many years. Several interfaces have been described and are now routinely used: continuous-flow fast atom bombardment (FAB) [4,5], frit FAB [6,7], ionspray [8,9] and thermospray (TSP) [10–16]. It has been shown that thermospray ionization can generate multiply charged ions from peptides [12–14,17,18], thereby extending the mass range of a quadrupole instrument.

We report here the first application of LC–thermospray MS and HPLC–photodiode-array detection to the peptide mapping recombinant human interferon-γ (rhIFN-γ). In the course of this study, spontaneous fragmentation of peptides in the thermospray device was observed.

* Corresponding author.
☆ Present address: Hopital Debrousse, Service de Biochimie, 29 Rue Soeur Bouvier, F-69005 Lyon, France.

EXPERIMENTAL

Chemicals

rhIFN-γ (RU 42369) is extracted from *Escherichia coli*, into which a plasmid coding for this protein has been transfected. rhIFN-γ contains the sequence of 143 amino acids, as found in the natural protein, with the addition of an additional N-terminal methionine. This recombinant protein is not glycosylated.

Protease from *Staphylococcus aureus* strain V8 is an endoprotease, which hydrolyses peptide bonds specifically at the carboxylic side of glutamic acid (pH of incubation about 4.5 or 7) and aspartic acid (pH of incubation about 7.5). The enzyme preparation used for this study was purchased from Boehringer (Mannheim, Germany).

Acetonitrile and glacial acetic acid were purchased from E. Merck (Darmstadt, Germany). Trifluoracetic acid (TFA) (sequence grade) was from Pierce. Water was obtained from a Millipore (France) Milli-Q filtration unit.

Materials

The separation of the peptides by HPLC was performed using a Model 600 low-pressure gradient HPLC pump system (Waters–Millipore) equipped with a Rheodyne Model 7010/7012 manual injector.

Separation was carried out on a Beckman Ultrasphere C_{18} column (750 mm × 4 mm I.D.) packed with 3-μm particles.

The elution profile of the peptides was recorded by means of a Waters–Millipore Model 990+ diode-array detector system. The detector was equipped with a special high-pressure-resistant cell, in order to permit on-line coupling with a thermospray mass spectrometer. The chromatograms were analysed using the program accompanying the detector.

Acetic acid solution (16%, v/v) was delivered by means of a Waters M45 HPLC pump.

Mass spectrometry

All experiments were carried out on a Finnigan Model 4600 GC–LC–MS quadrupole mass spectrometer (mass range 1800 u) equipped with a slightly modified TSP-I thermospray ionization source (Finnigan-MAT, San Jose, CA, USA).

The standard planar repeller electrode of the Finnigan thermospray source was modified by sealing the filament electron aperture and by using a needle repeller electrode placed very near the sampling cone orifice as described by Robins and Crow [19]. This modification improves the sensitivity at higher masses and the stability of the ion current.

The vaporizer consists of a length of 0.007 in. I.D. syringe tubing (1 in. = 2.54 cm), tipped with a sapphire orifice that has a nominal orifice of 0.0026 in. (Finnigan TSP II). The mass spectrometer was calibrated in the electron impact (EI) mode using TRZ9 [tris(perfluorononyl)-*s*-triazine] and alternatively in the TSP mode with polyethylene glycol. Initial tuning of the instrument was carried out by infusion of a dilute solution of a peptide mixture of Leu-enkephalin, angiotensin, gramicidine S and IFN 10–38 (peptide of rhIFN-γ), concentration 10 μ*M* each, in water–acetonitrile–acetic acid (67:29:4, v/v/v).

Typical operating conditions were as follows: jet (source block) temperature, 230°C; vaporizer temperature, 75–80°C; repeller voltage, 30 V; mass spectrometer high vacuum, $4.0 \cdot 10^{-5}$ Torr (1 Torr = 133.322 Pa); and flow-rate, 1.5 ml/min. Data were collected over the mass range of interest using 4-s scans in the centroid mode.

Methods

Hydrolysis. Limited digestion of rhIFN-γ (1 mg/ml) with endoprotease from *Staphylococcus aureus* at an enzyme-to-IFN-γ ratio of 1:50 (w/w) was performed in 50 m*M* Tris–HCl buffer (pH 7.0) for 15 h at 37°C.

HPLC. A 200-μg amount of the hydrolysed protein was injected directly on to the HPLC column. The peptides were eluted with a gradient of 0.1% TFA in acetonitrile (B) and 0.1% TFA in distilled water (A), as follows: Initial, 100% A; 0–40 min, linear gradient from 0 to 20% (v/v) B in A; 40–60 min, linear gradient from 20 to 40% (v/v) B in A; 60–65 min, linear gradient from 40 to 50% (v/v) B in A; and 65–70 min, linear gradient from 50 to 0% (v/v) B in A. A 10-min delay was allowed before reinjection. The flow-rate was 1.2 ml/min.

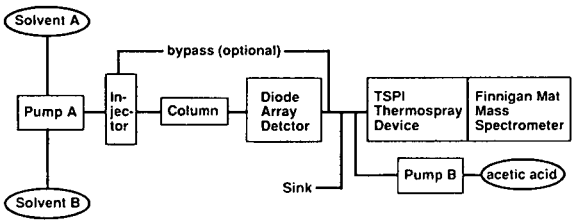

Fig. 1. Experimental set-up of the on-line RP-HPLC–diode-array UV detector–thermospray mass spectrometer system. Pump A, Waters Model 600 gradient pump; pump B, Waters M45 HPLC pump.

Spectra of the eluate in the wavelength range 220–290 nm were recorded at given intervals (about 1 s).

A solution of 16% (v/v) acetic acid in water was added at a flow-rate of 0.3 ml/min between the absorbance detector and the thermospray vaporizer.

The eluate was directed to waste during the 5 min immediately after injection of the sample, without passing through the thermospray ionizer, in order to prevent blockage by inorganic salt deposits. A schematic diagram of the experimental set-up is shown in Fig. 1.

RESULTS AND DISCUSSION

A typical peptide map obtained under the experimental conditions described above is shown in Fig. 2. The elution profile of the proteolytic digest is represented for the two modes of detection: total ion current from the mass spectrometer (Fig. 2b) and UV absorbance at 220 nm from the diode-array detector (Fig. 2a).

Two conclusions can be drawn from these chromatograms: first, the thermospray interface does not seem to affect the chromatographic resolution too dramatically, and second, if we consider that the absorbance at 220 nm is roughly proportional to the amount of material eluted from the column, it appears that the ionization efficiency by thermospray varies dramatically with the structure of the peptides, as the peak intensities given by the two detection modes are very different.

The results were analysed in the following way. For the absorbance profile, the absorption spectra between 240 and 290 nm of the peaks detected at 220 nm were analysed in the presence of phenylalanine (absorbance maximum at 250–260 nm), tyrosine (absorbance maximum at 280 nm, low absorbance at 290 nm) and tryptophan (absorbance maximum at 280 nm and relatively high absorbance at 290 nm). An example is given in Fig. 3, which represents the elution of the first peaks of the peptide map (peaks 1–6) together with the UV spectrum of each peak. The presence of an aromatic side-chain in peptides 3, 5 and 6, tryptophan, phenylalanine and tyrosine, respectively, was then concluded.

For the mass spectrometry profile, the 42 fractions numbered in Fig. 2b were analysed for the presence of fragments (peptides) in the mass range 300–1800 u. A search was made for each fraction to locate the amino acid sequence in rhIFN-γ that matches the observed mass, the absorption spectrum and with a C-terminal amino acid residue consistent with the specificity of the protease.

Table I summarizes the experimental data and the main conclusions in terms of identification of the peptides. All the peaks of the chromatogram were analysed in the same way. The retention time, the surface, the percentage of the total surface, the observed and theoretical mass, the proposed sequence and the nature of the UV chromophore of the peptide are given for each peak. The fragments printed in bold are characterized unambiguously as the parent fragments of a series. Sequences are coded by two numbers. The numbering is made according to the order of the first and the last amino acid of the peptide in the sequence of rhIFN-γ, assigning position 0 to the N-terminal methionine (this amino acid is absent in natural interferon gamma).

The amino acid sequence of rhIFN-γ is given in Fig. 4. The observed cleavage sites for *Staphylococcus aureus* strain V8 endoprotease are indicated.

Formation of multiply charged ions

The addition of acetic acid to the eluate after the diode-array detector (see Fig. 1) facilitates the ionization and in many instances the forma-

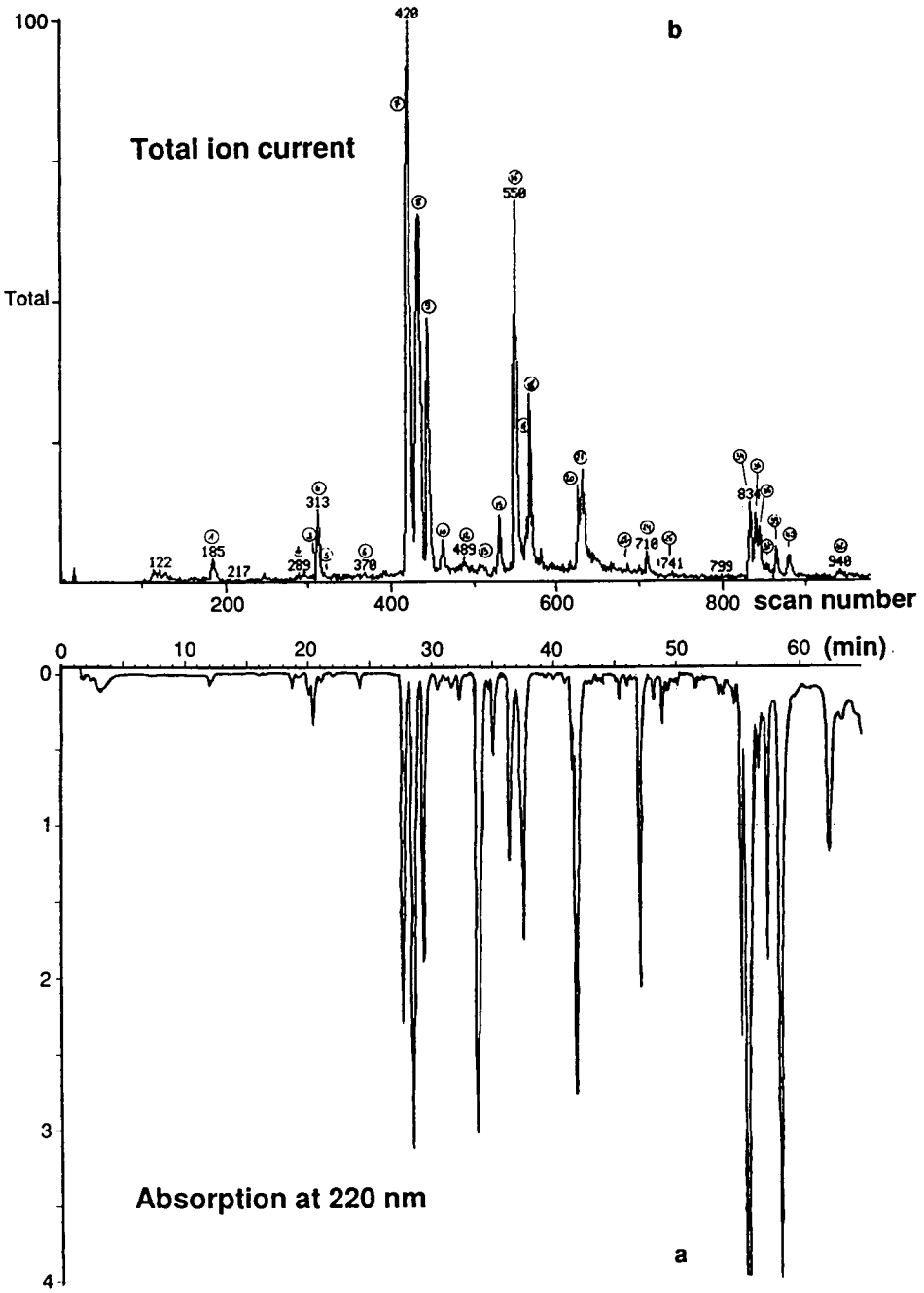

Fig. 2. Peptide map of rhIFN-γ. (a) Detection by UV absorbance at 220 nm; (b) detection by total ion current.

tion of multiply charged ions [17]. This extends the analytical power of the mass detector to peptides with masses over 1800 u and occasionally provides confirmation of sequence assignments for fragments appearing as several multiply charged ions in the spectra.

In this study we observed that direct thermospray ionization can generate multiply charged ions from the intact molecule for peptides of masses up to 3900 u. These multiply charged ions are represented in Table I. The presence of multiply charged ions was confirmed by the

TABLE I

ANALYSIS OF THE PEPTIDE OF rhIFN-γ HYDROLYZED BY *STAPHYLOCOCCUS AUREUS* STRAIN V8 ENDOPROTEASE IN Tris BUFFER, pH 7.0

200 μg hydrolyzate analyzed.

Retention time (min)	Surface (220 nm)[a]	% of total surface	Masses found $(M + xH)^{x+}$	Fragments identified	(M + H), theoretical	UV Spectrum
11.96 (peak 1)	2 581	0.2	490^{+}	**72–75**	489.6	No aromatics
18.71 (peak 2)	1 933	0.2	765^{2+}	**120–133**	1527.8	No aromatics
20.08 (peak 3)	3 740	0.3	705^{+} 912	35–39	704.7	Trp
20.44 (peak 4)	9 163	0.7	338^{2+}, 675^{+} 439^{2+}, 877^{+}	**42–46** **40–46**	674.9 877.0	No aromatics
21.07 (peak 5)	1 950	0.2	902^{+} 1748	77–83	899.1	Phe
24.22 (peak 6)	2 796	0.2	409^{+} 635^{+}	0–20X 3–7	408.0 634.7	Tyr
27.60 (peak 7)	74 555	5.9	605^{2+}, 1207^{+}	**103–112**	1207.4	No aromatics
28.44 (peak 8)	102 199	8.1	393^{+} 635^{+} 505^{2+}, 1009^{+}	0–2 3–7 **0–7**	392.4 634.7 1009.1	Tyr
29.28 (peak 9)	54 048	4.3	463^{2+}, 925^{+} 521^{2+}, 1040^{+}	94–101 **94–102**	925.0 1040.1	Tyr
30.46 (peak 10)	3 481	0.3	611^{2+}	**134–143**	1221.4	Phe
31.62 (peak 11)	4 046	0.3				Phe
32.27 (peak 12)	3 561	0.3	448 747 1126 1396 530^{2+}, 1059^{+}			Trp
33.68 (peak 13)	135 912	10.7	949 683^{4+}, 911^{3+}	 **120–143**	 2731.2	Phe
35.06 (peak 15)	14 472	1.1	640^{2+}, 1278^{+} 697^{2+}, 1393^{+}	10–20 **10–21**	1278.4 1393.5	Tyr
36.39 (peak 16)	40 921	3.2	804^{+}	**113–119**	803.0	No aromatics
37.30 (peak 17)	21 398	1.7	659^{2+}, 1317^{+} $869^{2+}/879^{2+}$ $927^{2+}/935^{2+}$ $985^{2+}/992^{2+}$ 1201^{+}	**92–102** 77–90 76–90 **76–91** 92–101	1316.4 1756.1 1871.1 1986.2 1201.3	Phe
37.55 (peak 18)	52 328	4.1	688^{2+}, 1375^{+} 782^{2+} 840^{2+}	10–21[b] 10–23 **10–24**	1393.5 1563.7 1678.8	Tyr
41.46 (peak 20)	11.461	0.9	$1022^{+}/1040^{+}$ 604^{2+}, 1208^{+} 744^{3+}, 1115^{2+}	94–102 103–112 **94–112**	1040.1 1207.4 2229.5	Tyr
41.75 (peak 21)	108 336	8.6	410^{+} $869^{2+}/877^{2+}$ $927^{2+}/936^{2+}$ 985^{2+} 1074^{2+} 754^{3+}, $1123^{2+}/1132^{2+}$ 975 998	91–93 77–90 76–90 76–91[b] 77–93 **76–93**	409.4 1756.1 1871.1 1986.2 2147.4 2262.5	Phe

(*Continued on p. 8*)

TABLE I *(continued)*

Retention time (min)	Surface (220 nm)[a]	% of total surface	Masses found $(M+xH)^{x+}$	Fragments identified	(M + H), theoretical	UV Spectrum
45.38 (peak 22)			1253^{2+}	92–112	2505.8	Tyr
			660			
			892			
47.02 (peak 24)	43 668	3.5	659^{2+}, 1317^{+}	91–101	1316.4	Tyr, Phe
			717^{2+}, 1432^{+}	91–102	1431.5	
			869^{2+}	76–89 or 77–90[b]	1756.1	
			927^{2+}	76–90[b]	1871.1	
			985^{2+}	76–91[b]	1986.2	
			1057^{3+}, 1586^{2+}	76–101 or 77–102	3169.6	
			821^{4+}, 1095^{3+}, 1643^{2+}	**76–102**	3284.6	
			1504			
48.13 (peak 25)	2 586	0.2				Trp
48.87 (peak 26)	5 859	0.5	605^{2+}	103–112	1207.4	Tyr, Phe
			927^{2+}	76–90	1871.1	
			984^{2+}	76–91	1986.2	
			538			
55.22 (peak 34)	46 005	3.6	881^{2+}, 1763^{+}	**25–39**	1762.0	Trp
			1007			
55.71 (peak 35)	144 335	11.4	$688^{2+}/696^{2+}$, 1377^{+}	10–21[b]	1393.5	Trp, Tyr
			824^{2+}	26–39	1647.9	
			$831^{2+}/839^{2+}$	10–24	1678.8	
			881^{2+}	25–39	1762.0	
			$888^{2+}/896^{2+}$	10–25	1792.9	
			1024^{2+}	22–39	2047.3	
			1143^{3+}, 1712^{2+}	**10–39**	3422.8	
			332			
56.03 (peak 36)	52 679	4.1	824^{2+}	26–39	1647.9	Trp
			$873^{2+}/882^{2+}$, 1763^{+}	25–39	1762.0	
			1024^{2+}	**22–39**	2047.3	
56.65 (peak 37)	21 352	1.7	824^{2+}	26–39		Trp, Tyr
			597			
			673			
			872^{2+}	25–39[b]	1762.0	
			947			
			1141^{3+}	10–39	3422.8	
57.32 (peak 39)	47 404	3.7	460^{2+}, 918^{+}	64–71	918.0	Tyr, Phe
			517^{2+}, 1033^{+}	63–71	1033.1	
			$997^{2+}/1004^{2+}$	47–62	2011.4	
			$1055^{2+}/1062^{2+}$	47–63	2126.4	
			755^{4+}, 1009^{3+}, 1514^{2+}	**47–71**	3026.4	
			901			
			981			
58.35 (peak 40)	154 985	12.2	459^{2+}, 918^{+}	64–71	918.0	Tyr, Phe
			517^{2+}, 1033^{+}	63–71	1033.1	
			951^{3+}, 1426^{2+}	40–62[b]	2870.4	
			990^{3+}, 1484^{2+}	40–63[b]	2985.5	
			1228^{3+}	42–71	3683.3	
			971^{4+}, 1295^{3+}	**40–71**	3885.5	
			901			

TABLE I *(continued)*

Retention time (min)	Surface (220 nm)[a]	% of total surface	Masses found $(M + xH)^{x+}$	Fragments identified	(M + H), theoretical	UV Spectrum
62.24 (peak 42)	51 349	4.1	418^{+}	22–25	417.4	Tyr
			472			
			517^{2+}, 1033^{+}	63–71	1033.1	
			555			
			584			
			601			
			688^{2+}, 1376^{+}	10–21[b]	1393.5	
			719			
			745			
			793			
			831^{2+}	10–24[b]	1678.8	
			841			
			872	25–39[b]	1762.0	
			918^{+}	64–71	918.0	
			975			
			1125			
			1228			

[a] Total surface = $1301.28 \cdot 10^{-3}$ AU (220 nm) · min.

[b] These fragments arise most probably from spontaneous degradation (see text). Their masses correspond to the masses of the peptide minus 18 (loss of H_2O).

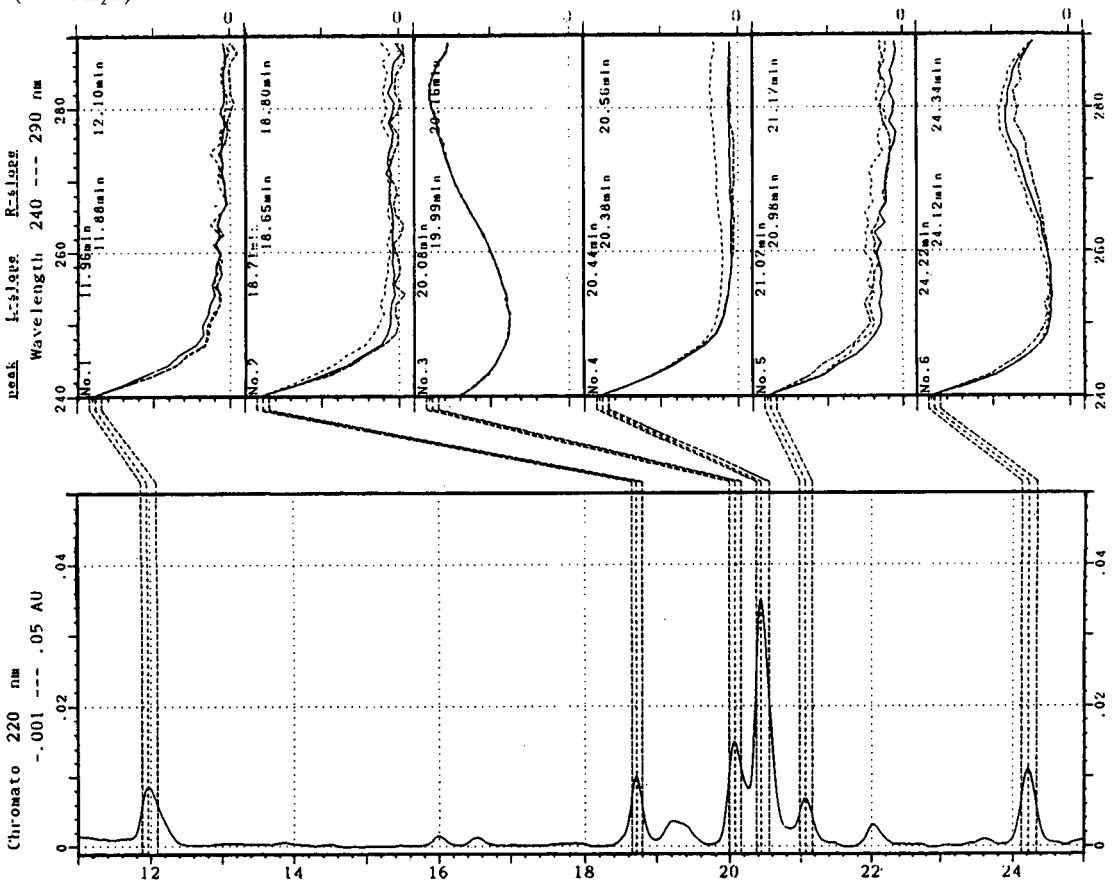

Fig. 3. Spectral analysis of the peptide map (detail). Left: expanded view of a part the chromatogram of Fig. 2. UV detection at 220 nm. Right: absorption spectra of the main peaks recorded from 240 to 290 nm.

```
                    5                                  10
MET GLN ASP / PRO TYR VAL LYS GLU // ALA GLU // ASN LEU LYS LYS
M   Q   D     P   Y   V   K   E       A   E       N   L   K   K

    15                  20                                 25
TYR PHE ASN ALA GLY HIS SER / ASP // VAL ALA / ASP // ASN GLY THR
Y     F   N   A   G   H   S     D       V   A     D       N   G   T

        30                          35                         40
LEU PHE LEU GLY ILE LEU LYS // ASN TRP LYS GLU GLU // SER ASP /
L   F   L   G   I   L   K       N   W   K   E   E       S   D

            45                          50                         55
ARG LYS ILE MET GLN //  SER GLN ILE VAL SER PHE TYR PHE LYS LEU R
K   I   M   Q       S   Q   I   V   S   F   Y   F   K   L
                60                          65                         70
PHE LYS ASN PHE LYS ASP // ASP // GLN SER ILE GLN LYS SER VAL
F   K   N   F   K   D       D       Q   S   I   Q   K   S   V

                    75                          80
GLU // THR ILE LYS GLU // ASP / MET ASN VAL LYS PHE PHE ASN SER
E       T   I   K   E       D     M   N   V   K   F   F   N   S

85                  90                          95
ASN LYS LYS LYS ARG ASP / ASP // PHE GLU // LYS LEU THR ASN TYR
N   K   K   K   R   D       D       F   E       K   L   T   N   Y

    100                 105                         110
SER VAL THR / ASP // LEU ASN VAL GLN ARG LYS ALA ILE HIS GLU //
S     V   T       D       L   N   V     Q   R   K   A   I   H   E

        115                 120                         125
LEU ILE GLN VAL MET ALA GLU //  LEU SER PRO ALA ALA LYS THR GLY L
I   Q   V   M   A   E       L   S   P   A   A   K   T   G

        130                 135                         140
LYS ARG LYS ARG SER GLN // MET LEU PHE ARG GLY ARG ARG ALA SER
K   R   K   R   S   Q       M   L   F   R   G   R   R   A   S


GLN
Q

//  peptide bonds subjected to enzymatic hydrolysis
/   peptide bonds susceptible to thermal hydrolysis.
```

Fig. 4. Observed enzymatic and thermal cleavage sites of rhIFN-γ.

apparent masses of the accompanying Na^+ and K^+ adducts, as is shown below.

Peptide fragmentation in the thermospray interface

Fragments resulting from the hydrolysis of a specific peptide bond are observed. In general, peptide bonds are acid labile. However, in dilute acid conditions, the peptide bond involving an aspartic acid is hydrolysed 100 times more rapidly than the other peptide bonds [20]. This mechanism explains certain fragmentations that occur during the thermospray injection. This phenomenon was observed after the installation of a new TSP II varporizer. We assume that the vaporizer contains a catalyst for this kind of hydrolysis or that the temperature conductance is changed, so that the sample is heated in a more efficient way. The observed thermal and/or enzymatic hydrolyses that have been observed with this interface are summarized in Fig. 4.

As an example of a mass spectrum, the spectrum of peak 21 (Fig. 2b) is given in Fig. 5. The

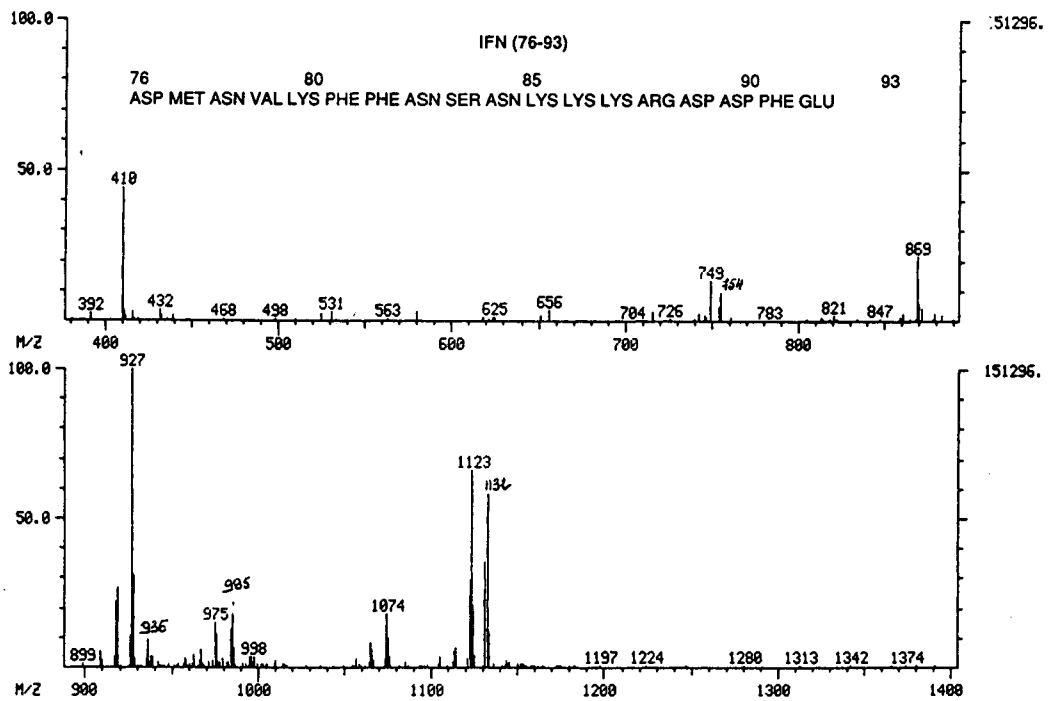

Fig. 5. Mass spectrum of peak 21 attributed to fragment IFN (76–93).

results of the analysis are given in Table I and illustrate the formation of multiply charged ions and hydrolysis of the aspartic peptide bond. The doubly charged ion from the molecular ion of peptide 76–93 (1132^{2+}) is shown in Fig. 6 and represents the 1100–1200 u region of Fig. 5. Doubly and singly charged ions from the peptides resulting from the cleavage of Asp–Met, Asp–Asp and Asp–Phe (1074^{2+}, 985^{2+}, 936^{2+}, 877^{2+}, 410^{+}) are also found.

It was not always possible to detect the singly charged parent ion for these peptides, but the apparent masses of the adducts of Na^{+} and K^{+} enabled us to assign these as multiply charged ions.

The finding of fragment 3–7 in two different peaks (6 and 8) also indicates postcolumn fragmentation. The apparent co-elution with fragment 0–2 or 0–2ox (oxidation of the methionine) must be due to the hydrolysis of the fragment IFN 0–7 after position 2 (Asp). In peak 8 the parent molecule is also found.

At the end of the peptide map, where large peptides are eluted, the presence of acid hydrolysis products enables us to retrace the parent peptide, which can be found as a series of multiply charged ions. For example, in peak 39 all hydrolysis products plus the parent molecule are observed.

Spontaneous fragmentation

Besides hydrolysis, spontaneous fragmentation can be used to explain the masses of certain fragments. Apparently this fragmentation cleaves the peptide bond, by a mechanism similar to that causing peptide bond cleavage in FAB or MS–MS ionization. It results in the loss of 18 u with respect to similar fragments obtained by hydrolysis. Consider, for example, peak 21 (Table I). The mass spectrum of this peak

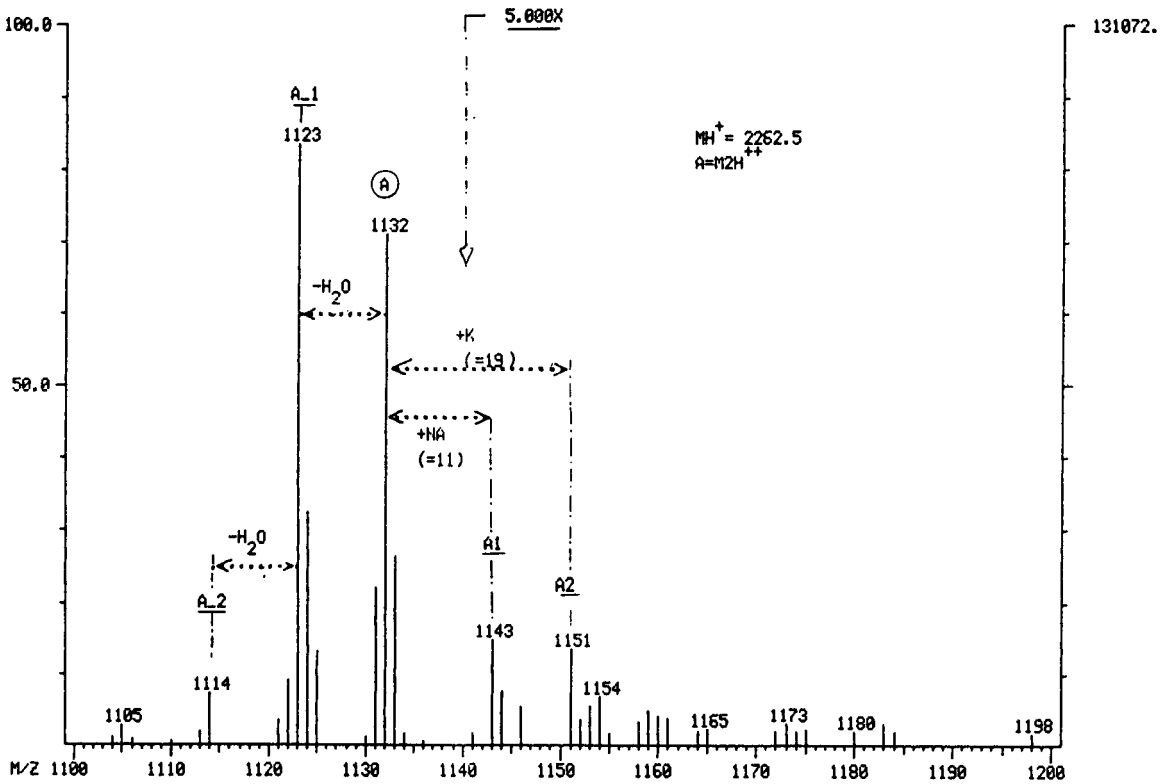

Fig. 6. 1100–1200 u region of the mass spectrum of peak 21 attributed to fragment IFN (76–93).

contains fragments due to acid hydrolysis, in addition to spontaneous fragmentation: fragment 77–90, masses $869^{2+}/877^{2+}$; fragment 76–90, masses $927^{2+}/936^{2+}$; and fragment 76–91, mass 985^{2+}.

It should also be noted that apparently abnormal cleavage sites are found, at the C-terminal side from Gln at positions 46 and 133. In these cases the complementary fragment is also found (40–46 with 47–71 and 120–133 with 134–143) elsewhere in the peptide map. The sequence around these sites, Met–Gln–Ser and Ser–Gln–Met, is remarkable. Another abnormal cleavage is found at the Lys–Asn bond (34–35).

Sensitivity

The amount of hydrolysate injected was 200 μg. We were able to determine masses in peaks that account for less than 0.2% of the total surface in the peptide map. We estimate the amount of material under this peak as 400 ng (less than 4 nmol of amino acids) (peaks 1, 2, 6, 10 and 12).

CONCLUSIONS

The peptide map of rhIFN-γ was determined by on-line RP-HPLC with diode-array absorbance and thermospray mass spectrometric detection. Fragmentation of the peptides by acid hydrolysis of the peptide bond involving aspartic acid and spontaneous fragmentation were observed. They were of great use in the identification of most of the peptides resulting from the digest of rhIFN-γ by *Staphylococcus aureus* strain V8 endoprotease. The recording of the UV absorption spectra of the fragments is of interest for the identification of the peptides and permits the extrapolation of the results to those obtained without coupling to a thermospray mass spectrometer.

REFERENCES

1 R.L. Garnick, N.J. Solli and P.A. Papa, *Anal. Chem.*, 60 (1988) 2546.
2 V.M. Ingram, *Methods Enzymol.*, 6 (1963) 831.
3 S.A. Carr, M.E. Hemling, M.F. Bean and G.D. Roberts, *Anal. Chem.*, 63 (1991) 2802.
4 Y. Ito, T. Takeuchi and D. Joto, *J. Chromatogr.*, 346 (1985) 161.
5 R.M. Caprioli, B. DaGue, T. Fan and W.T. Moore, *Biochem. Biophys. Res. Commun.*, 146 (1987) 291.
6 W.J. Henzel, J.H. Bourell and J.T. Stults, *Anal. Biochem.*, 187 (1990) 228.
7 A. Cappiello, P. Palma, I.A. Papayannopoulos and K. Biemann, *Chromatographia*, 30 (1990) 477.
8 A.P. Bruins, T.R. Covey and J.D. Henion, *Anal. Chem.*, 59 (1987) 2642.
9 E.C. Huang and J.D. Henion, *Anal. Chem.*, 63 (1991) 732.
10 C.R. Blakey, J.J. Carmody and M.L. Vestal, *Anal. Chem.*, 52 (1980) 1636.
11 H.Y. Kim, D. Pilosof, D.F. Dyckes and M.L. Vestal, *J. Am. Chem. Soc.*, 106 (1984) 7304.
12 D. Pilosof, H.Y. Kim, D.F. Dyckes and M.L. Vestal, *Anal. Chem.*, 56 (1984) 1236.
13 W.P. Blackstock, R.J. Dennis, S.J. Lane, J.I. Sparks and M.P. Weir, *Anal. Biochem.*, 175 (1988) 319.
14 P.J. Rudewicz, *Biomed. Environ. Mass Spectrom.*, 15 (1988) 461.
15 K. Stachowiak, C. Wilder, M.L. Vestal and D.F. Dyckes, *J. Am. Chem. Soc.*, 110 (1988) 1758.
16 K. Stachowiak and D.F. Dyckes, *Pept. Res.*, 2 (1989) 267.
17 K. Straub and K. Chan, *Rapid Commun. Mass Spectrom.*, 4 (1990) 267.
18 K. Chan, D. Wintergrass and K. Straub, *Rapid Commun. Mass Spectrom.*, 4 (1990) 139.
19 R.H. Robins and F.W. Crow, *Rapid Commun. Mass Spectrom.*, 2 (1988) 30.
20 C.M. Tsung and H. Fraenkel-Conrat, *Biochemistry*, 4 (1965) 793.

Journal of Chromatography, 647 (1993) 13–20
Elsevier Science Publishers B.V., Amsterdam

CHROMSYMP. 2852

Evaluation of the performance of capillary liquid chromatography–fast atom bombardment mass spectrometry systems with precolumn addition of glycerol as a viscous matrix

J.P. Gagné and A. Carrier

Regional Center for Mass Spectrometry, Department of Chemistry, University of Montreal, P.O. Box 6128, Montreal H3C 3J7 (Canada)

L. Varfalvy

Hydro-Québec, Montreal (Canada)

M.J. Bertrand*

Regional Center for Mass Spectrometry, Department of Chemistry, University of Montreal, P.O. Box 6128, Montreal H3C 3J7 (Canada)

ABSTRACT

A series of experiments were conducted in order to evaluate the boundaries within which precolumn addition of viscous matrices can be systematically used in capillary LC–fast atom bombardment MS systems and to evaluate the broadening caused by components of the systems such as the column, the transfer capillary tube and the probe interface. The effect of the addition of a viscous matrix on the capillary system was studied by monitoring important chromatographic parameters such as capacity factors, selectivity, number of theoretical plates, peak width and resolution. The results obtained indicate that glycerol contents in the mobile phase higher than 5% have a deleterious effect on most chromatographic indicators. The overall effect of the presence of glycerol on the chromatographic system can be rationalized in terms of the modification of the analyte distribution between the mobile and stationary phases and changes in the kinetics of the system created by an increase in the viscosity of the mobile phase. The main contribution to band broadening in the system can be attributed to the interface and is related to the formation of a liquid droplet at the tip of the probe. Other contributions such as broadening in the column and in the transfer capillary affect the total variance of the chromatographic system but to a smaller extent.

INTRODUCTION

Fast atom bombardment mass spectrometry (FAB-MS) and liquid secondary ion mass spectrometry (LSIMS) are commonly used to generate mass spectra from polar, thermally labile and involatile compounds. Each technique involves the bombardment of an analyte dissolved in a viscous organic matrix by high energy (3–10 keV) fast-moving neutral species (FAB) or by a high-energy Cs^+ ion beam guided to a static sample [1,2]. These techniques have extended the scope of their initial applications by the introduction of different continuous-flow devices allowing the dynamic introduction of sample [3–

* Corresponding author.

0021-9673/93/$06.00

6]. The advent of dynamic flow systems has not only increased the power of the techniques but has also allowed their interfacing with liquid chromatography (LC–FAB-MS). However, the need for low flow-rates (2–7 μl/min) and for the presence of a non-volatile matrix in the LC–FAB-MS systems have generated problems in the routine application of LC coupled to dynamic FAB-MS. To date, few stategies have been used to solve the constraints encountered in LC–FAB-MS analyses. The strategies developed initially have favored postcolumn splitting of the chromatographic effluent along with postcolumn addition of a matrix in conventional and microbore columns [7,8]. Recent strategies, however, have mostly been concerned with the direct coupling of the liquid capillary column with dynamic introduction systems [3,5,9–15]. In separation schemes using capillary columns, the analyst may use postcolumn addition of the viscous matrix in order to allow the independent optimization of the LC conditions [9]. However, in some instances such as when using open-tubular liquid chromatography coupled to FAB-MS, postcolumn addition is necessary as the efficient operation of the mass spectrometer requires that a make up liquid be added to the chromatographic effluent ($\leq$100 nl/min). In other situations, uncommon matrices may be necessary in order to produce good-quality mass spectra. These matrices may react with the stationary phase or metal parts of the chromatographic system [16] and in such instances postcolumn addition is a useful mitigating alternative.

Precolumn addition of the viscous matrix is the second option that can be used in order to introduce the matrix in LC–FAB-MS systems. However, the intrusion of a polar and viscous matrix in the chromatographic process necessarly introduces changes in the distribution of the analyte between the mobile and stationary phases. Also, the diffusive processes taking place inside and outside the column will usually be altered, as previously observed in conventional LC–FAB-MS systems [16–18], since the introduction of a viscous matrix in the mobile phase will change its physical properties. The primary objective of this study was to investigate and to quantify the perturbation in the chromatographic process induced by the precolumn addition of glycerol to the mobile phase of packed capillary liquid chromatographic systems. A second objective was to assess the extent of broadening induced by the presence of the FAB matrix in a frit-FAB system.

EXPERIMENTAL

Instrumentation

The liquid chromatographic system consisted of a Carlo-Erba Phoenix-20 pump connected to a Valco Model C14W 60-nl injector. Detection was achieved with an Isco uLC-10 variable-wavelength detector set at 280 nm. The chromatographic column used consisted of a laboratory-made capillary column (Spherisorb ODS-2, d_p = 5 μm, 225 mm $\times$ 0.250 mm I.D.). The temperature was maintained at 25°C by a temperature equalization chamber provided with the detector. Experiments involving continuous-flow FAB (CF-FAB) were performed on a VG Autospec-Q mass spectrometer using the dynamic LSIMS probe. This probe consists of a fused-silica transfer tube of 50 or 75 μm terminated by a stainless-steel frit of 2 mm diameter.

Chemicals

The peptides met-enkephalin and leu-enkephalin were obtained from Sigma (St. Louis, MO, USA). Glass-distilled glycerol (>99%) and trifluoroacetic acid were purchased from Aldrich (Milwaukee, WI, USA). All compounds were used without further purification and the mobile phase were prepared using HPLC-grade acetonitrile and distilled, deionized water obtained with a Milli-Q purification system (Millipore, Bedford, MA, USA).

Preparation of mobiles phases

The eluents were carefully prepared by mixing appropriate volumes of distilled, deionized water and organic modifiers. The mobile phase used for peptide analysis contained fixed proportions of trifluoroacetic acid (TFA) and acetonitrile

(ACN) and the proportion of water was adjusted to complement the volume of glycerol (GLY) in the solution (ACN–H_2O–GLY–TFA 30:70 – x:x:0.1). Sufficient amounts of mixture were prepared in order to ensure that all experiments would be conducted with the same mobile phase. In all instances, the solvents were filtered (0.45-μm filter) and degassed prior to use.

Chromatographic measurements

All chromatographic experiments were carried out at 25°C after the chromatographic system had been equilibrated for at least 45 min. Before the experiments were conducted in the presence of glycerol, the capillary column was tested to evaluate its efficiency by injection of a standard solution of amylbenzene ($k' = 5$) eluted with acetonitrile–water (75:25, v/v). Precise values for the volumetric flow-rates were measured for each experiment. The retention of sodium nitrate was taken as the dead volume (t_m) and the average linear velocity was calculated using the length of the chromatographic column. The number of theoretical plates (N) was estimated from the widths at half-height of the peaks. The Van Deemter plots were generated by measuring the theoretical plate height (H) with linear velocities over the range 0.02–4 mm/s.

Band broadening measurements

The evaluation of the variance related the broadening generated by the continous-flow introduction probe coupled to the mass spectrometric system was performed by indirect UV experiments and direct MS experiments. The variance associated with the capillary transfer tube found in the dynamic FAB interface was determined by replacing the column in the UV system by capillary tubes with the same inner diameter (50 or 75 μm) but with different lengths [19,20]. By plotting the total variance obtained from the width at the base W_b ($\sigma_t^2 = (W_b/4)^2$] *versus* the length of the capillary tube on a graph and by extrapolating the line obtained to the intercept on the ordinate, the instrumental variance originating from injector and detector can be estimated. The subtraction of the estimated instrumental variance from the total variance measured for a 1-m long capillary tube allows the determination of the broadening generated by the capillary transfer tube of the dynamic FAB-MS interface. Replacing the column in the system and doing the same subtraction for the extra-column contribution allows the determination of typical values for the broadening generated by a capillary column in presence of a FAB matrix in the mobile phase. The broadening produced at the tip of the dynamic introduction probe was evaluated by injecting a solution of met-enkephalin into the interface of to the mass spectrometer. The variance observed minus the previous variance evaluated for the capillary transfer tube allows the quantification of the broadening at the probe tip.

RESULTS AND DISCUSSION

It is important to characterize the influence of the presence of a FAB matrix in the mobile phase of the capillary liquid chromatographic system since this type of chromatography is becoming the standard in LC–FAB-MS analysis. In order to gain a descriptive and comprehensive view of the effect of the precolumn addition of a FAB matrix in packed capillary liquid chromatography coupled to dynamic FAB-MS systems, a series of experiments that should allow the determination of the effects induced on the key chromatographic indicators can be conducted.

The effect on the retention properties of some peptides induced by an increasing concentration of viscous matrix in the mobile phase can be seen in Figs. 1 and 2. Fig. 1 shows the changes in the capacity factors induced by variation of the glycerol content in the mobile phase between 0 and 10%. It can be seen that the capacity factors decrease with increase in the concentration of the matrix in the chromatographic eluent. This decrease, of the order of 40% for met-enkephalin and 46% for leu-enkephalin, is significant as the glycerol content is raised from 0 to 10%. This decrease in the capacity factors implies that the addition of a FAB matrix can cause severe compression of the retention times of the analytes. However, examination of Fig. 1 reveals that the acceleration of the elution becomes

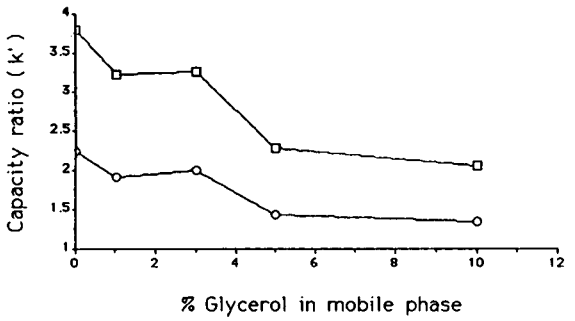

Fig. 1. Effect of concentration of glycerol in the mobile phase on the capacity factor (k'). ○ = Met-enkephalin; □ = leu-enkephalin.

significant only when more than 3% of matrix is added to the mobile phase. The decrease in the capacity factors that has been observed is greater than that previously observed in conventional chromatography in the presence of glycerol or thioglycerol [16,18]. Possible interactions at the fused-silica wall of the capillary column and the differences between the phase ratios of the capillary and the conventional columns may be involved in the differences noted. Further experiments are needed, however, in order to elucidate the causes of that effect. The addition of the FAB matrix to the liquid vector induces other changes in the separation of the analytes. As shown in Fig. 2, by plotting the variation in selectivity against the glycerol content in the mobile phase, the increased presence of glycerol decreases the selectivity for the pair met-enkephalin and leu-enkephalin. This decrease is not drastic but it varies regularly, passing from 1.69 with no matrix to 1.53 with 10% matrix added to the mobile phase. Such changes in selectivity indicate that the retention of compounds with higher capacity factors are more affected by the presence of glycerol.

The efficiency of the column is another parameter that it is important to characterize because it is an indicator of the potential of the chromatographic system to separate complex mixtures. In the presence of glycerol the efficiency must change as the addition of a viscous matrix to the chromatographic eluent perturbs most diffusive processes that control the kinetics of the chromatographic process. The effect on the number of theoretical plates (N) of increasing amounts of glycerol added to the mobile phase can be seen in Fig. 3, which shows the decrease in the normalized theoretical plate number (N_x/N_0) with increase in glycerol content in the capillary chromatographic system. Normalization of the number of theoritical plates at a specific matrix content (N_x) to the number of theoritical plates measured in absence of matrix (N_0) allows the quantification of the decrease in efficiency of the column in the presence of glycerol. The reduction is of the order of 33% and 38% for met-enkephalin and leu-enkephalin, respectively, with 10% of added matrix. As in Fig. 2, small changes are seen with the first 3% of added matrix and the decrease is faster at higher matrix contents. This decrease in efficiency comes from the broadening of the elution band. Fig. 4 shows the behavior of the normalized peak width ($w_{1/2}/t_r$) with glycerol content. The curves show that

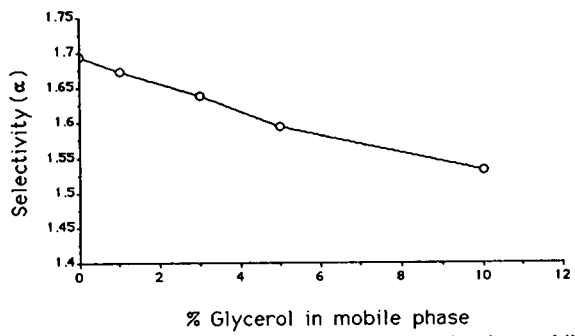

Fig. 2. Effect of concentration of glycerol in the mobile phase on the selectivity (α). ○ = Met-enkephalin; □ = leu-enkephalin.

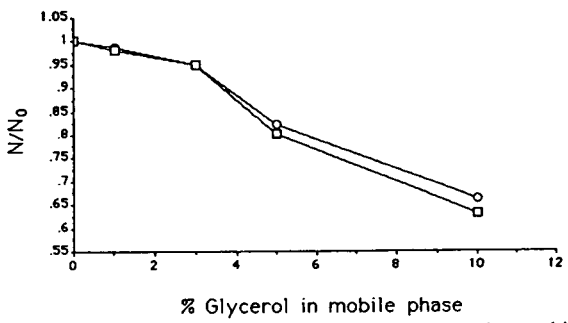

Fig. 3. Effect of concentration of glycerol in the mobile phase on the normalized number of theoretical plates (N_x/N_0). ○ = Met-enkephalin; □ = leu-enkephalin.

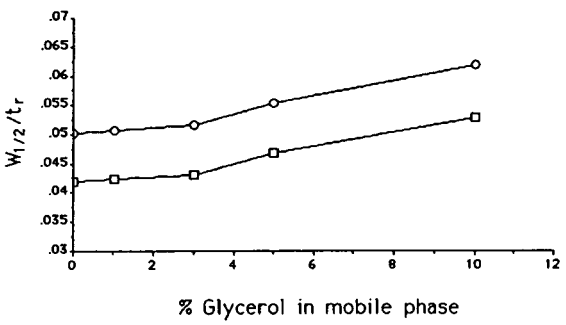

Fig. 4. Effect of concentration of glycerol in the mobile phase on the normalized peak width ($w_{1/2}/t_r$). ○ = Met-enkephalin; □ = leu-enkephalin.

broadening increases in the presence of glycerol. The band spreading increases by 25% at 10% of added matrix for the two peptides analysed. Hence, the decrease in efficiency observed for the leu-enkephalin (38%) *versus* met-enkephalin (33%) originates from both sources: the increase in broadening and the greater decrease in the retention time of leu-enkephalin. The net effect of the differential decrease in retention and increase in the peak width for met-enkephalin and leu-enkephalin can be seen in Fig. 5. The data in the figure, which shows the changes in resolution in the presence of glycerol, demonstrate that the addition of a FAB matrix to the mobile phase significantly decreases the resolution of the pair of peptides.

In order to characterize the effect of the presence of glycerol on the kinetics of the capillary system, Van Deemter plots at different matrix contents present in the mobile phase have

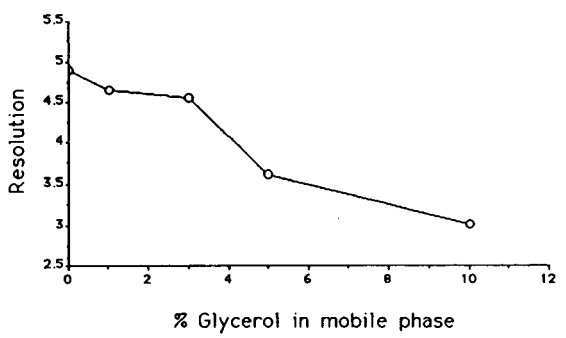

Fig. 5. Effect of concentration of glycerol in the mobile phase on the resolution (R_s). ○ = Met-enkephalin; □ = leu-enkephalin.

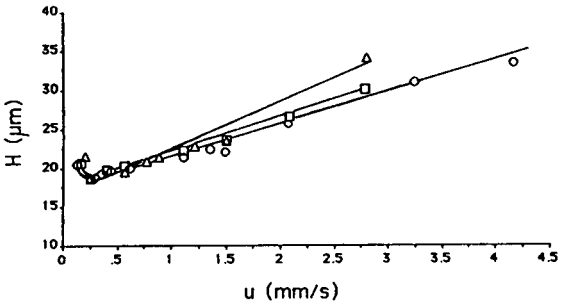

Fig. 6. Van Deemter plots for met-enkephalin at various glycerol concentrations in the mobile phase: ○ = 0%; □ = 3%; △ = 5%.

been generated. Fig. 6 shows the height equivalent to a theoretical plate in relation to the average linear velocity of the mobile phase in the capillary column. It can be seen that the addition of a FAB matrix such as glycerol mainly affects the mass transfer (right-hand side) processes involved in the chromatographic equilibrium. The similarity of the curves obtained at 0% and 3% of matrix added to the liquid vector is an indication that negligible or very small perturbations are caused by the presence of glycerol at low levels in the mobile phase. These observations explain why only small perturbations have been measured in the capacity factor, selectivity, efficiency, normalized peak width and resolution with less than a 3% matrix content in the mobile phase. Our observations on the Van Deemter plots are also in agreement with reported comments indicating that analyses with 1% matrix added to different mobile phases induce almost no change in chromatographic performance during LC–FAB-MS analysis [10–13]. The decrease in efficiency noted at high glycerol concentrations is related to less efficient mass transfer in the capillary column. As indicated by previous studies [16,17], this is caused by an increase in the viscosity of the mobile phase which produces a lower diffusivity of the solute, thus inducing more band spreading in the system.

In order to identify the factors responsible for band broadening, the variances associated with each component of the system were examined. Table I gives the measured variances associated with each component of the LC–FAB-MS system in the presence of a FAB matrix such as

TABLE I

MEASUREMENT OF THE BROADENING CAUSED BY THE COMPONENTS IN THE LC–FAB-MS SYSTEM

Glycerol (%)	σ^2_{col} (μl^2)	σ^2_{tu} (μl^2)						σ^2_d (μl^2)[a]
		50 μm I.D.			75 μm I.D.			
		2.5 μl/min	4.0 μl/min	5.0 μl/min	2.5 μl/min	4.0 μl/min	5.0 μl/min	
0	0.148	0.0083	0.0115	0.0137	0.0179	0.0259	0.0352	–
1	0.141	0.0086	0.0120	0.0141	0.0194	0.0264	0.0375	0.170
3	0.151	0.0090	0.0127	0.0147	0.0204	0.0301	0.0397	0.207
5	0.177	0.0095	0.0134	0.0152	0.0224	0.0323	0.0422	0.256
7	0.238	0.0101	0.0146	0.0158	0.0237	0.0344	0.0421	–

[a] Frit-FAB.

the variance associated with the chromatographic column (σ^2_{col}), the transfer tube (σ^2_{tu}) and the droplet (σ^2_d). The variance associated with the chromatographic system (σ^2_{CHR}) was calculated using eqn. 1, where H is the height equivalent to a theoretical plate, t_r is the retention time and L is the length of the column:

$$\sigma^2_{CHR} = \frac{Ht_r^2}{L} \quad (1)$$

The total variance of the chromatographic system (σ^2_{CHR}) can be expressed as the sum of the broadening occuring in the column (σ^2_{col}) and by components external to the column (σ^2_{ex}):

$$\sigma^2_{CHR} = \sigma^2_{col} + \sigma^2_{ex} \quad (2)$$

The subtraction from σ^2_{CHR} of the variances associated with the injector and the detector will result in the variance associated with the column. The results indicate that the variance associated with the column is between 0.148 and 0.238 μl^2 when the glycerol content in the mobile phase varies from 0 to 7% and therefore its contribution to the total variance is relatively important.

The data in Table I indicate that the variances associated with the probe tip are between 0.170 and 0.256 μl^2 when the glycerol content is varied from 1 to 5%. These variances are responsible for a dispersion of 1.6–2.0 μl for the frit-FAB interface used in this study. The widths of these bands, however, are smaller than those which can be observed in conventional CF-FAB interfaces, which are of the order of 2.5 μl [4,17]. It thus appears that variances associated with the interface are considerably more important than those associated with the chromatographic column.

Variances associated with transfer capillary tubes of 50 or 75 μm I.D. are between 0.0083 and 0.0421 μl^2, as indicated by the data of Table I. These are functions of the flow-rate as indicated by the Taylor–Golay equation (eqn. 3) [21], which allows the theoretical estimation of the variances associated with capillary tubing:

$$\sigma^2_{tu} = \frac{\pi r^4 LF}{24 D_m} \quad (3)$$

where F is the flow-rate and D_m is the diffusion coefficient. Comparison of the variances associated with the transfer capillaries (Table I) reveals that variances associated with tubing of 75 μm I.D. are systematically 15% of the variance associated with the probe tip at a flow-rate of 5 μl/min and a glycerol content of 5%. With a flow-rate of 2.5 μl/min and a 5% content of glycerol the same variance is around 4%. Hence the dispersion produced by this component appears to be relatively small and its contribution should not significantly affect the total variance of the system.

From the data presented, it can be concluded that the major contribution to broadening comes from the probe tip. However, broadening produced by the chromatographic column has to be considered relatively important under the present conditions as it accounts for almost 50% of the broadening induced by the probe tip. Both of these effects will obviously result in a decrease in the chromatographic resolution for the overall system. It is possible to reduce the total dispersion in the system by using a low concentration of glycerol in the system, but it must be realized that these contributions will still be important even at glycerol contents of the order of 1% (*ca.* 0.33 μl^2).

Thus it can be seen from Table I that the contribution of the interface is mainly due to the formation of a liquid droplet at the end of the probe tip. The dispersion occurring at the tip is relatively difficult to evaluate as there are many phenomena occurring in the droplet that forms at the end of the probe tip (evaporation, diffusion, sputtering, mixing, etc.). Two approaches can be used to estimate the dispersion of the system. One approach is to concentrate on the droplet itself and consider it as a connecting tube and the variance associated with it can be obtained from the Taylor–Golay relationship (eqn. 3). The other approach is to consider the droplet as a mixing chamber, in which case the variance associated with it can be obtained from the equation [22]:

$$\sigma^2_{drop} = V^2_{drop} = \pi^2 r^4_{tc} L^2_{tc} \quad (4)$$

TABLE III

ESTIMATED VARIANCE ASSOCIATED WITH A MIXING CHAMBER

Diameter × thickness (mm × mm)	σ^2_d (μl^2)
2 × 0.050	0.025
2 × 0.045	0.020
2 × 0.040	0.016
2 × 0.035	0.012
2 × 0.030	0.009

where r_{tc} is the radius of the droplet and L_{tc} is its length.

By assuming that the composition of the liquid phase is constant within the droplet, the variance can be estimated. The estimated values for the variance associated with the droplet that can be obtained using each model described above are given in Tables II and III. The comparison of the measured variance (Table I) with the estimated value (Tables II and III) shows that the first approach, "the connecting tube approach", seems to be a more suitable model that fits in with the data. The results obtained indicate that the variance would correspond to a film height of the order of 35–40 μm. Therefore, a decrease in the radius of the frit should lead to a significant decrease in the broadening due to the formation of the liquid droplet, as can be seen from eqn. 3 where the broadening is directly proportional to r^4. Further experiments are needed, however, in order to confirm that the formation of the liquid

TABLE II

ESTIMATED VARIANCE CAUSED BY A CAPILLARY TRANSFER TUBE

Diameter × thickness (mm × mm)	σ^2_d (μl^2)				
	0% glycerol	1% glycerol	3% glycerol	5% glycerol	10% glycerol
2 × 0.050	0.262	0.264	0.276	0.285	0.336
2 × 0.045	0.236	0.238	0.248	0.256	0.302
2 × 0.040	0.210	0.211	0.221	0.228	0.268
2 × 0.035	0.184	0.185	0.193	0.199	0.235
2 × 0.030	0.157	0.158	0.166	0.171	0.201

droplet can be estimated using this model, which gives a very good approximation of the variance associated with the formation of the droplet.

CONCLUSIONS

As previously observed for conventional LC–FAB-MS, the precolumn addition of a viscous matrix such as glycerol can also significantly alter the chromatographic conditions in capillary LC–FAB-MS systems. In general terms, the negative effect of precolumn addition of glycerol on the chromatographic indicators are comparable in conventional and in capillary LC–FAB-MS systems. The source of chromatographic broadening can be attributed mainly to changes in the diffusivity of the analytes induced by an increase in the viscosity of the mobile phase. The variance associated with the interface can be related mainly to effects occurring at the tip of the probe, as the variance with the dead volume of the transfer capillary tube is found to be small. However, as has been demonstrated, the dispersion induced in the chromatographic column by the presence of a matrix cannot be neglected as it is of the same order of magnitude as that induced by the probe tip.

ACKNOWLEDGMENTS

The authors acknowledge the financial support of the Natural Sciences and Engineering Council of Canada (NSERC) and of Hydro-Québec, which permitted this study.

REFERENCES

1 M. Barber, R.S. Bordoli, G.J. Elliot, R.D. Sedgwick and A.N. Tyler, *J. Chem. Soc., Chem. Commun.*, (1981) 325.
2 W. Aberth, K.M. Straub and A.L. Burlingame, *Anal. Chem.*, 54 (1982) 2029.
3 Y. Ito, T. Takeuchi, D. Ishii and M. Goto, *J. Chromatogr.*, 346 (1985) 161.
4 R.M. Caprioli, T. Fan and J.S. Cottrel, *Anal. Chem.*, 58 (1986) 2946.
5 M.A. Moseley, L.J. Deterding, K.B. Tomer, R.T. Kennedy, N. Bragg and J. Jorgenson, *Anal. Chem.*, 61 (1989) 1577.
6 M.C. Shih, T.C.L. Wang and S.P. Markey, *Anal. Chem.*, 61 (1989) 2582.
7 D.E. Games, S. Pleasance, E.D. Ramsey and M.A. McDowall, *Biomed. Environ. Mass Spectrom.*, 15 (1989) 179.
8 D.J. Bell, M.D. Brightwell, W.A. Neville and A. West, *Rapid Commun. Mass Spectrom.*, 4 (1990) 88.
9 J.E. Coutant, T.G. Chen and B.L. Ackerman, *J. Chromatogr.*, 529 (1990) 265.
10 D.B, Kassel, B.D. Musselman and J.A. Smith, *Anal. Chem.*, 63 (1991) 1091.
11 P. Boulenguer, Y. Leroy, J.M. Alonso, J. Montreuil, G. Ricard, C. Colbert, D. Duquet, C. Deweale and B. Fournet, *Anal. Biochem.*, 168 (1988) 164.
12 Y. Ito, T. Takeuchi, D. Ishii, M. Goto and T. Mizuno, *J. Chromatogr.*, 358 (1986) 201.
13 W.J. Henzel, J.H. Bourret and J.J. Stuits, *Anal. Biochem.*, 187 (1990) 228.
14 K.B. Tomer, J.R. Perkins, C.E. Parker and L.J. Deterding, *Biol. Mass. Spectrom.*, 20 (1991) 783.
15 S. Pleasance, P. Thibault, M.A. Moseley, L.J. Deterding, K.B. Tomer and J.W. Jorgenson, *J. Am. Soc. Mass Spectrom.*, 1 (1990) 321.
16 A. Carrier, J.P. Gagné and M.J. Bertrand, *J. Chromatogr.*, 591 (1992) 129.
17 J.P. Gagné, A. Carrier and M.J. Bertrand, *J. Chromatogr.*, 554 (1991) 47.
18 J.P. Gagné, A. Carrier and M.J. Bertrand, *J. Chromatogr.*, 554 (1991) 61.
19 H.A. Claessens, C.A. Cramers and M.A.J. Kuyken, *Chromatographia*, 23 (1987) 189.
20 H.H. Lauer and G.P. Rozing, *Chromatographia*, 14 (1981) 641.
21 G. Taylor, *Proc. R. Soc. London, Ser. A*, 255 (1956) 67.
22 J.C. Sternberg, *Adv. Chromatogr.*, 2 (1966) 205.

Journal of Chromatography, 647 (1993) 21–29
Elsevier Science Publishers B.V., Amsterdam

CHROMSYMP. 2807

Origin of the decrease in chromatographic resolution induced by the addition of viscous matrices in liquid chromatographic–fast atom bombardment mass spectrometric systems

J.P. Gagné and A. Carrier

Regional Center for Mass Spectrometry, Department of Chemistry, University of Montreal, P.O. Box 6128, Montreal H3C 3J7 (Canada)

L. Varfalvy

Hydro-Québec, Montreal (Canada)

M.J. Bertrand*

Regional Center for Mass Spectrometry, Department of Chemistry, University of Montreal, P.O. Box 6128, Montreal H3C 3J7 (Canada)

ABSTRACT

The monitoring of the chromatographic resolution for three pairs of analytes separated in different chromatographic systems using mobile phases with varying concentrations of viscous fast atom bombardment matrices showed that it exhibits a steady decrease with increasing matrix content in the mobile phase. The decrease in resolution is observed in the partition and ion-pair chromatographic modes at both low and high matrix contents in the eluent for both conventional and capillary chromatographic systems using precolumn addition of glycerol and thioglycerol. Careful examination of the normalized efficiency, capacity factor and selectivity terms contributing to the resolution allowed the identification of the sources of the decrease in resolution in the presence of a matrix in the eluent. The efficiency and capacity factor terms show decreases with increasing matrix content in all systems. Subtle variations in the selectivity term observed in the presence of a viscous matrix can increase or limit the decrease in resolution. The variations observed for the efficiency term show similar trends in all systems studied and appear to be independent of the analyte or the chromatographic mode. However, the variations in capacity factor and selectivity induced by the presence of the viscous matrix are dependent on the nature of the analyte, the type of chromatography and the nature of the matrix.

INTRODUCTION

The technique of continuous-flow fast atom bombardment mass spectrometry (CF-FAB-MS) is a powerful tool that allows repetitive and rapid determinations of polar and labile compounds in aqueous media. In complex mixture analysis, however, this technique used alone can suffer from ionization suppression and insufficient resolution capability [1,2]. In order to reduce these limitations, coupling of this technique with liquid chromatography (LC–FAB-MS) is often a way to gain supplementary temporal resolution which allows the efficient operation of the mass spectrometric system. As the presence of a viscous matrix is necessary to optimize ionization in

* Corresponding author.

0021-9673/93/$06.00

FAB-MS, premixing of the matrix with the chromatographic eluent is an easy method to admit involatile solvents in this coupled system. The inclusion of a viscous matrix in the mobile phase will, to some extent, affect the quality of the initial separation developed in the absence of the FAB matrix. In our previous studies on LC–FAB-MS systems [3–5], conducted with UV detection to allow the discrimination of chromatographic perturbations caused by the presence of a matrix in the mobile phase while excluding those induced by the mass spectrometric interface and operating parameters, it was observed that the presence of a matrix in the chromatographic eluent produces some alterations in the multiple chromatographic parameters that can affect the chromatographic system and reduce its performance [3–6].

This study pursued our investigation on the effect of the presence of FAB matrices in the mobile phase on the chromatographic separation. The changes in chromatographic resolution that result from precolumn addition of glycerol or thioglycerol to the chromatographic eluent in conventional and capillary liquid chromatographic systems used in LC–FAB-MS were specifically investigated. In this work, the effects on resolution produced by the presence of a FAB matrix in the mobile phase were monitored in partition and ion-pair chromatography. The results obtained show that the presence of a matrix, as noticed before, reduces the chromatographic resolution and affects both the physical and chemical processes taking place during the chromatographic separation. It was also observed that ion-pair chromatography seems to be much more sensitive than partition chromatography to the presence of a matrix in the liquid vector.

EXPERIMENTAL

Instrumentation

The conventional liquid chromatographic system used in this study consisted of a Perkin-Elmer Model 410 pump connected to a Rheodyne Model 7125 injector with a 6-μl sample loop. The UV detection system was a Perkin-Elmer LC 90 variable-wavelength detector operated at 280 nm. The conventional columns used (Spherisorb ODS-2, $d_p = 5$ μm, 125 mm × 4.6 mm I.D.) (CSC, Montréal, Canada) were maintained at 25°C by a water jacket regulated by a Haake (Berlin-Sterglitz, Germany) circulator. The capillary system used consisted of a Carlo Erba Phoenix-20 pump connected to a Valco C14W injector with a 60-nl sample loop. Detection at 280 nm was achieved with an ISCO μLC-10 variable-wavelength detector equipped with a 60-nl flow cell. The capillary columns were laboratory-made (180 mm × 0.25 mm I.D.) and packed with 5-μm particules (Spherisorb ODS-2). The temperatures of the injector, the capillary column and the detector flow cell were maintained at 25°C by a temperature equalization chamber supplied with the detector.

Chemicals

The peptides bradykinin, met-enkephalin and leu-enkephalin were obtained from Sigma (St. Louis, MO, USA). The acidic compounds 3,5-dihydroxybenzoic acid and vanillic acid were purchased from Aldrich (Milwaukee, WI, USA) along with thioglycerol (THIO) (<95%) and trifluoroacetic acid (TFA). Glass-distilled glycerol (GLY) (>99%) was obtained from BDH (Toronto, Canada). All compounds were used as received and the mobile phases were prepared using HPLC grade acetonitrile (ACN) and distilled, deionized water obtained with a Milli-Q purification system (Millipore, Bedford, MA, USA).

Mobile phases

The chromatographic systems used are summarized in Table I and are referred to in the text as systems A–C for conventional liquid chromatography and D for capillary liquid chromatography. The mobile phases were prepared as described previously [3]. In brief, the mobile phase was prepared by mixing well defined

TABLE I

CHROMATOGRAPHIC SYSTEMS INVESTIGATED

System	Column dimensions	Mobile phase[a]	Composition[b]	Model compounds
A	125 mm × 4.6 mm I.D.	ACN–H_2O–Gly–AcOH	10:(90 − x):x:1 ($x \leq 20$)	3,5-Dihydoxybenzoic acid, vanillic acid
B	125 mm × 4.6 mm I.D.	ACN–H_2O–Gly–TFA	30:(70 − x):x:0.1 ($x \leq 20$)	Met-enkephalin, bradykinin
C	125 mm × 4.6 mm I.D.	ACN–H_2O–Thio–TFA	30:(70 − x):x:0.5 ($x \leq 15$)	Met-enkephalin, leu-enkephalin
D	180 mm × 0.25 mm I.D.	ACN–H_2O–Gly–TFA	30:(70 − x):x:0.1 ($x \leq 10$)	Met-enkephalin, leu-enkephalin

[a] ACN = Acetonitrile; Gly = glycerol; Thio = thioglycerol; AcOH = acetic acid; TFA = trifluoroacetic acid.
[b] x = Proportion of matrix added to the mobile phase.

volumes of acetonitrile and organic acid and various volumes of water and viscous FAB matrices. The amount of water present was adjusted to complement the volume of liquid taking into account the proportions of added matrix (x in Table I). The composition of the mobile phases used in the experiments with conventional and capillary columns are given in Table I.

Chromatographic measurements

All chromatographic experiments are carried out at 25°C. Before the experiments conducted in the presence of a FAB matrix, each system was tested to evaluate its efficiency by injection of a standard solution of amylbenzene ($k' = 5$) eluted with acetonitrile–water (75:25, v/v). After the evaluation of the theoretical plate number, the mobile phase was changed and the system was allowed to equilibrate for at least 45 min. Measurements were made at average linear velocities around 1.5 mm/s. These conditions correspond to typical flow-rates of 0.8 ml/min for conventional columns and 2.5 μl/min for capillary columns. The retention of sodium nitrate was taken as a dead-time indicator (t_m) and the capacity factor (k') and the selectivity (α) were estimated from the retention of the solutes (t_r) in the usual way. The number of theoretical plates in the system (N) was calculated using peak widths at half-height ($W_{1/2}$) and the resolution (R_s) was calculated from the peak widths of the base (W_b).

RESULTS AND DISCUSSION

It is customary in LC–FAB-MS analysis to determine the optimum chromatographic conditions for separation prior to the inclusion of small proportions of viscous matrix in the mobile phase in order to optimize the sensitivity during the acquisition of mass spectral data. It is important, for this reason, to understand the effect that the presence of a matrix in the mobile phase will produce on the chromatographic separation so as to maintain the quality of separation. Fig. 1 shows the changes in resolution induced by the precolumn addition of glycerol or thioglycerol that occurred in the chromatographic systems used in this study. The addition of increasing amounts of matrix to the liquid vector induces a decrease in resolution under all chromatographic conditions used. It should be stressed that this addition has a deleterious effect on separation irrespective of the nature or concentration of the added matrix. As shown in Fig. 1A and B, this observation was confirmed in systems using both conventional and capillary columns. The de-

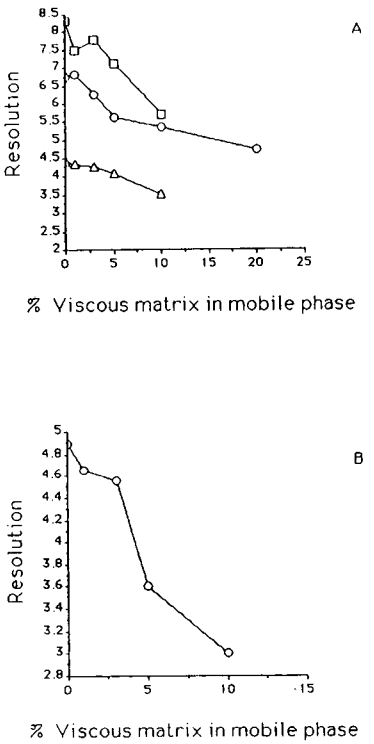

Fig. 1. Influences of FAB matrices on the resolution (R_s) achieved in (A) conventional and (B) capillary liquid chromatographic systems. ○ = System A; □ = system B; △ = system C; ○ = system D (see Table I).

crease in resolution caused by the presence of the matrix in the mobile phase can be minimized by using a low matrix content. However, for capillary columns the sharp decrease in resolution observed with matrix contents above 3% seems to indicate that capillary systems can be more sensitive than conventional systems to the presence of a matrix. It is therefore desirable to limit the addition of the matrix in the chromatographic system to a value that is less than 3% of the composition of the mobile phase.

The decrease in resolution previously demonstrated can originate from many sources. The widths of the chromatographic peak at the base (W_b) and the retention times (t_r) are the most important parameters in determining resolution, as shown in its operational definition given by the equation

$$R_s = \frac{2(t_{r_2} - t_{r_1})}{(W_{b_2} - W_{b_1})} \quad (1)$$

This important practical equation does not, however, give ample information on the physical or chemical processes involved in the separation. In order to obtain more insight into the physical and chemical processes that control the separation, a more descriptive equation has to be used, so as to reveal the true causes of the decrease in resolution that is observed under the present experimental conditions.

As the peak width depends on diffusional processes occurring in the column, the peak width expressed in terms of the number of theoretical plates (N) can be used as an indirect indicator of the physical processes taking place in the analytical system. On the other hand, the retention time can act as a probe for the chemical distribution of the analyte between the mobile and stationary phases. The capacity factor (k') and the selectivity coefficient (α), which are related to retention times, are suitable parameters that can be used in order to gain insight into the chemical equilibrium occurring in the chromatographic system. The three parameters N, k' and α can be combined to give the classical expression of resolution:

$$R_s = \frac{N^{1/2}}{4} \cdot \left(\frac{k'}{k'+1}\right) \cdot \left(\frac{\alpha - 1}{\alpha}\right) \quad (2)$$

The monitoring of the changes in N, k' and α induced by the presence of the matrix in the mobile phase can now be used in order to explore in more detail and to elucidate the specific effects altering the separation in the presence of glycerol or thioglycerol. This exploration may be instructive in providing a better understanding of the perturbation induced by the presence of the matrix in the chromatographic system. Further, it can also provide guidance in making better choices in selecting matrices and their concentrations in the mobile phase for LC–FAB-MS analysis.

In order to compare the relative importance of the contributions of parameters affecting resolution, it is desirable, in the present instance, to normalize all the data to a reference state. In this study, the 0% matrix content was chosen as the reference state as this state corresponds to the

usual conditions under which the method development will have been conducted. Normalization of all the diagnostic parameters was done by dividing the measurements acquired at a specific matrix content by the values obtained in the reference state. In this study, the normalized terms for the efficiency, the capacity factor and the selectivity contributing to the resolution will be designated by $\sqrt{N_x}/\sqrt{N_0}$, $f(k')_x/f(k')_0$ and $f(\alpha)_x/f(\alpha)_0$, respectively. This nomenclature will be used in presenting and discussing the data.

The effect of the addition of a FAB matrix in conventional liquid chromatography was initially studied for partition chromatography in system A using 3,5-dihydroxybenzoic acid and vanillic acid as model compounds eluted with ACN–H_2O–GLY–AcOH. Fig. 2 shows the variations in the normalized ratios with glycerol present in the mobile phase. The data in Fig. 2 indicate a decrease in the three normalized parameters as the content of glycerol is increased. However, the key factor that controls the observed decrease in resolution is the efficiency term, which decreases more than the other factors. For example, at a 20% glycerol content in the eluent the decreases in the normalized capacity factor and normalized selectivity terms are limited to less than 4% and 8%, respectively, of their initial values obtained in the absence of a matrix. These data indicate that the presence of a matrix in the eluent does not produce dramatic changes in the initial nature of the mobile phase, nor does it affect the mechanisms governing the separation and selectivity. In this system, the added glycerol replacing part of the water in the mobile phase seems to act in a very similar manner to water on the distribution of the analytes between the mobile and stationary phases. In contrast, the normalized efficiency term shows a decrease of 1% under the same boundary conditions. The large decrease in the normalized efficiency term for partition chromatography suggests that physical processes are more significantly affected than chemical processes occurring in the column.

The second chromatographic system was used to examine the effect of glycerol in ion-pair chromatography. In system B, met-enkephalin and bradykinin were chosen as reference compounds and were eluted with ACN–H_2O–GLY–TFA as the mobile phase. Fig. 3 shows the dependence of the three normalized parameters on the concentration of glycerol present in the mobile phase. It can be seen that the presence of glycerol influences the normalized efficiency, capacity factor and selectivity terms. The similar decreases observed in the ratios $\sqrt{N_x}/\sqrt{N_0}$, $f(k')_x/f(k')_0$ and $f(\alpha)_x/f(\alpha)_0$ with increasing content of matrix indicate that all parameters may contribute to the decrease in resolution, in contrast to the previous system studied, in which the efficiency term was the most active. The reduction in the normalized parameters, of the order of 10–20% at a 20% matrix content in the chromatographic eluent, suggests that ion-pair chromatography can be much more sensitive to the presence of the matrix than in partition chromatography. This also implies that in ion-

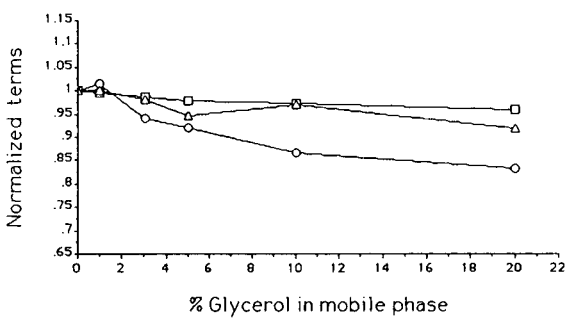

Fig. 2. Influence of glycerol on the normalized efficiency, capacity factor and selectivity terms in partition chromatography (system A). ○ = $\sqrt{N_x}/\sqrt{N_0}$; □ = $f(k')_x/f(k')_0$; △ = $f(\alpha)_x/f(\alpha)_0$.

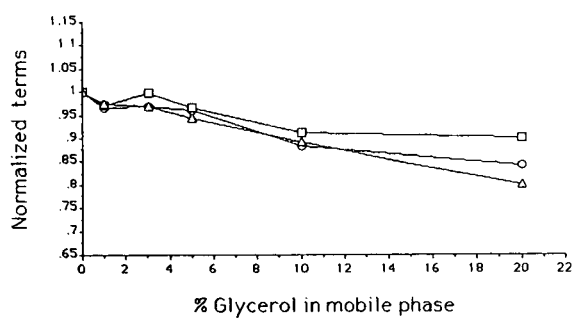

Fig. 3. Influence of glycerol on the normalized efficiency, capacity factor and selectivity terms in ion-pair chromatography (system B). ○ = $\sqrt{N_x}/\sqrt{N_0}$; □ = $f(k')_x/f(k')_0$; △ = $f(\alpha)_x/f(\alpha)_0$.

pair chromatography the presence of a matrix in the mobile phase will make the control of the chromatographic system more difficult since the physical and chemical processes in the system are altered.

In order to confirm the sensitivity of ion-pair systems to the presence of a matrix in the mobile phase, a second ion-pair chromatographic system consisting of leu-enkephalin and met-enkephalin in the presence of thioglycerol was studied. Fig. 4 shows, for system C, the changes induced in $\sqrt{N_x}/\sqrt{N_0}$, $f(k')_x/f(k')_0$ and $f(\alpha)_x/f(\alpha)_0$ with increasing content of thioglycerol in the mobile phase. The presence of thioglycerol produces a decrease in the $\sqrt{N_x}/\sqrt{N_0}$ term of the order of 10% at a 10% matrix content, as was similarly observed in systems A and B. This supports the idea that some common processes related to the parameter N are, in a systematic manner, affected in each system under study. The changes in the $f(k')_x/f(k')_0$, and $f(\alpha)_x/f(\alpha)_0$ terms, which are of the order of −30% and +15%, respectively, at a 15% matrix content in the mobile phase, confirm the sensitivity of ion-pair chromatography to the presence of a FAB matrix. The variations in $f(k')_x/f(k')_0$, and $f(\alpha)_x/f(\alpha)_0$ are different and more dramatic than previously observed in system B in the presence of glycerol. This shows that thioglycerol substantially perturbs the chemical distribution of the analyte in the chromatographic system in a fashion which is different to that of glycerol. In system C this results in an increase in selectivity in the presence of thioglycerol, contrary to the decrease in selectivity previously observed in the presence of glycerol in the other ion-pair system studied (system B).

In order to determine the influence of the presence of a FAB matrix on the results generated by packed capillary ion-pair liquid chromatography, the peptides met-enkephalin and leu-enkephalin were separated using ACN–H_2O–GLY–TFA as the mobile phase in which the glycerol content was increased to a maximum of 10% of the composition. The capillary column was flushed with 4 ml of HPLC-grade water, 2 ml of 0.1% TFA in water, 2 ml of 2-propanol, 2 ml of acetonitrile and 2 ml of HPLC-grade water prior to allowing the mobile phase ACN–H_2O–GLY–TFA to percolate through the column. Fig. 5 shows the changes observed in the $\sqrt{N_x}/\sqrt{N_0}$, $f(k')_x/f(k')_0$ and $f(\alpha)_x/f(\alpha)_0$ terms with the percentage of glycerol added to the mobile phase in capillary system D. In this system the normalized efficiency ratio $\sqrt{N_x}/\sqrt{N_0}$ shows a net decrease of the order of 22% at a 10% matrix content and the ratios $f(k')_x/f(k')_0$ and $f(\alpha)_x/f(\alpha)_0$ show a decrease of the order of 15%. The decrease observed in the two latter parameters in the capillary system is significantly higher than those measured in conventional systems A or B in the presence of glycerol. However, the decrease in all three parameters measured in system D are very similar to those observed in system B. It should be mentioned that using capillary systems it has been observed that the lifetime and usage of the column can affect the results obtained for the normalized

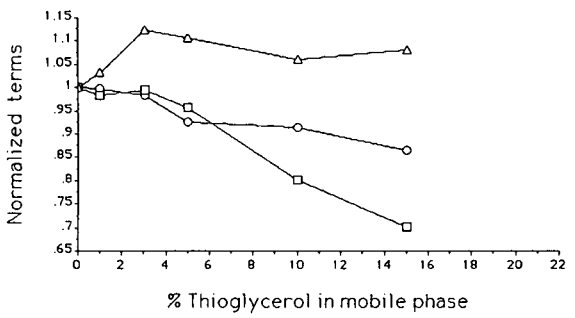

Fig. 4. Influence of thioglycerol on the normalized efficiency, capacity factor and selectivity terms in ion-pair chromatography (system C). ○ = $\sqrt{N_x}/\sqrt{N_0}$; □ = $f(k')_x/f(k')_0$; △ = $f(\alpha)_x/f(\alpha)_0$.

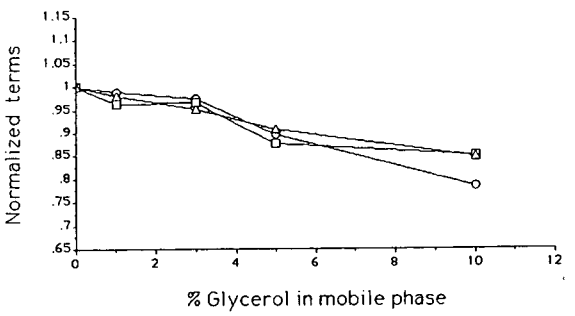

Fig. 5. Influence of glycerol on the normalized efficiency, capacity factor and selectivity terms in ion-pair chromatography (system D). ○ = $\sqrt{N_x}/\sqrt{N_0}$; □ = $f(k')_x/f(k')_0$; △ = $f(\alpha)_x/f(\alpha)_0$.

selectivity ratio. This parameter seems to be subject with time and number of analyses to irreversible adsorption of some compounds, which modifies the trends observed in the selectivity factor.

It therefore appears from monitoring of the chromatographic resolution for three pairs of analytes in three mobile phases containing different concentrations of FAB matrix that it steadily decreases with increasing matrix content in the mobile phase. The decrease in resolution is observed in the presence of glycerol or thioglycerol at both low and high matrix concentrations in conventional or capillary columns. This phenomenon is observed in partition and ion-pair systems and can be rationalized by analyzing the subtle processes that are related to each of the normalized ratios.

The degradation of the quality of the separation as measured by means of the normalized efficiency term $(\sqrt{N_x}/\sqrt{N_0})$ contributing to the resolution shows that the efficiencies of conventional and capillary systems are both decreased in the presence of a FAB matrix. The extent of the decrease seems to be independent of the nature of the FAB matrix, of the acid added to the mobile phase and of the initial proportions of ACN and H_2O present in the mobile phase. However, in capillary systems the decrease in efficiency is higher than that observed in conventional systems. There are four basic processes that control band broadening, which determines the efficiency in chromatographic systems: axial molecular diffusion, flow dispersion in a packed bed, mass transfer in the column and extra-column band broadening. In our experiments with conventional columns, the extra-column broadening was made negligible by using small connecting tubes and small injector and detector volumes. Also, the importance of longitudinal diffusion was maintained low by using average linear velocities of the order of 1.5 mm/s. As a result of choosing such experimental conditions, the efficiency of the conventional systems used should be under mass transfer control. In this instance, as shown in a previous study [4,5], the mass transfer process in the presence of a FAB matrix is governed by the extent of the change in the viscosity of the mobile phase, which is similar for all matrices studied. An increase in viscosity causes a lower diffusivity of the analyte [4], which results in a decrease in efficiency, as has been observed. In the capillary liquid chromatographic system used, an increase in viscosity also reduces the efficiency. However, as the capillary systems are very sensitive to dispersive effects in dead volumes [7–10], it is probable that extra-column broadening occurs in our capillary systems owing to the connexions between the column and injector and the column and detector, and this will decrease the efficiency in the capillary systems as measured by the ratio $\sqrt{N_x}/\sqrt{N_0}$ given in Fig. 5. From the break in the resolution curves of system D (Fig. 1B), it seems that dead volume effects become important when more than 3% of glycerol is present in the mobile phase. Decreases in resolution that may originate from changes in capacity factors and selectivity can also be rationalized. Considering the chromatographic systems studied, only system A, based on partition chromatography, seems to be controlled mainly by changes in the efficiency term. For the other systems, based on ion-pair chromatography, chemical alteration of the distribution of the analytes between the mobile and stationary phases appears to play an important role in the decrease in resolution.

The capacity factors and selectivity, which characterize the interactions responsible for retention, are dependent on the nature of the analytes, the nature of the stationary phase and the composition of the mobile phase. The variations observed in $f(k')_x/f(k')_0$ and $f(\alpha)_x/f(\alpha)_0$ as an increasing amount of viscous matrix is added to the mobile phase clearly indicate that the interactions between participants in the chromatographic equilibrium are changed. In the case of the $f(k')_x/f(k')_0$ term the steady decrease observed in the four systems monitored in the presence of increasing amounts of FAB matrix indicates that the analyte distribution is shifted towards the mobile phase in both the partition (system A) and the ion-pair (system B to D) chromatographic modes. The rationale for this observation is that glycerol and thioglycerol behave as organic moderators which increase the eluotropic force of the mobile phase, thus favoring the elution of the analytes. The data ob-

tained in the conventional systems indicate that thioglycerol is more efficient than glycerol in that role as a larger decrease in the $f(k')_x/f(k')_0$ term occurs in its presence.

The previous decrease observed in the $f(k')_x/f(k')_0$ term can also find a rational explanation on the basis of the molecular interactions occurring in the system. In the systems studied, the interactions between the analytes and the ODS moities are mainly dispersive and inductive, as the alkyl chain bonded to silica has a weak dipole moment [11]. Hence the addition of a polar matrix such as glycerol or thioglycerol should not significantly affect the dispersive interactions responsible for the retention of the analyte. In the present instance, the addition of a substance such as glycerol that has a lower dielectric constant than water ($\varepsilon_{glycerol} = 42.5$ and $\varepsilon_{water} = 78.5$ [12]) should lower the overall dielectric constant of the mobile phase [13–15]. As there is an inverse relationship between intermolecular interactions and the dielectric constant, the interactions between the solute and the mobile phase become stronger, which results in a decrease in analyte retention. This is clearly supported by the measured decrease in the normalized capacity factor term that occurs in all systems. However, it is noteworthy that each system (A, B and D) exhibits a different rate of decrease which reflects that role of the composition of the mobile phase and its interaction with the stationary phase in the perturbation caused by addition of glycerol.

The presence of a matrix in the mobile phase also affects the nature and the composition of the stationary phase. It is well known that bonded stationary phases adsorb constituents such as water, acetonitrile or alcohols from the mobile phase [16–20]. This adsorption would vary in accordance with the eluotropic strength of the eluent. Hence the addition of glycerol or thioglycerol should then favor the intrusion of these molecules in the stationary phase. It is to be expected that, because the matrices are efficient organic moderators, they will compete with water and, to an extent, with acetonitrile for adsorption. Therefore, any modification in the stationary zone that is participating in the separation can result in subtle and sometimes unpredicable changes in retention and selectivity, as has been observed in this work. However, some important changes in selectivity observed in the analysis of peptides appear to be related to the role and the presence of TFA in the mobile phase. This acid, which is added to mobile phases, has three distinct functions [21–25]: it promotes the protonation of peptides by affecting the pH, it is involved in ion pairing as the counter ion and it minimizes the interactions of the cationic residues in the molecule with the support by decreasing the ionization of the nonderivatized silanol groups. The addition of a FAB matrix to the ion-pair chromatographic systems will affect the distribution and mode of action of TFA. The presence of a polyhydroxylated matrix such as glycerol or thioglycerol can shield the silanol groups, making them less accessible to TFA. Further, the decrease in the dielectric constant of the mobile phase in the presence of a matrix should increase electrostatic interactions in the mobile phase, thus favoring ion pairing and affecting capacity factors and ultimately the selectivity of the system. In ion-pair systems, it was observed that the normalized selectivity term decreased in the presence of glycerol whereas it increased in the presence of thioglycerol. The increase in the normalized selectivity term in the presence of thioglycerol may be related to a differential competition for common sites. Both thioglycerol and met-enkephalin contain sulfur groups which are likely to interact in a similar way. Thus, as the matrix becomes more concentrated in the mobile phase it can saturate the retention sites and decrease the retention of met-enkephalin, which results in a decrease in the capacity factor. As leu-enkephalin is not affected to the same extent by this phenomenon because it does not contain sulfur, the net result is an increase in selectivity. Caution should be used, however, in attributing this effect strictly to thioglycerol, as this FAB matrix was only 95% pure in its commonly used form. It is possible, as stated previously, that impurities in the thioglycerol which was continuously percolated through the system were adsorbed irreversibly by the stationary phase and that this factor can also be involved in the changes observed.

CONCLUSIONS

It was demonstrated that a decrease in chromatographic resolution occurs in the presence of glycerol or thioglycerol in the mobile phase for peptides and phenolic compounds separated in both conventional and capillary chromatographic systems. The monitoring of the efficiency, the capacity factor and the selectivity terms contributing to chromatographic resolution permitted the identification of the decrease in capacity factors and in efficiency as constant sources causing the decrease in resolution in the presence of a FAB matrix. In the systems studied it was observed that selectivity can be affected in different ways and that changes in selectivity can increase or limit the decrease in resolution in the presence of a FAB matrix. The efficiency parameter were observed to exhibit similar changes in all systems studied and they were independent of the nature of the analyte and the matrix, whereas the variations observed in the capacity factor and selectivity term appear to be intimately related to the mode of chromatography and the nature of the analyte and of the matrix used. Impurities in the mobile phase may be involved in some of the changes in selectivity observed.

ACKNOWLEDGEMENTS

The authors acknowledge the financial support of the Natural Sciences and Engineering Council of Canada (NSERC) and of Hydro-Québec, which permitted this study.

REFERENCES

1 S. Naylor, A.F. Findies, B.W. Gibson and D.H. Williams, *J. Am. Chem. Soc.*, 108 (1986) 6359.
2 R.M. Caprioli, in R.M. Caproli (Editor), *Continuous Flow Fast Atom Bombardment Mass Spectrometry*, Wiley, Chichester, 1990, Ch. 1.
3 J.P. Gagné, A. Carrier and M.J. Bertrand, *J. Chromatogr.*, 554 (1991) 61.
4 J.P. Gagné, A. Carrier and M.J. Bertrand, *J. Chromatogr.*, 554 (1991) 47.
5 A. Carries, J.P. Gagné and M.J. Bertrand, *J. Chromatogr.*, 591 (1991) 129.
6 S. Pleasance, P. Thibault, M.A. Moseley, L.J. Deterding, K.B. Tomer and J.W. Jorgenson, *J. Am. Soc. Mass Spectrom.*, 1 (1990) 312.
7 J.C. Sternberg, *Ad. Chromatogr.*, 2 (1966) 205.
8 G. Guiochon and H. Colin, in P. Kucera (Editor), *Microcolumn High-Performance Liquid Chromatography*, Elsevier, Amsterdam, 1984, pp. 1–38.
9 M. Novotny, in P. Kucera (Editor), *Microcolumn High-Performance Liquid Chromatography*, Elsevier, Amsterdam, 1984, pp. 194–259.
10 M. Verzele, C.D. Dewaele and M. De Weerdt, *LC · GC*, 6 (1988) 966.
11 R. Kaliszan, in P.R. Brown and R.A. Hartwick (Editors), *High-Performance Liquid Chromatography*, Wiley, New York, 1988, pp. 563–599.
12 R.C. Weast (Editor), *CRC Handbook of Chemistry and Physics*, CRC Press, Cleveland, OH, 57th ed., 1976–77, pp. E55–E60.
13 R.M. Caprioli, *Anal. Chem.*, 55 (1983) 2387.
14 W.R. Melander and Cs. Horváth, in Cs. Horváth (Editor), *High-Performance Liquid Chromatography, Advances and Perspectives*, Vol. 2, Academic Press, New York, 1980, pp. 165–170.
15 A. Le Berre, *Analusis*, 18 (1990) 51.
16 P. Jandera, H. Colin and G. Guiochon, *Anal. Chem.*, 54 (1982) 435.
17 R.P.W. Scott and P. Kucera, *J. Chromatogr.*, 142 (1977) 213.
18 R.M. McCormick and B.L. Karger, *J. Chromatogr.*, 142 (1977) 213.
19 E.H. Slaats, W. Marskovski, F. Fekete and H. Poppe, *J. Chromatogr.*, 207 (1981) 299.
20 K.G. Wahlund and I. Beijersten, *Anal. Chem.*, 54 (1982) 128.
21 G. Gonnet and G. Gonot, *Analusis*, 18 (1990) 381.
22 R.L. Potter and R.V. Lewis, in Cs. Horváth (Editor), *High-Performance Liquid Chromatography*, Vol. 4, Academic Press, Orlando, 1980, pp. 1–44.
23 K.D. Nugent, W.G. Burton, T.K. Slattery, B.F. Johnson and L.R. Snyder, *J. Chromatogr.*, 443 (1988) 381.
24 X. Geng and F.E. Regnier, *J. Chromatogr.*, 296 (1984) 15.
25 S. Linde and B.S. Welinder, *J. Chromatogr.*, 536 (1991) 43.

Journal of Chromatography, 647 (1993) 31–38
Elsevier Science Publishers B.V., Amsterdam

CHROMSYMP. 2788

Deuterium oxide as a reagent for the modification of mass spectra in electrospray microcolumn liquid chromatography–mass spectrometry

K.-E. Karlsson

Department of Analytical Chemistry, Pharmaceutical Research and Development, Astra Hässle AB, S-431 83 Mölndal (Sweden)

ABSTRACT

Microcolumn liquid chromatography was used in combination with a quadrupole mass spectrometer equipped with an electrospray ionization interface. Deuterium oxide was used as a reagent to induce peak shifts in mass spectra. The peak shift obtained gives the number of heteroatoms carrying hydrogen atoms that are present in a molecule. Examples relating to amino alcohols, peptides and sugars are given. Two different modes of operation were investigated; postcolumn addition of the reagent to the eluent from the column and the use of deuterium oxide as a mobile phase component. The latter technique makes use of a dynamic exchange reaction on-column. Exchanged hydrogen atoms are carried away from the migrating zone (as H^2HO or H_2O) containing the target compound, leading to a high yield of the deuterated compound. On-column exchange was found to be more useful, especially if the compounds contained several exchangeable hydrogen atoms. No significant changes were observed with regard to chromatographic selectivity or efficiency.

INTRODUCTION

Recent developments in instrumentation for mass spectrometry, particularly the introduction of the electrospray interface (ESI), have had an enormous impact in the field of bioanalytical separations. Several review papers have already been published, dealing with both fundamentals and applications [1–4]. In parallel, liquid chromatography (LC) using packed fused silica columns has been developed into a powerful separation technique offering high separation efficiency and the capability to deal with small amounts of sample [5,6]. Another attractive feature of microcolumn LC is the low volumetric flow-rate of the mobile phase, of the order of 1 μl/min. This makes it possible to use fairly expensive or for other reasons uncommonly used mobile phases. High-resolution LC can now be combined with a powerful detector without compromises to either LC or the mass spectrometer, at least with respect to liquid flow-rates. Consequently, several papers have been published [7–9] describing the combination of slurry-packed capillary columns and a mass spectrometer using the ESI. High separation efficiency and high sensitivity were demonstrated.

Many of the new types of interface for LC–MS, especially the ESI, produce in the positive-ion mode only the protonated molecular ion with no or very few structurally significant fragment ions. Additional information can be obtained by using tandem mass spectrometry (MS–MS). Unfortunately, the resulting daughter ion spectrum is often difficult to interpret without a comparison with some structurally related compounds. An additional disadvantage with this technique is that more of the sample is usually needed. Other methods that have been used to induce fragmentation include thermally induced

0021-9673/93/$06.00

dissociation [10] and the technique of accelerating the ions in the intermediate pressure region between the nozzle and the skimmer [8].

Derivatization of the target molecule has been used successfully in GC–MS for many years but also to some extent in LC–MS [11,12]. In an LC–MS system, it is sometimes beneficial to modify the properties of the mobile phase. Halogenated mobile phase additives improved the sensitivity in the negative ion mode [13,14] and recently sodium acetate was used in a thermospray source to help detect oligosaccharides [15]. A postcolumn modification of the mobile phase is commonly used in ESI. The sheath liquid introduction [8,16] of an organic solvent is aimed at changing the bulk properties of the mobile phase such as reducing the surface tension, changing the pH [17] or adjusting the total flow-rate into the interface as in capillary zone electrophoresis (CZE) [3,17].

Deuterium oxide has been used as a reagent for determining the number of exchangeable hydrogen atoms in organic molecules using various analytical techniques including NMR [18] and mass spectrometry [19]. More recently, exchange reactions were investigated using thermospray [20,21], electrospray [22] and fast atom bombardment (FAB) [23].

The aim of this work was to evaluate the use of deuterium oxide as a mobile phase constituent in an *on-column* exchange reaction and to compare the results obtained with those of continuous postcolumn addition.

EXPERIMENTAL

Chemicals

LC-grade acetonitrile was obtained from Rathburn (Walkerburn, UK) and used as received. Water was purified using a Milli-Q system (Millipore). Deuterium oxide (99.8% isotopic purity) was purchased from Dr. Glaser (Basle, Switzerland) and angiotensin I and II (human, synthetic) from Sigma (St. Louis, MO, USA). Other compounds studied were obtained in-house.

Sheath liquid and postcolumn addition of deuterium oxide

Deuterium oxide as a mixture [acetonitrile–deuterium oxide (50:50)] was delivered at various flow-rates by a low-pressure syringe pump (Harvard Apparatus, South Natic, MA, USA) and mixed with the sample stream using either of the two configurations, A and B, as shown in Fig. 1. The sample [1×10^{-5} *M* in acetonitrile–water (50:50)] was infused continuously through a short column (200 mm × 250 μm I.D., creating a slight back-pressure) using a Carlo Erba (Milan, Italy) Phoenix 20 CU pump and a Model 7010 500-μl loop injector (Rheodyne, Berkeley, CA, USA) at a flow-rate of 1 μl/min. Ion intensities were determined in the profile mode and averaged for 1 min.

The correction for the heavy isotope effect was made by measuring the natural isotopic ratio for the $[M+1]^+$ (C-12) and $[M+2]^+$ (C-13) ions before using deuterium oxide. In cases where two hydrogen atoms were exchanged also the $[M+3]^+$ (S-34) ion had to be measured. The area ratios determined will be constant in experiments with deuterium oxide also. In the presence of deuterium oxide, using the area of the remaining (original) M + 1 ion and the determined ratios, the shifted peak area can be corrected.

Microcolumn liquid chromatography

Isocratic elution was applied throughout using a Phoenix 20 CU pump operated in the constant-pressure mode. The injector was a Valco (Houston, TX, USA) CI4W (200 nl), which was used in the time split mode to introduce about 100 nl of the sample. A second injector (Rheodyne Model 7010), equipped with a 500-μl loop, was placed between the pump and the sample injector. This injector served as the mobile phase reservoir in experiments with deuterium oxide. Columns of 200–250 μm I.D. were prepared

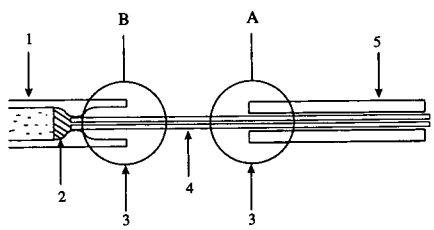

Fig. 1. (A) Sheath liquid and (B) postcolumn addition of deuterium oxide. 1 = chromatographic column; 2 = porous Teflon; 3 = Swagelock tee; 4 = fused-silica tubing; 5 = stainless-steel capillary.

from empty fused-silica tubes (Polymicro Technologies, Phoenix, AZ, USA) as described previously [24]. The packing material was 5-μm Kromasil C_8 (EKA Nobel, Surte, Sweden), held in place by a 0.2-mm long section of glass-wool ("frit") as described previously [25]. The column was connected to the electrospray needle using a 300 mm × 50 μm I.D. × 150 μm O.D. empty fused-silica tube.

Electrospray mass spectrometry

Experiments were carried out on a Finnigan TSQ 700 triple quadrupole mass spectrometer equipped with an electrospray interface (Analytica of Branford, Branford, CT, USA). All spectra were obtained using unit mass resolution. The electrospray needle was made in house using a 150 mm × 160 μm I.D. stainless-steel capillary. The fused-silica capillary from the column ended about 0.5 mm outside the needle.

RESULTS AND DISCUSSION

Addition of deuterium oxide

Two different modes of introduction of deuterium oxide were used; sheath liquid introduction (Fig. 1A) and what will be referred to as postcolumn introduction (Fig. 1B). In the latter configuration, some extra time is provided for mixing in the capillary tube. If the target molecules contain exchangeable hydrogen atoms, a fraction of the molecules will be converted into the deuterated form. The extent of this exchange will be determined by the equilibrium constants and the kinetics of the reaction. When the two liquid streams meet, a complex mixture will be formed, consisting of acetonitrile, water, deuterium oxide and H^2HO in addition to several charged species due to autoprotolysis. In the absence of a strict mathematical model for proton transfer in the electrospray process, a simple equation based on relative rates of formation for the competing ions was used:

$$\frac{I_{A^2H^+}}{I_{AH^+}} = K \cdot \frac{F^2_{H_2O}}{F_{H_2O}} \quad (1)$$

where $I_{A^2H^+}$ and I_{AH^+} represent the ion intensities for the deuterated and the corresponding protonated analyte (corrected for the heavy isotope effect) and $F^2_{H_2O}$ and F_{H_2O} are the flow-rates of the solution of deuterium oxide and water, respectively. For molecules containing exchangeable hydrogen atoms, the exchange reaction is assumed to reach an equilibrium before charging takes place, *i.e.*, in the transfer capillary. A plot based on eqn. 1 is shown in Fig. 2, for four different compounds (Fig. 3). If there is no difference between water and deuterium

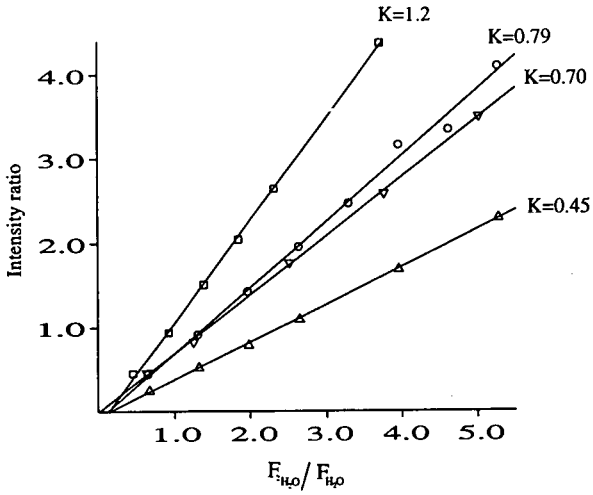

Fig. 2. Evaluation of relative formation rate constants. □ = N-methylhomatropine; ○ = N-methylomeprazole; ▽ = scopolamine; △ = omeprazole. D = deuterium.

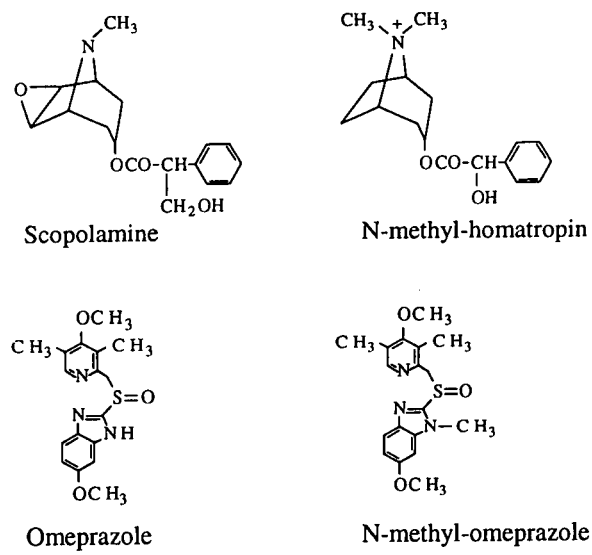

Fig. 3. Compounds studied in postcolumn experiments.

oxide systems with respect to the charging process, one would expect from statistical considerations that $K \approx 1$ for molecules that accept either a deuteron or a proton. The highest conversion efficiency ($K = 1.2$) was obtained for a permanently charged quaternary ammonium ion (N-methylhomatropine), where only one proton was exchanged. The large positive deviation ($K > 1$) seen for this compound could be due to several factors. Many species in the solution like such as $^2H_2HO^+$ and $^2HH_2O^+$ might favour the deuteron in the charging process. An additional complication is that back-exchange reactions can occur in the gas phase by ion–molecule reactions. The overall result could therefore be different for different types of molecules. This could possibly explain why the corresponding constant for N-methylomeprazole ($K = 0.8$) was found to be slightly less than unity. In such a case, one has to assume that a deuterium atom bound in a hydroxyl group (N-methylhomatropine) is bonded more strongly than an adduct deuteron ($M + D^+$) formed in the spray process and therefore less sensitive to a back-exchange reaction.

For compounds that can accept two deuterium atoms (omeprazole, scopolamine), one would expect a K value of about 0.5. This seems to be the case for omeprazole ($K = 0.45$). To summarize, the K values are higher than expected for N-methylhomatropine and scopolamine and slightly less than expected for the other two compounds.

In experiments using the liquid sheath method (Fig. 1A), linear relationships were also observed but the slopes of the lines (K) were about 10–15% lower, possibly indicating less efficient mixing of the two liquid streams.

The relative recovery (comparing only the intensities measured) of the fully deuterated compounds can be calculated using a rearranged form of eqn. 1 and will be about 83% for N-

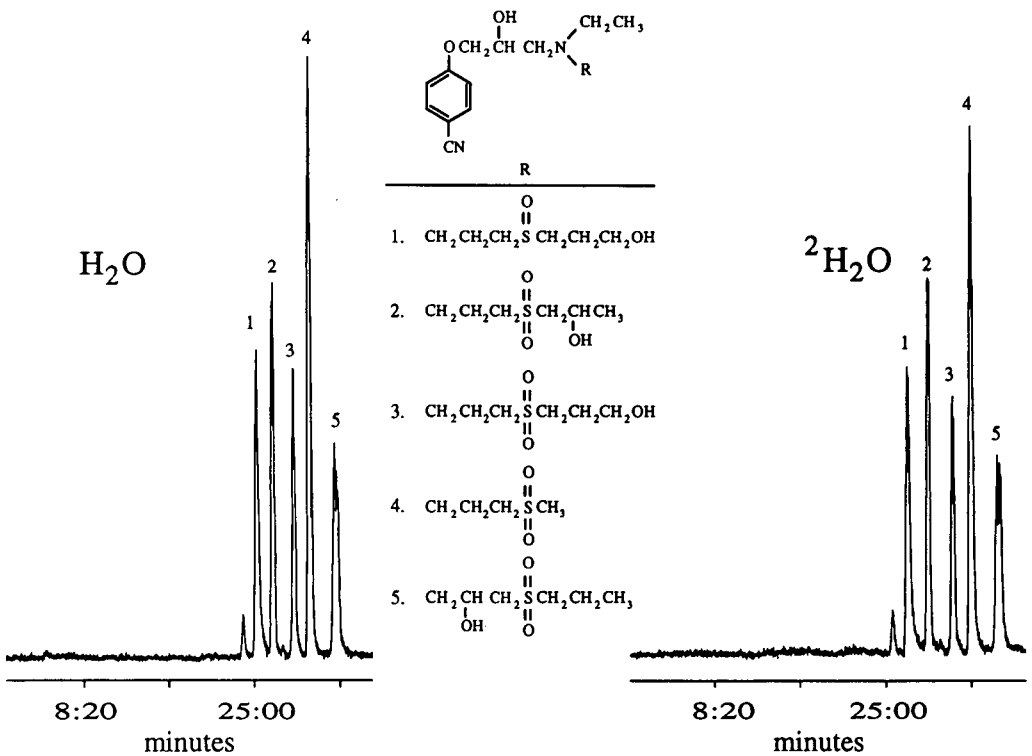

Fig. 4. Microcolumn separation using (left) water or (right) deuterium oxide in the mobile phase. Reconstructed total ion current trace using a scan range from 200 to 400 u at 0.7 s per scan. The amount injected ranged from 20 to 30 pmol. The column was 900 mm × 200 μm I.D., packed with 5-μm Kromasil C_8. The mobile phase was acetonitrile–5 mM ammonium acetate in water or deuterium oxide (55:45). Flow-rate, 0.95 μl/min.

methylhomatropine but only 64% for omeprazole using the constants given in Fig. 2 at a flow ratio of 4. A higher efficiency for the conversion will be necessary when the number of exchangeable hydrogen atoms increases, otherwise an envelope of ions will result. A possibility is to increase the percentage of deuterium oxide added postcolumn. A disadvantage with this approach is that the sensitivity will decrease with increasing deuterium oxide content owing to increasing surface tension. Another possibility is to decrease the flow of water by drastically reducing the column flow-rate via a reduction of the column diameter or a change to CZE or open-tubular LC.

Deuterium oxide as a mobile phase component

Although the techniques described above are fairly easy to use, difficulties arise when several exchangeable hydrogen atoms are present in the analyte. A postcolumn addition of deuterium oxide can be regarded as a batchwise operation where there always will be some water present to decrease the yield of the fully deuterated analyte. A change from a static system (fixed concentration ratio of ^2H_2O to H_2O) to a dynamic system can be done by using a chromatographic column and replacing mobile phase deuterium oxide with water. Hydrogen atoms will be exchanged and the equilibrium below forced to the right as water will migrate faster ($k' \approx 0$) on the column than a zone containing the sample ($k' > 0$):

$$RH_n + 0.5n^2H_2O \rightleftharpoons R^2H_n + 0.5nH_2O$$

In a chromatographic system there will be adequate mixing and enough time available to give a high recovery of the fully deuterated compound. Sources of protons that will decrease the recovery are to be found in the organic modifier, deuterium oxide and various buffer components.

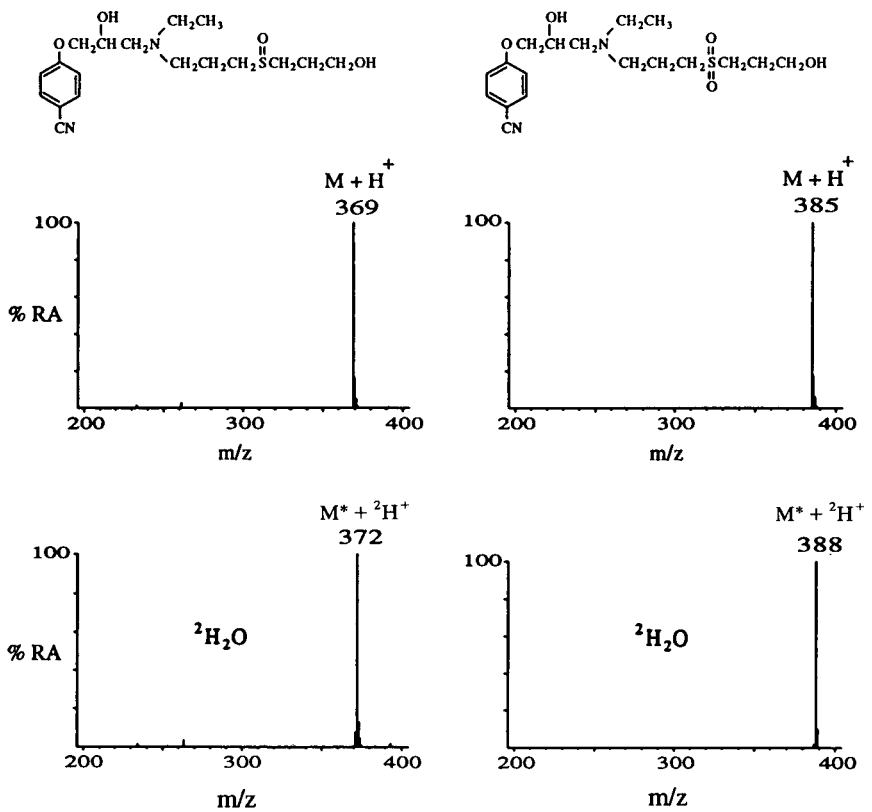

Fig. 5. Mass spectra obtained using (top) water or (bottom) deuterium oxide in the mobile phase.

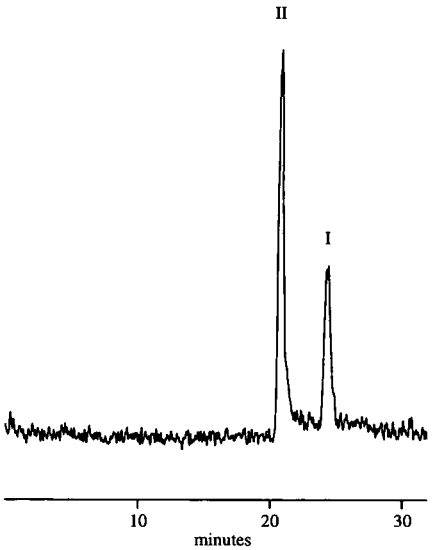

Fig. 6. Microcolumn separation of angiotensin I and II. Column, 900 mm × 0.25 mm I.D., packed with 5-μm Kromasil C_8; mobile phase, acetonitrile–5 m*M* ammonium acetate solution in deuterium oxide (40:60) at a flow-rate of 1.1 μl/min. Total ion current trace obtained by scanning from 500 to 1320 u in 2 s.

Fig. 4 shows a separation of some amino alcohols using acetonitrile–water (50:50) (left) and acetonitrile–deuterium oxide (50:50) (right) as mobile phases. A retention time a few minutes longer is observed using deuterium oxide instead of water in the mobile phase. This can probably be explained by the higher viscosity (*ca.* 20%) for deuterium oxide. No change was observed that relates to selectivity or efficiency. The latter could be degraded if there is a slow hydrogen–deuterium exchange resulting in a mixture of compounds with varying degrees of substitution. Molecules containing deuterium instead of hydrogen are differently retained [26].

Fig. 5 shows a comparison of some ESI mass spectra obtained in water and deuterium oxide systems, respectively. These compounds are metabolites of a drug ($[M + H]^+ = 353$) that lacks a hydroxyl group in the carbon chain attached to the sulphur atom (Fig. 5, top left). The peak shift of 3 u for the compound in the top left corner reveals that two exchangeable hydrogen atoms are present; the third one is responsible for the charge ($[M + {}^2H]^+$). As the molecular mass is increased by 16 u (*m/z* 353→369), a hydroxylated metabolite could be expected. Another metabolic pathway for the parent drug is oxidation of the sulphur atom to the corresponding sulphone, again an increase of 16 u. This could be easily ruled out as the peak shift would then be only 2 u. The top right spectrum corner shows that the molecular mass

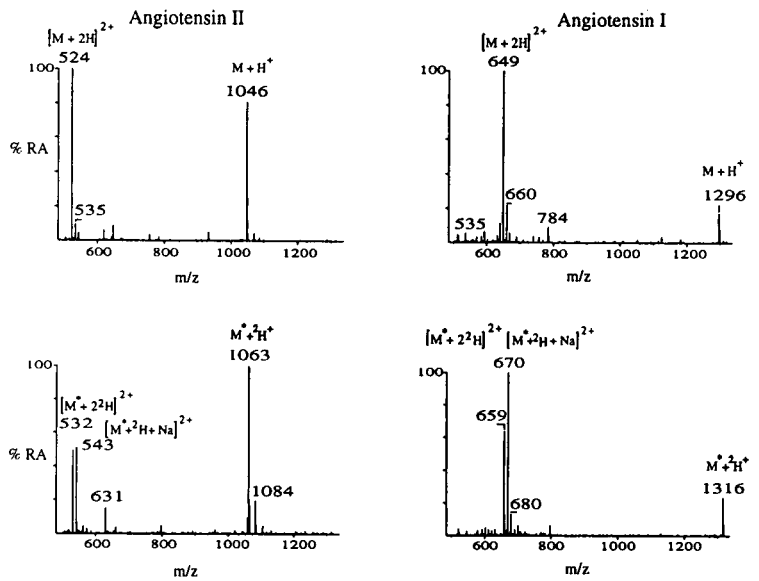

Fig. 7. Mass spectra of angiotensins I and II obtained using (top) water and (bottom) deuterium oxide in the mobile phase.

for this metabolite has increased by 32 u. The peak shift was only 3 u, which suggests that only one hydroxyl group has been formed, and the other oxygen atom should therefore be bound to sulphur.

An area that has attracted considerable interest in the last few years is peptide mapping using mass spectrometry [7,27,28]. The molecular masses of the peptides, formed by tryptic digest of a protein, are determined using either FAB or ESI methods. Sequence information on the individual peptides can be obtained in MS–MS experiments [7]. However, when only small amounts of material are available, the latter technique may not give a definite answer. Additional information can be obtained without using a higher sample load by modifying the mobile phase using deuterium oxide. Fig. 6 shows an isocratic separation of a synthetic mixture of angiotensin I (15 pmol) and II (18 pmol) using acetonitrile–5 m*M* ammonium acetate solution in ^2H_2O (40:60). The mass spectra obtained before and after changing the mobile phase are shown in Fig. 7. The small amount of ammonium acetate used as buffer obviously did not cause any problem in locating the molecular ion. Both peptides show the protonated molecular ion at *m/z* 1046 and 1296 together with the doubly charged ions ($[M + 2H]^{2+}$) at *m/z* 524 and 649, respectively. In the deuterium oxide system, the molecular ions have shifted to *m/z* 1063 and 1316, respectively. The peak shift obtained for angiotensin II is 17 u and that for angiotensin I is 20 u. These values correspond exactly to the number of exchangeable hydrogen atoms in both molecules, including the proton responsible for the charge. Knowing the exact number of heteroatoms carrying a proton in an unknown peptide will make it easier to determine which amino acid residues are present. An interesting detail here is that in the ^2H_2O system, other doubly charged molecular ions appear, carrying both a deuteron and a sodium ion. The relative intensities of these ions are consistently larger than those of the corresponding ions in the water system.

Additional information that can be obtained that will be of value concerns the presence of impurities, *e.g.*, compounds that are not peptides, especially in the very complex mixture obtained after an enzymatic digestion. For an unknown compound to be a peptide, the mass shift must be at least 5 u for a dipeptide; three hydrogen atoms from the N- and C-termini and one from the peptide bond in addition to the proton carrying the charge.

The peak shift technique was also used to help identify an unknown degradation compound found in a pharmaceutical formulation. The tablets contained hydralazine, metoprolol and hydrochlorothiazide. The mass spectra obtained with and without deuterium oxide are shown in Fig. 8. The protonated molecular ion (*m/z* 485) suggests a molecular mass much larger than that

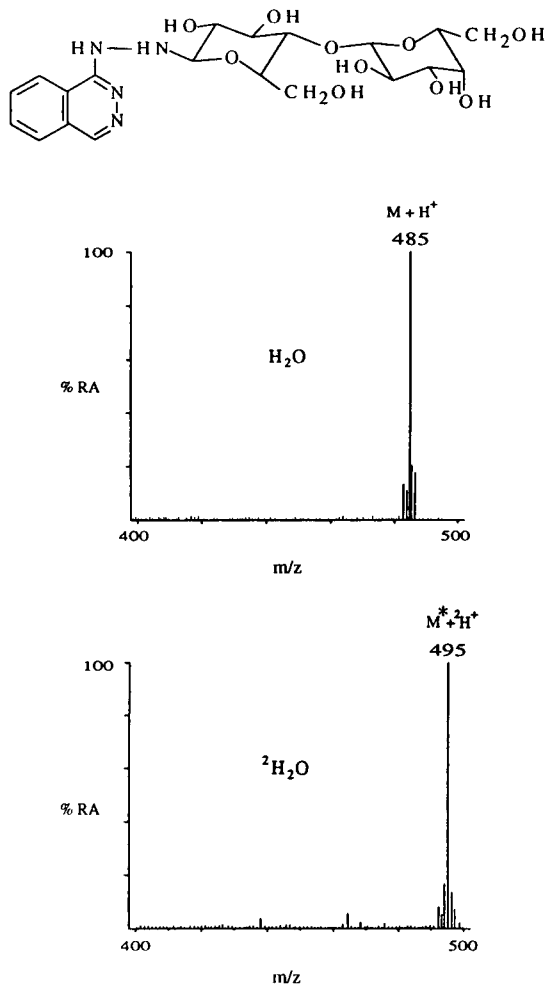

Fig. 8. Mass spectra obtained for an "unknown" degradation compound. Column and mobile phase as in Fig. 6.

of any of the active ingredients. The large peak shift of 10 u focused attention on lactose, an "inactive" ingredient in the tablets. The structure given in Fig. 8 was finally verified using NMR spectroscopy. It can be seen that all the hydrogen atoms on the sugar moiety and also on the nitrogen atoms have been exchanged.

REFERENCES

1 J.B. Fenn, M. Mann, C.K. Meng and S.F. Wong, *Mass Spectrom. Rev.*, 9 (1990) 37.
2 E.C. Huang, T. Wachs, J.J. Conboy and J.D. Henion, *Anal. Chem.*, 62 (1990) 713A.
3 R.D. Smith, J.A. Loo, R.R. Ogorzalek, M. Busman and H.R. Udseth, *Mass Spectrom. Rev.*, 5 (1991) 359.
4 A.P. Bruins, *Mass Spectrom. Rev.*, 10 (1991) 53.
5 M. Novotny and D. Ishii (Editors), *Microcolumn Separations (Journal of Chromatography Library*, Vol. 30), Elsevier, Amsterdam, 1985.
6 F.J. Yang (Editor), *Microbore Column Chromatography (Chromatographic Science Series*, Vol. 45), Marcel Dekker, New York, Basle, 1988.
7 M. Hail, S. Lewis, I. Jardine, J. Liu and M. Novotny, *J. Microcol. Sep.*, 2 (1990) 285.
8 J.R. Perkins, C.E. Parker and K.B. Tomer, *J. Am. Soc. Mass Spectrom.*, 3 (1992) 139; and references cited therein.
9 E.C. Huang and J.D. Henion, *Anal. Chem.*, 63 (1991) 732.
10 A.L. Rockwood, M. Busman, H.R. Udseth and R.D. Smith, *Rapid Commun. Mass Spectrom.*, 5 (1991) 582.
11 D.E. Games and E.D. Ramsey, *J. Chromatogr.*, 323 (1985) 67.
12 J. van der Greef, W.M.A. Niessen and U.R. Tjaden, *J. Chromatogr.*, 474 (1989) 5.
13 R.B. Geerdink, F.A. Maris, G.J. de Jong, R.W. Frei and U.A.Th. Brinkman, *J. Chromatogr.*, 394 (1987) 51.
14 Y. Kato and Y. Numajiri, *J. Chromatogr.*, 562 (1991) 81.
15 W.M.A. Niessen, R.A.M. van der Hoeven, J. van der Greef, H.A. Schols and A.G.J. Voragen, *Rapid Commun. Mass Spectrom.*, 6 (1992) 197.
16 L.W. Hershberger, J.B. Callis and G.D. Christian, *Anal. Chem.*, 51 (1979) 1444.
17 R.D. Smith, C.J. Barinaga and H.R. Udseth, *Anal. Chem.*, 60 (1988) 194.
18 F.M. Hughson, P.E. Wright and R.L. Baldwin, *Science*, 249 (1990) 1544.
19 M.V. Buchanan, *Anal. Chem.*, 54 (1982) 570.
20 M.M. Siegel, *Anal. Chem.*, 60 (1988) 2090.
21 C.G. Edmonds, S.C. Pomerantz, F.F. Hsu and J. McCloskey, *Anal. Chem.*, 60 (1988) 2314.
22 V. Katta and B.T. Chait, *Rapid Commun. Mass Spectrom.*, 5 (1991) 214.
23 A. Guarini, G. Guglielmetti and N. Andriollo, *Anal. Chem.*, 64 (1992) 204.
24 K.-E. Karlsson and M. Novotny, *Anal. Chem.*, 60 (1988) 1662.
25 K.-E. Karlsson, *J. Microcol. Sep.*, 3 (1991) 449.
26 Y. Hirata and K. Jinno, in M. Novotny and D. Ishii (Editors), *Microcolumn Separations (Journal of Chromatography Library*, Vol. 30), Elsevier, Amsterdam, 1985, p. 50.
27 D.S. Jones, W. Heerma, P.D. van Wassenaar and J. Haverkamp, *Rapid Commun. Mass Spectrom.*, 5 (1991) 192.
28 D.J. Bell, M.D. Brightwell, M. Haran, W.A. Neville and A. West, *Org. Mass Spectrom.*, 26 (1991) 454.

Journal of Chromatography, 647 (1993) 39–50
Elsevier Science Publishers B.V., Amsterdam

CHROMSYMP. 2860

Radiofrequency-only daughter scan mode to provide more spectral information in liquid chromatography–thermospray tandem mass spectrometry

Paul G.M. Kienhuis

RIZA, P.O. Box 17, 8200 AA Lelystad (Netherlands)

ABSTRACT

A method is presented for increasing the number of specific ions in LC–thermospray mass spectra by means of a quadrupole tandem mass spectrometer (Finnigan TSQ-70) in the radiofrequency-only daughter (RFD) scan mode. The method can be used for screening a large number of compounds eluted from an HPLC system. MS–MS in the usual daughter, parent or neutral loss scan mode (on retention time altered for each eluted compound) in this particular instance is very laborious or even impossible. In the RFD scan mode the first quadrupole is operating as a high-pass mass filter. Only ions with masses equal to or above the arbitrary selected cut-off mass will enter the collision cell. With a low collision offset voltage mainly molecular ions will be present in the third quadrupole, which is acting as a mass analyser in the full-scan mode. With medium and high collision offset voltages, daughter ions are generated in the collision cell. By using two or three different alternating collision offset voltages during one analysis, both molecular and daughter ions can be acquired, increasing the specificity of the mass spectrum. First, data on optimization of the low collision offset voltage and the collision gas (argon) pressure with a mixture of alachlor, atrazine, aldicarb and barban are presented. Next, spectral information and data about the sensitivity of twenty compounds (alachlor, aldicarb, aniline, atrazine, benzothiazole, carbendazim, chloridazon, diazinon, dimethoate, diuron, ethylenethiourea, isocarbamide, isoproturon, metamitron, metolachlor, monolinuron, propachlor, sethoxydim, simazine and warfarin) in the RFD scan mode at three collision offset voltages (−6, −20 and −40 V) are presented and compared with the single-stage Q3MS scan mode. The sensitivity proved to be the same or better at collision offset voltages of −6 and −20 V, partly because adducts and eluent clusters were decreased significantly or even disappeared. At a collision offset of −40 V the sensitivity decreased for many compounds and the more intense ions mainly had low m/z values, which are less specific. The RFD scan mode, using a −6 and −20 V collision offset voltage alternating in each scan, is demonstrated by screening a surface water sample (river Rhine) spiked with ten compounds at a level of 1 μg/l. It resulted in chromatograms with increased spectral information, the same or better signal-to-noise ratios, less eluent clusters and no adducts.

INTRODUCTION

Thermospray is one of the most popular techniques for interfacing HPLC with mass spectrometry. However, compared with GC–MS systems with electron impact ionization there is, in addition to the lower separation power of the HPLC system, a great lack of specific ions. For most compounds only one or two specific ions are generated, mainly with molecular mass information, unless extreme repeller or vaporizer settings are used and a far lower sensitivity is accepted [1,2].

For the unambiguous identification of an analyte by gas chromatography–low resolution mass spectrometry, the European Community recommends that at least four diagnostic ions (including the molecular ion, if possible) should be measured and that the relative abundances of all diagnostic ions should match those of the standard analyte [3]. The US Environmental Protection Agency (EPA) demands at least five

0021-9673/93/$06.00

ions for confirmation [4]. These requirements are based on the statistical occurence of mass and abundance values in mass spectra [5] and are much higher than thermospray can give for many compounds.

The abundant generation of eluent clusters, mainly in the lower mass range, is another disadvantage of the thermospray ion source. They decrease the sensitivity of ions with the same m/z ratio or make it even impossible to analyse such masses [2].

Thermospray MS–MS with parent, daughter and neutral loss scan modes can overcome these problems in many instances. These methods generate additional specific ions, which makes it possible to indentify compounds unambiguously. Thermospray MS–MS, in combination with HPLC separation or with flow-injection analysis (FIA), is now widely accepted [6–9].

In surface water, however, an enormous number of compounds are present. Nearly 40% of the organic compounds in the river Rhine are polar low-molecular-mass substances [7]. Several HPLC methods with UV or MS detection have been reported for the screening of aqueous environmental samples in the presence of 30–80 compounds in one analysis [2,10–12].

MS–MS with parent, daughter or neutral loss scans selected and programmed on retention time, however, is possible with only a limited number of target compounds. A "general" daughter scan mode, selecting each mass in a window of, *e.g.*, m/z 100–500 as parent mass followed by a full range daughter scan of 0.5 s, needs more than 3 min for one complete cycle and is therefore not compatible with HPLC.

To overcome this restriction, the radiofrequency (RF)-only daughter (RFD) scan mode of a triple quadrupole mass spectrometer (Fig. 1) has been investigated [13].

The first quadrupole (Q1) acts as a high-pass mass filter with an arbitrary selected cut-off mass, the second quadrupole (Q2) as a collision cell with a target gas (argon) admitted to the cell and the third quadrupole (Q3) as mass analyser to scan the ions in the full-scan mode. Every ion generated in the thermospray ion source and equal to or above the cut-off mass is allowed to enter the collision cell without the need to select parents for each compound. It can be seen as a

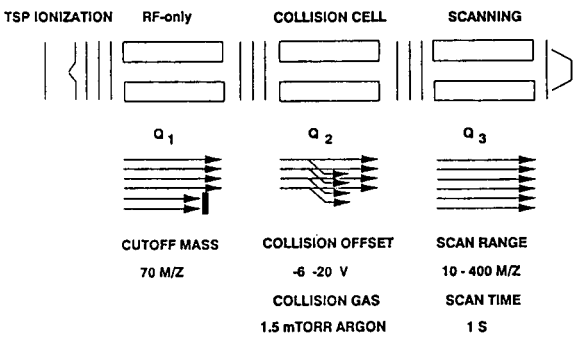

Fig. 1. Triple quadrupole mass spectrometer in the RFD scan mode.

mass spectrometer with separated ionization and fragmentation chambers, compared with electron impact where both actions take place in the ion source.

In the RFD scan mode the collision offset (COFF) voltage can be changed every scan. The chromatographic peak width in LC is generally 20–40 s. Hence, during peak elution, two or three different COFF voltages at a scan time of 0.5–1 s can be applied, to acquire 7–40 scans at each voltage for every peak.

The cut-off mass can be used to retard at least part of the eluent clusters entering the collision cell. For the experiments m/z 70 is selected to reject the clusters ions of m/z 59 and 60, allowing the lowest molecular ion of the tested compounds (aniline, M_r 93.06) to enter the collision cell.

In the thermospray ion source mainly ions are formed with intact molecules, *e.g.* $[M+H]^+$, revealing the molecular mass of a compound [2,9]. It is very important to maintain this information, but this aim is contrary to the admittance of a collision gas to the collision cell, necessary for the generation of daughter ions. It is not possible to change the argon pressure in a short time, just as the COFF voltage is changed every scan. Therefore, an argon pressure will be needed, low enough to allow the ions to pass at a low COFF voltage and high enough to generate daughter ions with higher COFF voltages.

First, by altering the COFF voltage and collision gas pressure in the RFD scan mode, the intensities of the molecular ions were optimized at a low COFF voltage range. Second, twenty compounds were tested in the RFD scan mode at the selected and at higher COFF voltages to

establish whether extra ions are generated at the optimized argon pressure without losing the molecular ions.

EXPERIMENTAL

Chemicals

All test compounds were obtained from Riedel-de Haën (Hannover, Germany). Ammonium formate (analytical-reagent grade) was obtained from Sigma (St. Louis, MO, USA), dichloromethane (analytical-reagent grade) from Merck (Darmstadt, Germany), acetonitrile (HPLC grade) from Promochem (Wesel, Germany) and ammonium acetate (analytical-reagent grade), ascorbic acid (analytical-reagent grade), methanol (HPLC grade), HCl (37%) and trifluoroacetic acid (TFA) (>99%) from J.T. Baker (Deventer, Netherlands). Water was purified in a Milli-Q system (Millipore, Bedford, MA, USA) before use.

MS

A Finnigan TSQ-70 mass spectrometer in combination with a TSP-2 thermospray interface (Finnigan Mat, San Jose, CA, USA) equiped with a liquid nitrogen solvent trap was used, with argon (quality 5.0; Hoek Loos, Schiedam, Netherlands) as collision gas. The MS–MS correction factor was set to zero while using the RFD scan mode.

Because a large number of compounds were used in the experiments, a general optimization of the repeller voltage was used each day, based on the intensity of the eluent clusters around m/z 100 [1]. Although in all experiments buffer ionization was applied, an additional discharge voltage was used. From earlier experiments some of the compounds proved to have a better signal-to-noise ratio with buffer ionization in combination with a relative low discharge voltage, without losing the sensitivity for the other compounds.

The vaporizer temperature and source block temperature were kept at 100 and 200°C, respectively, during all experiments except tuning. Tuning was performed on TFA clusters produced by methanol–water–TFA (15:84.5:0.5, v/v/v) containing 0.1 *M* ammonium acetate [14] delivered at a flow-rate of 1.5 ml/min. Tuning clusters were m/z 18.0, 78.0, 149.05, 280.07, 542.11 and 804.15 in the positive mode and m/z 31.0, 69.0, 113.0, 227.0, 341.0, 472.1 and 603.2 in the negative mode. The exhaust valve was heated with an heating ribbon to 70°C during the tuning procedure to prevent condensation of ammonium trifluoroacetate in the valve. Tuning the TSQ-70 with a thermospray ion source takes several days for all quadrupoles and lenses in all modes and is only performed after each cleaning of the quadrupoles. The system proved to be very stable for months [15].

FIA–MS

An LKB (Bromma, Sweden) Model 2150 pump was used to deliver the solvent at a flow-rate of 1.5 ml/min. An ASPEC system (Gilson, Villiers Le Bel, France) with a 500-μl loop was used to inject the samples. Each injection was followed by an injection of acetonitrile–water (50:50, v/v) to clean the loop, lines and vaporizer.

HPLC–MS

The HPLC system was connected on-line with an UV detector and the mass spectrometer in series. The LC system consists of a Rheodyne, (Cotati, CA, USA) Model 7125 injection valve (100-μl loop) and a Milton Roy (Riviera Beach, FL, USA) Model CM4000 gradient pump. Separation was carried out on a silica-based C_{18} column (3 mm I.D., 5-μm particles) (Chrompack, Bergen op Zoom, Netherlands) at a flow-rate of 0.6 ml/min and a gradient from 100% A to 100% B in 60 min [A = 0.1 *M* ammonium acetate (or formate)–acetonitrile (95:5, v/v), B = acetonitrile]. After UV detection at 235 nm (Milton Roy Spectromonitor 3100), the eluent was mixed with a postcolumn flow of 1.2 ml/min (LKB Model 2150) 0.1 *M* ammonium acetate (or formate) to increase the flow-rate to the vaporizer and to reduce the concentration of the organic modifier.

Sample concentration

The procedure of Di Corcia and Marchetti [11] was used to concentrate surface water samples (river Rhine). Samples of 500 ml were spiked with ten compounds at 1 μg/l and forced by vacuum to pass through ENVI-Carb SPE car-

tridges (6 ml, filled with 250 mg of Carbopack B, 40–100 μm particles) (Supelco, Bellafonte, PA, USA) within 1 h. Each cartridge was conditioned with 5 ml of dichloromethane–methanol (80:20, v/v) followed by 2 ml of methanol and 15 ml of 10 g/l ascorbic acid in HCl-acidified water (pH 2).

After loading with sample, the cartridge was washed with 7 ml of water and dried for several minutes by drawing room air through it. Desorption was performed with 1 ml of methanol followed by 6 ml of dichloromethane–methanol (80:20, v/v). The extract was evaporated with a stream of nitrogen to reduce the volume to 100 μl. Methanol–water (50:50, v/v) was added to adjust the total volume to 500 μl.

RESULTS AND DISCUSSION

Optimization of lower COFF voltage and collision gas pressure

A mixture of alachlor, atrazine, aldicarb and barban (500 ng/ml each) in 0.1 *M* ammonium acetate in water–acetonitrile (90:10, v/v) was analysed by FIA at different collision gas pressures of argon in the range 0.5–3.5 mTorr (1 Torr = 133.322 Pa). The collision offset voltage was continuously changed (from −2 to −10 V in 2-V steps) from scan to scan. The cut-off mass was *m/z* 70, the daughter scan range was *m/z* 10–500 in 0.5 s, the repeller voltage was 160 V and the discharge voltage was 500 V.

The results revealed that each compound has its own optimum, which depends on the presence of adduct ions at a COFF of −2 V (aldicarb, alachlor and barban) and/or the presence of fragments or daughter ions at the whole COFF range of −2 to −10 V, but especially at values of −8 and −10 V. High intensities of $[M + H]^+$ ions were obtained in the COFF voltage range −4 to −6 V for most compounds. Both COFF voltages are shown in Fig. 2A and B, with the intensity of the $[M + H]^+$ ions plotted against the collision gas pressure. The optimum pressure is between 1

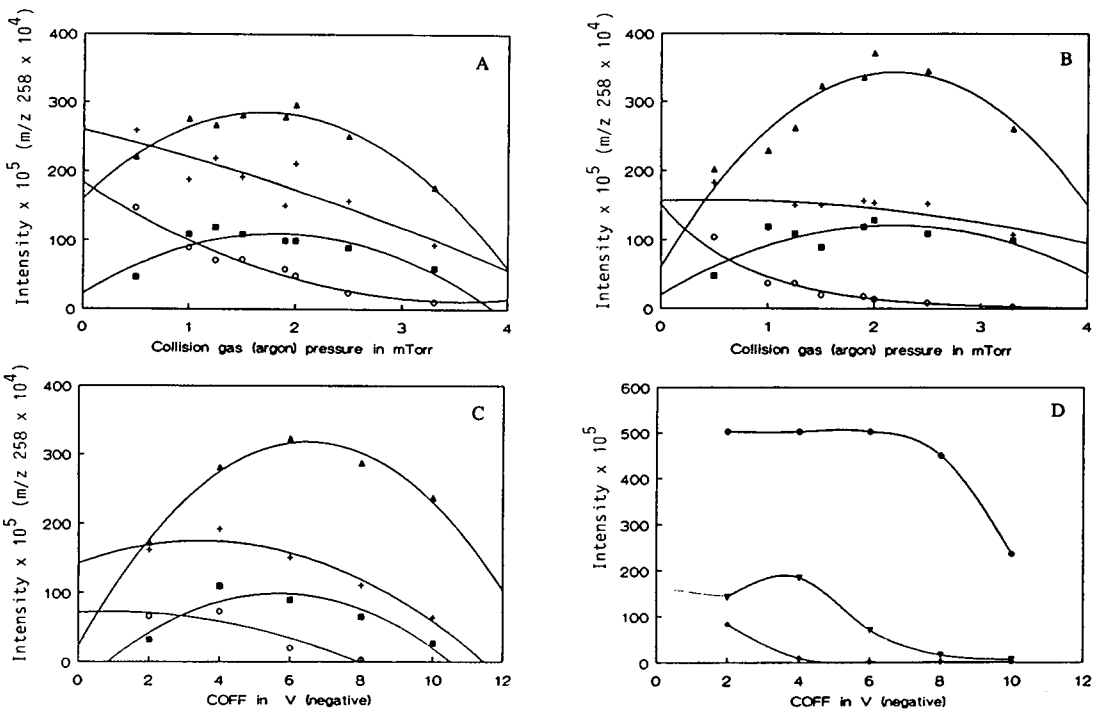

Fig. 2. Optimization of the lower COFF voltage and the collision gas (argon) pressure. Based on the intensities of the molecular ions $[M + H]^+$ of (+) alachlor (*m/z* 270), (▲) atrazine (*m/z* 218; *m/z* 216 was overloaded), (○) aldicarb (*m/z* 191), (■) barban (*m/z* 258), and eluent clusters (●) *m/z* 59 saturated between −2 to −6 V, (▼) *m/z* 77 and (◆) *m/z* 100, analysed by FIA–RFD. (A) COFF, −4 V; (B) COFF, −6 V; (C) argon, 1.5 mTorr; (D) argon, 1.5 mTorr.

and 2 mTorr at both COFF voltages and therefore 1.5 mTorr of argon was selected for further experiments.

In Fig. 2C the influence of the COFF voltage on the intensity of the $[M+H]^+$ ions is plotted at an argon pressure of 1.5 mTorr and shows an optimum at about −4 to −6 V. In Fig. 2D the intensity of some major eluent clusters (note that m/z 59 is below the cut-off mass and therefore a daughter ion) are plotted against the COFF voltage at a collision gas pressure of 1.5 mTorr. The intensity of these unwanted ions are decreased strongly from −4 to −10 V. From the combined information in Fig. 2C and D a COFF of −6 V was selected and used in further experiments.

Higher COFF voltages

Additional specific ions can be obtained at higher COFF voltages. Therefore, the RFD scan mode was evaluated with three COFF voltages (−6, −20 and −40 V), alternately changed each scan at a collision gas pressure of 1.5 mTorr of argon. For twenty compounds, listed in Table I, flow-injection analyses were performed in the single stage scan mode (Q3MS; scan range m/z 65–500; scan time 0.5 s; electron multiplier voltage 1500 V) and in the RFD scan mode (scan range 10-500 m/z; scan time 0.5 s; cut-off mass m/z 70; electron multiplier voltage 1500 V) with thermospray ionization at a repeller voltage of 160 V and a discharge voltage of 500 V. The sample solution and FIA eluent was 0.1 *M* ammonium acetate in water–acetonitrile (90:10, v/v). Compounds were separately injected at a concentration of 450 ng/ml.

At a COFF of-6 V in the RFD scan mode the intensities of the base peaks are comparable to those in the Q3MS scan mode (Table I). In MS–MS scan modes in which the first quadrupole is used as a mass filter, the transmission is about 10% relative to a first quadrupole operating in the RF-only mode [13]. However, in both the RFD and Q3MS scan modes the first quadrupole is in the RF-only mode, so the transmission should be equal and a difference in intensity is mainly evoked by the situation in the collision cell. The spectral information regarding the molecular mass is slightly less in the RFD scan mode, because for none of the compounds were adduct ions acquired. The aim to maintain the molecular $[M+H]^+$ ions is achieved for all analytes, unless they were not present in the single-stage Q3MS scan mode (sethoxydim). The decreased noise level in the RFD scan mode with a COFF of −6 V resulted for many compounds in a better signal-to-noise ratio and lower detection limit.

At a COFF of −20 V the optimized argon pressure of 1.5 mTorr proved to be high enough to generate additional ions for most of the compounds (in Table II the remaining ions besides the base peaks are listed). However, the detection limits shown in Table I are also important. Compared with the Q3MS scan mode, the intensities at a COFF of −20 V are lower (note: values from 10^6 to 10^5), but due to a lower noise level the detection limits are about the same. Compared with −6 V, the detection limit at −20 V is higher. This is mainly caused by the decrease in intensity of the base peak due to the increased fragmentation, rather than by an increased noise level. Hence the generated spectra give more specific information without sacrificing much sensitivity.

At a COFF of −40 V increased fragmentation results in mainly high detection limits and low m/z values. These m/z values are less suitable for diagnostic purposes, *i.e.*, they are less unique. Therefore, the COFF of −40 V was not used in the remaining experiments. If it is nessecary to acquire these masses, *e.g.*, for structural elucidation, it will be better to use the more common MS–MS scan modes. The relationship between a parent ion and low m/z daughter ions is better defined in those modes.

HPLC–MS

The HPLC–RFD method was tested at a collision gas pressure of 1.5 mTorr of argon and with COFF voltages of −6 and −20 V alternating each scan. A cut-off mass of m/z 70 was used. Ammonium acetate and ammonium formate were used separately in the HPLC and post-column eluent. The scan range was m/z 33–400 for the Q3MS mode and m/z 10–400 for the RFD mode. For both modes the scan time was 1

TABLE I

INTENSITY OF BASE PEAKS AND NOISE WITH FIA ANALYSES IN Q3MS AND RFD SCAN MODES

DL = Detection limit (signal-to-noise ratio = 5) in ng calculated on the base peak. Peak width is 20–30 s, comparable to HPLC–MS.

Compound	M_r	Q3 MS				RFD, COFF −6V				RFD, COFF −20V				RFD, COFF −40V			
		Base peak		Noise intensity ($\times 10^4$)	DL (ng)	Base peak		Noise intensity ($\times 10^4$)	DL (ng)	Base peak		Noise intensity ($\times 10^3$)	DL (ng)	Base peak		Noise intensity ($\times 10^3$)	DL (ng)
		m/z	($\times 10^6$)			m/z	($\times 10^6$)			m/z	($\times 10^5$)			m/z	($\times 10^5$)		
Alachlor	269.12	270	2	1.6	2.3	238	2.2	0.35	0.4	162	7	3	1.2	147	2.4	1.4	1.6
Aldicarb	190.08	208	1.3	0.64	1.4	116	1.6	0.9	1.6	89	5	7	3.9	89[a]	0.75	2	7.5
Aniline	93.06	135	0.1	0.7	20	94	0.2	0.25	3.5	94	0.6	2	9.4	51	0.18	2	31
Atrazine	215.09	216	4.7	0.5	0.3	216	4	0.28	0.2	174	7	2	0.8	68	2.4	3	3.5
Benzothiazole	135.01	136	0.5	3	17	136	0.56	0.24	1.2	136	2.3	3	3.7	65	0.4	10	70
Carbendazim	191.07	192	3.2	0.5	0.4	192	2.4	0.5	0.6	160	9.5	2.5	0.7	160	0.9	1	3.2
Chloridazon	221.04	222	4	1	0.7	222	2.7	0.5	0.5	222	6.5	2.5	1.1	77	3	30	28
Diazinon	304.10	305[a]	3.2	2.5	2.2	305	2.6	2	2.2	153	7.5	5	1.9	97	2.4	10	12
Dimethoate	229.00	230	11	1	0.3	230	7.5	1.5	0.6	125	16	9	1.6	125[a]	3.2	4	3.5
Diuron	232.02	233[a]	1	1	2.8	233	0.73	0.9	3.5	46	6.4	5	2.2	72	1.6	5	8.8
Ethylenethiourea	102.02	103	13	3	0.6	103	9.4	2	0.6	103[a]	9	10	3.1	103[a]	1	8	23
Isocarbamide	185.12	186	15	6	1.1	186	13	5	1.1	87	40	10	0.7	87[a]	5	4	2.3
Isoproturon	206.14	179	6.7	3	1.3	179	6	2	0.9	137[a]	7	13	5.2	72[a]	1.7	6	10
Metamitron	202.09	203	13	10	2.2	203	9	3	0.9	203	4	15	10	104[a]	1.1	5	13
Metolachlor	283.13	284	16	3	0.5	284	10	2	0.6	252	43	5	0.3	133	4	6	4.2
Monolinuron	214.05	215	4	1.4	1.0	215	3.2	0.9	0.8	126	7	4	1.6	127[a]	1	2	5.6
Propachlor	211.05	212	9	2	0.6	212	10	1	0.3	170	24	4	0.5	94[a]	8	3	1.1
Sethoxydim	327.19	282	15	3	0.6	282	12	1	0.2	178	13	3	0.6	107	4	7	4.9
Simazine	201.08	202	13	4	0.9	202	11	2.5	0.6	132[a]	10	3	0.8	68	8	5	1.8
Warfarin	308.11	309	6	3	1.4	309	3.5	1.5	1.2	251	8	5	1.8	163[a]	0.7	3	12

[a] No base peak, but more specific and/or lower DL.

TABLE II

REMAINING IONS HIGHER THAN 10% OF THE BASE PEAK (% OF THE BASE PEAK)

Compound	M_r	m/z (relative intensity, %)		
		Q3 MS	RFD, COFF −6V	RFD, COFF −20V
Alachlor	269.12	226 (12); 238 (37); 240 (12); 271 (14); 272 (31); 287 (25)[a]	226 (14); 239 (14); 240 (30); 270 (45); 272 (16)	90(13); 238 (50); 240 (19)
Aldicarb	190.08	116 (13); 191(80)	191 (13)	41 (16); 70 (22); 116 (16)
Aniline	93.06	94 (13)	–	–
Atrazine	215.09	218 (33)	218 (33)	96 (25); 132 (12); 146 (11); 176 (33); 216 (40); 218 (12)
Benzothiazole	135.01	177 (28)[a]	–	–
Carbendazim	191.07	134 (14); 193 (10)	134 (20); 193 (10)	134 (17)
Chloridazon	221.04	224 (33)	224 (33)	92 (12); 104 (20); 224 (33);
Diazinon	304.10	153 (110); 306 (13)	153 (113); 306 (13)	84 (19); 93 (21); 97 (15); 125 (16); 169 (70); 249 (17)
Dimethoate	229.00	–	199 (40)	88 (31); 171 (35); 199 (17)
Diuron	232.02	87 (212)[a]; 205 (36); 207 (24); 222 (23); 224 (12); 235 (61); 250 (12)[a]	46 (123); 205 (57); 207 (38); 235 (67)	72 (42)
Ethylenethiourea	102.02	–	–	44 (177); 86 (19)
Isocarbamide	185.12	–	–	–
Isoproturon	206.14	87 (33)[a]; 196 (12); 207 (41)	46 (15); 207 (37)	46 (117); 72 (69); 94 (87); 120 (12); 179 (20)
Metamitron	202.09	204 (11)	204 (11)	31 (21); 77 (37); 79 (19); 104 (95); 106 (16); 145 (17); 174 (47); 175 (76)
Metolachlor	283.13	285 (17); 286 (33)	252 (35); 254 (11); 285 (17); 286 (33)	176 (43); 253 (16); 254 (33)
Monolinuron	214.05	171 (16); 217 (33); 232 (35)[a]; 234 (11)[a]	171 (21); 217 (33)	62 (23), 93 (11); 128 (33); 148 (66)
Propachlor	211.05	213 (12); 214 (33); 229 (22)[a]	213 (12); 214 (33)	94 (40); 106 (24); 172 (32);
Sethoxydim	327.19	283 (18)	283 (18)	107 (91); 108 (20); 150 (15); 151 (12); 176 (82); 220 (45); 282 (47)
Simazine	201.08	204 (33)	204 (33)	68 (29); 71 (44); 96 (87); 104 (48); 106 (16); 124 (110); 134 (33); 174 (13); 202 (61); 204 (20)
Warfarin	308.11	310 (20)	310 (20)	45 (24); 147 (21); 163 (97); 252 (15)

[a] Adductions.

s, electron multiplier voltage 1500 V, repeller voltage 100 V and discharge voltage 500 V.

A Q3MS and an RFD analysis of a concentrated (on Carbopack B) Rhine water sample spiked at 1 μg/l are shown in Fig. 3. The RFD chromatogram (Fig. 3B) looks "strange" owing to the different noise and ion intensity levels at a COFF voltage of −6 and −20 V and is difficult to interpret both manually as automatically. Therefore, the scans were copied alternately to different files (Fig. 3C and D). The retention time was copied together with each scan, so the resulting chromatograms can be compared (same compound, different spectra) and interpreted as usual.

In Fig. 4 background spectra from chromatograms of a standard mixture (ten compounds, listed in Fig. 3, in methanol–water (50:50, v/v) at a concentration of 1 μg/ml) are shown. In the Q3MS scan mode it is difficult to analyse below m/z 143 because of the eluent clusters generated with both ammonium acetate and ammonium formate as ionization buffers. In the RFD scan mode with a cut-off mass of m/z 70 this value is decreased to m/z 78 (COFF −6 V) and m/z 62 (COFF −20V). Remaining ions such as those of m/z 227 and 243 in the formate spectra are probaly due to the chemical background.

Fig. 5 shows the spectra of dimethoate and metolachlor in a spiked Rhine water sample after

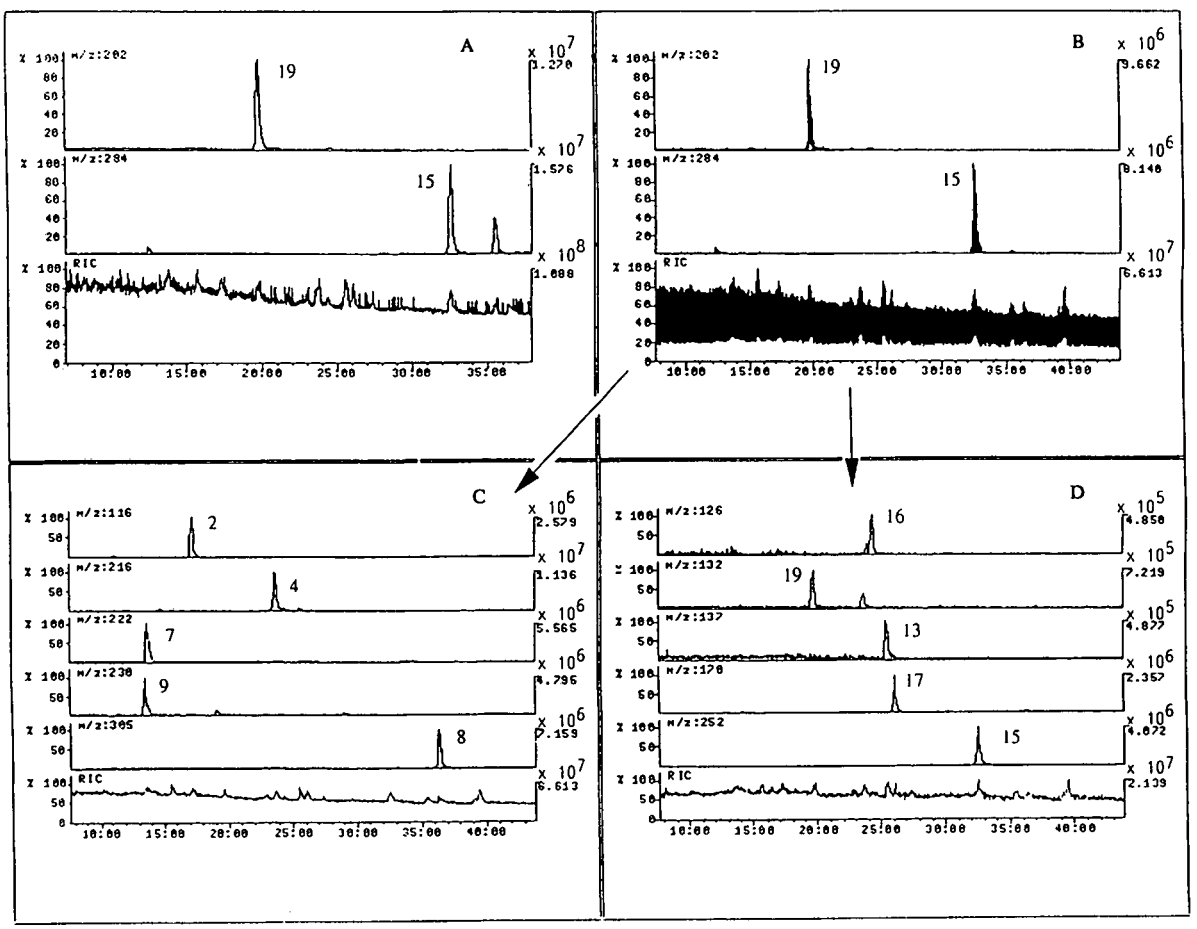

Fig. 3. Chromatograms of Rhine water spiked with ten compounds at 1 μg/l. Injected amount after concentration, *ca.* 100 ng. Ionization buffer with ammonium formate. (A) Q3MS; (B) RFD with COFF of −6 and −20 V alternately; (C) RFD with COFF of −6 V, copied from (B); (D) RFD with COFF of −20 V, copied from (B). Peaks: 2 = aldicarb; 4 = atrazine; 7 = chloridazon; 8 = diazinon; 9 = dimethoate; 13 = isoproturon; 15 = metolachlor; 16 = monolinuron; 17 = propachlor; 19 = simazine.

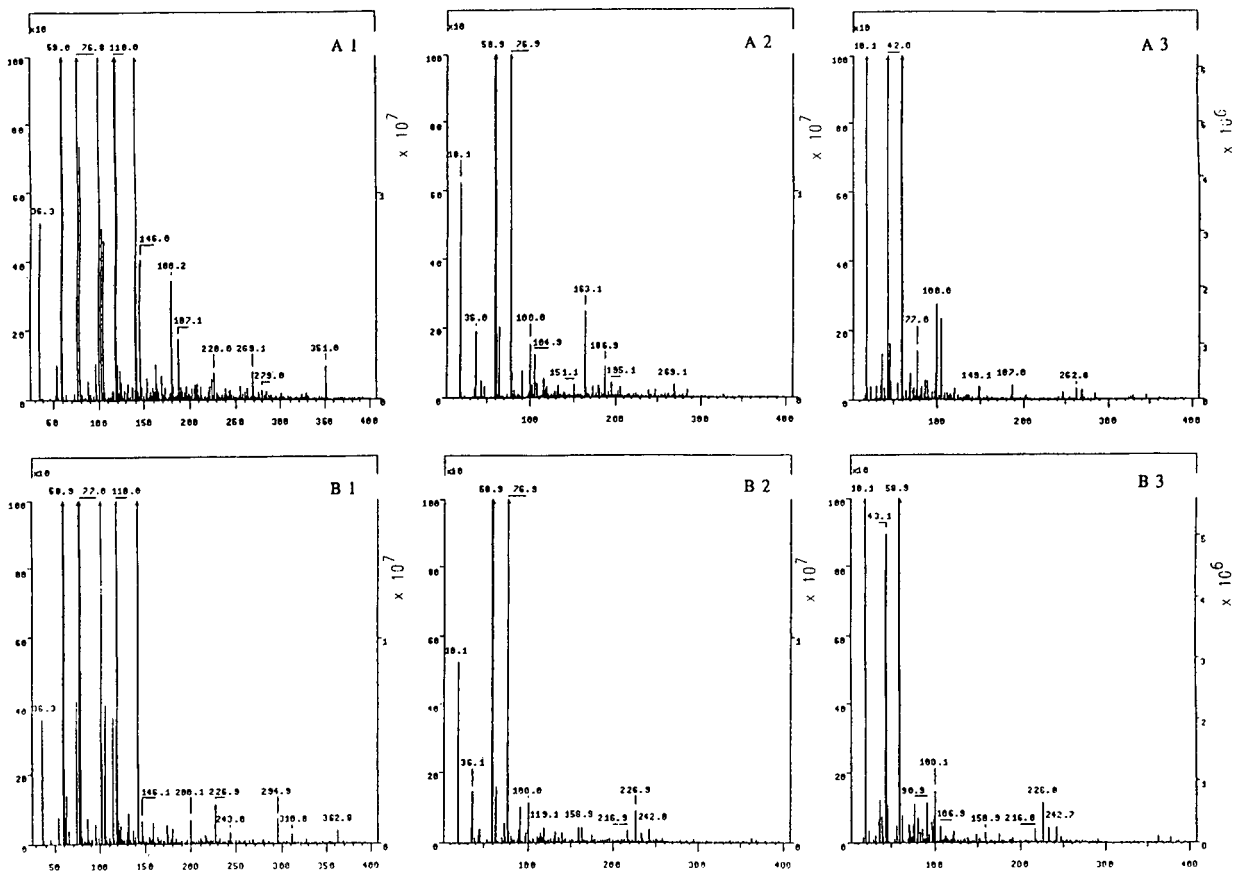

Fig. 4. Background spectra of 0.1 *M* ammonium acetate (or formate)–acetonitrile (*ca.* 90:10) in the Q3MS and RFD scan modes. (A) Acetate; (B) formate; 1 = Q3MS; 2 = RFD, −6 V; 3 = RFD, −20 V. Blow-up factor = 10 for all spectra.

background subtraction in both the Q3MS and RFD scan modes. On going from the Q3MS to the RFD scan mode with a COFF voltage of −6 V, the NH_4^+ adduct of dimethoate (*m/z* 247) disappears, but molecular information for both compounds is retained. At a COFF voltage of −20 V extra ions are acquired. By combining the information from both COFF voltages for both compounds at least five diagnostic ions are obtained. A problem is how to deal with the ions with the same *m/z* ratio in both spectra (COFF −6 and −20 V). In fact, they are the result of different collisionally activated decomposition processes. The ratio between them depends on the stability of the ion and is therefore additional information. How far this ratio is stable between the standard analyte and the analyte in a sample and whether it can be used for confirmation will be investigated in future work.

One of the chromatograms of the standard mixture was acquired with a cut-off mass of *m/z* 105 to remove the intense eluent clusters around *m/z* 77 and 100 generated in the thermospray ion source, to test the stability of the spectra in the RFD scan mode. With a cut-off mass of *m/z* 70, ions from the eluent are still entering the collision cell together with an analyte. Using a cut-off mass of *m/z* 105 the number of eluent ions is decreased strongly, which may influence the collision and fragmentation process. Fig. 6 shows the spectra of simazine with cut-off values of *m/z* 70 (Fig. 6A and C) and *m/z* 105 (Fig. 6B and D). The spectra show a further decrease in the intensity of the remaining eluent clusters (*e.g.*, *m/z* 59, Fig. 6A and B). Subtraction of the background results in comparable spectra (Fig. 6C and D) indicating that the number of ions entering the collision cell together with the

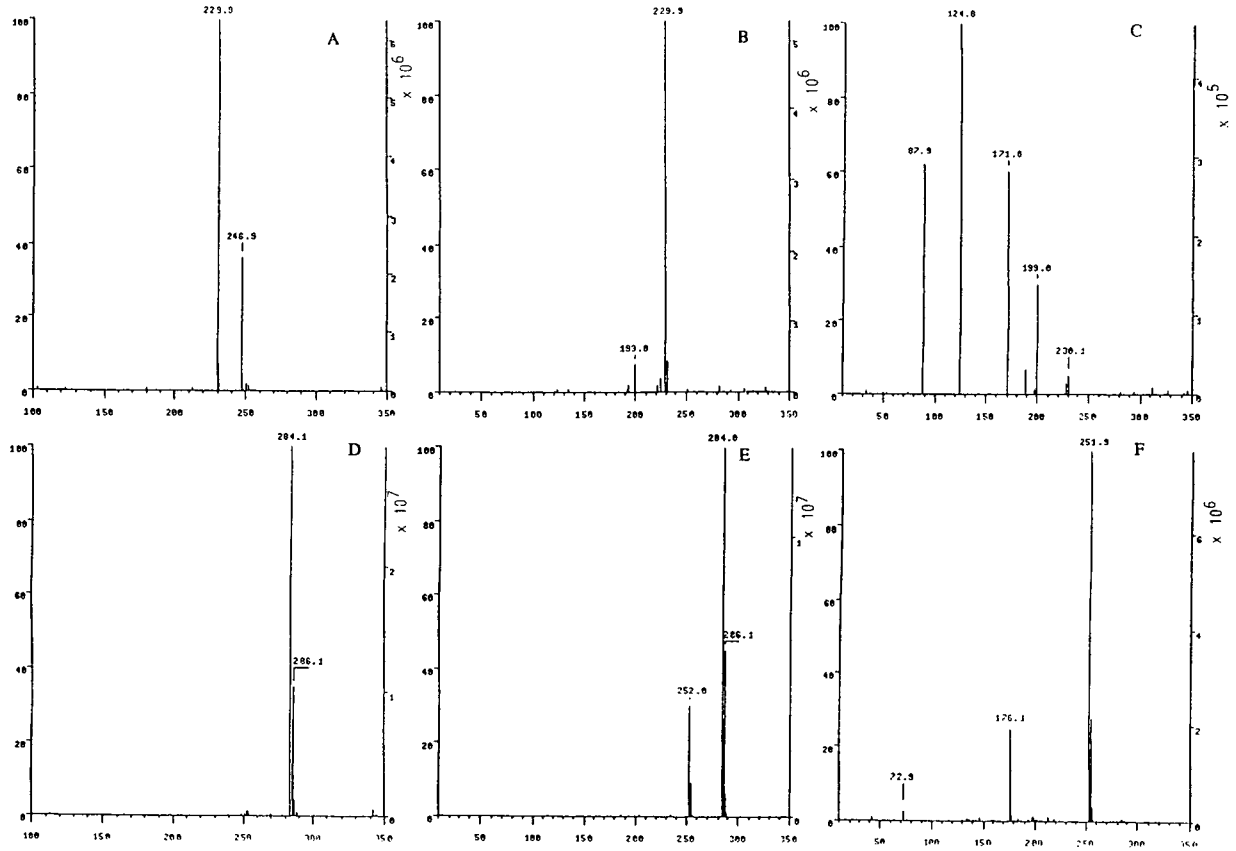

Fig. 5. Spectra of (A–C) dimethoate and (D–F) metolachlor from chromatograms in Fig. 3 after background subtraction. (A, D) Q3MS; (B, E) RFD with −6 V; (C, F) RFD with −20 V.

analyte is not very critical. In what way the optimization of the argon pressure at a relatively low cut-off mass has influenced this stability has not been investigated.

CONCLUSIONS

The RFD scan mode of a triple quadrupole mass spectrometer has been used to generate additional ions for twenty pesticides. The results indicate that, for most of the compounds, spectra with more ions are acquired with the same or better base peak signal-to-noise ratios compared with the single-stage Q3MS scan mode. The number of ions depends on the stability of a compound; *e.g.*, aniline and benzothiazole did not generate extra ions at a COFF voltage of −20 V, but even the fact that a compound does not break down at a medium COFF voltage is already extra information. By combining the diagnostic ions with different m/z values at both COFF voltages, at least four ions, with an intensity of more than 10% of the base peak at each COFF voltage, are available for sixteen of the twenty compounds.

The aim of not to lose molecular mass information was achieved. All compounds tested (Table I) have spectra with intense $[M+H]^+$ ions in the RFD scan mode with a COFF voltage of −6 V, unless they were not present in the single-stage MS mode (sethoxydim).

Adduct ions of the tested compounds disappear in the RFD mode. The importance of adducts is twofold. In many instances they are useful to trace the molecular mass of a com-

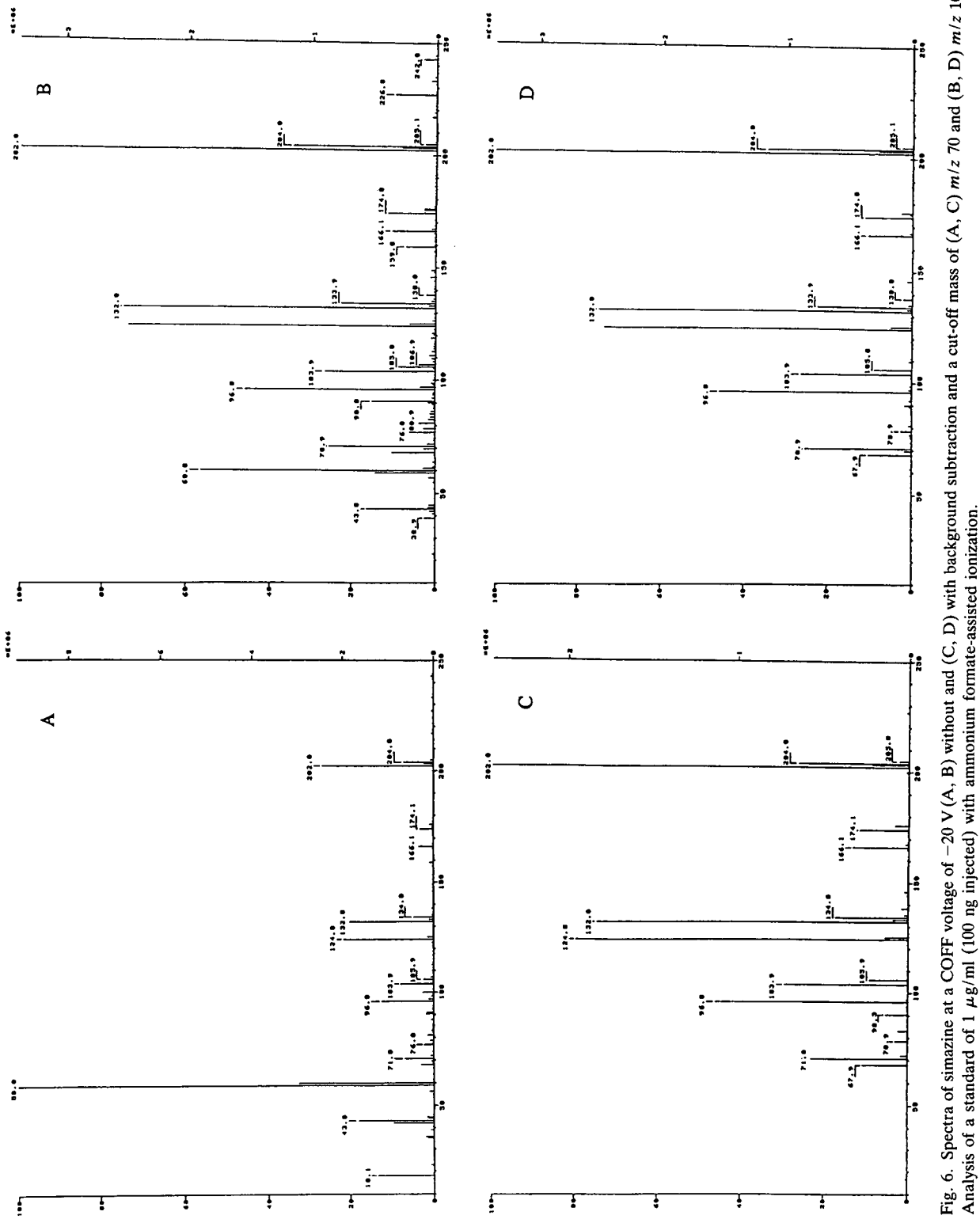

Fig. 6. Spectra of simazine at a COFF voltage of −20 V (A, B) without and (C, D) with background subtraction and a cut-off mass of (A, C) m/z 70 and (B, D) m/z 105. Analysis of a standard of 1 μg/ml (100 ng injected) with ammonium formate-assisted ionization.

pound, but they are also not very specific, matrix and source dependent and sometimes rather confusing if an adduct represents the base peak (aniline).

Eluent clusters are strongly decreased compared with the single-stage Q3MS scan mode. With a cut-off mass of m/z 105 spectra can be acquired in the whole mass range down to m/z 10 with only a few masses from eluent clusters with medium intensities (compare Fig. 6B and D).

The method was used to analyse a Rhine water sample spiked at 1 μg/l with ten compounds. Owing to the different noise levels at both COFF voltages the chromatograms look "strange", but after separation of the scans the resulting chromatograms can be evaluated as usual.

The principle of the RFD scan mode is not restricted to positive ionization. Preliminary investigations with phenoxyacid herbicides in the negative mode revealed that optimization of the argon pressure and the COFF voltage in relation to the intensity of the molecular ions $[M-H]^-$ resulted in values of 1.5 mTorr and +6 V, respectively. At a COFF of +20 V extra ions could be acquired. The RFD scan mode acted in the same way as the positive mode.

REFERENCES

1 P.J. Arpino, *Mass Spectrom. Rev.*, 9 (1990) 631–669.
2 T.A. Bellar and W.L. Budde, *Anal. Chem.*, 60 (1988) 2076–2083.
3 *Off. J. Eur. Commun.*, L 223 (1987) 26.
4 *Method 1625 Revision C*, US Environmental Protection Agency, Washington, DC, 1989.
5 G.M. Pesyna, F.W. McLafferty, R. Venkataraghavan and H.E. Dayringer, *Anal. Chem.*, 47 (1975) 1161.
6 A.L. Burlingame, D.S. Millington, D.L. Norwood and D.H. Russel, *Anal. Chem.*, 62 (1990) 268R–303R.
7 H.Fr. Schröder, *J. Chromatogr.*, 554 (1991) 251–266.
8 R.B. Geerdink, P.G.M. Kienhuis and U.A.Th. Brinkman, *J. Chromatogr.*, 647 (1993) 329.
9 R.D. Voyksner, W.H. McFadden and S.A. Lammert, in J.D. Rosen (Editor), *Application of New Mass Spectrometry Techniques in Pesticide Chemistry*, Wiley, New York, 1987, pp. 247–258.
10 I. Liska, E.R. Brouwer, A.G.L. Ostheimer, H. Lingeman, U.A.Th. Brinkman, R.B. Geerdink and W.H. Mulder, *Int. J. Environ. Anal. Chem.*, 47 (1992) 267–291.
11 A. Di Corcia and M. Marchetti, *Environ. Sci. Technol.*, 26 (1992) 66–74.
12 R. Reupert and E. Plöger, *Vom Wasser*, 72 (1989) 211–233.
13 S.A. McLuckey, G.L. Glish and B.C. Grant, *Anal. Chem.*, 62 (1990) 56–61.
14 J.S. Stout and A.R. daCunha, *Anal. Chem.*, 61 (1989) 2126–2128.
15 E.J. Reiner, D.H. Schellenberg and V.Y. Taguchi, *Environ. Sci. Technol.*, 25 (1991) 110–117.

Journal of Chromatography, 647 (1993) 51–61
Elsevier Science Publishers B.V., Amsterdam

CHROMSYMP. 2770

Ion spray mass spectrometric detection for liquid chromatography: a concentration- or a mass-flow-sensitive device?

Gérard Hopfgartner, Karen Bean and Jack Henion*

Drug Testing and Toxicology, New York State College of Veterinary Medicine, Cornell University, 925 Warren Drive, Ithaca, NY 14850 (USA)

Richard Henry

Keystone Scientific, Inc., Penn Eagle Industrial Park, 320 Rolling Ridge Drive, Bellefonte, PA 16823 (USA)

ABSTRACT

As the mass spectrometer becomes more accepted as a detector for HPLC, its characteristics should become better understood by those performing routine LC–MS experiments. In particular, the ion current response for quantitative analysis studies involving significant dynamic range in concentration for target analytes must be determined as well as other factors that affect MS response. This work describes the concentration-sensitive response for the ion spray (pneumatically-assisted electrospray) LC–MS interface from the chromatographer's perspective. A comparison of LC–MS ion current response in the isocratic mode resulting from studies of a synthetic mixture containing alkyl benzoates is presented. LC–MS total ion current chromatograms from three different column sizes (1 mm I.D., 2.1 mm I.D. and 4.6 mm I.D.) with and without a post-column split, and high-flow ion spray LC–MS without a post-column split illustrates that the former behaves as a concentration-sensitive detector whereas the latter behaves as a mass-flow-sensitive detector. The flexibility of ion spray to high-flow applications allows the use of HPLC eluent flow ranging from 0.001–2.0 ml/min. The use of solvent–buffer post-column addition also allows optimization for improved analyte ion current response.

INTRODUCTION

Liquid chromatography (LC) is largely used for the determination of polar or thermolabile compounds with UV, fluorescence, or electrochemical detection. More recently mass spectrometry (MS) has been introduced as a highly specific and sensitive detector for HPLC for quantitative or qualitative studies. Several approaches have been used to combine LC and MS including direct liquid introduction (DLI) [1], thermospray (TS) [2], particle beam (PB) [3] and more recently electrospray [4] and ion spray (IS) [5].

Unfortunately, LC–MS combinations often place restrictions on LC flow range or eluent composition [6,7]. For thermospray LC–MS applications, an eluent flow or 1 ml/min using reversed-phase conditions and volatile buffers are typical. Particle beam LC–MS applications allow similar HPLC conditions, but with effluent flow restricted to between 0.2–0.5 ml/min. Both of these LC–MS approaches sometimes provide disappointing limitations regarding detection limits for trace analyses. In contrast, pure electrospray can only handle eluent flow in the 0.002–0.005 ml/min range, yet provides very high sensitivity for certain polar analytes. Re-

* Corresponding author.

0021-9673/93/$06.00

cently, an ultrasonic nebulizer device has increased electrospray flow capability to 0.4 ml/min [8], but little is known presently about on-line LC–MS capabilities with this approach. Intermediate between thermospray and pure electrospray flow ranges is pneumatically assisted electrospray or ion spray [5]. This simple modification of electrospray performs best with flow rates from 1–100 μl/min, and many applications of LC–MS have been reported [1,5]. Ion spray LC–MS is thus compatible with reduced diameter micro-bore columns without post-column splitting while larger bore columns require a post-column split that confines the interface flow to this range. Recently, we have extended the application of ion spray to flow-rates up to 2 ml/min using a liquid shield [9], which avoids the need for conventional post-column splitting with HPLC columns up to 4.6 mm I.D.

The analyst is faced with the challenge of coupling different HPLC column diameters and their corresponding optimum flow-rates to the LC–MS interfaces mentioned above, each of which has its own limitations regarding effluent flows. Electrospray, for example, has required a substantial post-column split with 4.6 mm I.D. columns in order to restrict the 1 ml/min column effluent flow at the electrospray interface to less than 5 μl/min. The question that often arises is does diverting 95% of the HPLC effluent away from the mass spectrometer reduce LC–MS sensitivity? Similarly, if 1 mm I.D. HPLC columns are used with electrospray, does one obtain improved sensitivity? An understanding of these factors affecting these questions is important for optimizing an experimental set-up for LC–MS experiments.

In general a mass spectrometer equipped with an electron ionization (EI) or chemical ionization (CI) ion source behaves as a mass-flow-sensitive detector [7]. In contrast, both electrospray [4] and ion spray [5] LC–MS techniques behave as a concentration-sensitive detector [10], where the ion current response is directly proportional to the analyte concentration in a chromatographic peak. The latter is dependent on the column inside diameter. The first part of this work re-investigates the benefits and the limitations of HPLC–IS-MS with different column I.D.s including 1 mm (micro-bore), 2 mm (narrow-bore), and 4.6 mm (standard-bore). Alkyl benzoate esters are used as model compounds for low-molecular-mass analytes to compare with LC–UV performance in the isocratic mode. The isocratic mode was chosen relative to the gradient mode to minimize instrumental variables.

The second part of this report describes an approach that significantly increases the analyte ion current response in IS-MS. Since the ion spray ion current is dependant upon the nature of the analyte as well as the composition of the mobile phase, we have studied various means for improving the analyte response without affecting the chromatographic conditions. In some cases, the analyst must compromise MS response to achieve desired HPLC separation. Voyksner *et al.* [11] have demonstrated for thermospray that post-column addition or buffer addition can sometimes significantly improve the overall response of the analytes. The limited flow capabilities of pure electrospray have precluded this ploy for LC–MS applications using larger-bore HPLC columns. Using high-flow ion spray [9], where the detector behaves like a mass-flow-sensitive device, we have investigated the potential of post-column addition using two pesticides as model compounds to improve IS-MS response.

GENERAL CONSIDERATIONS

Chromatographic separation

A chromatographic separation is based on two principles: resolution between two compounds and analyte dilution in the mobile phase [12]. The latter dilution can be described by a Gaussian distribution [13], where the maximum peak concentration (C_{max}) of the eluting compound is a function of injected analyte (m), the efficiency of the column (N), the capacity factor (k') of the analyte and the dead volume of the column (V_0) which is also dependent on the length (l) and internal diameter (d) of the column. The relationship between these parameters is shown in eqn. 1 [13].

$$C_{max} = \frac{mN^{1/2}}{(2\pi)^{1/2}V_0(1+k')} \quad (1)$$

The C_{max} is directly proportional to the mass of analyte and the efficiency of the column and retention time also affects C_{max}. High plate numbers and short retention time will provide the best sensitivity for a concentration-sensitive device. One of the most important parameters which affects C_{max} is the column internal diameter. For two columns with the same packing material and the same length, but different internal diameter (d_{c1} and d_{c2}) the C_{max} ratio can be described by eqn. 2

$$C_{max}\ \text{ratio} = \frac{d_{c1}^2}{d_{c2}^2} \quad (2)$$

Table I shows the relative increase in C_{max} *versus* different column inside diameters based on a ratio of cross-sectional areas. The theoretical increase in sensitivity using a column with 1 mm I.D. instead of a 4.6 mm I.D. is about a factor of 21 due to smaller V_0 and less sample dilution.

Mass-flow-sensitive detector

A mass-flow-sensitive detector is defined as one where the response is directly proportional to the amount of analyte reaching the detector *per unit time* [7]. Typical mass-flow-sensitive devices are the flame ionization detector and the classical EI mass spectrometer. Both of these are also destructive detectors [14]. The response (R) can be described by eqn. 3 with (m) the analyte mass, (F) the flux, (S) the splitting ratio, (a) response factor, and (t) time. C_{max} is the maximum concentration of the analyte.

$$R = a \cdot \frac{\partial m}{\partial t} = aC_{max}FS \quad (3)$$

The response R with a mass-flow-sensitive detector is directly proportional to the flux and a decrease of flow-rate, as with post-column splitting, will produce a decrease in response. When the flow-rate is maintained constant, the response is directly proportional to C_{max}. In the case of an "infusion" experiment with a constant analyte concentration, an increase in flow will result in a linear increase in signal. This means that for flow injection analysis a reduction in flow for example, will lower the peak height but the peak area will remain the same when the same quantity of material is injected.

TABLE I

THEORETICAL INCREASE IN C_{max} FOR DIFFERENT COLUMN I.D.s

	d_c (mm)		
	4.6	2.0	1
Increase in C_{max}	1	5	21

Concentration-sensitive detector

For a concentration-sensitive device the detector signal depends on the concentration of the sample in the carrier flow. Most of the detectors used in liquid chromatography, such as UV and fluorescence devices, are concentration-sensitive detectors where the response R is directly proportional to C_{max} and can be described by eqn. 4 where a is a response factor [15].

$$R = aC_{max} \quad (4)$$

Concentration-sensitive detectors are generally non-destructive and the flow-rate does not affect the response because the physical measurement of the analyte is much faster than the sample flow-rate [14]. For an infusion experiment with a constant analyte concentration the response stays constant with an increase of flow-rate. This means that for flow injection analysis a decrease in flow will increase the peak area but the peak height will remain the same. This report describes a series of experiments designed to demonstrate and compare the results obtained from on-line ion spray LC–MS experiments, in the isocratic mode, with a view of those factors important to consider for optimizing conditions for LC–MS analyses.

EXPERIMENTAL

Chemicals

The water used was obtained from a Barnstead Nanopure cartridge system (Boston, MA, USA). Acetonitrile and methanol were of Fischer Optima grade and ammonium acetate was of Fischer HPLC grade (Fair Lawn, NY, USA).

High-purity trifluoroacetic acid (TFA), and tetradecyl ammonium bromide (TDAB) were obtained from Sigma (St Louis, MO, USA), Tetrabutyl ammonium hydroxide (TBAH) was purchased from Southwestern Analytical Chemicals (Austin, TX, USA). Ethyl, propyl and butyl benzoate esters were purchased from Aldrich (Milwaukee, WI, USA). Monuron and carbofuran were obtained from the US Environmental Protection Agency Repository (Research Triangle Park, NC, USA).

Liquid chromatography

The synthetic compound mixture was analyzed on 100 mm length Keystone BDS-Hypersil 5 μm C_8 columns (Keystone Scientific, Bellefonte, PA, USA) with internal diameters of 1.0, 2.0 and 4.6 mm. The packing material for each of these columns was from the same lot. Mobile phase was delivered by an Hitachi L-6200A pump (Hitachi Instruments, Danbury, CT, USA). Isocratic separation of the alkyl benzoate esters was achieved with an 0.15% TFA in acetonitrile–water (60:40) mobile phase. The use of TFA does not affect the chromatographic separation of the alkyl benzoate esters, but does improve the IS-MS response of these neutral organic compounds. Isocratic separation of the two pesticides used in this study was achieved with a 5 m*M* ammonium acetate in acetonitrile–water (40:60) solution. HPLC mobile phases were filtered and degassed prior to use by sparging with helium. The compounds were loaded on the HPLC columns using an external loop Model 7125 injector with a 5-μl loop or a Model 7520 injector with a 0.5-μl internal loop (Rheodyne, Cotati, CA, USA). The splitting and post-column experiments were performed with a low-dead-volume tee (Upchurch Scientific, Oak Harbor, WA, USA).

UV detection

For UV detection an Applied Biosystems (San José, CA, USA) Model 757 variable-wavelength UV detector was used with interchangable 0.5-μl (1 mm path length) and 2.4-μl cells (6 mm path length). The LC–UV experiments were performed using the 4.6, 2 and 1 mm I.D. columns with the 0.5-μl cell. For the post-column experiments with the 1 mm column the 2.4-μl cell was

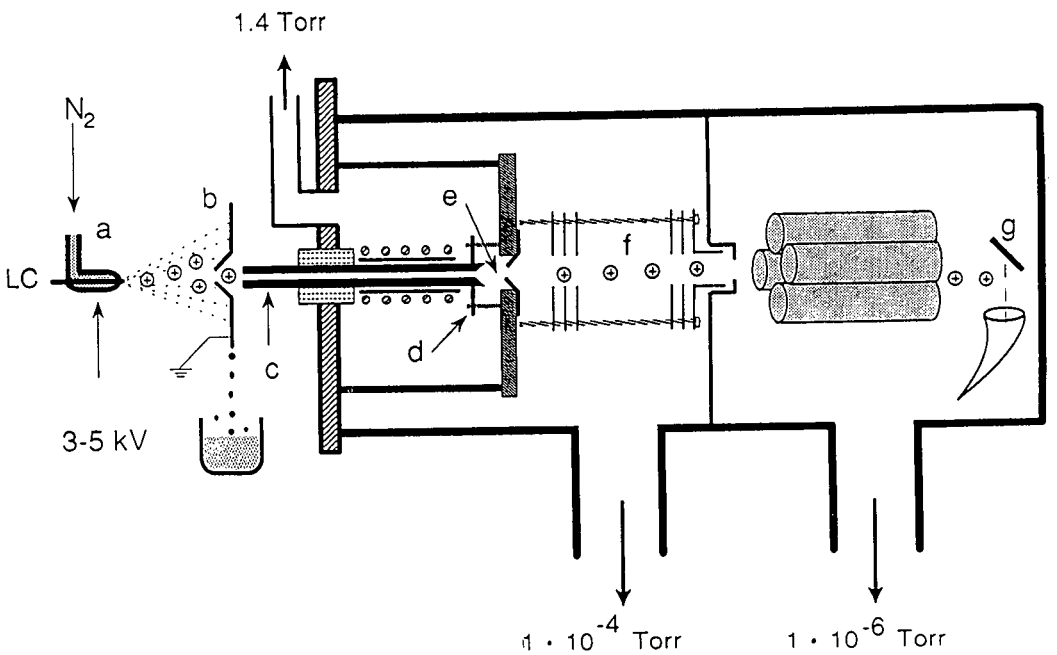

Fig. 1. General schematic of the ion spray LC–MS system incorporated on an HP 5985B mass spectrometer. a = Ion spray: b = liquid shield; c = heated ion capillary; d = centering device; e = skimmer; f = Einzel lenses; g = high-energy dynode detector. 1 Torr = 133.322 Pa.

used. Every effort was made to minimize extra-column dead volume in these experiments, in particular minimum bore tubing (I.D. = 100 μm) and zero-dead-volume fittings were used. The wavelength was set at 254 nm for the benzoate esters and at 214 nm for the pesticides. UV chromatograms were recorded by a Hewlett-Packard 3390A integrator (Avondale, PA, USA).

Ion spray mass spectrometric detection

All LC–MS measurements were performed under selected ion monitoring (SIM) conditions on a Hewlett-Packard Model 5985B mass spectrometer (Hewlett-Packard, Palo Alto, CA, USA) with an in-house constructed interface capable of sampling ions formed at atmospheric pressure [9]. Fig. 1 shows a schematic drawing of the system. The standard EI source and its associated Einzel lens system were replaced by a two-stage vacuum region designed to sample ions formed at atmospheric pressure. The system is patterned after that reported by Chait *et al.* [16], and is composed of the following key features (Fig. 1): (a) ion spray LC–MS interface, (b) grounded liquid shield, (c) heated ion sampling capillary in the first vacuum region, (d) centering device, (e) ion sampling skimmer, (f) second vacuum region housing the ion optics lens, (g) high-vacuum region housing the quadrupole mass analyzer and high-energy dynode electron multiplier. A complete description of this system is given elsewhere [9].

The setup for high-flow ion spray is similar to conventional ion spray which has been described previously. The LC column effluent (1–2000 μl/min) travels through a connecting fused-silica capillary (100 mm length × 0.1 mm I.D. × 0.25 mm O.D.) that protrudes from a stainless-steel capillary (0.004 in I.D. × 0.009 in O.D.) housed in the ion spray LC–MS tee fitting [4]. High voltage (3–5 kV) is applied to the effluent near the sprayer tip via an electrical contact on a stainless steel tee fitting that houses the two concentric capillaries positioned by graphite ferrules. Nitrogen gas (50–80 p.s.i.; 1 p.s.i. = 6894.76 Pa) is passed through the annular space between the inner and the outer capillaries to affect pneumatically-assisted electrospray (ion spray) ionization. For HPLC experiments the sprayer is positioned off-center (5 mm) and about 10 mm distant from the orifice in the liquid shield. The excess eluent is allowed to drip from the liquid shield into a beaker (Fig. 1). Some safety precautions should be taken to vent the excess solvent vapor.

The mass spectrometer data acquisition was performed using the standard Pascal Workstation with release 3.1.1. HP software (Hewlett-Packard). The tuning and mass calibration of the HP-5985B were achieved via a 4 μl/min infusion of a 10 pmol/μl methanol solution of either TBAH while monitoring m/z = 242.24, 142.16, 100.01, 57.07 or tetradecyl ammonium bromide (TDAB) while monitoring m/z = 578.66, 310.35, 184.21 using the manual tune software. Fragment ions were obtained by increasing the potential difference between the ion sampling capillary (Fig. 1, c) and the skimmer (Fig. 1, e) which produces collision-induced dissociation using a potential difference of 85 V for TBAH and 160 V for TDAB [4]. The mass resolution was adjusted to provide peak widths of 0.6 u. at half-height across the mass range (50–1000 u).

RESULTS AND DISCUSSION

Conventional ion spray

Fig. 2 shows the LC–UV traces of three alkyl benzoate (ethyl, butyl, propyl) esters using three different column I.D.s: (A) 1, (B) 2 and (C) 4.6 mm. The flow-rates were optimized to obtain similar analysis times for all three columns with the same mobile phase composition. The same hardware (pump, injector, detector equipped with a micro cell) was used for all three experiments and special care was taken to minimize extracolumn variance for the micro-bore separation, in particular tubing (100 μm I.D.) and connections. The injection volume (5 μl) and the injected amount was indentical on all three columns. When the column I.D. is reduced from 4.6 to 1 mm the increased peak height (butyl benzoate ester) is only 7.4 *versus* 21 which is theoretically expected. All our efforts failed to produce the theoretical 21-fold increase presumably because it is not practical to eliminate all extra-column dead volume in the micro-bore system. A smaller injection volume of 0.5 μl

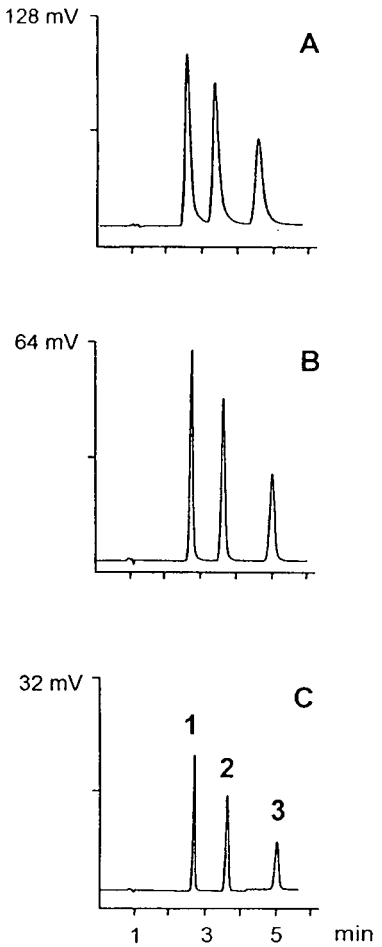

Fig. 2. LC–UV traces of alkyl benzoate esters on three different column I.D.s: (A) 1 mm I.D., flow-rate = 65 μl/min; (B) 2.0 mm I.D., flow-rate = 210 μl/min; (C) 4.6 mm I.D., flow-rate = 1000 μl/min. UV Detector with a 0.5-μl cell, 254 nm, 5-μl injection. Peaks: 1 = ethyl benzoate; 2 = propyl benzoate; 3 = butyl benzoate.

with an internal loop injector did not provide improved resolution. It is also well-known that packing techniques for micro-bore columns are more critical so these 1 mm I.D. columns often do not provide comparable separation efficiencies to 4.6 mm I.D. columns. The separation efficiency achieved on the butyl benzoate ester ($N = 1588$) for the 1 mm I.D. column, as illustrated in Fig. 2A is not as good as for the 4.6 mm column ($N = 6774$) result shown in Fig. 2C. Similarly, for the 2 mm I.D. column (Fig. 2B) the loss of chromatographic performance is about 35% resulting in a 3.8-fold increase in response rather than 5 which is theoretically expected.

The same experiments were repeated with HPLC–IS-MS conditions using a post-column split for the larger I.D. columns to give the results shown in Fig. 3 where the flow to the mass spectrometer was maintained at 65 μl/min. Similar detector response behavior is observed for HPLC–IS-MS as for LC–UV. In this case the increase in peak height for the butyl benzoate ester is about 8.5 using the 1 mm I.D. column compared to the 4.6 mm I.D. column as shown

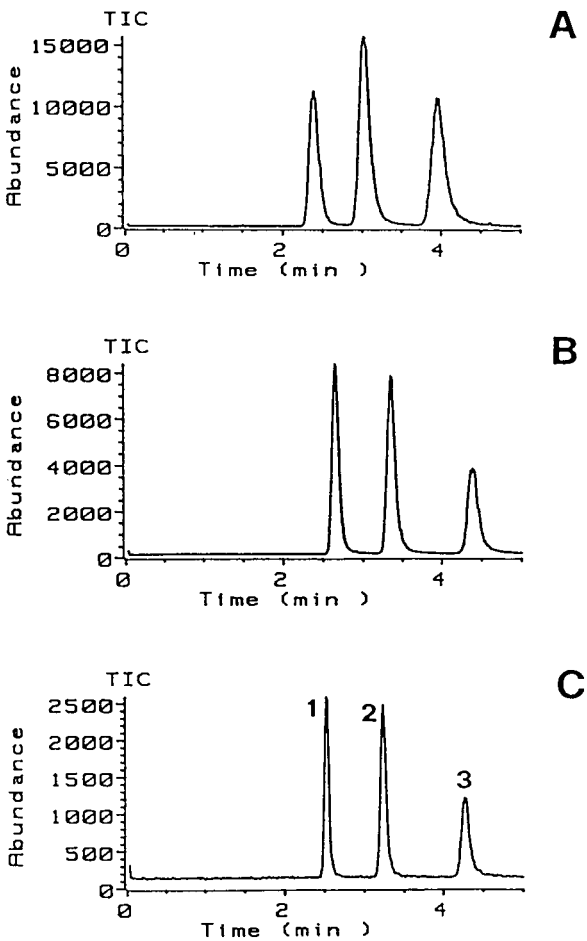

Fig. 3. LC–IS-MS traces of alkyl benzoate esters on three different column I.D.s with post-column splitting. (A) 1 mm I.D., flow-rate = 65 μl/min; (B) 2.0 mm I.D., flow-rate = 210 μl/min, splitting flow-rate to mass spectrometer 65 μl/min; (C) 4.6 mm I.D., flow-rate = 1000 μl/min, splitting flow-rate to mass spectrometer 65 μl/min, injection volume 5 μl. TIC = Total ion current.

TABLE II

OBSERVED RELATIVE INCREASE IN RESPONSE AS A FUNCTION OF COLUMN I.D.

Butyl benzoate ester, $n = 3$.

	1/4.6	2.0/4.6	4.6/4.6
LC–UV (peak height)	7.4	3.8	1
LC–UV (peak area)	13.8	4.6	1
LC–MS (peak height)	8.5	3.5	1
LC–MS (peak area)	15.5	4.5	1

in Fig. 3A and C. For the narrow-bore column the increase in response is about 3.5-fold as shown in Fig. 3B. Under these conditions where the flow to the mass spectrometer is constant, the analyte response is directly proportional to the analyte concentration. Table II summarizes the results for all three columns for peak area and peak height for LC–UV and HPLC–IS-MS. Since the detection limit may be defined as the ratio between the signal and the baseline noise (S/N) [14], then the peak height relative to the baseline noise is an important factor for determining sensitivity. For these reasons, peak areas are given only for reference. Table III shows the plate numbers obtained for butyl benzoate ester with the different columns and the two detectors. Table III also shows that the current design of the LC–MS ion spray interface does not affect chromatographic performance when eluent flow from the 4.6 mm column is split to 65 μl/min.

Post-column splitting does not affect the concentration of the analyte, but it does affect the quantity of analyte delivered per unit time. The effect of post-column splitting for a concentration-sensitive detector is illustrated in Fig. 4 where the split delivers reduced flow to the UV detector with no significant decrease in signal while good chromatographic performance is maintained. For Fig. 4C a slightly lower signal is observed which is due to some extra-column dispersion. As expected from eqn. 3 a post-column split for a mass-flow-sensitive device will result in a significant decrease in response, and direct coupling with micro-bore columns will provide the best overall sensitivity. This has been described previously for micro-LC–MS with DLI [1] under CI conditions. The analyte response from ion spray and electrospray as a function of flow rate has been studied by Ikonomou *et al.* [18]. The authors observed that an increase in flow of a given solution by infusion does not correspond to a significant increase in total ion current. In the flow range 1 to 100 μl/min conventional ion spray behaves like a UV detector and post-column splitting does not affect the analyte response in terms of peak height or total ion current. These facts suggest that post-column splitting using larger-bore HPLC columns coupled with electrospray or ion spray will not result in dramatic LC–MS sensitivity loss as would be expected in the case of mass-flow sensitive device from eqn. 3. The split effluent can of course be directed to, for example, a diode array for complementary spectroscopic information. However, HPLC plumbing problems associated with maintaining precisely controlled flow to the interface may occur which detracts from the apparent ease of these experiments and in particular for quantitative work.

Micro-bore columns provide better response than standard-bore columns for the same injected amount with ion spray, but chromatographic

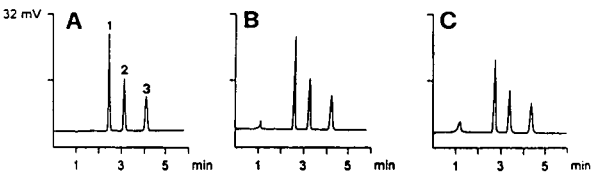

Fig. 4. LC–UV response with post-column splitting. The separation of the alkyl benzoates was performed on a 100 × 4.6 mm column, UV detector with a 2.8-μl cell, 254 nm. (A) No split, 1000 μl/min to the detector: (B) split 5:1, 200 μl/min to the detector; (C) split 20:1, 50 μl/min to the detector.

TABLE III

OBSERVED LOSS OF EFFICIENCY UPON SCALE DOWN TO 1 mm I.D. COLUMN

$n = 5.54(t_R/W_{0.5})^2$.

Column I.D. (mm)	N (LC–UV)	N (LC–IS-MS)
1.0	1588	2547
2.0	4422	6936
4.6	6774	8948

performance is often compromised. This results not from problems with MS, but practical limitations with minimizing extra-column volume resulting from connecting tubing and HPLC fittings. The increase in response is mainly related to increased C_{max} of the analyte with the smaller column internal diameter. Micro-bore columns with smaller I.D. than 1 mm or even open tubular columns have shown increased separation efficiencies and resolution because the latter have greater permeability and minimized diffusion which allows the use of longer packed HPLC columns. However, in the case of packed columns the diameter of the particles is still an important parameter for chromatographic resolution. Optimizing the design of small diameter columns and packing as well as automated HPLC systems will certainly be of benefit to similarly improve LC–MS sensitivity.

The available injection volume is also an important factor to consider when evaluating the overall sensitivity of an LC–MS system. Micro-bore columns will tolerate a limited injection volume of about 5 μl in the isocratic mode under most common HPLC conditions. On standard-bore columns injection volumes of 50 μl or more of biological fluid extracts are common. When large volumes of sample must be introduced for trace investigation, the highest efficiency is obtained with sample solvents weaker than the mobile phase. "Peak compression" may be used to inject larger amounts of samples on micro-bore columns. However, these columns are very sensitive to pressure changes and injection of large amounts of plasma extracts, for example, will require special care for sample work-up. On the other hand the mass spectrometer is a very specific detector and quantitative analysis with high through-put in the isocratic mode is preferred for speed, simplicity and analytical ruggedness.

When minimal sample consumption is required micro-bore columns are the best choice for maximum ion spray LC–MS sensitivity. Another important advantage of micro-bore columns is reduced solvent consumption where about 15 times less solvent is used compared to 4.6 mm I.D. columns. However, when sufficient sample is available to allow larger injection volumes, maximum overall response, best chromatographic performance and analytical ruggedness will be obtained with a 4.6 mm I.D. HPLC column. An intriguing alternative to 4.6 mm I.D. columns for HPLC–IS-MS are short 2 mm I.D. columns packed with 3-μm particles. These columns offer reduced solvent consumption and increased in sensitivity without compromizing chromatographic performance or analytical ruggedness.

High-flow ion spray

Recently we extended the application of ion spray techniques to HPLC flows up to 2 ml/min by adding a simple grounded liquid shield between the sprayer and the ion sampling capillary of a heated capillary-type atmospheric pressure interface (Fig. 1). Using this interface LC–MS experiments can be carried out over a large range of flow-rates which provides benefits for conventional LC–MS applications where previously the post-column split was required for standard HPLC columns [9]. We have shown that under high-flow ion spray conditions the analyte ion current signal increases with flow-rate for a solution with a fixed concentration. This behavior is in contrast to conventional ion spray described above and is characteristic of a mass-

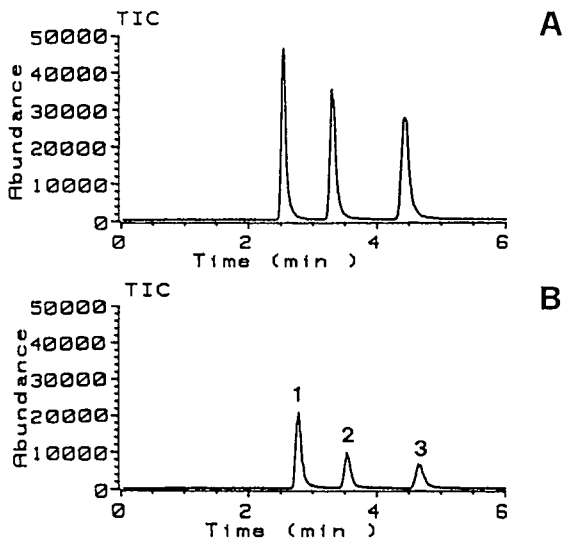

Fig. 5. High-flow ion spray *versus* conventional ion spray of alkyl benzoate esters on a 100 × 4.6 mm column SIM of m/z = 151, 165, 179 (MH^+), dwell time = 300 ms. (A) High-flow ion spray without post-column split and liquid shield; (B) conventional ion spray with post-column split and no liquid shield.

flow-sensitive detector [7]. Higher ion current response is obtained at 1 ml/min than with lower flow due presumably to a mass-flow effect as might expected for a mass spectrometer [7]. Fig. 5A shows the SIM LC–MS comparison of the alkyl benzoate esters using a 4.6 I.D. Column without post-column splitting using the liquid shield (1 ml/min to mass spectrometer) and Fig. 5B with conventional post-column splitting (40 μl/min to mass spectrometer). The position of the sprayer was optimized for each experiment. In both cases chromatographic performance is conserved and for the higher flow a 3-fold increase in analyte ion current signal is observed. Most chromatographic separations are still based on standard-bore columns so high-flow ion spray provides HPLC–IS-MS capability without post-column splitting while retaining good sensitivity. It also allows simple transfer of established conventional (using 4.6 mm I.D. columns) LC–UV separations to LC–MS experiments. In electrospray and ion spray we have at least two important steps. The first is the formation of the spray while the second is the generation of gas-phase ions at atmospheric pressure. These ions must then be sampled from atmospheric pressure into the high-vacuum region of the mass spectrometer. The mass flow or the concentration behavior of ion spray may depend upon these two steps and the particular design of the atmospheric pressure ionization interface.

Post-column addition

A convenient feature of the ion spray interface compared to, for example, electrospray or particle beam LC–MS approaches, is its ability to handle a wider range of flow-rates including those common to micro- and standard-bore eluent flows. Since ion spray analyte response is dependent on the nature of the analyte and the eluent composition such as the organic modifier and ionic salt content, post-column addition is an alternative for improving sensitivity and has also been demonstrated for thermospray LC–MS applications [11]. However, the addition of a post-column liquid essentially dilutes the analyte concentration and hence the analyte response if detection is based upon concentration. This effect is illustrated in Fig. 6A–C for the LC–UV determination of monuron and carbofuran and

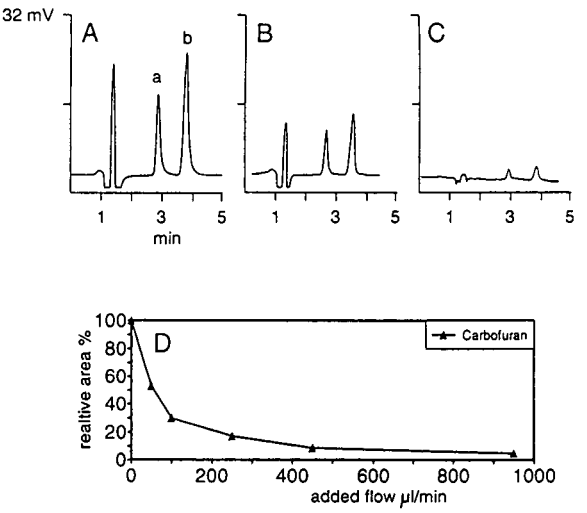

Fig. 6. LC–UV response of monuron (a) and carbofuran (b) with post-column addition on a 100 × 1 mm I.D. column (see Experimental for conditions). (A) No post-column addition; (B) 50 μl/min post-column addition; (C) 450 μl/min post-column addition; (D) summary of LC–UV response for carbofuran with various post-column additions of column eluent.

summarized for carbofuran in Fig. 6D. Fig. 6A shows the separation of the two pesticides on a 1 mm I.D. column with a 5 m*M* ammonium acetate in water–acetonitrile (60:40) mobile phase maintained at 50 μl/min. The addition of 50 μl/min of the same eluent via a post-column tee located between the column exit and the UV detector reduces the analyte response by a factor of two as illustrated in Fig. 6B. A 9-fold dilution (Fig. 6C) results in a loss of about 84% of the UV signal. Fig. 7A shows the SIM trace of monuron and carbofuran (50 ng each) under conventional ion spray LC–MS conditions separated on the 1 mm I.D. column with no post-column addition and with the same mobile phase as for LC–UV at 50 μl/min (see Fig. 6). If the liquid shield is placed in the spray region of the ion spray interface so that high-flow ion spray conditions are used [9], post-column eluent addition may be readily implemented. When 450 μl/min mobile phase is added to the effluent of the HPLC column an approximatively 70% decrease in analyte response is also observed (Fig. 7B). This LC–MS behavior parallels that of the LC–UV detector response described above (Fig. 6A–D) and suggests that the dilution effect is a

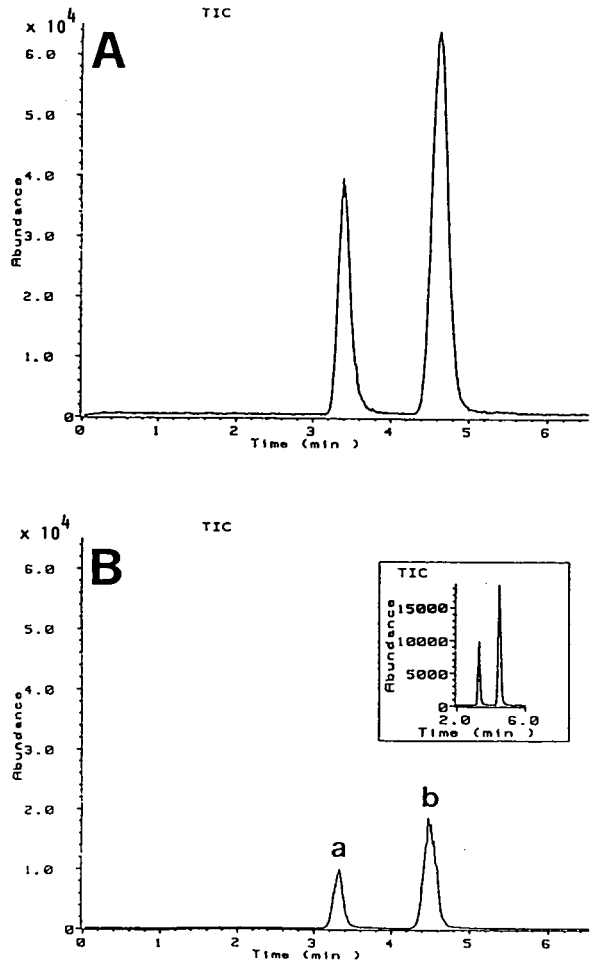

Fig. 7. SIM LC–MS response of monuron (a) and carbofuran (b) (50 ng on-column) on a 100 × 1 mm I.D. column at 50 μl/min (m/z = 199, 222, dwell time = 300 ms). (A) Conventional ion spray with no post-column addition; (B) high-flow ion spray post-column addition of 450 μl/min using the liquid shield.

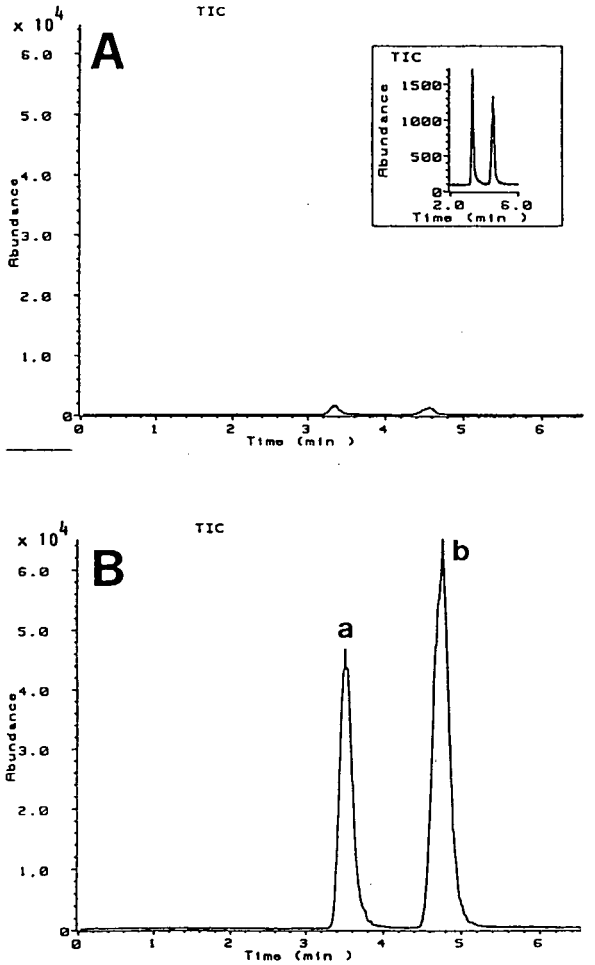

Fig. 8. SIM LC–MS response of monuron (a) and carbofuran (b) (see Fig. 7 for conditions). (A) High-flow ion spray with post-column addition of 450 μl/min 100% CH_3CN; (B) high-flow ion spray post-column addition of 450 μl/min 100% MeOH using the liquid shield.

more important parameter than the increase in flow, and negatively affects the overall analyte ion current response in this case.

Acetonitrile and methanol are well known to enhance analyte response under ion spray conditions [18]. However, the post-column addition of 100% acetonitrile under high-flow ion spray LC–MS conditions significantly suppresses the ion current response for the two pesticides as illustrated in Fig. 8A. Addition of 0.1% formic acid (not shown) produces some improvement in the analyte ion current response. In contrast, when 100% methanol is used we observe a considerable enhancement of the signal (Fig. 8B) which appears to compensate for the dilution effect. Since under ion spray conditions it is generally accepted that high organic content improves the analyte response, the observed difference between acetonitrile and methanol may be related to the nature of the solvent and in particular to ion solvation where acetonitrile is aprotic compared to the protic nature of methanol. Raffaelli and Bruins [19] investigated the response of quaternary ammonium salts, which are preformed ions, *versus* acetonitrile and methanol

and observed the opposite effect. Thus they observed a better analyte signal using acetonitrile than for methanol. In contrast to quaternary ammonium salts, the two pesticides studied here do not carry their own positive charge. In the case of acetonitrile the weak signal may be partially due to the fact that the compounds are not preformed ions in solution and this may result in an inefficient ion release from the condensed phase. The improved response by the addition of formic acid is consistent with this explanation. However, gas-phase processes involving proton transfer cannot be excluded.

Post-column addition is very useful for enhancing MS response without compromising the HPLC separation. We illustrate here the feasibility of post-column addition with simple solvents and with a high dilution factor. More appropriate solvent ratios and even post-column chemistry may be an appropriate way to extend the application of IS-MS to molecules which under normal conditions show a poor IS-MS ion current signal. Under these conditions the behavior of the detector may be difficult to predict, because the MS response is primarily dependent on the mobile phase composition and the analyte.

CONCLUSIONS

In contrast to typical EI and CI mass spectrometric performance conventional ion spray behaves as a concentration-sensitive detector so that post-column splitting under LC–MS conditions does not affect the LC–MS response. The practical increase in sensitivity with 1 mm I.D. *versus* 4.6 I.D. columns with the same length and the same packing material in the isocratic mode while injecting the same quantity of sample is about 8-fold, but chromatographic performance and analytical ruggedness are compromised. Micro-bore columns are the best choice when minimum consumption of the sample is required. Better 1 mm I.D. columns in the future will certainly improve these results. For LC–MS applications 2 mm I.D. columns may be a practical alternative for lower solvent consumption, increased analyte response, and good chromatographic performance. High-flow ion spray with the liquid shield behaves more like a mass-flow-sensitive detector. Higher liquid flow allows post-column addition to micro-bore separations which is a useful approach for improving MS response without compromising HPLC performance.

ACKNOWLEDGEMENTS

The authors gratefully acknowledge K. Ogan of Hitachi Instruments for the HPLC pump used in this work. We also thank Hewlett-Packard and Gallileo Instruments for the high-energy dynode used on the HP-5985B. G.H. thanks the Swiss National Science Foundation for financial support during his stay at Cornell.

REFERENCES

1 E.D. Lee and J.D. Henion, *J. Chromatogr. Sci.*, 23 (1985) 253.
2 P. Arpino, *Mass Spectrom. Rev.*, 11 (1992) 3.
3 P.C. Winkler, D.D. Perkins, W.K. Williams and R.F. Browner, *Anal. Chem.*, 60 (1988) 489.
4 S.F. Wong, C.K. Meng and J.B. Fenn, *J. Phys. Chem.*, 92 (1988) 546.
5 A.P. Bruins, T.R. Covey and J.D. Henion, *Anal. Chem.*, 59 (1987) 2642.
6 W.M.A. Niessen, U.R. Tjaden and J. van der Greef, *J. Chromatogr.*, 554 (1991) 3.
7 B.L. Karger and P. Vouros, *J. Chromatogr*, 323 (1985) 13.
8 S. Shen, C. Whitehouse, F. Banks and J.B. Fenn, *Proceedings of the 40th ASMS Conference on Mass Spectrometry and Allied Topics, Washington, DC, May 31, 1992.*
9 G. Hopfgartner, T. Wachs, K. Bean and J. Henion, *Anal. Chem.*, 65 (1993) 439.
10 A.P. Bruins, *Mass Spectrom. Rev.*, 10 (1991) 53.
11 R.D. Voyksner, J.T. Bursey and E.D. Pellizzari, *Anal. Chem.*, 56 (1984) 1507.
12 C.A.M. Meijers, J.A.R.J. Hulsman and J.F.K. Huber, *Z. Anal. Chem.*, 261 (1972) 347.
13 B.L. Karger, M. Martin and G. Guiochon, *Anal. Chem.*, 46 (1974) 1640.
14 I. Halász, *Anal. Chem.*, 36 (1964) 1428–1430.
15 S.R. Bakalyar and R.A. Henry, *J. Chromatogr.*, 126 (1976) 327.
16 S.K. Chowdhury, V. Katta and B.T. Chait, *Rapid Comm. Mass Spectrom.*, 4 (1990) 81.
17 G.L. Long and J.D. Winefordner, *Anal. Chem.*, 55 (1983) 713*A*.
18 M.G. Ikonomou, A.T. Blades and P. Kebarle, *Anal. Chem.*, 63 (1991) 1989.
19 A. Raffaeli and A.P. Bruins, *Rapid Comm. Mass Spectrom.*, 5 (1991) 269.

Journal of Chromatography, 647 (1993) 63–72
Elsevier Science Publishers B.V., Amsterdam

CHROMSYMP. 2781

New ionization strategies in particle-beam liquid chromatography–mass spectrometry based on the principle of surface ionization

A.P. Tinke, R.A.M. van der Hoeven, W.M.A. Niessen*, U.R. Tjaden and J. van der Greef

Division of Analytical Chemistry, Leiden/Amsterdam Center for Drug Research, P.O. Box 9502, 2300 RA Leiden (Netherlands)

ABSTRACT

The potential of surface ionization (SI) as an ionization technique in particle-beam (PB) LC–MS was investigated. Using a laboratory-built surface ionization probe with a platinum tip, several ionization phenomena were observed, *i.e.*, thermal surface ionization (TSI), hyperthermal surface ionization (HSI) and alkali metal addition. Although TSI experiments suggest that kinetic energy is added to the molecules in the PB, the increase in kinetic energy is still insufficient to induce efficient HSI. TSI in combination with LC–PB-MS leads to highly improved detection limits of tetraalkylammonium salts. The use of the SI probe as a thermionic emitter of alkali metal ions for the formation of alkali metal adduct ions leads to sensitive detection of crown ethers and to a considerably extended upper mass limit for polyethylene glycol samples in comparison with standard ammonia chemical ionization conditions.

INTRODUCTION

In 1923, Langmuir and Kingdon [1] described the phenomenon of surface ionization (SI) for the emission of alkali metal ions from metal surfaces. Further research in this field revealed that an atom or a molecule that adsorbs on a surface can be desorbed as either a positive or a negative ion, depending on its ionization potential or its electron affinity, the surface workfunction and the temperature of the surface. Surface ionization appeared to offer the highest possible ionization efficiency, but unfortunately only for compounds with a low ionization potential, *i.e.*, alkali metals [2,3], or compounds with a high electron affinity. Therefore, surface ionization never became a standard ionization technique in organic mass spectrometry. This situation might change because Amirav and co-workers [4–6] demonstrated that the energy barrier for the hyperthermal surface ionization of compounds can be overcome by increasing the molecular kinetic energy. The use of a supersonic or a so-called hyperthermal molecular beam in combination with gas chromatography–mass spectrometry (GC–MS) offers an improved ionization efficiency [4–6].

Because the particle-beam (PB) interface forms a high-velocity beam of molecules and molecule aggregates by expansion of the mobile phase into the momentum separator of the interface [7], the potential of SI in combination with particle-beam mass spectrometry has been investigated in our laboratory. The use of SI in particle-beam liquid chromatography–mass spectrometry (LC–PB-MS) may widen the applicability range of the particle-beam interface and improve its performance in terms of achiev-

* Corresponding author.

0021-9673/93/$06.00

able detection limits as a result of improved ionization efficiencies.

In our experiments it appeared that several ionization phenomena could be observed, *i.e.*, thermal surface ionization (TSI), hyperthermal surface ionization (HSI) and alkali metal addition. Therefore, in our research into the potential of surface ionization as an ionization technique in LC–PB-MS, three strategies were investigated. It is important to realize that all SI data presented here were obtained in the filament-off mode. For the TSI analysis of tetraalkylammonium (TAA) salts, a comparison was made between TSI and electron impact (EI) ionization with respect to the ions generated and the detection limits achieved. For the analysis of polyethylene glycol (PEG) samples a comparison was made between alkali metal addition and standard ammonia chemical ionization (CI) conditions.

EXPERIMENTAL

Apparatus

The experiments were performed on a Finnigan MAT (San José, CA, USA) TSQ-70 triple quadrupole mass spectrometer. For the LC–PB-MS experiments the mass spectrometer was equipped with a Hewlett-Packard (Palo Alto, CA, USA) HP 59980 particle-beam interface. The particle-beam interface was coupled to the mass spectrometer with a *ca.* 15 cm laboratory-made stainless-steel transfer tube. A pneumatic nebulizer with helium as a nebulization gas was used. The solvent-delivery system consisted of an LKB (Bromma, Sweden) Model 2150 LC pump, while samples were introduced via a Rheodyne (Cotati, CA, USA) Model 7125 injection valve with a 20-μl sample loop.

For the surface ionization experiments a special water-cooled surface ionization probe was built, which was inserted into the ion volume of the ion source through the direct insertion probe inlet. Slightly modified source ion volumes were used in order to insert the SI probe. The tip of the probe was made of platinum and was positioned in such a way that the angle between the particle beam and the surface was 45°, as illustrated in Fig. 1. The tip of the probe could

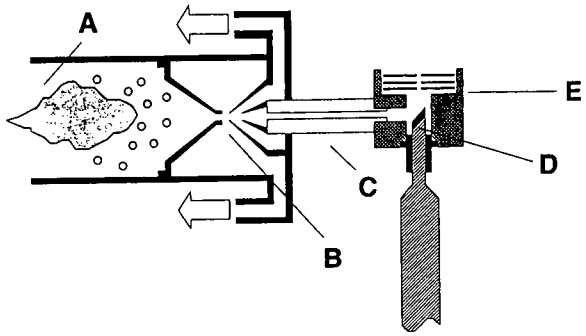

Fig. 1. Schematic representation of the LC–PB-SI-MS system. A = Desolvation chamber; B = momentum separator; C = *ca.* 15-cm transfer tube; D = surface ionization probe with platinum surface; E = ion source.

be heated to about 1300°C. The surface probe-tip temperature was monitored via a platinum *vs.* platinum–10% rhodium thermocouple, which was connected to the lens 41 (L41) potential connection in order to bias the probe tip 0–5 V with respect to the ion volume for positive ions. Prior to every experiment the probe bias was optimized for the signal of the molecular species (molecular ion or cationized molecule). All surface ionization experiments were performed in the filament-off mode, monitoring only positive ions. The source temperature for the SI, EI and CI experiments was set at 250°C.

Thermal surface ionization

For the TSI experiments several tetraalkylammonium (TAA) salts were used [8]. EI mass spectra were obtained using a standard GC–EI ion volume at a source temperature of 250°C. The EI experiments were carried out in the filament-on mode, whereas SI experiments were performed in filament-off mode at an oxygen source pressure of *ca.* 150 Pa using a slightly modified EI ion volume.

For nebulization into the desolvation chamber, 1.5–2.5 l/min of helium was used. Methanol was used as the mobile phase at a flow-rate of 0.1–1.0 ml/min. The temperature of the desolvation chamber was kept at 45°C. All experiments were performed in the flow-injection analysis mode, monitoring the ions either in the single-ion or full-scan mode.

Hyperthermal surface ionization

In the LC–SI-MS experiments, 0.5 ml/min of acetonitrile was used as the mobile phase for the column bypass injection of 280 ng of anthracene ($M_r = 178$) at a surface probe tip temperature of 1100°C. The desolvation chamber was adjusted to 45°C.

For the GC–SI-MS experiments the mass spectrometer was coupled to a Varian (Sunnyvale, CA, USA) capillary GC system equipped with a 0.5-m CP-Sil 5 capillary column. A 1-μl volume of anthracene in acetonitrile was injected in the splitless mode at injector and column temperatures of 200 and 100°C, respectively. The transfer line was set to the highest possible temperature of 350°C for maximum response.

Both LC–MS and GC–MS experiments were performed with a modified EI ion volume. For the oxidation of the platinum probe surface in both the LC–MS and GC–MS experiments oxygen was introduced into the ion source via the CI reagent gas inlet at a source pressure of 150–200 Pa. Most experiments were performed in the single-ion detection mode, monitoring the molecular ion at m/z 178.

Alkali metal addition

Methanol was used at a flow-rate of 0.5 ml/min for the column bypass injection of several crown ethers in NH_3 CI and in combination with the SI probe. The desolvation chamber was adjusted to 45°C. The SI probe tip was inserted into a modified CI ion column. For source pressure experiments both O_2 and NH_3 were introduced into the ion source via the reagent gas inlet.

For the chromatographic separation of PEG samples, a 25 cm × 4.6 mm I.D. Hypersil 5-μm C_{18} column was used. The separation of a 10 mg/ml of PEG 1540 in water was performed with methanol–water (55:45, v/v) as the mobile phase at a flow-rate of 0.5 ml/min, monitoring the alkali metal adduct ions in the full-scan mode. The desolvation chamber was adjusted to a slightly higher temperature of 50°C. Optimum response in LC–SI-MS was achieved at a surface temperature of 1100°C. For the SI experiments the O_2 source pressure was 30 Pa whereas for the CI experiments the NH_3 source pressure was adjusted to 500 Pa.

Chemicals

Tetraalkylammonium (TAA) salts were purchased from Aldrich-Chemie (Steinheim, Germany). Anthracene ($M_r = 178$) was obtained from Merck (Darmstadt, Germany), benzo-15-crown-5 ($M_r = 268$), dibenzo-18-crown-6 ($M_r = 360$) and dicyclohexano-18-crown-6 ($M_r = 372$) from Fluka (Buchs, Switzerland), PEG 1540 from Sigma (St. Louis, MO, USA) and methanol and acetonitrile (analytical-reagent grade) from J.T. Baker (Deventer, Netherlands).

RESULTS AND DISCUSSION

Thermal surface ionization

The limited sensitivity of ionic compounds in the EI mode, which is related to their low volatility, makes LC–PB-MS less suitable for the analysis of this type of compound. The sample consumption for the EI-MS analysis of tetraalkylammonium salts as described in the literature [9,10] is of the order of 1 mg. As far as we known, only Hsu [11] has reported the combination of ion chromatography with particle-beam mass spectrometry for the determination of organic anionic compounds. However, the full-scan detection limits of *ca.* 100 ng were high.

Thermal emission of cations and anions can be achieved simply by heating a surface on which salts have been deposited [12]. Thermal surface ionization mass spectra for several tetraalkylammonium (TAA) salts have been reported by Schade *et al.* [13] using surface temperatures of at least 500°C.

The use of thermal surface ionization as an ionization technique in LC–PB-MS results in the formation of TAA ions at SI probe temperatures as low as 250°C [8]. In Fig. 2 both the PB-EI and PB-TSI spectra of *ca.* 100 ng of tetrahexylammonium perchlorate are shown. For TAA compounds with the general formula R_4N^+ the $R(CH_3)N=CH_2^+$ and $R_2N=CH_2^+$ fragment ions are the major ions observed in the EI mass spectrum, whereas in TSI no fragmentation is observed and the mass spectrum is determined

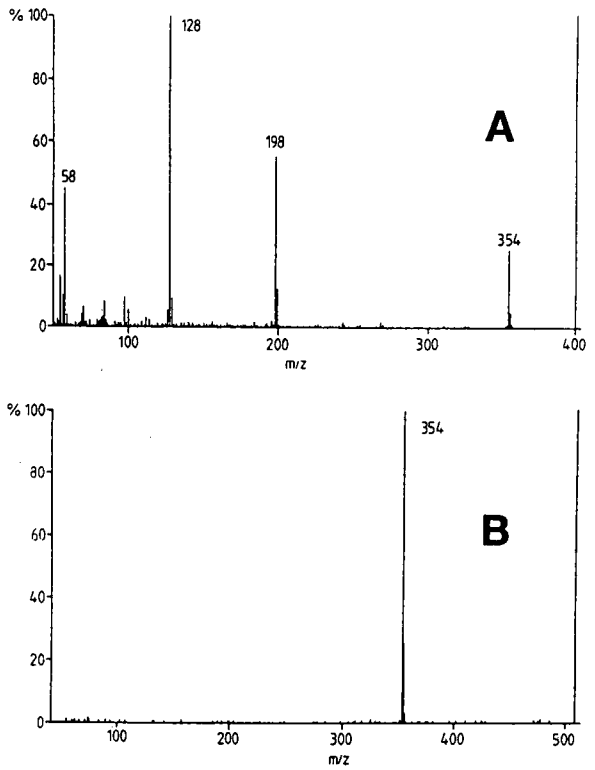

Fig. 2. Mass spectra of tetrahexylammonium (formula mass = 354) perchlorate obtained in (A) filament-on (EI) mode and (B) filament-off (SI) mode at a probe temperature of 250°C.

by an intense signal due to the molecular cation, R_4N^+.

It should be noted that the mass spectra obtained in TSI with the particle-beam interface differ from those reported by Schade *et al.* [13,14]. They observed considerable fragmentation, whereas in our experiments no significant fragmentation was observed. This indicates a difference in heat transfer to the molecules, which in fact may already be concluded from the differences in the experimental set-up. In TSI with PB the thermal energy is also used for the evaporation of solvent molecules partly clustered to the analyte in the particles. However, it is important to emphasize that soft ionization of ionic compounds can be achieved in this way.

The effect of the probe temperature on the intensity of various TAA salts shows slightly different optima [8]. However, the appearance of TSI at temperatures as low as 250°C, instead of the 500°C reported by Schade *et al.* [13], suggests that kinetic energy is transferred to the molecules in the particle beam by the expansion of the mobile phase into the momentum separator of the interface.

The performance of TSI under PB conditions is expected to be determined by two factors: the temperature of the TSI surface and a kinetic component. The kinetic energy of the molecular beam can be influenced by the flow-rates of the mobile phase and of the nebulization gas. A decrease in the liquid flow-rate from 1 to 0.2 ml/min resulted in a tenfold increase in the signal for tetrabutylammonium, whereas an increase in the gas flow-rate from 1.5 to 2.5 l/min resulted in a fourfold increase in signal. These effects are common in particle-beam interfacing, as these parameters affect the transmission through the interface in two ways: a decrease of the droplet size, improving the evaporation rate of the droplets, and an enlargement of the pressure difference between the desolvation chamber and the first pumping stage in the momentum separator, resulting in a higher kinetic energy of the particles [15].

By optimizing the LC–PB-TSI-MS system, a very sensitive method is obtained for the determination of TAA salts. This is demonstrated in Fig. 3, which represents the chromatogram for two injections of 2 pg of tetrabutylammonium bromide. The chromatogram was recorded in the single-ion detection mode at m/z 242, applying a

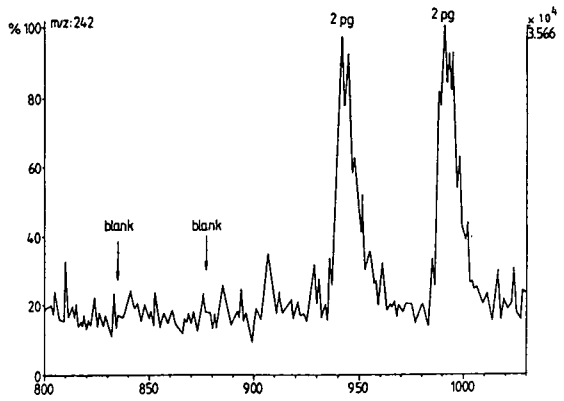

Fig. 3. TSI mass chromatogram for two injections of 2 pg of tetrabutylammonium (formula mass = 242) bromide recorded in the single-ion detection mode at m/z 242, applying a probe temperature of 600°C.

probe temperature of 600°C. The detection limit increases for larger TAA salts. As an example, for tetraoctylammonium bromide a *ca.* fivefold higher detection limit over tetrabutylammonium bromide is observed. These results show that detection limits obtained in particle-beam SI for TAA salts compare well with those obtained using other techniques such as electrospray [16] and ionspray [17]. The calibration graphs for particle-beam TSI show non-linearity at lower concentrations. This is in accordance with PB-EI results reported by others [18]. The observation of this phenomenon under TSI conditions indicates that the non-linearity is caused by decreased transmission in the momentum separator rather than by ionization problems in the ion source. It has been shown that the problem of non-linearity in quantification can be solved by the use of isotope dilution procedures [18,19].

(Hyperthermal) surface ionization

As pointed out in the Introduction, SI as an ionization technique in organic mass spectrometry is suitable for only a very limited class of compounds [20–23]. This is illustrated by the Saha–Langmuir equation for the formation of positive ions [24,25]:

$$\alpha = A \exp[(\phi - IP)/kT] \quad (1)$$

where $\alpha = n^+/n^0$ is the ratio of the number of positive ions to neutral species evaporating from the surface, A is the ratio of the statistical weights of the ionic and neutral states of the compound, ϕ is the workfunction of the surface, IP is the ionization potential of the compound, k is the Boltzmann constant and T is the absolute temperature of the surface. For an arbitrary compound with a defined ionization potential, the yield of positive ions desorbing from a surface is determined by the surface workfunction and the surface temperature. The highest yield is obtained for surfaces with a high workfunction or at high surface temperatures. Various materials such as tungsten, rhenium, platinum and diamond are often used as surfaces in SI experiments because of their high surface workfunction [5,20]. The theoretical surface workfunction for the platinum probe used in our experiments is 5.7 eV, which is much lower than the ionization potential of most compounds, explaining the low yield of desorbed positive ions. Additionally, this yield is very much affected by modifications of the surface. As an example, oxidation of the surface increases the surface workfunction [5,20], whereas contamination of the surface with various salts lowers the surface workfunction.

Another way to increase the yield of desorbed ions is to increase the surface temperature. This is illustrated by the fact that an increase in the platinum probe tip temperature results in the emission of larger amounts of sodium, potassium and caesium ions, as illustrated in Fig. 4 for sodium and potassium. The formation of alkali metal ions can be explained by alkali metal contamination, which readily occurs on the tip of the SI probe. The high yield of alkali metal ions is explained by the fact that alkali metals are characterized by a very low ionization potential. The reason why the formation of potassium cations starts at a lower temperature compared with the formation of sodium cations is that the ionization potential of potassium (4.3 eV) is lower than that of sodium (5.1 eV).

Anthracene has an ionization potential of 7.5 eV, which is relatively low. However, when 280 ng (14 ng/μl) of anthracene is injected into the LC–PB-SI-MS system at a probe temperature of about 1100°C, a full-scan spectrum is obtained with a signal-to-noise ratio of only 20. Increasing the surface workfunction by oxidizing the platinum surface, realized by introducing oxygen

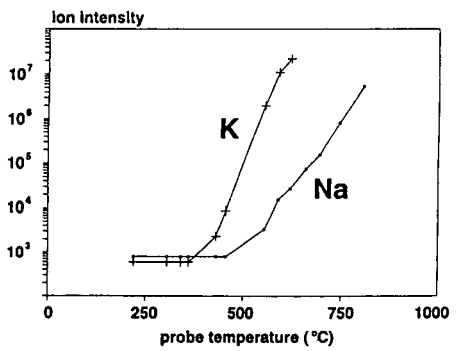

Fig. 4. Potassium and sodium background intensity as a function of the surface probe tip temperature. No liquid was introduced into the particle-beam interface.

into the ion source at a source pressure of 150–200 Pa, results in an improvement in the signal-to-noise ratio. Still, under these experimental conditions sensitive detection of anthracene was not achieved. Improvement of the ionization efficiency and the resulting detection limits for anthracene and other compounds can theoretically be achieved by increasing the probe-tip temperature. However, too high surface temperatures result in serious thermal degradation of many organic compounds.

In order to approach more sensitive HSI conditions [5] in combination with GC–MS, a capillary GC system with a short column and a splitless injector was coupled to the mass spectrometer. With this set-up the solvent is easily separated from the analyte and retention times are low. The analyte expanding at the end of the capillary column into the vacuum of the ion source collides with the surface, as illustrated in Fig. 5. A 1.4 ng (1.4 ng/μl) injection of anthracene resulted in a spectrum (Fig. 6) with a much better signal-to-noise ratio than was the case for the 14 ng/μl sample solution in the PB-SI experiments, even when it is taken in account that the transmission of the particle-beam interface at high concentrations of *ca.* 20% [8] results in a loss of analyte. The increase in the temperature of the transfer line from 250 to 350°C resulted in a more than tenfold improvement in detectability, because of a more pronounced expansion at the end of the capillary column. The signal-to-noise ratio for anthracene under GC–HSI-MS conditions is at least a factor of 1000 better than under LC–SI-MS conditions. A

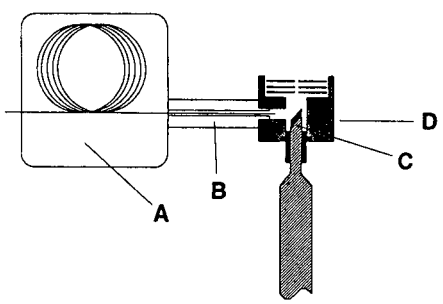

Fig. 5. Schematic representation of the GC–SI-MS system. A = Capillary GC system with splitless injector and a 0.5-m column; B = heated transfer line; C = surface ionization probe with platinum surface; D = ion source.

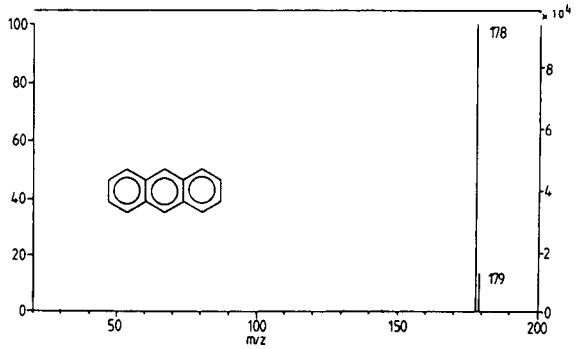

Fig. 6. GC–HSI mass spectrum of 1.4 ng of anthracene (M_r = 178) after splitless injection at a surface temperature of 1100°C.

lower GC–HSI-MS sensitivity is observed for compounds with an ionization potential of >7.5 eV, *i.e.*, the ionization potential of anthracene, which can be explained by differences in the experimental setup. An important difference with the GC–HSI-MS system as described by Amirav [5] is that the use of a nozzle–skimmer arrangement by the latter and of H_2 as an expanding gas instead of He result in a much higher kinetic energy of the molecular beam up to 30 eV.

A very important conclusion that can be drawn from these experiments is that the increase in kinetic energy in case of the PB-SI experiments, caused by the expansion of the mobile phase into the momentum separator of the interface, is too low to overcome the energy barrier for increasing the ionization efficiency. Additionally, contamination of mobile phases with various salts and the resulting permanent delivery of surface-contaminating compounds to the probe surface in particle-beam MS will lower both the surface workfunction and the ionization efficiency. Experiments are currently being performed to improve the nozzle–skimmer part of the interface in order to create supersonic molecular beams in LC–PB-MS.

Alkali metal addition

Alkali metal cations are easily formed by so-called thermionic emitters [26]. They cationize most compounds containing π- or n-donor sites to produce alkali metal adduct ions. Various

studies have been performed using alkali metal ions as reagent ions under atmospheric pressure CI [27] and under normal CI conditions [28,29] and in combination with laser desorption mass spectrometry [30,31]. The use of metal ions as special reagents in analytical mass spectrometry has been reviewed by Teesch and Adams [32]. Alkali metal addition is assumed to be a three-body process, in which a neutral molecule collides with an ion–molecule complex and removes an excess amount of energy, thus stabilizing the alkali metal adduct ion. On the basis of this model, the cationization process would be especially efficient in a high-pressure environment, as the major component gas molecules serve as the third body in the analyte addition reaction with alkali metal ions. Bombick *et al.* [29] reported the addition of potassium to various compounds at helium and acetone source pressures varying between 1 and 100 Pa.

In this section, the applicability of alkali metal metals as a source of CI reagent ions in combination with the use of the SI probe in LC–PB-MS is discussed. Several crown ethers were used as model compounds. Liou and Brodbelt [33] reported the relative alkali metal ion affinities of various crown ethers. Injection of 200 ng of dicyclohexano-18-crown-6 at a probe temperature of 750°C leads to a spectrum that is mainly characterized by $[M + Na]^+$ and very small $[M + K]^+$ ions. It is remarkable that, despite the *ca.* twofold higher affinity of 18-C-6 crown ethers [33] for potassium and the *ca.* fifteenfold higher potassium background over sodium under the experimental conditions, the $[M + Na]^+$ ion is the base peak in the spectrum.

Several studies have been carried out of the exact mechanism of the alkali metal adduct formation [30,31]. Purely thermal desorption of $[M + Na]^+$ ions has been reported for a mixture of a crown ether with sodium iodide [12]. The $[M + Na]^+$ ions are observed at temperatures below the onset for thermionic emission of Na^+, thus excluding a gas-phase ionization mechanism by ion–molecule reactions. The thermal desorption of alkali metal adduct ions was ascribed to the high stability of the $[M + Na]^+$ complex and to a low Coulomb binding energy between the alkali metal and halogen ions. However, for sucrose Stoll and Röllgen [31] reported a gas-phase ionization mechanism via ion–molecule reactions without any contribution from direct evaporation of preformed cationized molecules.

In Fig. 7, the sodium background intensity and the peak area for the sodiated species of several 200-ng injections of dicylohexano-18-crown-6 ($M_r = 372$) are plotted as a function of the probe tip temperature. It is clearly demonstrated that the optimum for the sodium adduct formation lies well below the minimum temperature required for thermionic emission of sodium ions. This observation corresponds with the former theory, that the alkali metal adduct formation for crown ethers is a surface ionization process, which excludes a direct relationship to the background intensity of the various alkali metal ions in the spectrum. Variation of the source pressure between 10 and 200 Pa had only a slight influence on the alkali metal adduct intensity, suggesting that the alkali metal adduct formation is a surface process rather than a three-body gas-phase process. Additional experiments were performed by contaminating the probe surface with lithium acetate. Despite the lack of lithium in the mobile phase, $[M + Li]^+$ ions were observed in the spectrum. This phenomenon seems to prove that the alkali metal adduct formation is the result of surface cationization rather than thermal desorption of preformed alkali metal adduct ions.

Repetitive injections of some crown ethers

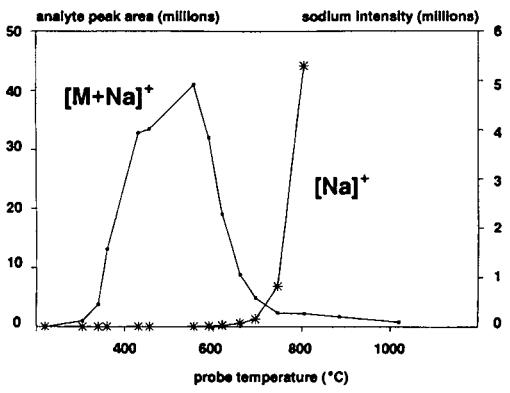

Fig. 7. Sodium background intensity and peak area for the sodiated species of several 200-ng injections of dicyclohexano-18-crown-6 ($M_r = 372$) plotted as a function of the probe-tip temperature.

result in reproducible peak areas for a long period of time, because the permanent contamination of mobile phases results in a permanent delivery of alkali metals to the surface. Therefore, no sodium or potassium needs to be added to the mobile phase. Addition of 0.5 m*M* of lithium acetate to the mobile phase results in the onset of lithium cations in the background spectrum. Under these conditions the spectrum of dicyclohexano-18-crown-6 is now dominated by the $[M + Li]^+$. It takes almost 1 h to condition the probe surface before optimum ionization conditions are obtained. A minor disadvantage of the addition of alkali metal salts (>0.1 m*M*) to the mobile phase is the serious contamination of the first skimmer in the PB interface. At a probe temperature of 600°C and with addition of 0.5 m*M* lithium acetate, the minimum detectable amount for dibenzo-18-crown-6 after some minor optimization is *ca.* 200 pg, as is illustrated in Fig. 8. This minimum detectable amount can be lowered significantly by improving the linear dynamic range of the particle-beam interface as a result of the simultaneous injection of a large amount of a carrier [18,34]. For instance, for 100 ng of benzo-15-crown-5 ($M_r = 268$) with simultaneous injection of 20 μg of dibenzo-18-crown-6 ($M_r = 360$), a fifteenfold improvement in response for the 15-C-5 crown ether is obtained.

The influence of the probe temperature on the alkali metal adduct formation was investigated for various PEG samples. It appears that a higher probe temperature is needed for molecules with a higher molecular mass. For a PEG 1540 sample maximum sensitivity is obtained at a probe temperature of *ca.* 1000°C. Optimum ionization conditions far above the onset temperature for thermionic emission of sodium ions seem to prove that the alkali metal adduct formation for PEG molecules is a gas-phase process, in contrast to the crown ethers for which the alkali metal addition is SI process (see above).

Fig. 9 shows the spectra that are obtained for a PEG component of a PEG 1540 sample after

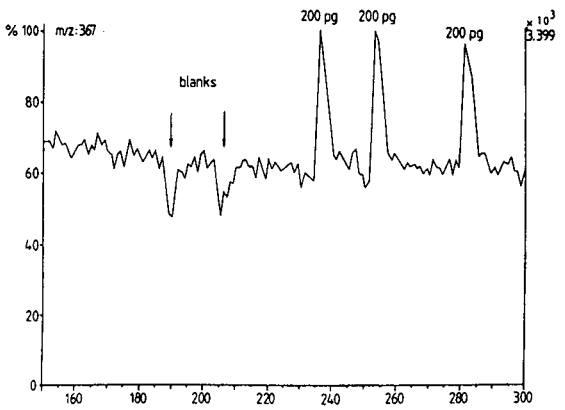

Fig. 8. Mass chromatogram for three 200-pg injections of dibenzo-18-crown-6 ($M_r = 360$) with 0.5 m*M* lithium acetate in methanol as the mobile phase at a probe temperature of 600°C, obtained by single-ion monitoring of the $[M + Li]^+$ intensity at *m/z* 367.

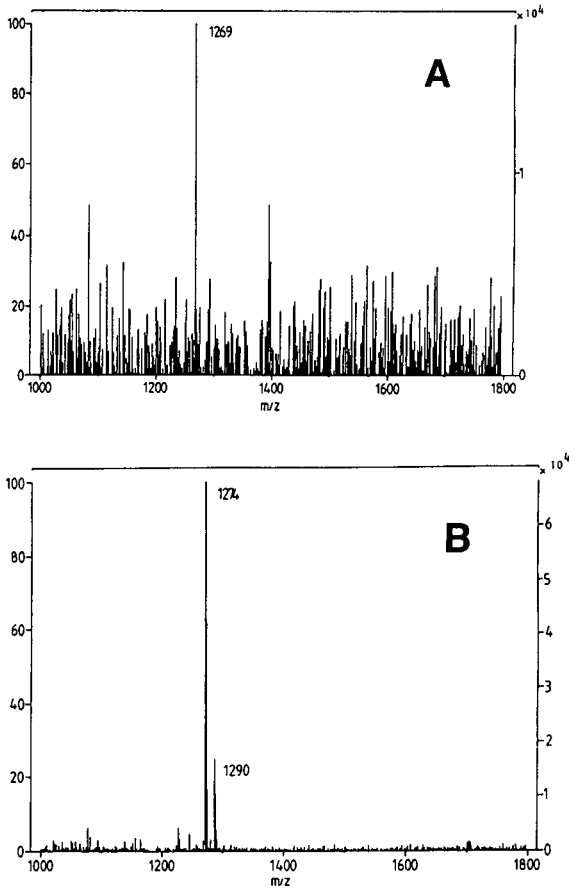

Fig. 9. Spectra from the PEG component $HO[C_2H_4O]_{28}H$ ($M_r = 1251$) of a PEG 1540 sample after chromatographic separation. (A) Obtained under CI conditions at an NH_3 source pressure of 500 Pa; (B) obtained under SI conditions at a probe temperature of 1100°C at a O_2 source pressure of 30 Pa.

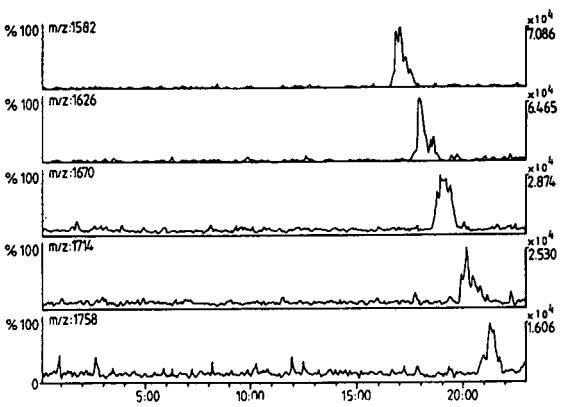

Fig. 10. Partial representation of the chromatogram for the separation of a PEG 1540 sample (200 μg) using methanol–water 55:45 (v/v) as the mobile phase at a flow-rate of 0.5 ml/min and a 25 cm × 4.6 mm I.D. Hypersil 5-μm C_{18} column.

chromatographic separation. In combination with the surface ionization probe, much better sensitivity can be obtained compared with standard CI conditions with NH_3 as the reagent gas. In fact, the $[M + NH_4]^+$ peak at m/z 1269 is the largest ammoniated molecule observed in PB-CI. Additionally, the upper mass limit for LC–PB-MS combination with the heated probe is higher compared with CI conditions, as is shown in Fig. 10. The chromatogram was recorded in the full-scan mode at a probe temperature of 1100°C, while no alkali metal salts were added to the mobile phase. Under these conditions the highest mass that could be observed was the $[M + Na]^+$ ion at m/z 1758. This upper mass limit for the polar PEG 1540 sample is close to the highest reported upper mass limit for the LC–PB-MS detection of non-polar styrene oligomers [35].

CONCLUSIONS

Owing to the expansion of the mobile phase into the momentum separator of the particle-beam interface, a certain amount of kinetic energy is added to the molecules in the beam of particles. However, this increase in kinetic energy is insufficient to induce efficient hyperthermal surface ionization. Thermal surface ionization appears to be a soft ionization technique for the sensitive detection of tetraalkylammonium ions. For tetrabutylammonium bromide, detection limits as low as 2 pg can be achieved. Introduction of O_2 into the ion source leads to improved sensitivity for various compounds, probably owing to the increase in the workfunction as a result of oxidation of the SI probe tip. The formation of alkali metal adduct ions for crown ethers is probably the result of surface cationization, rather than thermal desorption of preformed alkali metal adduct ions. Because the alkali metal contamination of mobile phases results in a permanent delivery of sodium and potassium to the probe surface, for alkali metal addition experiments no alkali metals have to be added to the liquid. The alkali metal adduct formation can be influenced by adding other alkali metal salts such as lithium acetate to the mobile phase. At a probe temperature of 600°C and with addition of 0.5 m*M* lithium acetate to the mobile phase, the minimum detectable amount for dibenzo-18-crown-6 is *ca.* 200 pg. For the analysis of PEG samples the upper mass limit for LC–PB-MS in combination with the heated probe is much higher compared with standard NH_3 CI conditions. The highest mass that could be observed for a PEG 1540 sample was the $[M + Na]^+$ ion at m/z 1758. Improvement of the nozzle–skimmer configuration for the creation of supersonic molecular beams in LC–PB-MS in combination with the surface ionization probe will offer a wider applicability range for this type of LC–MS.

ACKNOWLEDGEMENT

The authors thank Hans Robbers for his contribution to the development of the surface ionization probe.

REFERENCES

1 I. Langmuir and K.H. Kingdon, *Phys. Rev.*, 21 (1923) 380.
2 J.P. Blewett and E.J. Jones, *Phys. Rev.*, 50 (1936) 464.
3 M.J. Hogan, P.P. Ong, J.L. Ang and K.K. Cheang, *Int. J. Mass Spectrom. Ion Processes*, 116 (1992) 249.
4 A. Danon and A. Amirav, *Isr. J. Chem.*, 29 (1989) 443.
5 A. Amirav, *Org. Mass Spectrom.*, 26 (1991) 1.

6 S. Dagan, A. Danon and A. Amirav, *Int. J. Mass Spectrom. Ion Processes*, 113 (1992) 157.
7 R.C. Willoughby and R.F. Browner, *Anal. Chem.*, 56 (1984) 2626.
8 R.A.M. van der Hoeven, A.P. Tinke, W.M.A. Niessen and J. van der Greef, *Rapid Commun. Mass Spectrom.*, 7 (1993) 37.
9 T.D. Lee, W.R. Anderson and G.D. Daves, Jr., *Anal. Chem.*, 53 (1981) 304.
10 K. Isa and Yayoi Yamada, *Org. Mass Spectrom.*, 18 (1983) 229.
11 J. Hsu, *Anal. Chem.*, 64 (1992) 434.
12 R. Stoll and F.W. Röllgen, *Org. Mass Spectrom.*, 16 (1981) 72.
13 U. Schade, R. Stoll and F.W. Röllgen, *Org. Mass Spectrom.*, 16 (1981) 441.
14 U. Schade, R. Stoll and F.W. Röllgen, *Int. J. Mass Spectrom. Ion Phys.*, 46 (1983) 337.
15 A.P. Tinke, R.A.M. van der Hoeven, W.M.A. Niessen, U.R. Tjaden and J. van der Greef, *J. Chromatogr.*, 554 (1991) 119.
16 A. Raffaelli and A.P. Bruins, *Rapid Commun. Mass Spectrom.*, 5 (1991) 269.
17 J.J. Conboy and J.D. Henion, *Anal. Chem.*, 62 (1990) 800.
18 A. Apffel and M.L. Perry, *J. Chromatogr.*, 554 (1991) 103.
19 F.R. Brown and W.M. Draper, *Biol. Mass Spectrom.*, 20 (1991) 521.
20 T. Fujii, *Int. J. Mass Spectrom. Ion Processes*, 57 (1984) 63.
21 T. Fujii and T. Kitai, *Int. J. Mass Spectrom. Ion Processes*, 71 (1986) 129.
22 T. Fujii and H. Jimba, *Int. J. Mass Spectrom. Ion Processes*, 79 (1987) 221.
23 T. Fujii, H. Ishi and H. Jimba, *Int. J. Mass Spectrom. Ion Processes*, 93 (1989) 73.
24 K.H. Kingdon and I. Langmuir, *Proc. R. Soc. London, Ser. A*, 107 (1925) 61.
25 E.Y. Zandberg and U.K. Rasulev, *Russ. Chem. Rev.*, 51 (1982) 819.
26 M.J. Hogan, P.P. Ong and K.K. Cheang, *Int. J. Mass Spectrom. Ion Processes*, 116 (1992) 249.
27 T. Fujii, *Anal. Chem.*, 64 (1992) 775.
28 R.V. Hodges and J.L. Beauchamp, *Anal. Chem.*, 48 (1976) 825.
29 D. Bombick, J.D. Pinkston and J. Allison, *Anal. Chem.*, 56 (1984) 396.
30 G.J.Q. van der Peyl, K. Isa, J. Haverkamp and P.G. Kistemaker, *Org. Mass Spectrom.*, 16 (1981) 416.
31 R. Stoll and F.W. Röllgen, *Z. Naturforsch., Teil A*, 37 (1982) 9.
32 L.M. Teesch and J. Adams, *Org. Mass Spectrom.*, 27 (1992) 931.
33 C.C. Liou and J.S. Brodbelt, *J. Am. Soc. Mass Spectrom.*, 3 (1992) 543.
34 T.A. Bellar, T.D. Behymer and W.L. Budde, *J. Am. Soc. Mass Spectrom.*, 1 (1990) 92.
35 G.G. Jones, R.E. Pauls and R.C. Willoughby, *Anal. Chem.*, 63 (1991) 460.

Journal of Chromatography, 647 (1993) 73–78
Elsevier Science Publishers B.V., Amsterdam

CHROMSYMP. 2848

Applications of dual-beam thermospray liquid chromatography–mass spectrometry

Wim J.L. Genuit* and Janjaap de Boer

Koninklijke/Shell-Laboratorium, Amsterdam (Shell Research B.V.), P.O. Box 3003, 1003 AA Amsterdam (Netherlands)

ABSTRACT

A dual-beam thermospray system has been constructed, by which the requirements of the electrolyte ion evaporation process have been decoupled from those of the separation and volatilization of the analytes. The dual-beam system has a high flexibility with regard to mobile phase polarity, flow-rate and eluent vaporizer temperature. Results are presented from applications of dual-beam thermospray in the coupling of organic gel permeation chromatography with mass spectrometry, and in gradient elution liquid chromatography. In a comparison of the dual-beam with the single-beam thermospray technique for two thermolabile compounds, the mass spectra obtained with the dual-beam system show much less degradation.

INTRODUCTION

Coupled liquid chromatography–mass spectrometry (LC–MS) has emerged as an important analytical tool since the introduction of the thermospray LC–MS interfacing technique several years ago [1]. Thermospray is compatible with standard reversed-phase liquid chromatographic (RPLC) methods employing aqueous mobile phases, provided that they do not contain non-volatile buffer salts. Ionization of the sample is effected by means of a volatile electrolyte added to the LC eluent, or, alternatively, by chemical ionization with reagent ions which are generated by means of electron bombardment of the solvent vapour, in a "filament-on" or a "discharge" mode of operation. Although somewhat more universal, the last two ionization methods are often not preferred because of their tendency to induce solvent–analyte and fragmentation reactions that complicate the spectra obtained and hamper their interpretation.

A number of limitations of the thermospray technique have to do with conflicting requirements of electrolyte ion evaporation, on the one hand, and of analyte separation and/or volatilization on the other. The vaporizer temperature window for optimum electrolyte ion evaporation is generally narrow. In gradient-elution LC, this necessitates the programming of the temperature according to the varying eluent composition, which implies the determination of the optimum vaporizer temperature at two points along the gradient at least [2]. Eluents with a high water content require a high vaporizer temperature, which may be detrimental to the analysis of compounds that are susceptible to thermal degradation. Furthermore, in our experience, thermospray has serious limitations with regard to chromatographic methods employing non-aqueous mobile phases. In this case, the addition of electrolytes as ionizing agents poses solubility problems. "Filament-on" ionization does not produce sufficiently high ion yields in most cases, while in "discharge" ionization mode the discharge electrode tends to become rapidly contaminated by a carbonaceous deposit produced from the organic solvent. Probably because of such problems, very few reports have appeared

* Corresponding author.

0021-9673/93/$06.00

in the literature on the application of thermospray in combination with non-polar mobile phases [3,4].

The flexibility of the thermospray technique with regard to mobile phases and vaporizer operating conditions can be significantly enhanced by decoupling the ion evaporation process from the analyte volatilization process in a "dual-beam" arrangement with two independently heated vaporizers, in which the eluent is carried by one vaporizer and the electrolyte solution that is used as the ionizing agent is pumped through a second vaporizer (Fig. 1). This dual-beam concept was pioneered by Bütfering *et al.* [5,6] several years ago, but did not find analytical application at that time. An alternative, recently reported [7], approach is based on the introduction of a chemical ionization gas in the thermospray source in combination with filament-on or discharge ionization. We have constructed a dual-beam thermospray source with the initial aim of coupling organic gel permeation chromatography (GPC), with tetrahydrofuran as solvent, to mass spectrometry. Today, the dual-beam system is also used in the majority of all standard reversed-phase LC–MS applications in our laboratory. This paper presents a few examples of applications of dual-beam thermospray in combination with non-polar mobile phases, in gradient-elution LC, and in the analysis of thermolabile compounds.

EXPERIMENTAL

Liquid chromatography

The liquid chromatographic system consisted of a Waters 600MS multisolvent delivery system, and a Waters 490MS multiwavelength UV detector connected in series with the mass spectrometer. For GPC, a 60-cm-long, 100 Å pore size, PL gel column (Polymer Laboratories) was used, with tetrahydrofuran (Merck Lichrosolv HPLC grade) as the mobile phase, at a flow-rate of 1.0 ml/min. Reversed-phase separations were performed with a Waters Novapak C_{18} column, 15 cm × 3.9 mm I.D., and a mobile phase consisting of a mixture of water (purified by a Millipore purification system) and acetonitrile (Rathburn HPLC grade), either in a constant 1:1 composition ratio or in a gradient from 100% water to 100% acetonitrile in 40 min. In both cases, the flow-rate was 1.0 ml/min.

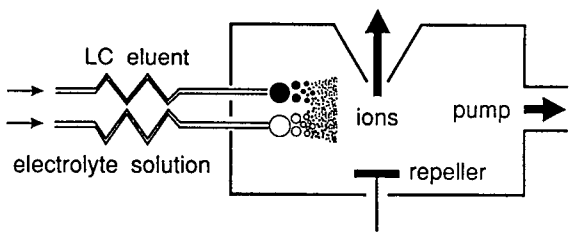

Fig. 1. Diagram of the dual-beam thermospray system.

Mass spectrometry

A Finnigan 4500 triple-stage quadrupole (TSQ) mass spectrometer with a Finnigan INCOS data system was used. The data were obtained in full-scan mode, with a typical scan range of m/z 150–850, at a rate of 1 scan/s. The UV detector signal was fed into the data system through an auxiliary input.

Dual-beam thermospray

A Finnigan MAT 4500 thermospray source was modified into a dual-beam system. The only modification of the source itself relates to the original Vespel® vaporizer plug, which was changed for a similar plug with two parallel holes, 3.0 mm apart, to accommodate the two vaporizer capillaries. The second vaporizer was fed into the vacuum chamber through a port, which in the original design was connected to a vent valve. Both vaporizers were of the original Finnigan MAT type, with sapphire tip. Electrical connections to the second vaporizer were made through the spare pins on one of the electrical feedthrough plugs. The two independent vaporizer temperature-control circuits were similar to the control system that has been described before [8]. In this system, the original time-proportional control circuit has been replaced by one based on phase-angle control, which yielded a much better vaporizer temperature stability. The LC eluent vaporizer was held at a temperature of 65°C, typically. A 0.1 *M* ammonium acetate (Baker reagent grade) aqueous solution was pumped through the second vaporizer at a flow-rate of 1.2 ml/min by a Waters 510 pump. The

temperature of this electrolyte vaporizer was set at 140°C for maximum background ion intensity. For single-beam thermospray operation the ammonium acetate solution, at a flow-rate of 1.0 ml/min, was added post column to the LC eluent. The optimum vaporizer temperature in this case was determined to be 124°C.

RESULTS AND DISCUSSION

Gel permeation chromatography–mass spectrometry

The combination of GPC and MS is a particularly attractive one, because GPC is a relatively fast and easy technique with regard to method development, but it has only limited separation efficiency. In GPC–MS, overlapping elution profiles may be deconvoluted into selected ion chromatograms. Furthermore, mass spectrometry provides GPC with an accurate mass scale calibration in applications where appropriate calibration standards are not available. Fig. 2 shows results of a GPC–MS analysis of a polystyrene A300 standard calibration mixture. The upper five traces represent ion chromatograms at five selected m/z values, corresponding to the ammoniated polystyrene oligomers $n = 3$ to $n = 7$. The bottom trace shows the UV absorbance chromatogram. The mobile phase, tetrahydrofuran, would be incompatible with the ionizing agent, ammonium acetate, in a single-beam thermospray system. Using the dual-beam system, the elution profiles of polystyrene oligomers from $n = 7$ down to $n = 3$ are easily observed. Remarkably, ions corresponding to polystyrene monomers and dimers were not detected. Apparently, these two compounds have a lower ammonium affinity than the higher polystyrene oligomers.

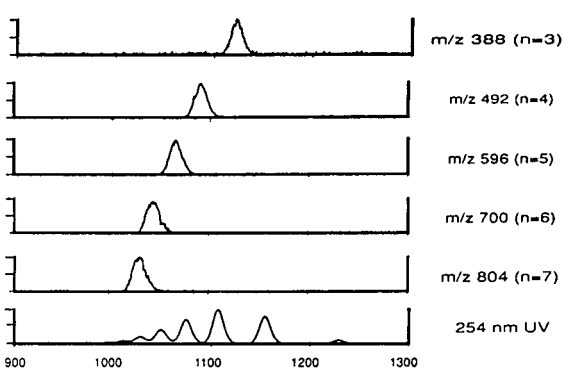

Fig. 2. GPC–MS analysis of a polystyrene A300 sample.

Gradient elution

In the dual-beam system, only the operating conditions (flow-rate, temperature) of the electrolyte vaporizer are critical. The eluent vaporizer conditions are much less critical. The eluent flow-rate and the vaporizer temperature may be varied over a wide range without an appreciable change in sensitivity. On the other hand, the temperature may be kept constant during a change in solvent composition. This is illustrated on an LC–MS analysis of a mixture of polyethylene glycol (PEG400) and alcohol ethoxylate (octanol to dodecanol ethoxylates). For reversed-phase separation, a linear solvent gradient was applied from pure water to pure acetonitrile in 40 min. The eluent vaporizer was set at 65°C and was kept constant. Fig. 3 shows the total ion current trace (bottom) and three mass spectra, the first obtained at high water content of the eluent (summed spectrum of PEG400), and the other two spectra at low water content (spectra of nonanol and undecanol ethoxylates).

Thermolabile compounds

Bütfering *et al.* [6] compared mass spectra obtained by single-beam thermospray and by the dual-beam system, for a number of thermally labile compounds. They reported very similar mass spectra and sensitivities for the two different thermospray modes. However, they used the same vaporizer temperatures in both modes. We find that in the dual-beam set-up, a much lower eluent vaporizer temperature can be applied, without an appreciable loss of sensitivity. We compared the performance of the dual-beam thermospray system, operating at a low eluent vaporizer temperature, with that of the standard single-beam system on two thermolabile compounds, shown in Fig. 4. The first compound, the 2,4-dinitrophenylhydrazone of mesityl oxide, was produced by derivatization of mesityl oxide (4-methyl-3-penten-2-one), an industrial solvent, with 2,4-dinitrophenylhydrazine. This selective UV labelling of aldehydes and ketones by the

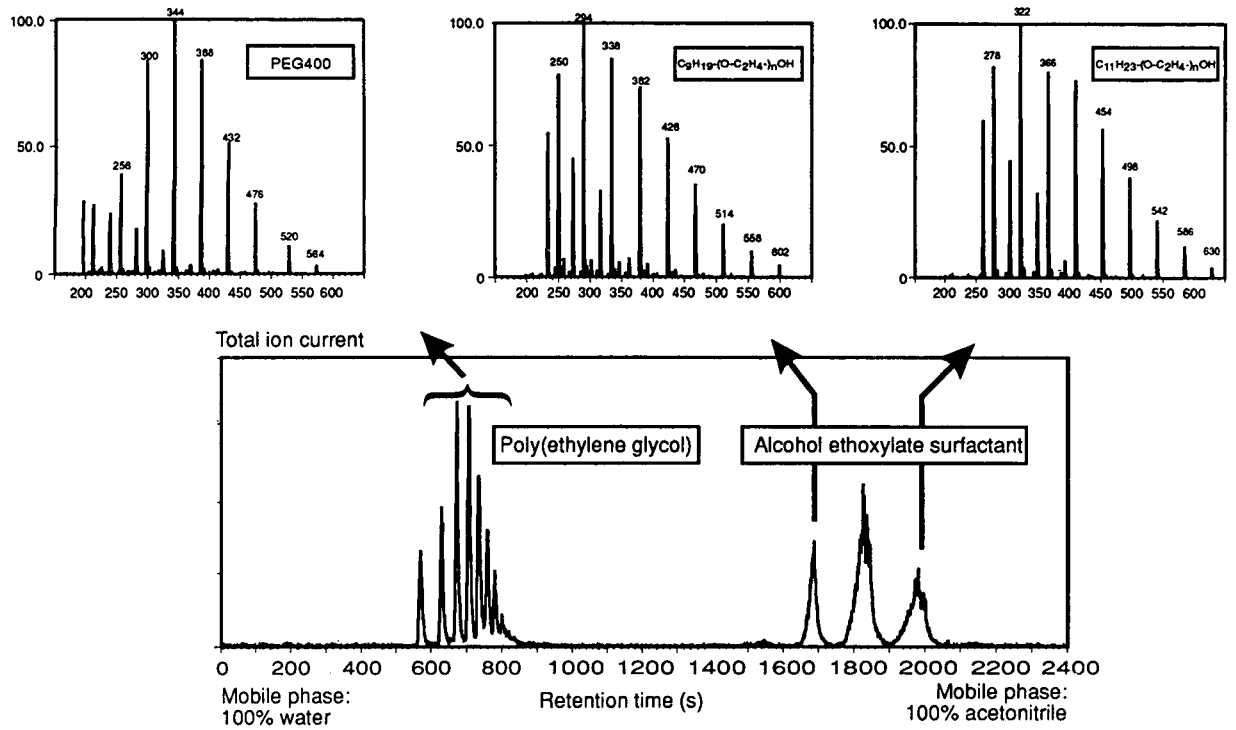

Fig. 3. Gradient elution LC–MS analysis of a mixture of polyethylene glycol (PEG400) and an alcohol ethoxylate surfactant.

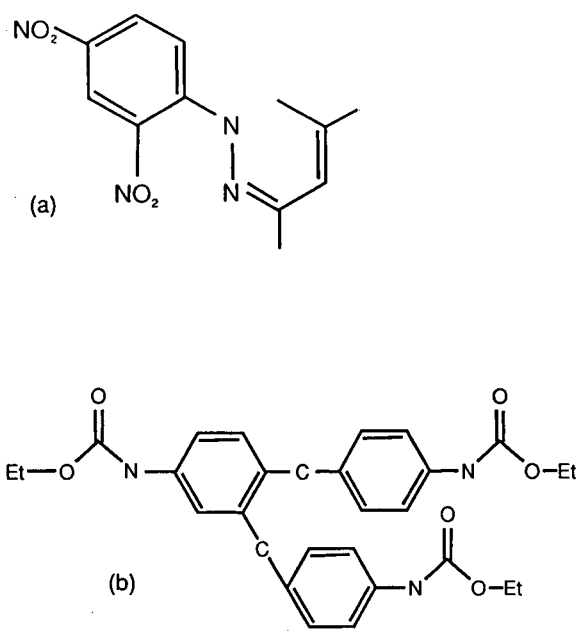

Fig. 4. Structures of (a) 2,4-dinitrophenylhydrazone of mesityl oxide (molecular mass 278) and (b) an urethane prepolymer (molecular mass 519).

reaction with dinitrophenylhydrazine is a well-known method in liquid chromatography. The urethane prepolymer is a product used for the manufacture of polyurethane materials.

Fig. 5 shows the single-beam (top) and the dual-beam (bottom) mass spectra of the first compound. The single-beam spectrum was recorded at a vaporizer temperature of 124°C. Apart from the protonated molecular ion peak at m/z 279, a large number of decomposition product peaks are observed in the spectrum, corresponding to losses of 30 (NO), 32 (O_2) and 46 u (NO_2) and so on. The dual-beam thermospray spectrum was obtained at an eluent vaporizer temperature of 65°C. In contrast to the single-beam spectrum, only two significant peaks are observed, corresponding to the protonated molecular ion and to a loss of 30 mass units (NO) from the molecular ion. Fig. 6 shows the single-beam (top) and the dual-beam (bottom) thermospray mass spectra of the urethane prepolymer. In this example, the difference between the two systems is even more dramatic. Whereas in the dual-beam spectrum fragment ion inten-

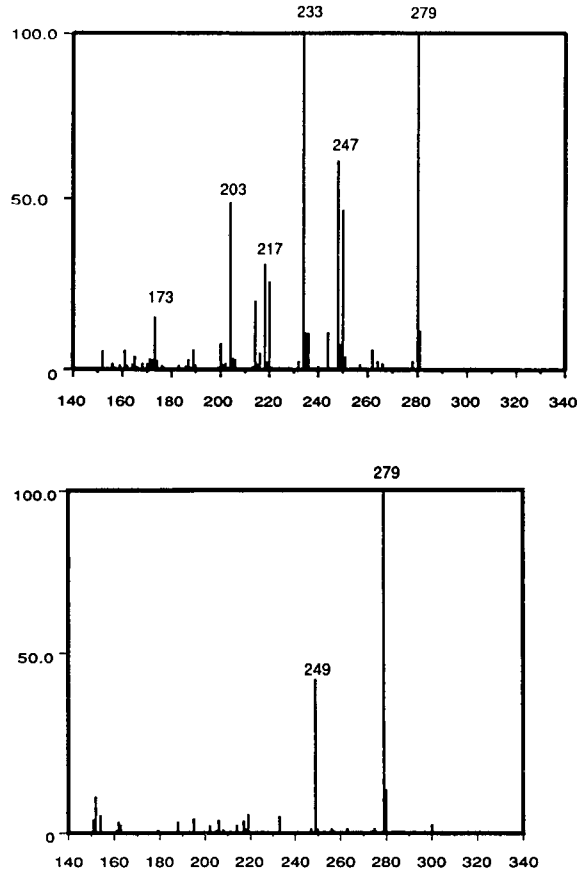

Fig. 5. Comparison of the single-beam (vaporizer 124°C) (top) and dual-beam (vaporizer 65°C) (bottom) thermospray mass spectra of the dinitrophenylhydrazone of mesityl oxide.

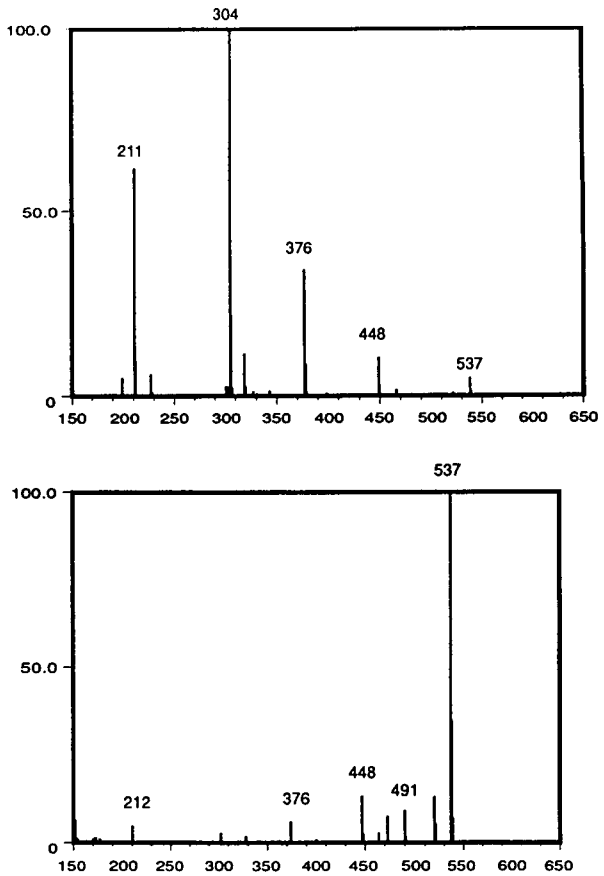

Fig. 6. Comparison of the single-beam (vaporizer 124°C) (top) and dual-beam (vaporizer 65°C) (bottom) thermospray mass spectra of an urethane prepolymer.

sities are less than 15% of the ammoniated molecular ion intensity (m/z 537), in the single-beam thermospray mass spectrum this ammoniated molecular ion peak is hardly observed.

CONCLUSIONS

Applications of dual-beam thermospray in the areas of organic GPC–MS, gradient elution LC and thermolabile compounds have been shown. They highlight the advantages of a dual-beam arrangement over the standard single-beam thermospray system. Much higher flexibility is obtained with regard to mobile phase polarity and flow-rate, and with regard to vaporizer temperature. The dual-beam system enables the soft electrolyte ionization method to be used in combination with non-polar mobile phases, it eliminates the need for vaporizer temperature programming in gradient elution LC and it has a superior performance in the analysis of thermolabile compounds.

ACKNOWLEDGEMENT

We thank H. van Binsbergen and L.M. van der Sman for their technical assistance.

REFERENCES

1 C.R. Blackley, J.J. Carmody and M.L. Vestal, *J. Am. Chem. Soc.*, 102 (1980) 5931.
2 C.H. Vestal, G.J. Fergusson and M.L. Vestal, *Int. J. Mass Spectrom. Ion Proc.*, 70 (1986) 185.
3 D. Barceló, *Org. Mass Spectrom.*, 24 (1989) 898.

4 D. Barceló, G. Durand, R.J. Vreeken, G.J. de Jong and U.A.Th. Brinkman, *Anal. Chem.*, 62 (1990) 1696.
5 L. Bütfering, G. Schmelzeisen-Redeker and F.W. Röllgen, *J. Chem Soc., Chem. Commun.*, (1986) 579.
6 L. Bütfering, G. Schmelzeisen-Redeker and F.W. Röllgen, *J. Chromatogr.*, 394 (1987) 109.
7 R.G.J. van Leuken and G.T.C. Kwakkenbos, *J. Chromatogr.*, 626 (1992) 81.
8 W. Genuit and H. van Binsbergen, *J. Chromatogr.*, 474 (1989) 145.

Journal of Chromatography, 647 (1993) 79–90
Elsevier Science Publishers B.V., Amsterdam

CHROMSYMP. 2786

Particle beam liquid chromatography–mass spectrometry behaviour of polynuclear metal carbonyl compounds

M. Careri*, A. Mangia, P. Manini and G. Predieri

Istituto di Chimica Generale ed Inorganica, Università di Parma, Viale delle Scienze, 43100 Parma (Italy)

V. Raverdino and G. Tsoupras

Hewlett-Packard S.A., Rue de Veyrot 39, 1217 Meyrin 1 (Switzerland)

E. Sappa

Dipartimento di Chimica Inorganica, Chimica Fisica e Chimica dei Materiali, Università di Torino, Via P. Giuria 7, 10125 Turin (Italy)

ABSTRACT

High-performance liquid chromatography (HPLC)–mass spectrometry (MS) was applied to organotransition-metal chemistry with the aim of studying the relationship between chromatographic behaviour and structural features of polynuclear organometallic compounds and of developing the methodological aspects of application of the combined technique in this field. In order to obtain significant structural information about organometallic compounds separated by HPLC, a particle beam LC–MS interface was used. As a first approach, some alkyne-carbonyl ruthenium derivatives and cyclopentadienyl nickel–ruthenium and nickel–osmium carbonyl clusters were considered; all these compounds are of relevant interest in the field of both homogeneous and heterogeneous catalysis. The separation of all the examined clusters was performed under reversed-phase conditions with non-aqueous mobile phases. Full-scan electron impact and chemical ionization mass spectra were obtained from the LC eluates.

INTRODUCTION

The on-line coupling of HPLC–MS was used in a research programme with the aim of studying the relationship between structure and chromatographic behaviour of polynuclear organometallic compounds and, more generally, to develop the methodological aspects of the application of this technique in organometallic chemistry, a field of great interest from the industrial, environmental and toxicological points of view.

Chromatographic techniques are widely used to separate and purify complex mixtures of organometallic compounds in preparative procedures; for this purpose column and thin-layer chromatography are used in most cases. From the analytical point of view, it has been proved that HPLC has great capability even in this field: in fact, HPLC allows rapid and adequately efficient separations of a large number of organometallic compounds, including homo- and heterometallic clusters of different nuclearity [1–5].

HPLC makes use of a variety of sensitive, liquid-phase detectors such as the spectrophotometric, fluorimetric and amperometric

* Corresponding author.

0021-9673/93/$06.00

ones. Owing to the structural complexity of the above substances, these detectors give scant information about the nature of the compounds in the column eluates. Moreover, since conventional HPLC does not provide the high efficiency available from capillary GC, LC chromatograms may contain unresolved peaks that non-specific detectors cannot differentiate. In this context the need for a more sensitive and specific detection system has generated considerable interest in developing the on-line LC–MS technique: mass spectrometry is an excellent tool for analyte identification and structural confirmation in chemical analysis. LC–MS allows the separation and identification of non-volatile, polar compounds, providing structural information for mixtures of components not suitable for GC–MS.

Although LC–MS has been applied extensively in the organic and biochemical analysis [6–11], the field of organotransition-metal chemistry is as yet unexplored with regard to this coupled technique. The problems associated with the interfacing of these two techniques are considerable, but recently there has been significant progress towards their solution. Furthermore, there is a need for structurally useful fragmentations (such as electron impact-like fragmentation) from LC–MS experiments: thermospray LC–MS and LC–atmospheric pressure ion source MS provide very mild ionization, resulting in a limited fragmentation and in a poor mass spectral specificity; nevertheless, thermospray provides more analytical information than other conventional LC detectors and it proves helpful for the characterization of unknown compounds also having high molecular mass, together with other analytical information that may be available.

The possibility of obtaining electron impact (EI) mass spectra, rich in structurally significant fragmentations, is provided by the recent MAGIC (monodisperse aerosol generation for introduction of liquid chromatographic effluents) and particle beam (PB) interfaces; chemical ionization (CI) mass spectra are also available from these interface devices.

With the aim of achieving significant structural information about organometallic compounds separated by HPLC, a particle beam LC–MS interface was used. Full-scan EI and CI mass spectra were obtained from three groups of carbonyl clusters: two groups made up of hydrido-acetylido carbonyl triruthenium clusters, deriving from the basic triangular metal framework $HRu_3(C{\equiv}CR)(CO)_9$. The first one was obtained from the cluster $HRu_3(C{\equiv}C\text{-}tert.\text{-}Bu)(CO)_9$ through substitution of the carbonyl ligands by group 15 donor ligands EPh_3 (E = P, As, Sb). The second one was obtained by varying the R acetylenic substituent in the parent cluster [R = iso-Pr, *tert.*-Bu, $C(Me)_2OH$,

TABLE I

FORMULAS, STRUCTURES AND MOLECULAR MASSES OF THE CLUSTERS

Compound		Mol. mass
	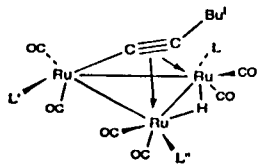	
I	L = L′ = L″ = CO	637.45
IIa	L = L″ = CO, L′ = PPh_3	871.73
IIb	L = L″ = CO, L′ = $AsPh_3$	915.68
IIc	L = L″ = CO, L′ = $SbPh_3$	962.50
III	L = CO, L′ = L″ = PPh_3	1106.01
IV	L = L′ = L″ = PPh_3	1340.29
	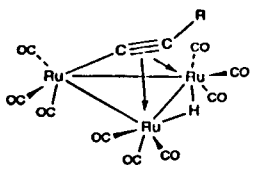	
V	R = iso-Pr	623.42
VI	R = $C(Me)_2OH$	639.42
VII	R = C(Me)(Ph)OH	701.49
	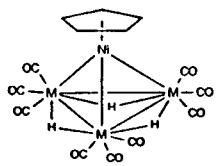	
VIII	M = Os	682.11
IX	M = Ru	949.50

C(Me)(Ph)OH]. In the third group, the tetrahedral cyclopentadienyl-hydrido nickel–osmium and nickel–ruthenium carbonyl clusters (η-C_5H_5)$NiM_3(\mu_2$-H)$_3$(CO)$_9$ [M = Os, Ru] were also considered.

All these compounds are of relevant interest in the field of both homogeneous and heterogeneous catalysis. The schemes of the structures of these complexes are reported in Table I, together with the respective formulas and the molecular masses.

Mass spectra of some acetylenic derivatives of iron and ruthenium carbonyl have been reported [12–15]; the spectra have been obtained for the single compounds, using a direct insertion probe.

The chromatographic behaviour of mono- and polynuclear metal clusters has been already intensively investigated [2–4,16] with the aim of studying the influence of the steric and electronic features on the retention and of verifying the analytical applications of HPLC in this field.

In this paper the results of the use of the on-line HPLC–MS in the separation and identification of the polynuclear carbonyl compounds are reported; these results demonstrate the application capabilities of this combined technique even in the field of organometallic chemistry.

EXPERIMENTAL

Compound HRu_3(C≡C-*tert.*-Bu)(CO)$_9$ (I) and its monosubstitution products with the EPh_3 ligand (IIa–IIc) were prepared as described in the literature for the derivative having E = P [17]. The triphenylphosphine di- and trisubstituted clusters were obtained, purified and identified as reported earlier [16]. Other acetylido derivatives (V–VII) were obtained from the corresponding alkynes using the same synthetic procedure described for I. Nickel–osmium and nickel–ruthenium clusters were synthesized by applying established methods [15,18].

HPLC conditions

The HPLC system consisted of a Hewlett-Packard Model HP1090 chromatograph (Palo Alto, CA, USA), equipped with a Rheodyne 7125 injector. A stainless-steel column (25 cm × 0.4 cm I.D.) filled with 5-μm LiChrosorb RP-18 (Merck, Darmstadt, Germany) was used. In order to check the maintenance of chromatographic resolution, a Perkin Elmer (Norwalk, CT, USA) LC-75 variable-wavelength UV–Vis detector was used, monitoring the eluates at 254 or 265 nm, depending on the position of the absorption maxima; acetonitrile solutions of the compounds (20 μl) were injected. The amounts of metal injected ranged between 0.1 and 0.5 μg when UV detection was used and between 0.5 and 5 μg in LC–MS mode. The flow-rate was 0.8 cm^3/min and 1 cm^3/min in the case of separations obtained in LC–MS and LC-UV mode, respectively. An acetonitrile–methanol (80:20) mixture was used for the isocratic elution of the first and the second set of clusters. Methanol was utilized as eluent for the separation of heterometallic complexes VIII and IX. In every case, data based on injections in flow injection analysis mode were primarily achieved, using methanol as mobile phase at 0.4 cm^3/min.

The solvents used were HPLC grade (Carlo Erba, Milan, Italy).

Interface conditions

A Hewlett-Packard Model HP 59980A particle beam LC–MS interface was used. The nebulizing gas was high-purity helium maintained at 50 p.s.i. (1 p.s.i. = 6894.76 Pa); the desolvation chamber temperature was held at 55°C. The particle beam nebulizing conditions were chosen first by injection of a test solution of benzidine (20 ng/μl in acetonitrile) supplied by Hewlett-Packard and then optimized with the studied compounds.

MS conditions

The mass spectrometer was a Hewlett-Packard Model HP5989A; the HP MS engine was equipped with a dual EI–CI ion source, a hyperbolic quadrupole mass analyser, a continuous dynode electron multiplier detector and a differentially pumped vacuum system with diffusion pumps. The HP MS 59940A ChemStation (HP-UX series) was used as analytical workstation.

Both EI and CI sources were utilized. The optimum source temperature was chosen within the range 250–320°C as a compromise between lower values for abundant molecular ions in the

spectrum and higher temperatures for total ion abundance. The overall best source temperature was 260°C. Using the electron impact source, mass spectra were obtained under these conditions: ionization energy of 30 eV and electron multiplier of 2300 V. In CI data acquisition, methane–ammonia (95:5) mixture was used as the reagent gas; in this case the ionization energy was 230 eV and the voltage applied to the electron multiplier was 2100 V. Both positive and negative ions were monitored in the CI mode.

The quadrupole temperature was held at 100°C.

For scan acquisition the system was scanned from 150 to 750 μ for compounds I and V–VII, from 250 to 1350 μ for compounds I–IV and from 100 to 980 μ for the heterometallic clusters VIII and IX.

RESULTS AND DISCUSSION

For preliminary adjustment of operating conditions flow injection analysis (FIA) was used, by injecting solutions of individual compounds into a mobile phase from an HPLC pump and transferring the mixture into the LC–PB-MS system, without the HPLC column. However, since overall system performance is controlled by the chromatographic conditions (type of column, variable eluent compositions for gradient elution), final optimization was carried out using the LC column.

With regard to the interface tuning, a determining factor of adjustment was found to be

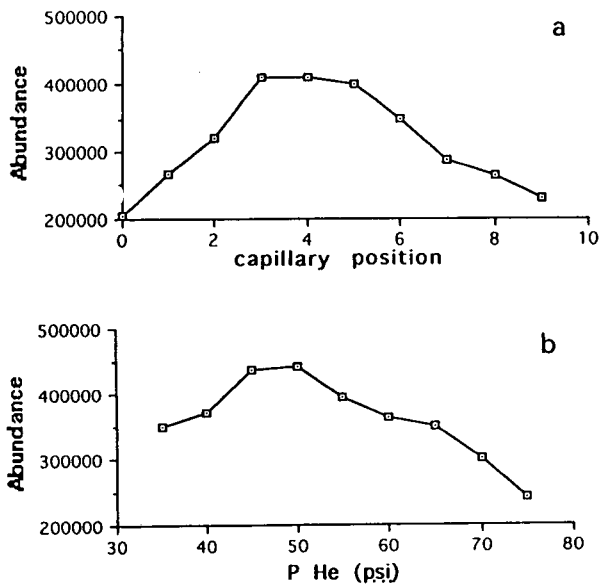

Fig. 1. Effect on peak abundance of $HRu_3(C{\equiv}C\text{-}tert.\text{-}Bu)(CO)_9$ of: (a) position of the end of the capillary in the nebulizer (arbitrary setting units); (b) nebulizing gas helium pressure. Operating conditions: FIA; eluent, methanol; flow-rate, 0.4 cm^3/min; source temperature, 260°C.

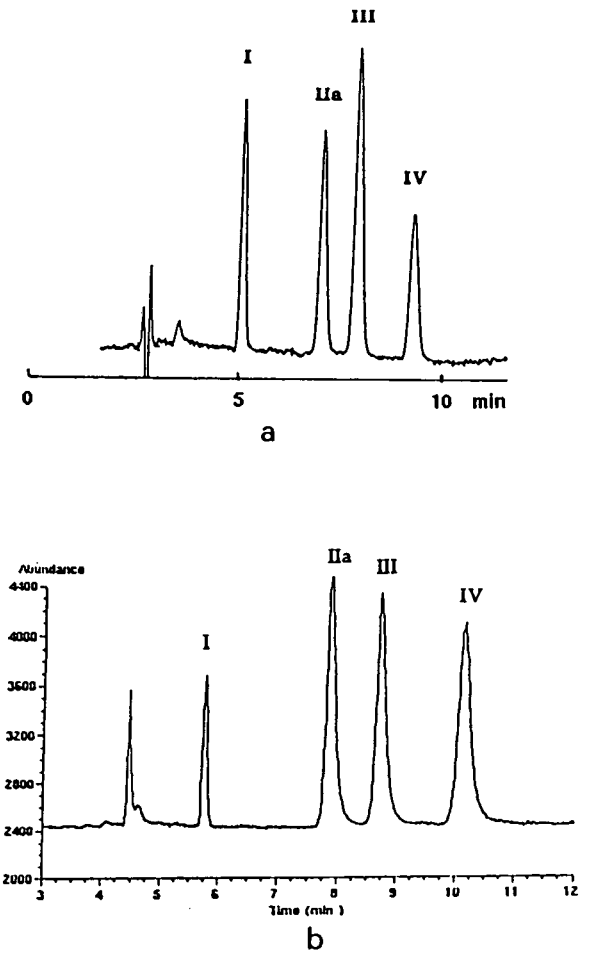

Fig. 2. Comparison of chromatograms of the cluster mixture I–IV with: (a) UV detection, $\lambda = 265$ nm; (b) MS detection, TIC signal. Chromatographic conditions: column, LiChrosorb RP-18; mobile phase, acetonitrile–methanol (80:20); flow-rate, 1.0 cm^3/min for LC–UV, 0.8 cm^3/min for LC–MS. MS conditions: CI source; source temperature, 260°C; reagent gas, methane–ammonia (95:5); scan range, 250–1350 μ; ionization energy, 230 eV, negative-ion signal.

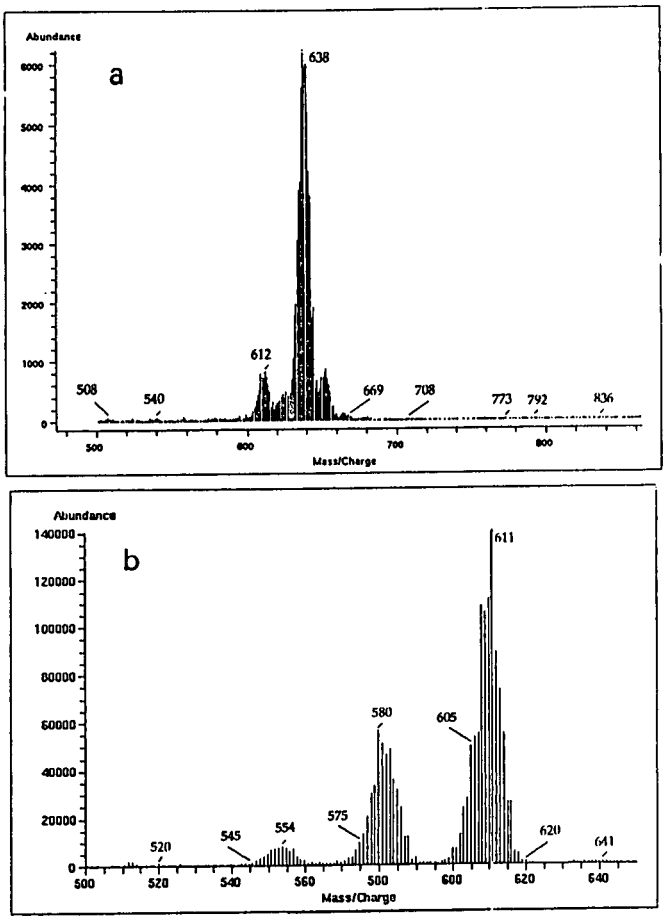

Fig. 3. LC–CI-MS spectra of $HRu_3(C{\equiv}C\text{-}tert.\text{-}Bu)(CO)_9$: (a) positive-ion signal; (b) negative-ion signal. Conditions as in Fig. 2.

the position of the end of the fused-silica capillary in the nebulizer, resulting in a different signal intensity for all compounds. The helium flow-rate in creating the aerosol in the interface was also found to affect sensitivity significantly, the optimum flow-rate being about 2 l/min. The effect of the variations in capillary position and of the helium flow-rate on the signal intensity is represented in Fig. 1 for the compound $HRu_3(C{\equiv}C\text{-}tert.\text{-}Bu)(CO)_9$, which was chosen as the reference compound. Of minor importance was the desolvation chamber temperature in the normal operating range 50–70°C, which was held constant at 55°C.

All the examined clusters were separated under reversed-phase conditions with non-aqueous mobile phases. The most efficient separations were obtained using a standard column (25 cm × 0.4 cm) requiring LC flows higher than those normally accommodated (0.4–0.5 cm^3/min) for the PB interface nebulizer. However, even though the optimum signal intensity was found to be in correspondence with 0.3–0.4 cm^3/min flow-rates, only a slight reduction in sensitivity was observed at a flow–rate of 0.8 cm^3/min. With regard to the solvent composition, methanol or acetonitrile–methanol mixtures were utilized for the elution of the organometallic compounds. In agreement with the results reported by other authors [19], under FIA conditions and at a flow-rate of 0.4 cm^3/min, a slight reduction in signal intensity was observed, changing solvent composition from 100% methanol to 100% acetonitrile on observing the molecular ion of cluster $HRu_3(C{\equiv}C\text{-}tert.\text{-}Bu)(CO)_9$. On the other hand, in the case of homometallic

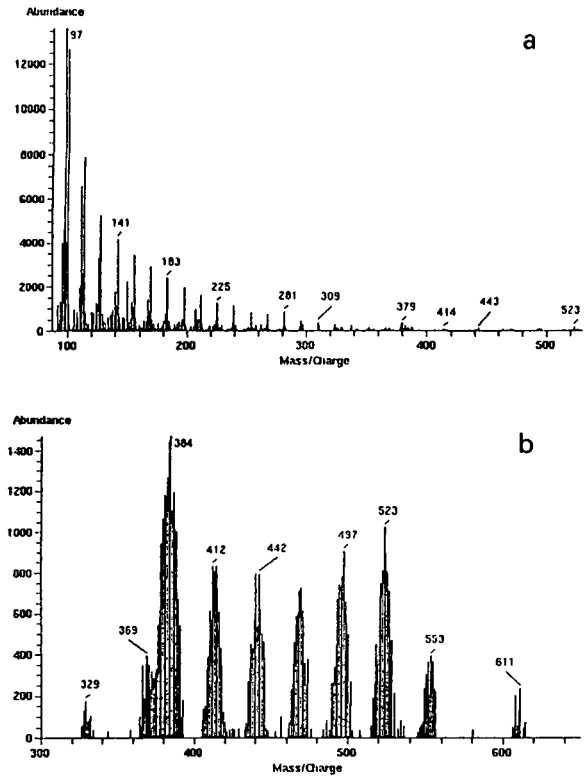

Fig. 4. LC–EI-MS mass spectra of $HRu_3(C{\equiv}C\text{-}tert.\text{-}Bu)(CO)_9$ at different ionization energy: (a) 70 eV; (b) 30 eV. Scan range, 150–750 μ; electron multiplier, 2300 V; positive-ion signal.

triruthenium clusters, it was necessary to use a high percentage of acetonitrile for an optimum elution of compounds.

In order to check the maintenance of the chromatographic resolution when the LC–PB-MS system was used, a UV detector was utilized together with MS for the substitution products of cluster I with the PPh_3 ligands. Fig. 2 provides a comparison of chromatograms of clusters I–IV obtained with UV detection at 265 nm and with the total ion signals from LC–MS, which shows excellent chromatographic fidelity and just a slight loss of resolution in the total-ion chromatogram (TIC) compared with the UV chromatogram. The effects of the nature and the number of the ligands on the separation obtained from LC–UV has already been discussed [16].

The total ion chromatogram of Fig. 2 was obtained by using chemical ionization source monitoring negative-ion signals (NICI mode) of the mixture under conditions reported in the figure. Mass spectra were recorded also in positive-ion (PI) CI mode with the same conditions of reagent gas, source temperature and scan range utilized under NICI conditions. The fragmentation patterns of the compounds in the eluates obtained in the positive-ion mode differ relevantly from that achieved in NICI mode.

Fig. 3 shows a portion of the mass spectra of the parent cluster $HRu_3(C{\equiv}C\text{-}tert.\text{-}Bu)(CO)_9$ in both PICI and NICI modes: the positive-ion spectrum is mainly characterized by the protonated molecular ion ($m/z = 638$), whereas the spectrum obtained by monitoring the negative-ion signal shows more intense fragments corresponding to the loss of up to three CO groups.

The mass spectrum of I was also obtained using electron impact source in two different conditions of ionization energy, as shown in Fig. 4. Using the usual value of collision energy of 70 eV, the compound underwent greater fragmentation than that achieved under milder conditions (30 eV). In this second case, fragments containing the triangular framework of the cluster are present and the gradual loss of all carbonyl groups (up to nine) is favoured. When operating at 30 eV the relative intensities of the ions arising from the breaking of the weaker bonds, namely Ru–CO coordinate bonds, increase and the demolition of the cluster is not observed; therefore lower values of electronic energy are needed to maintain the cluster skeleton.

Concerning the polysubstituted derivatives of cluster I with PPh_3, the PICI mass spectra appeared to be similar for all complexes; in fact they contained only fragments of phosphinic ligands at $m/z = 262$ ($[PPh_3]^+$) and $m/z = 183$ ($[PPh_2 - 2H]^+$), and the ruthenium isotopic pattern was not observed. In the NICI mode the spectra contained several groups of peaks at 28-μ intervals, arising from the loss of CO groups, together with fragments due to the loss of PPh_3 ligands, as shown in Fig. 5: the multiplet of the molecular ion (at m/z 871, 1105, 1338 μ for compounds IIa, III and IV, respectively) is scarcely visible even though always present.

Under reversed-phase conditions, it was observed that the monosubstitution products of the

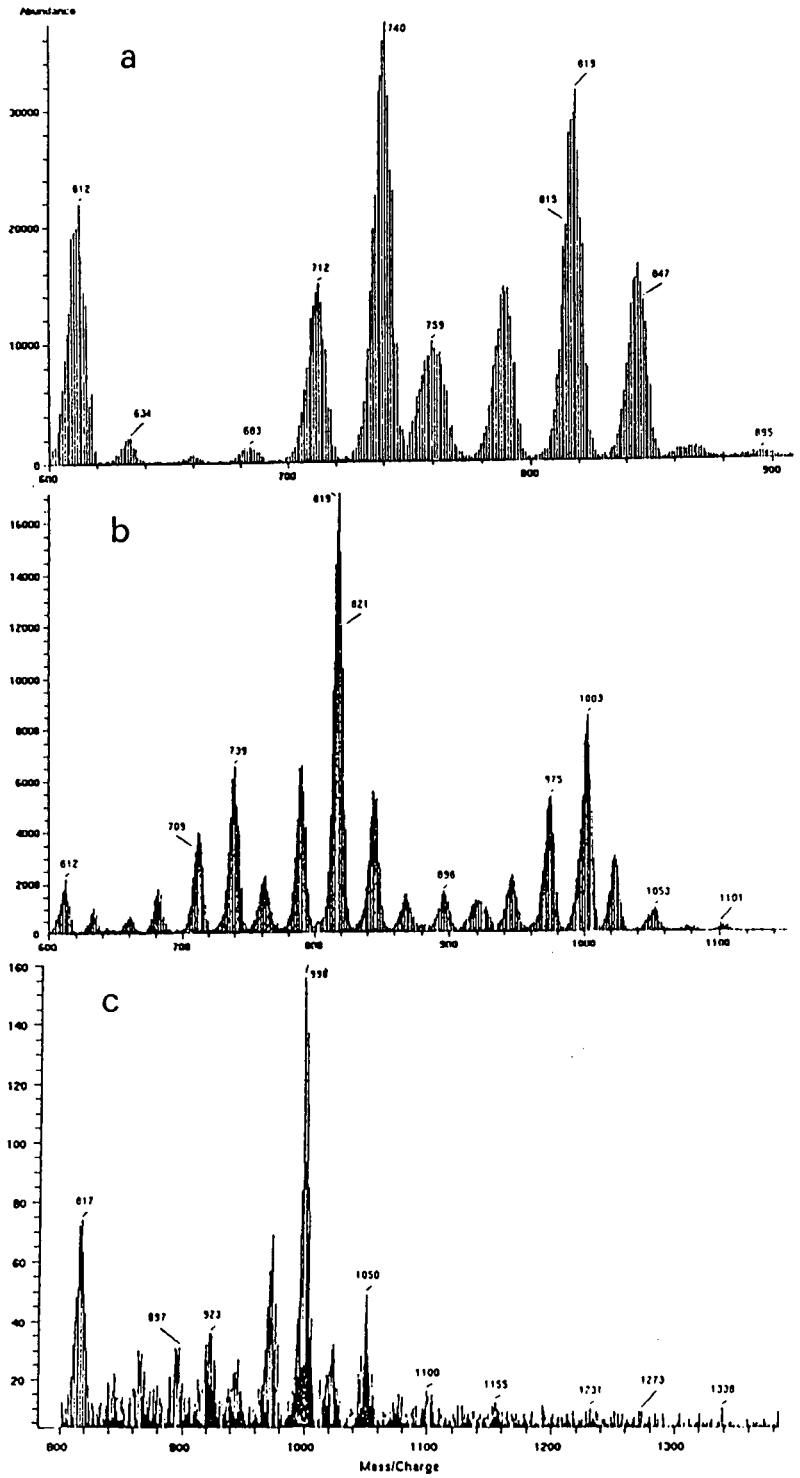

Fig. 5. LC–NICI-PB-MS mass spectra of: (a) $HRu_3(C{\equiv}C\text{-}tert.\text{-}Bu)(CO)_8(PPh_3)$; (b) $HRu_3(C{\equiv}C\text{-}tert.\text{-}Bu)(CO)_7(PPh_3)_2$; (c) $HRu_3(C{\equiv}C\text{-}tert.\text{-}Bu)(CO)_6(PPh_3)_3$. Conditions as in Fig. 2.

TABLE II

MASS SPECTRA OF $HRu_3(C{\equiv}C\text{-}tert.\text{-}Bu)(CO)_8EPh_3$ (E = As, Sb)

m/z	Abundance	Ion
NICI		
583.55	58	$[HRu_3(C{\equiv}C\text{-}tert.\text{-}Bu)(CO)_7]^-$
611.60	100	$[HRu_3(C{\equiv}C\text{-}tert.\text{-}Bu)(CO)_8]^-$
756.05	77	$[HRu_3(C{\equiv}C\text{-}tert.\text{-}Bu)(CO)_5AsPh_2]^-$
784.10	2	$[HRu_3(C{\equiv}C\text{-}tert.\text{-}Bu)(CO)_6AsPh_2]^-$
858.40	4	$[HRu_3(C{\equiv}C\text{-}tert.\text{-}Bu)(CO)_6AsPh_3]^-$
917.40	1	$[HRu_3(C{\equiv}C\text{-}tert.\text{-}Bu)(CO)_8AsPh_3]^-$
554.50	7	$[HRu_3(C{\equiv}C\text{-}tert.\text{-}Bu)(CO)_6]^-$
583.55	56	$[HRu_3(C{\equiv}C\text{-}tert.\text{-}Bu)(CO)_7]^-$
611.60	100	$[HRu_3(C{\equiv}C\text{-}tert.\text{-}Bu)(CO)_8]^-$
802.05	41	$[HRu_3(C{\equiv}C\text{-}tert.\text{-}Bu)(CO)_5SbPh_2]^-$
830.10	4	$[HRu_3(C{\equiv}C\text{-}tert.\text{-}Bu)(CO)_6SbPh_2]^-$
937.50	1	$[HRu_3(C{\equiv}C\text{-}tert.\text{-}Bu)(CO)_7SbPh_3]^-$
963.60	1	$[HRu_3(C{\equiv}C\text{-}tert.\text{-}Bu)(CO)_8SbPh_3]^-$
PICI		
861.05	8	$[HRu_3(C{\equiv}C\text{-}tert.\text{-}Bu)(CO)_6AsPh_3]^+$
888.95	47	$[HRu_3(C{\equiv}C\text{-}tert.\text{-}Bu)(CO)_7AsPh_3]^+$
917.90	100	$[HRu_3(C{\equiv}C\text{-}tert.\text{-}Bu)(CO)_8AsPh_3]^+$
904.75	10	$[HRu_3(C{\equiv}C\text{-}tert.\text{-}Bu)(CO)_6SbPh_3]^+$
933.90	32	$[HRu_3(C{\equiv}C\text{-}tert.\text{-}Bu)(CO)_7SbPh_3]^+$
964.95	100	$[HRu_3(C{\equiv}C\text{-}tert.\text{-}Bu)(CO)_8SbPh_3]^+$

parent cluster I with 15-group donor ligand EPh_3 (E = P, As, Sb) have almost the same retention volumes [16], so that the mass spectra of the compounds were obtained by FIA. In PICI mode, the fragmentation pattern of the derivatives with $AsPh_3$ and $SbPh_3$ ligands (IIb and IIc) showed interesting features compared with the cluster substituted with PPh_3 discussed above: in the first case, the most abundant ions observed were the protonated molecular ions ($m/z = 918$ and $m/z = 965$ μ for IIb and IIc, respectively); the low abundance of the peaks $[M - nCO]^+$ ($n = 1, 2, 3$) indicated a minor stability of the relative fragments. In the mass spectra recorded in NICI conditions, differences in the relative intensities of the peaks were observed: in compounds IIb and IIc, the release of the $AsPh_3$ and $SbPh_3$ ligands is easily obtained, whereas compound IIa showed easier loss of two carbonyls and one phenyl compared with the release of the whole PPh_3 group, suggesting the formation of a diphenylphosphido group bridged to an edge of the cluster [20]; the corresponding ion relative abundances are quoted in Table II.

As for the chromatographic behaviour of the clusters $HRu_3(C{\equiv}CR)(CO)_9$ [R = iso-Pr, *tert.*-Bu, $C(Me)_2OH$, C(Me)(Ph)OH], the reversed-

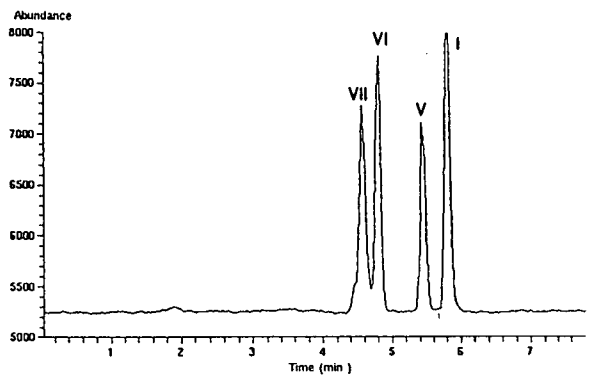

Fig. 6. Total-ion chromatogram of the cluster mixture $HRu_3(C{\equiv}CR)(CO)_9$. Chromatographic conditions: column, LiChrosorb RP-18; mobile phase, acetonitrile–methanol (80:20); flow-rate: 0.8 cm^3/min. MS conditions: source as in Fig. 2; NICI signal; scan range, 150–750 μ.

phase chromatographic separation of the ruthenium derivatives was performed by using an acetonitrile–methanol mixture as eluent: in these conditions, the nature and the electron-donor properties of the R acetylenic substituents appear to be effective in determining the retention order of these structurally related species.

Fig. 6 shows the total ion current profile obtained from the LC–PB-MS system and the mixture of clusters I, V, VI, VII. The CI mass spectrum of the cluster $HRu_3(C{\equiv}C\text{-}tert.\text{-}Bu)(CO)_9$ has been discussed above.

Of particular interest are the chemical ionization mass spectra of clusters V, VI and VII obtained by monitoring both positive- and negative-ion signals.

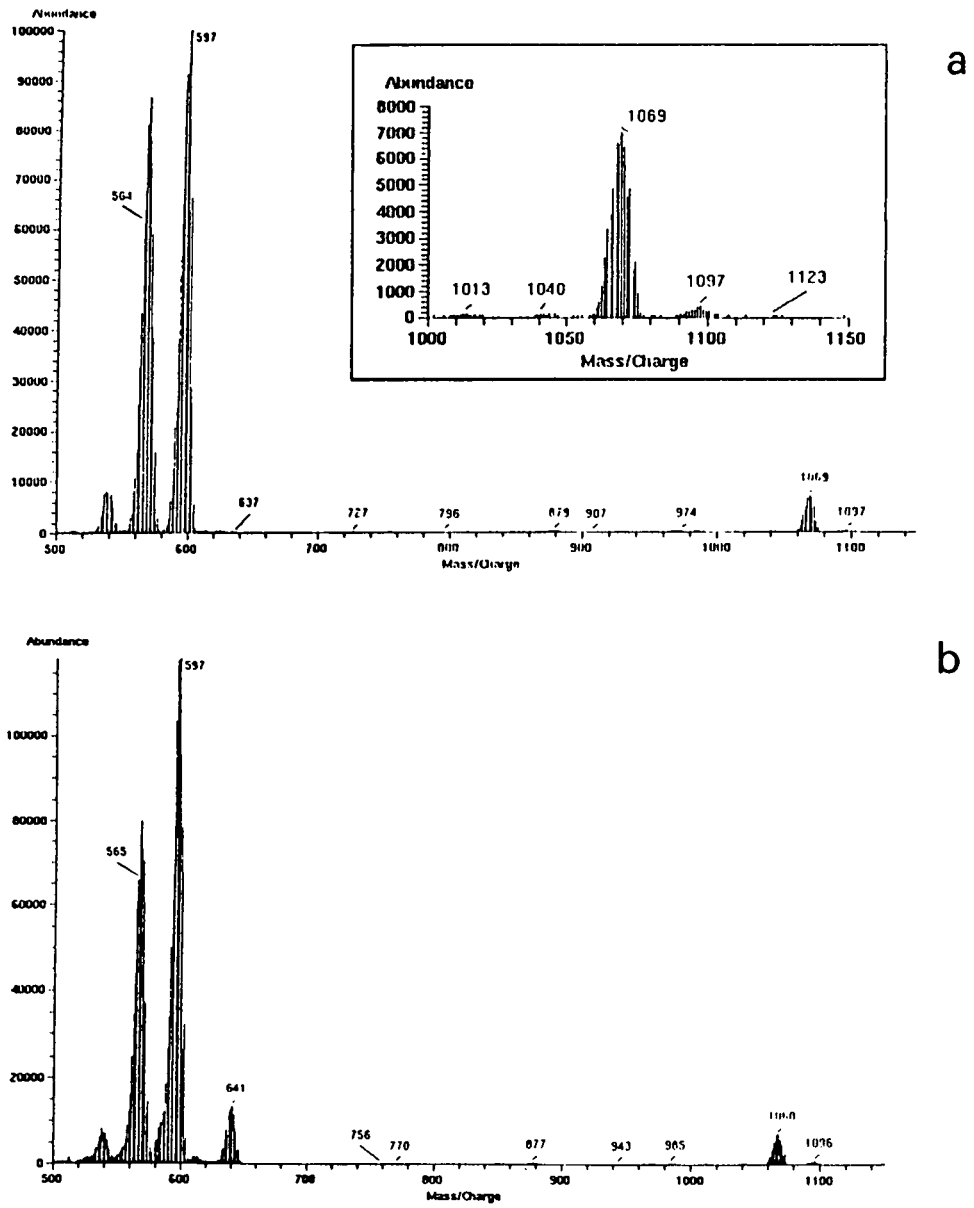

Fig. 7. Negative-ion LC–PB-MS mass spectra of: (a) $HRu_3(C{\equiv}C\text{-}C(Me)_2H)(CO)_9$; (b) $HRu_3(C{\equiv}C\text{-}C(Me)_2OH)(CO)_9$. Same conditions as in Fig. 6.

The fragmentation of V and VI is noteworthy on the NICI mode (Fig. 7); as in the case of the derivative I, the loss of carbonyls (up to three) was favoured and, in the particular case of V, the ion $[M - CO]^-$ ($m/z = 597$) was the most stable, whereas the molecular ion $[M]^-$ represented the most abundant ion for VI. Surprisingly, the mass spectra of both compounds show an isotopic pattern at $m/z = 1069$, suggesting that a dimerization process occurred. A possible explanation is that the acetylide ligand of both clusters generates a dimethyl allenyl fragment by loss of a proton or a hydroxyl group. The allenyl groups of two cluster units can interact in the gas phase, giving rise to dimers with a subsequent release of six CO groups. In contrast, in the signal obtained

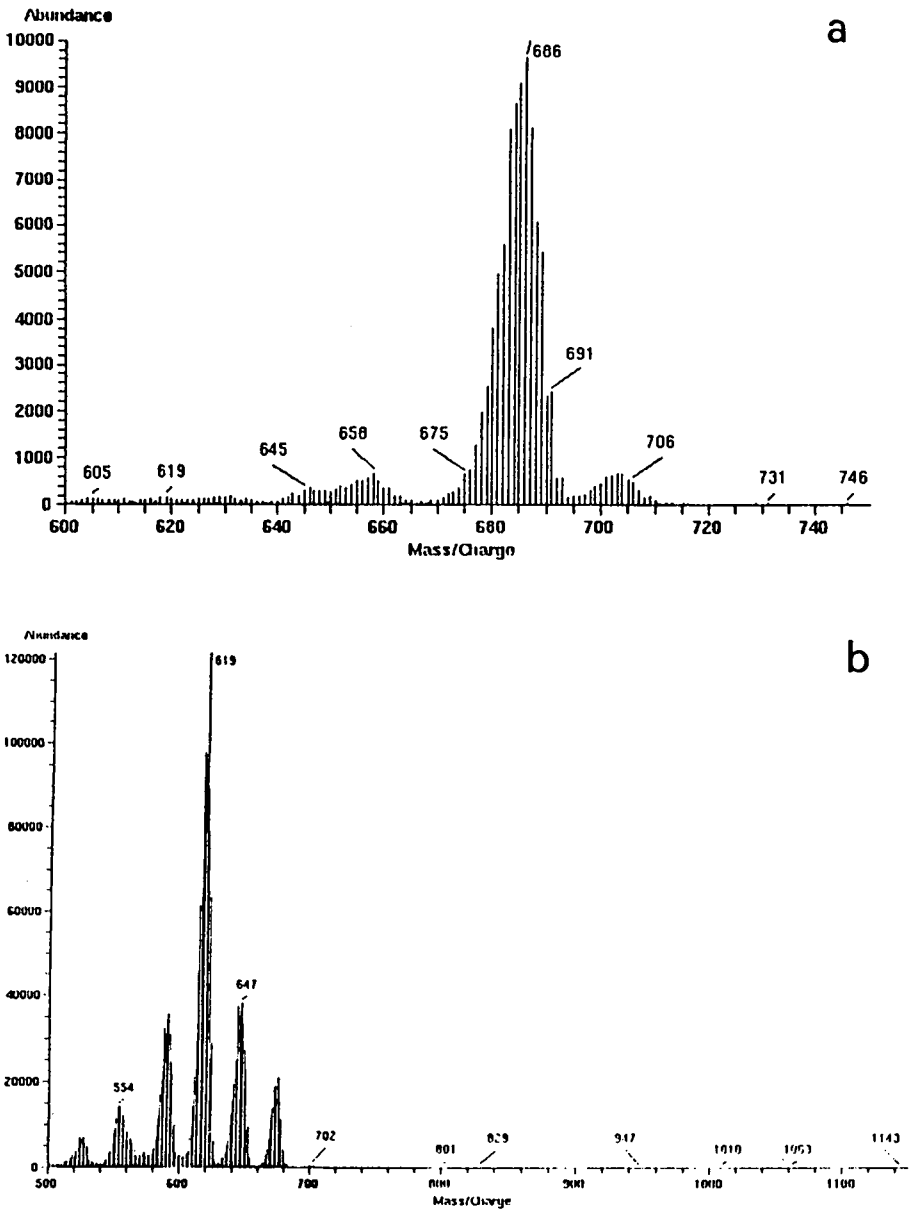

Fig. 8. LC–CI-MS spectrum of $HRu_3(C{\equiv}C{-}C(Me)(Ph)OH)(CO)_9$: (a) positive ion signal; (b) negative ion signal. Same conditions as in Fig. 6.

by monitoring positive ions of the clusters V and VI, fragments at $m/z = 1069$ arising from the dimerization process were not detectable. The PICI mass spectrum of V showed an intense multiplet of molecular ion ($m/z = 626$) and the release of not more than one CO; for compound VI the most abundant fragment was attributable to the ion $[M - OH + C_2H_5]^+ (m/z = 651)$; in addition, adduct ions $[M + C_2H_5]^+$ and $[M + C_3H_5]^+$ were present.

Finally, in the cluster with R = C(Me)(Ph)OH, the easy loss of all nine CO groups was observed under NICI conditions, the ion $[M - 3CO]^-$ being the main fragment (Fig. 8): the different behaviour in release of the carbonyls with respect to the other hydrido–alkyne carbonyl clusters is in agreement with that previously observed [21], namely the loss of the terminal CO groups was found to be effected by the electron-withdrawing power of the substituents on the acetylide.

The figure also contains the positive-ion mass spectrum of compound VII, which shows fragmentation processes different from those of the similar cluster VI having $R = C(Me)_2OH$. In contrast to cluster VI, for which a reaction with the reactant gas together with the loss of an OH group was observed, for compound VII the ion $[M - OH]^+$ ($m/z = 686$) showed the highest stability: this behaviour can be explained on the basis of the presence of the aromatic ring on the acetylide, which stabilizes the system. However, in the case of cluster VII, the release of an OH group does not involve a dimerization process as

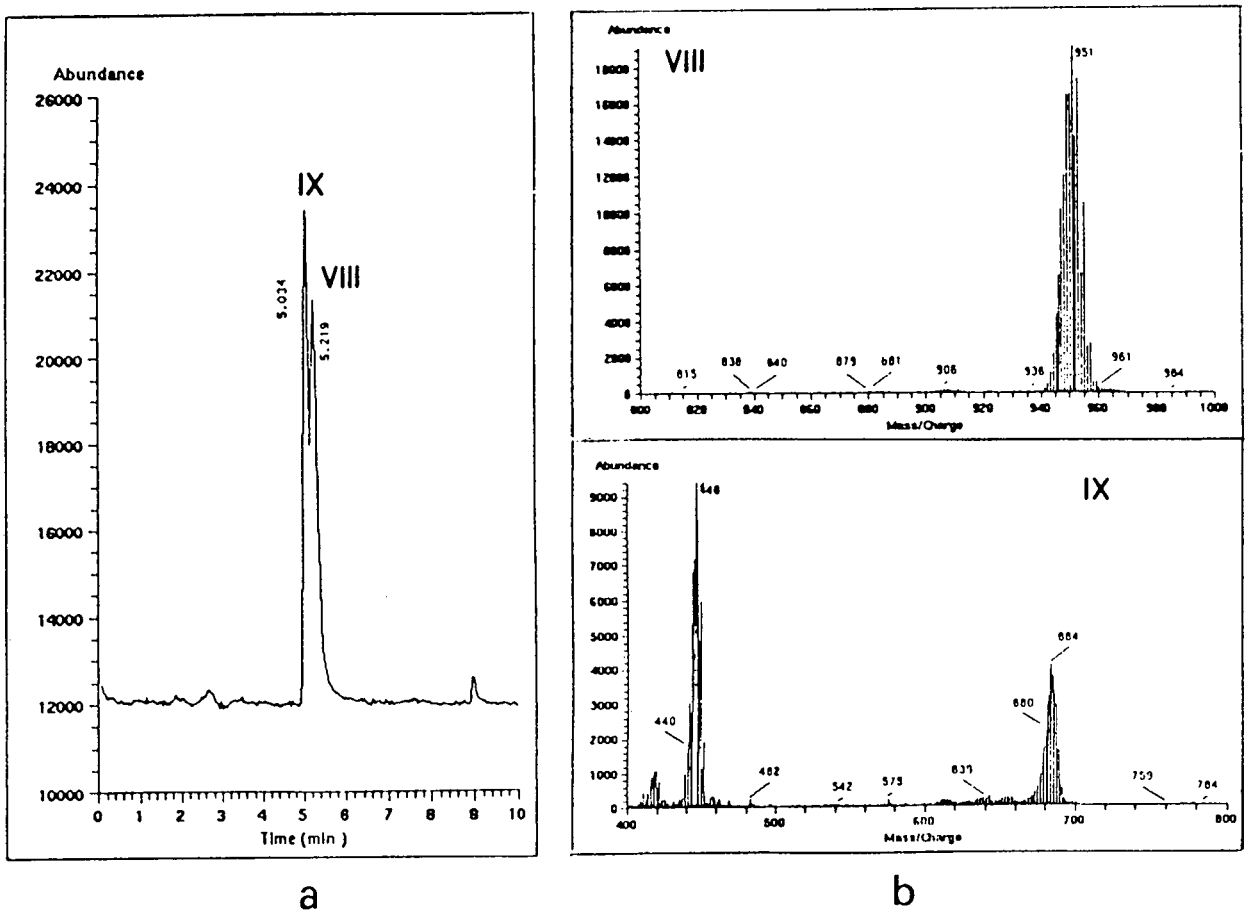

Fig. 9. (a) Separation of the nickel–ruthenium and nickel–osmium heterometallic clusters by LC–PB-MS (TIC) Chromatographic conditions: column, LiChrosorb RP-18; mobile phase, methanol; flow-rate, 0.8 cm^3/min. MS conditions as in Fig. 2, with scan range 100–980 μ. (b) MS spectra (PICI) for the clusters VIII and XI corresponding to the separation in (a).

in the case of the structurally related cluster VI: the allenyl ligand is probably sterically or electronically stabilized by the presence of the aromatic ring. Moreover, adducts with $[C_2H_5]^+$ or $[C_3H_5]^+$, while observed in the case of VI, were not detected for VII.

The chromatographic and mass spectral behaviour of the heteronuclear clusters VIII and IX were investigated. Under reversed-phase conditions, as reported in Fig. 9a, the elution order corresponded to the electronegativity of the metallic centres. Particularly noteworthy are the spectra of the eluates obtained in positive-ion mode (Fig. 9b): in fact, for the nickel–osmium derivative (VIII), only the protonated molecular ion was observed ($m/z = 951$), whereas, surprisingly, the spectrum of the nickel–ruthenium compound (IX) showed, in addition to the molecular ion, an intense signal due to $[NiRu_3(CO)_3]^+$, deriving from the loss of the cyclopentadienyl group and six carbonyls. Also when monitoring the negative-ion signals, the mass spectra of the two clusters presented a different pattern: the nickel–osmium derivative gave rise to the molecular ion ($m/z = 951$) and to the fragment $[M - CO]^-$ with almost the same intensity. The EI mass spectrum obtained by means of direct insertion probe of compound VIII has been reported [15]; in that case the parent ion was not observed and the highest fragment was at $m/z = 920$.

The fragmentation pattern of the nickel–ruthenium cluster was more complex: the loss of up to three CO groups was favoured and the peak corresponding to the molecular-ion ($m/z = 681$) had an intensity of about 50% compared with the most abundant one ($m/z = 653$).

From the results it can be inferred that the LC–PB-MS system can be successfully used even for compounds of particularly complex structure, such as the examined organometallic clusters; for the carbonyl derivatives the NICI mode proves to give more intense spectra and fragmentation patterns more suitable for the identifications.

ACKNOWLEDGEMENT

This work was financially supported by CNR, Italy.

REFERENCES

1 H. Veening, B.R. Willeford, *Adv. Chromatogr.*, 22 (1983) 117.
2 A. Casoli, A. Mangia, G. Predieri and E. Sappa, *J. Chromatogr.*, 355 (1986) 285.
3 A. Casoli, A. Mangia, G. Predieri and E. Sappa, *J. Chromatogr.*, 447 (1988) 187.
4 A. Casoli, A. Mangia, G. Predieri and E. Sappa, *J. Chromatogr.*, 483 (1989) 443.
5 H.G. Ang, W.L. Kwik and W.K. Leong, *J. Organomet. Chem.*, 379 (1989) 325.
6 K.B. Tomer, C.E. Parker, *J. Chromatogr. Biomed. Appl.*, 84 (1989) 189.
7 J.J. Conboy, J.D. Henion, M.W. Martin and J.A. Zweigenbaum, *Anal. Chem.*, 62 (1990) 800.
8 E.C. Huang, T. Wachs, J.J. Conboy and J.D. Henion, *Anal. Chem.*, 62 (1990) 713A.
9 T.D. Behymer, T.A. Bellar and W.L.Budde, *Anal. Chem.*, 62 (1990) 1686.
10 G.J. Van Berkel, S.A. McLuckey and G.L. Glish, *Anal. Chem.*, 63 (1991) 1098.
11 M. Sakairi, A.L. Yergey, K.W.M. Siu, J.C.Y. Le Blanc, R. Guevremont and S.S. Berman, *Anal. Chem.*, 63 (1991) 1488.
12 V. Raverdino and E. Sappa, *Ann. Chim. (Rome)*, 67 (1977) 423.
13 E. Sappa, M.L. Nanni-Marchino and V. Raverdino, *Ann. Chim. (Rome)*, 68 (1978) 349.
14 E. Sappa and V. Raverdino, *Ann. Chim. (Rome)*, 69 (1979) 349.
15 M. Castiglioni, E. Sappa, M. Valle, M. Lanfranchi and A. Tiripicchio, *J. Organomet. Chem.*, 241 (1983) 99.
16 M. Careri, G. Mori, G. Predieri, N. Souza de Rezende and E. Sappa, *J. Chromatogr.*, 634 (1993) 143.
17 C. Jangala, E. Rosenberg, D. Skinner, S. Aime, L. Milone and E. Sappa, *Inorg. Chem.*, 19 (1980) 1571.
18 E. Sappa, A.M. Manotti Lanfredi and A. Tiripicchio, *J. Organomet. Chem.*, 221 (1981) 93.
19 W.V. Ligon, Jr. and S.B. Dorn, *Anal. Chem.*, 62 (1990) 2573.
20 S. Nucciarone, S.A. MacLaughlin, N.J. Taylor and A.J. Carty, *Organometallics*, 7 (1988) 106.
21 O. Gambino, G. A. Vaglio, R. P. Ferrari and M. Valle, *J. Organomet. Chem.*, 76 (1974) 89.

Journal of Chromatography, 647 (1993) 91–94
Elsevier Science Publishers B.V., Amsterdam

CHROMSYMP. 2841

Characterization of the products formed in the reaction between 1,3-butadienemonoxide and 2′-deoxyadenosine by liquid chromatography–continuous-flow fast atom bombardment mass spectrometry

R. Kostiainen*

Environmental Laboratory of Helsinki, Helsinginkatu 24, 00530 Helsinki (Finland)

P. Koivisto and K. Peltonen

Institute of Occupational Health, Topeliuksenkatu 41 aA, 00250 Helsinki (Finland)

ABSTRACT

1,3-Butadiene, a widely produced industrial chemical, has recently been identified as a strong rodent carcinogen. Butadiene is metabolized to reactive 3,4-epoxy-1-butene (BM), which may bind to DNA. The reaction between 3,4-epoxy-1-butene and 2′-deoxyadenosine (dAdo) was studied. The reaction was carried out in trifluoroethanol–triethylamine and the reaction mixture was analysed by liquid chromatography–continuous-flow fast atom bombardment mass spectrometry. The recorded total-ion chromatogram showed four peaks. The spectra of the peaks exhibited a protonated molecule of BM adducts of dAdo (m/z 322), indicating formation of different isomers of the adducts. One alkylation site was shown to be at the exocyclic amino group of the 2′-deoxyadenosine.

INTRODUCTION

1,3-Butadiene (BD) is one of the most commonly produced petrochemicals in the world. Toxicological research has been focused on 3,4-epoxy-1-butene (BM), the main metabolite of butadiene catalysed by microsomes. It has been shown that BM is mutagenic, has carcinogenic activity in the mouse, is a substrate of human placental glutathione *S*-transferase and binds to haemoglobin [1–4]. Citti *et al.* [5] also reported binding to DNA *in vitro* and formation of two N-7 isomeric guanine adducts.

Of the numerous methods available for the detection and quantitation of DNA adducts in biological systems, the ^{32}P post-labelling assay of Randerath and co-workers [6,7] is perhaps the most widely utilized technique. However, the method is not inherently chemospecific and it does not reveal structural information about the modified nucleotides. This problem can be overcome by the use of mass spectrometry, the specificity of which is superior to that of most of the other analytical methods. Direct chemical desorption mass spectrometry (DCI-MS) [8] and tandem mass spectrometry [9] have been applied successfully to the characterization of the alkyldeoxynucleosides. However, owing to thermal decomposition of the compounds during the

* Corresponding author.

0021-9673/93/$06.00

desorption process in DCI, the intensities of the protonated molecules are low and the intensities of the fragment ions are not reproducible. The recently introduced electrospray [10] and fast atom bombardment [11] techniques are gentler ionization methods than DCI. Furthermore, a liquid chromatograph can be connected easily with a mass spectrometer through electrospray or continuous-flow fast atom bombardment (CF-FAB). These techniques provide a very powerful tool for the identification of polar, thermally labile and non-volatile molecules. In this study we have applied HPLC–CF-FAB-MS to the characterization of the reaction products of 3,4-epoxy-1-butene and 2′-deoxyadenosine (dAdo).

EXPERIMENTAL

All the chemicals were from commercial sources: BM, trifluoroethanol (TFE) and triethylamine (TEA) were from Aldrich (Milwaukee, WI, USA) and dAdo was from Sigma (St. Louis, MO, USA). Distilled, deionized water (Milli-Q, Millipore, Finland) mixed with glycerol (99.5%, Prolabo, France) was used as an eluent in HPLC. Xenon (99.995%) used in FAB was from Aga (Finland).

The reaction was carried out in a trifluoroethanol–triethylamine (1:1) mixture by refluxing the reaction mixture at 50°C for 5 days. At the end of the reaction the sample was evaporated to dryness, dissolved in water and subjected to HPLC–CF-FAB-MS analysis.

The measurements were made with a Finnigan MAT 95 high-resolution mass spectrometer connected to an HPLC system by a Finnigan MAT Bio-Probe interface. The ionization chamber temperature was 50°C, the xenon particle energy 8 kV, the emission current 10 mA, the accelerating voltage 5 kV and the magnetic field scanning range m/z 70–500 (3 s per scan). In order to increase the evacuation speed of the ion source, a liquid nitrogen trap was used. The effluent deliver was done by using two high-pressure pumps (Waters 600 MS, Milford, MA, USA). The column was a Novapak C_{18} (15 cm × 4.6 mm I.D.), and samples were introduced into the LC system with a 10-μl loop. The reaction products were separated isocratically using water–glycerol (90:10) as a mobile phase at a flow-rate of 0.8 ml/min. The high viscosity of the mobile phase was compensated by using elevated temperature (57°C). The HPLC effluent was split after the column by a simple T-piece splitter [12], leaving a flow-rate of 6 μl/min to be directed to the mass spectrometer.

RESULTS AND DISCUSSION

Fig. 1 shows a background-subtracted total-ion chromatogram of the reaction mixture recorded by HPLC–CF-FAB-MS with whole-mass-range scanning. The spectra of each of the five peaks detected are presented in Fig. 2. Although the spectra are affected by interference from the background ions, they are still indicative of the

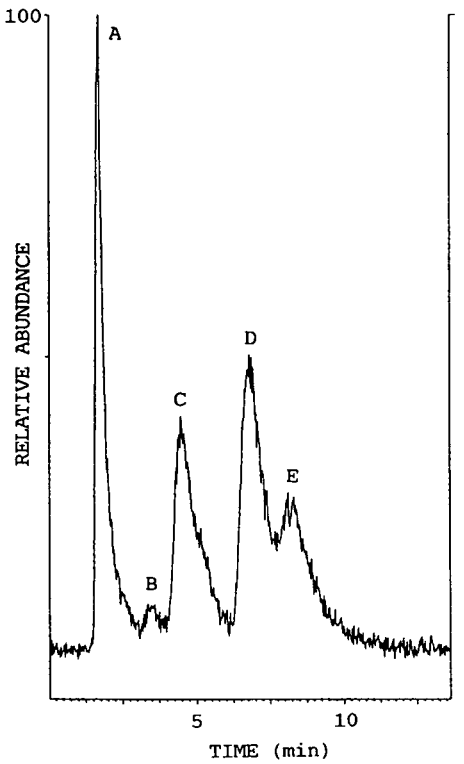

Fig. 1. Background-subtracted total-ion chromatogram of the reaction mixture recorded by HPLC–CF-FAB-MS.

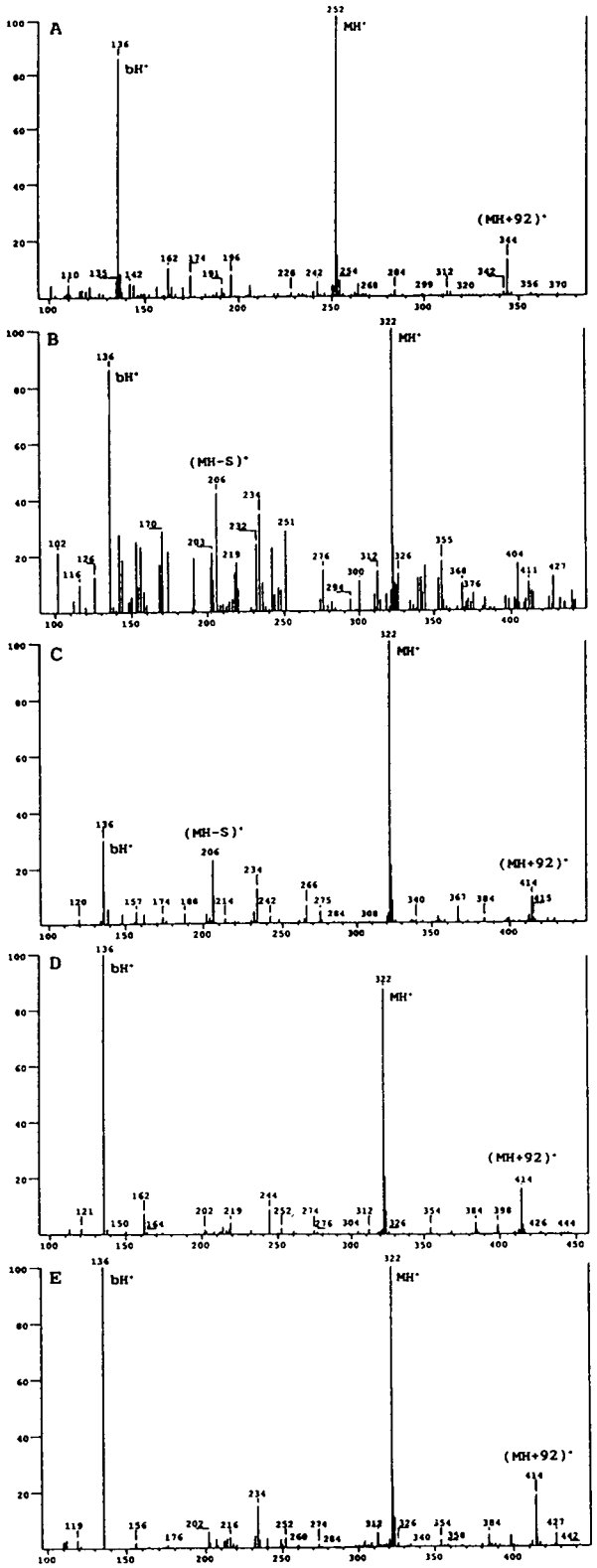

structure. All the spectra contain an abundant protonated molecule and also glycerol adduct ion. The spectrum of peak A exhibits an abundant protonated molecule of dAdo (m/z 252) and an ion at m/z 136 (bH^+) formed by the cleavage of the glycosidic bond with hydrogen transfer. The spectra of the other peaks (B–E) exhibit abundant protonated molecules of BM adducts of dAdo (m/z 322), indicating the formation of isomeric adducts.

The spectra of the peaks B and C exhibit an abundant ion m/z 206, formed by the cleavage of the glycosidic bond with a hydrogen transfer. The ion m/z 206 decomposes further by the loss of BM adduct, producing the ion m/z 136 (bH^+). The presence of the ion m/z 206 in the spectra of B and C indicates that the alkylation site is on the base moiety. Unfortunately, the spectra are affected by interference from the background ions so that the exact site of alkylation cannot be determined. Based on the reaction conditions shown in Fig. 3 (aprotic, basic) the most probable alkylation site is the exocyclic amino group of dAdo, *i.e.* the N^6 position.

In the case of D and E it is not obvious that the alkylation site is N^6 of dAdo, since the spectra do not exhibit the characteristic ion m/z 206. Therefore we are suggesting that the alkylation site could be N-3 of dAdo. This makes possible rearrangement and simultaneous loss of BM and sugar. The chemistry of expoxides does not support the modification of sugar hydroxyls.

The results suggest that N^6 isomers can be separated from the other isomers and identified. Based on the nature of the starting materials and the reaction chemistry of epoxides, an isomeric pair of diastereomers of N^6-dAdo adducts is expected. So, we realize that we were not able to separate all the four N^6 isomers of BM and dAdo adducts. Our future research will be focused on the separation of all N^6 isomers and their use as standards in a post-labelling assay.

Fig. 2. The FAB spectra of 2′-deoxyadenosine (A) and 3,4-epoxy-1-butene 2′-deoxyadenosine adducts (B–E).

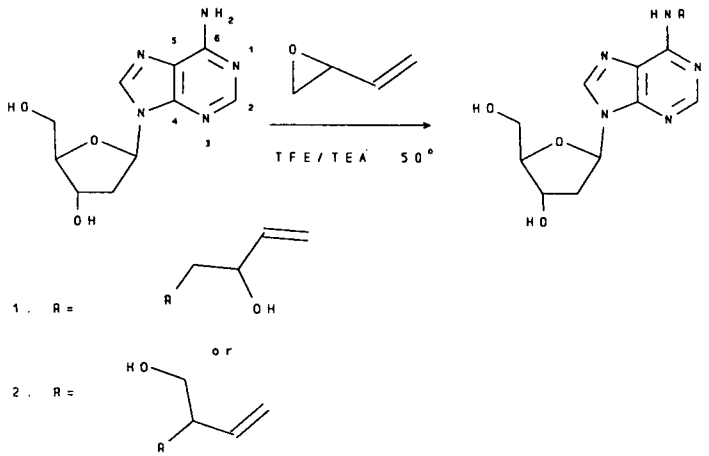

Fig. 3. Reaction of 2′ deoxyadenosine and 3,4-epoxy-1-butene.

ACKNOWLEDGEMENTS

The Oskar Öflund Foundation and CEC/STEP Project No. CT 91-0152 are gratefully acknowledged for financial support.

REFERENCES

1 A.A. Elfarra, R.J. Duescher and C.M. Pasch, *Arch. Biochem. Biophys.*, 286 (1991) 244.
2 C. de Meester, F. Poncelet, M. Roberfroid and M. Mercier, *Biochem. Biophys. Res. Commun.*, 80 (1978) 298.
3 P.L. Van Duuren, N. Nelson, L. Orris, E.D. Palmes and F.L. Schmitt, *J. Natl. Cancer Inst.*, 31 (1963) 41.
4 J.E. Sharer, R.J. Duescher and A.A. Elfarra, *Chem. Res. Toxicol.*, 4 (1991) 430.
5 L. Citti, P.G. Gervasi, G. Turchi, G. Bellucci and R. Bianchini, *Carcinogenesis*, 5 (1984) 47.
6 R.C. Gupta, M.V. Reddy and K. Randerath, *Carcinogenesis*, 3 (1982) 1081.
7 M.V. Reddy and K. Randerath, *Carcinogenesis*, 7 (1986) 1543.
8 J.J. Solomon, F. Mukai, J. Fedyk and A. Segal, *Chem.–Biol. Interactions*, 67 (1988) 275.
9 A. Hesso, R. Kostiainen, T. Kotiaho and K. Hemminki, in J.F.J. Todd (Editor), *Advances in Mass Spectrometry*, Part B, Wiley, Chichester, 1985, p. 1465.
10 H. Yamashita and J.B. Fenn, *J. Phys. Chem.*, 88 (1984) 4451.
11 R.M. Caprioli (Editor), *Continuous-Flow Fast Atom Bombardment Mass Spectrometry*, Wiley, New York, 1990.
12 P. Kokkonen, W.M.A. Niessen, U.R. Tjaden and J. van der Greef, *J. Chromatogr.*, 474 (1989) 59.

Journal of Chromatography, 647 (1993) 95–100
Elsevier Science Publishers B.V., Amsterdam

CHROMSYMP. 2756

Organic acid analysis by ion chromatography–particle beam mass spectrometry

James N. Alexander, IV* and Chad J. Quinn

Rohm and Haas Company, Spring House, PA 19477 (USA)

ABSTRACT

Ion chromatography–mass spectrometry (IC–MS) has been investigated, using the particle beam interface, as an analytical technique for the analysis of weak organic acids. Ion-exclusion chromatography is a technique for separating weak acids. Using dilute HCl as the mobile phase, weak acids are separated on a cation-exchange resin. IC–MS was used to detect and identify weak acids in commercial grape juices and red wine. Analyses were performed using both electron (EI) and chemical ionization (CI). Isobutane CI readily produced protonated molecular ions, and combined with structural information obtained from EI analyses, identification of weak acids was possible. A main advantage of this technique is that co-eluting acids can be identified, whereas with conductivity and UV detection this is difficult. To simplify these analyses, solid-phase extraction was used to remove sugars from the juice and wine samples.

INTRODUCTION

Organic acids are found in a variety of complex matrices. They can be found in biological samples, such as urine, blood and bile; in food products, such as wine, juice drinks and milk [1]. Small carboxylic acids are extremely important in wines and juice drinks because they contribute to taste and product stability [2,3].

Monocarboxylic acids can be analyzed by gas chromatography (GC), but dicarboxylic acids are difficult to analyze because of their high polarity and boiling points. A number of investigators have analyzed these compounds by GC using derivatization. Because sample preparation can take as long as 24 h in some cases, acids are often analyzed by liquid chromatography [4–9].

Although there are a variety of liquid chromatographic techniques for the analysis of weak acids, ion-exclusion chromatography [10–15], ion-exchange chromatography [3,11,17–19] and reversed-phase HPLC [2,20–22] have received the most attention. These separation techniques usually employ conductivity, UV or refractive index detection. Ion-exclusion chromatography with conductivity or UV detection has proven to be a sensitive technique for the analysis of weak acids. However, these analyses give limited information about the compounds of interest and provide no information on possible co-elution of compounds.

The focus of this study was to interface ion-exclusion chromatography with mass spectrometry using the particle beam interface. Others have used ion chromatography (IC) coupled to mass spectrometry (MS) [15,16]. Pacholec *et al.* [15] investigated IC–MS using the thermospray interface and was able to produce only the molecular ions for each acid. However, the particle beam interface provides the chromatographer with the ability to distinguish and identify unknown compounds from mass spectral data that contains both molecular mass (CI) and structural information (EI). The mass spectrometer also provides the analyst with a tool to deconvolute the co-elution of acids. Therefore, IC–MS makes identification of weak acids an

* Corresponding author.

0021-9673/93/$06.00

easier process by providing the analyst with spectral information in addition to the retention time of compounds.

EXPERIMENTAL

Reagents

Deionized water was obtained from a Milli-Q reagent water system (Millipore, Bedford, MA, USA). The HPLC-grade methanol, sodium hydroxide (Baker Analyzed), sulfuric acid (Baker Instra-Analyzed Reagent), hydrochloric acid (ULTREX II Ultrapure Reagent) were used as received from J.T. Baker (Phillipsburg, NJ, USA). The organic acids were purchased from Aldrich (Milwaukee, WI, USA). The grape juices were purchased from a local supermarket, and the red wine was from a local winery.

Standard and sample solutions

The acid standards (citric, fumaric, malic, tartaric and succinic acids) were prepared at the 75 ppm (w/w) level in deionized water. The grape juice and red wine samples were diluted 1:5 in deionized water.

The neutral compounds were separated from the organic acids by passing the diluted samples through a 2.8 ml Bond Elut strong anion-exchange (SAX) solid-phase extraction cartridge (Analytichem International, Harbor City, CA, USA). First, the tube was conditioned with 5 ml of methanol followed by 5 ml of deionized water. The pH of the diluted sample was adjusted to pH 7–8 with 10 *M* sodium hydroxide, and then 1 ml of sample was passed through a SAX cartridge at 1 ml/min. The neutral compounds (sugars) were eluted from the SAX cartridge with 2 ml of water at 1 ml/min. The acid compounds were eluted with two 0.5-ml aliquots of 0.5 *M* sulfuric acid at 1 ml/min [17].

Chromatography

The liquid chromatograph consisted of a Hewlett-Packard (HP) 1090 and a Rheodyne 7125 injector fitted with a 100-μl sample loop. A Kratos Spectroflow 783 UV detector (210 nm) was placed in series with the particle beam interface. A flow-rate of 0.5 ml/min and a Waters Fast Fruit Juice (Milford, MA, USA) 15 cm × 7.8 mm column (7 μm particle size) was used for all separations. The mobile phase was 1.0 m*M* HCl and was thoroughly degassed before use.

Mass spectrometer

The experiments were performed on a HP 5988 quadrupole mass spectrometer with a mass range of 2000 u. The HP particle beam LC–MS interface Model 5998A was used to couple the mass spectrometer to the liquid chromatograph and UV detector. The mass spectrometer was operated in the positive ion full scan mode for all experiments. The mass range scanned was 40–400 u and 100–500 u for EI and CI analyses, respectively. The source temperature was 200°C for both EI and CI analyses. The source pressure for isobutane CI was approximately 0.5 Torr (1 Torr = 133.322 Pa). Methane CI was approximately 0.9 Torr. The particle beam interface desolvation chamber was 70°C, the nebulizer helium pressure was 55 p.s.i. (1 p.s.i. = 6894.76 Pa), and the capillary position was extended approximately 0.6 mm from the flush position of the nebulizer.

RESULTS AND DISCUSSION

Chromatography

Ion-exclusion chromatography is an ion chromatography technique that is used to separate weak organic acids from strong acids. The stationary phases are cation-exchange resins in the H^+ form that can vary in the degree of resin cross-linking. The mobile phases are usually prepared from strong acids, such as hydrochloric and sulfuric acids. At an operating pH of 2–3 the cation-exchange resin and organic acids (*i.e.* carboxylic acids) are protonated. The acids are separated by mechanisms which include: Donnan exclusion, steric exclusion and adsorption [23].

Sulfuric acid (1 m*M*) was initially used for the separation, but, because of the interference of the sulfuric acid the mass spectrometer could not be scanned below m/z 98 (M_r of H_2SO_4) during EI analyses. This would have increased the background signal and interfered with the sensitivity of the analysis. Therefore, HCl was chosen as the mobile phase which allowed us to

start scanning the mass spectrometer from m/z 40, just above the HCl background. The use of HCl as a mobile phase with a stainless-steel HPLC system is not ideal, and thorough washing of the HPLC and the particle beam interface with water was necessary to reduce corrosion problems.

Initially, both mono- and dicarboxylic acids were analyzed. Sensitivity for the monocarboxylic acids was poor (500 ppm), while the dicarboxylic acids gave excellent responses at 75 ppm. We believe this behavior is due to the design of the particle beam interface [24]. To eliminate the solvent from entering the mass spectrometer, the interface employs a two-stage momentum separator. Because of the low molecular mass and volatility of the monocarboxylic acids, these compounds are skimmed away with the solvent, and therefore only high concentrations of the monocarboxylic acids will produce a signal in the mass spectrometer. For this reason we concentrated on the analysis of the dicarboxylic acids: fumaric, malic, succinic, tartaric and citric (Fig. 1). The CI total ion chromatograms of succinic, citric, malic, tartaric and fumaric acid standards are shown in Fig. 2.

Mass spectrometry

EI, negative CI (NCI), and positive CI (PCI) techniques were investigated. EI provided the highest counts while the negative and positive CI analyses were essentially identical using flow

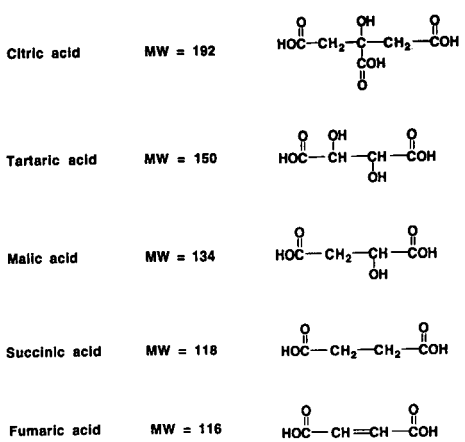

Fig. 1. Chemical structures of weak acid standards. MW = Molecular mass.

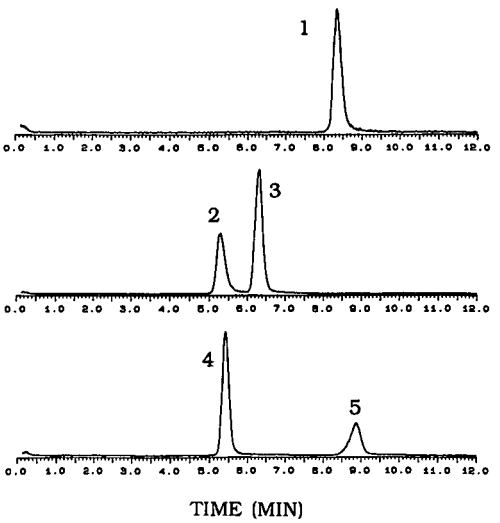

Fig. 2. CI total ion chromatograms for 75 ppm weak acid standards. Peaks: 1 = succinic acid; 2 = citric acid; 3 = malic acid; 4 = tartaric acid; 5 = fumaric acid.

injection analyses of organic acids at a concentration of 500 ppm.

NCI analyses produced molecular ions of the standards with no other significant amount of fragmentation. PCI analyses produced protonated molecular ions of the standards with little fragmentation. The base peak ion in the CI isobutane mass spectra of all the acid standards, except for citric acid, was the protonated molecular ion $(M+H)^+$. The loss of H_2O from the protonated molecular ion produces the ion with the next greatest intensity in the mass spectra. Fig. 3a is an example of succinic acid analyzed by CI. Ion m/z 119 is the protonated molecular ion and ion m/z 101 is the loss of H_2O. Fig. 3b and c are the CI mass spectra of malic and tartaric acids, respectively. The base peak in the CI mass spectra of citric acid is ion m/z 147 which corresponds to the loss of 46 (CH_2O_2) from the protonated molecular ion m/z 193 (Fig. 3d).

The molecular ion peak in the EI analyses of the dicarboxylic acid standards was either weak or absent. This is common for polycarboxylic acids. The loss of CO_2 is often found in the EI mass spectra of dicarboxylic acids [25]. This loss is observed in the EI mass spectra for malic, tartaric and succinic acids which are shown in Fig. 4a, b and c, respectively.

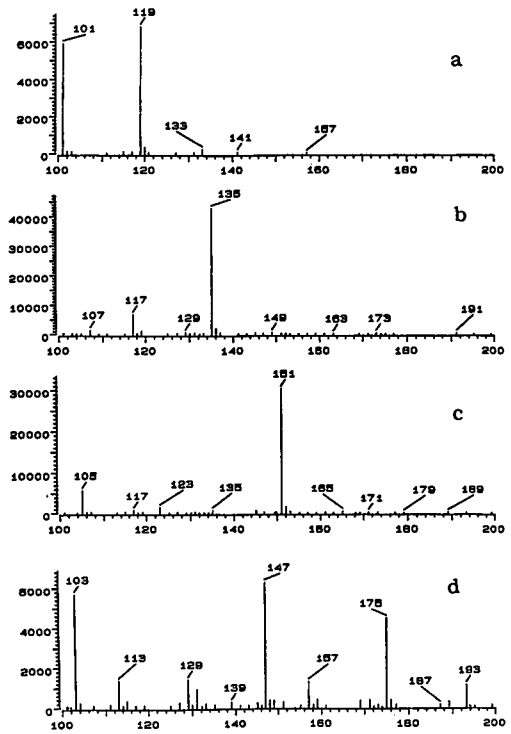

Fig. 3. CI mass spectra for 75 ppm weak acid standards: (a) succinic acid; (b) malic acid; (c) tartaric acid; (d) citric acid.

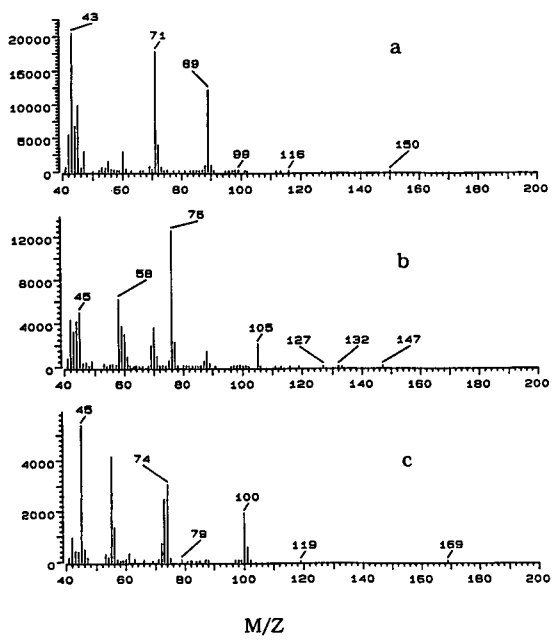

Fig. 4. EI mass spectra for 75 ppm weak acid standards: (a) malic acid; (b) tartaric acid; (c) succinic acid.

Applications

When analyzing commercial grape juice samples that contained sugar, it was necessary to separate the sugars from the sample to simplify the analysis. The sugars do not have a chromophore and are not detected by UV detection. Fig. 5a shows the CI total ion chromatogram for grape juice A before the SAX extraction. This chromatogram is very complex compared to the UV chromatogram of the same sample, Fig. 5b. Although the mass spectrometer has the ability to extract the characteristic ions of the acids from the chromatogram and identify their presence, it was decided for simplicity that solid-phase extraction would be used. Fig. 5c shows the CI total ion chromatogram of acid extract of commercial grape juice A. The major peaks in this chromatogram correlate well with the chromatographic profile obtained for the same sample (using UV detection) before extraction (Fig. 5b). The retention times differ because the analyses were performed on two different days.

The identification of the acid components of a mixture can be readily determined from the extracted ion profiles. The CI total ion chromatogram of the acid extract of commercial grape juice A is shown in Fig. 6a. The extracted ion

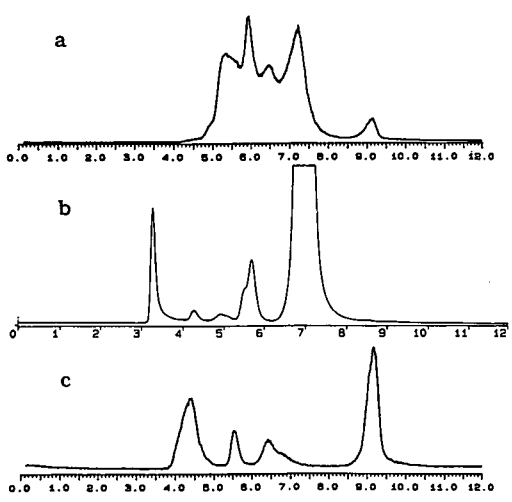

Fig. 5. Analysis of grape juice A before SAX extraction: (a) CI total ion chromatogram; (b) UV chromatogram. Analysis of grape juice A after SAX extraction: (c) CI total ion chromatogram.

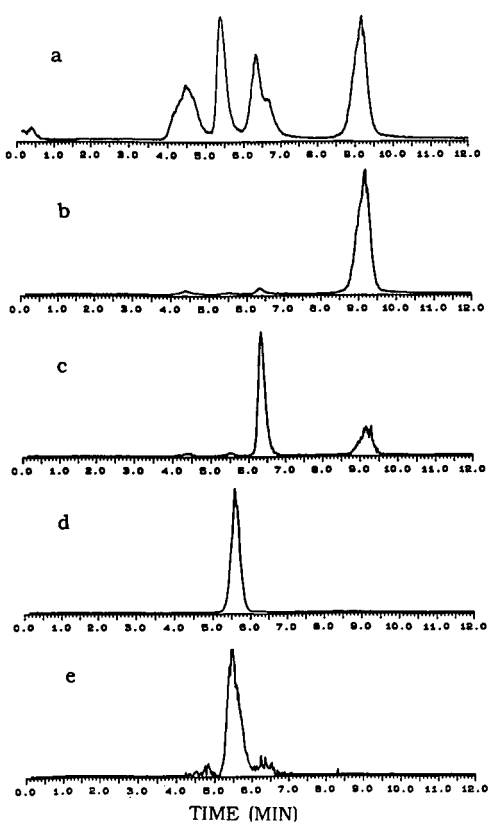

Fig. 6. Analysis of the grape juice A acid extract. (a) CI total ion chromatogram. Extracted ion profiles for (b) fumaric acid (m/z 117), (c) malic acid (m/z 135), (d) tartaric acid (m/z 151) and (e) citric acid (m/z 193).

profiles for ions m/z 117, m/z 135, m/z 151 and m/z 193 correspond to the protonated molecular ions for fumaric, malic, tartaric and citric acids, respectively. The retention times and mass spectra of the peaks confirm the presence of these acids in grape juice A. The extracted ions m/z 151 and m/z 193 (Fig. 6d and e) show the strength of the mass spectrometer to identify the co-elution of tartaric (m/z 151) and citric (m/z 193) acids. The peak at retention time 4.5 min is still unidentified but has characteristic ions of a carboxylic acid. Another acid extract from a different commercial grape juice (B) is shown in Fig. 7. The extracted ion profiles for the protonated molecular ions m/z 135 and m/z 151 correspond to malic and tartaric acids, respectively. The retention times and mass spectra of the peaks confirm the presence of these acids in

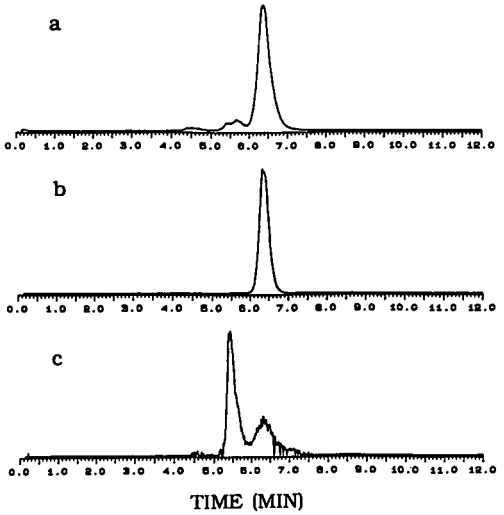

Fig. 7. Analysis of the grape juice B acid extract. (a) CI total ion chromatogram. Extracted ion profiles for (b) malic acid (m/z 135) and (c) tartaric acid (m/z 151).

grape juice B. Malic and tartaric acids were identified in both grape juices, while fumaric and citric acids were identified only in grape juice A.

The CI total ion chromatogram of the acid extract of a red wine is shown in Fig. 8. The extracted ion profiles for the protonated molecular ions m/z 119, m/z 135, m/z 151, and m/z 193 correspond to succinic, malic, tartaric and citric acids, respectively. The retention times and mass spectra of the peaks confirm the presence of these acids in this sample of red wine. Again the deconvolution of ions m/z 151 and m/z 193 (Fig. 8d and e) show the strength of the mass spectrometer to identify the co-elution of tartaric (m/z 151) and citric (m/z 193) acids.

CONCLUSIONS

Ion chromatography coupled to particle beam mass spectrometry has been shown to generate characteristic mass spectra for the identification of weak acids. Due to co-elution of sugars with the weak acids, solid phase extraction was used to eliminate the interference of the sugars present in the samples. This extraction simplified the total ion chromatograms and mass spectra obtained for each analysis. Positive CI analysis produced protonated molecular ions, and EI

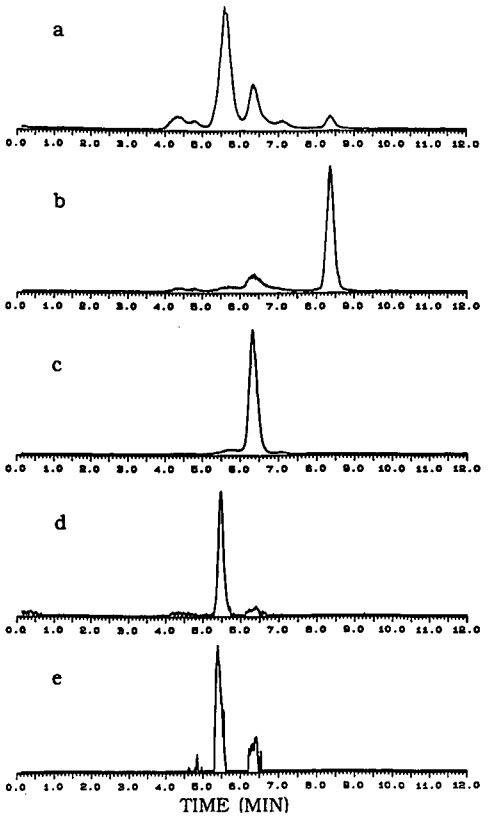

Fig. 8. Analysis of the red wine acid extract. (a) CI total ion chromatogram. Extracted ion profiles for (b) succinic acid (*m/z* 119), (c) malic acid (*m/z* 135), (d) tartaric acid (*m/z* 151) and (e) citric acid (*m/z* 193).

analysis provided structural information of the acid standards. With the combination of the two analyses, dicarboxylic acids were detected and identified in commercial grape juices and red wine.

REFERENCES

1 P.R. Haddad and P.E. Jackson, *Ion Chromatography —Principles and Applications (Journal of Chromatography Library*, Vol. 46), Elsevier, Amsterdam, New York, 1990, pp. 215, 216.
2 F. Cacamo, G. Carfagnini, A. DiCorcia and R. Samperi, *J. Chromatogr.*, 362 (1986) 47.
3 S.A. Kupina, C.A. Pohl and J.L. Gannotti, *Am. J. Enol. Vitic.*, 42 (1991) 1.
4 G.W. Chapman and R.J. Horvat, *J. Agric. Food Chem.*, 37 (1989) 947.
5 C.J. Belke and A.J. Irwin, *J. Am. Soc. Brew. Chem.*, 50 (1992) 26.
6 M. Morvai, I. Molnar-Perl and D. Knausz, *J. Chromatogr.*, 552 (1991) 337.
7 M. Morvai, I. Molnar-Perl and D. Knausz, *J. Chromatogr.*, 520 (1990) 201.
8 E.J. Gallegos, *J. Chromatogr. Sci.*, 25 (1987) 296.
9 P. Pfaffli, H. Savolainen and H. Keskinen, *Chromatographia*, 27 (1989) 9.
10 J. Haginaka, J. Wakai, H. Yasuda and T. Nomura, *J. Chromatogr.*, 447 (1988) 373.
11 R.D. Rocklin, R.W. Slingsby and C.A. Pohl, *J. Liq. Chromatogr.*, 9 (1986) 757.
12 K. Tanaka, T. Ishizuka and H. Sunahara, *J. Chromatogr.*, 174 (1979) 153.
13 R. Widiastui, P.R. Haddad and P.E. Jackson, *J. Chromatogr.*, 602 (1992) 43.
14 E. Papp and P. Keresztes, *J. Chromatogr.*, 506 (1990) 157.
15 F. Pacholec, D.R. Eaton and D.T. Rossi, *Anal. Chem.*, 58 (1986) 2581.
16 S. Kim, F.I. Sasinos, R.D. Stephens and M.A. Brown, *J. Agric Food Chem.*, 38 (1990) 1223.
17 M. Calull, R.M. Marcé and F. Borrull, *J. Chromatogr.*, 590 (1992) 215.
18 R.F. Frayne, *Am. J. Enol. Vitic.*, 37 (1986) 281.
19 R.W. Slingsby, *J. Chromatogr.*, 371 (1986) 373.
20 M. Llorente, B. Villarroya and C. Gómez-Cordovés, *Chromatographia*, 32 (1991) 555.
21 D. Tusseau and C. Benoit, *J. Chromatogr.*, 395 (1987) 323.
22 V. Raverdino, *J. Chromatogr.*, 554 (1991) 125–140.
23 P.R. Haddad and P.E. Jackson, *Ion Chromatography —Principles and Applications (Journal of Chromatography Library*, Vol. 46), Elsevier, Amsterdam, New York, 1990, pp. 195–202.
24 R.C. Willoughby and R.F. Browner, *Anal. Chem.*, 56 (1984) 2626.
25 F.W. McLafferty, *Interpretation of Mass Spectra*, University Science Books, Mill Valley, CA, 3rd ed., 1980, pp. 206–207

Journal of Chromatography, 647 (1993) 101–105
Elsevier Science Publishers B.V., Amsterdam

CHROMSYMP. 2737

Application of particle-beam mass spectrometry to drugs

An examination of the parameters affecting sensitivity

P.R. Tiller

Structural Chemistry Department, Glaxo Group Research Ltd., Greenford Road, Greenford, Middlesex, UB6 0HE (UK)

ABSTRACT

The qualitative performance of a particle-beam interface is evaluated by an examination of the effects of altering the pressure of the nebulisation gas, the nebuliser position, the desolvation chamber temperature, the temperature of the nebulisation gas, the temperature of the source and the solvent composition. All these parameters have an impact on performance excepting the nebulisation gas temperature. A summary of the "optimum" settings for routine operation is given.

INTRODUCTION

In recent years several new liquid chromatography–mass spectrometry (LC–MS) interfaces have become commercially available, increasing the range of compounds amenable to analysis by LC–MS; one of these being the particle-beam interface. Several papers have been published dealing with the optimisation of the interface [1] and outlining some of its limitations such as linearity [2], peak broadening [3] and matrix effects [4]. The performance of the interface in this laboratory did not reflect that expected, based upon published data [1], so it was thought prudent to perform an evaluation of the interface to determine what parameters concerned with its operation are crucial to performance.

This paper describes an evaluation of the particle-beam interface using three drug compounds of commercial interest to Glaxo [Lacidipine (anti-hypertensive, M_r 455.56), Ondansetron (anti-emetic, M_r 293.37) and Sumatriptan (anti-migraine, M_r 295.41)]. The parameters examined were the effects of altering the pressure of the nebulisation gas, the nebuliser position, the desolvation chamber temperature, the temperature of the nebulisation gas, the temperature of the source and the solvent composition. The solvent flow-rate is known to be of importance with a recommended rate of 0.4–0.6 ml/min being optimum [1]. In this laboratory flow-rates much in

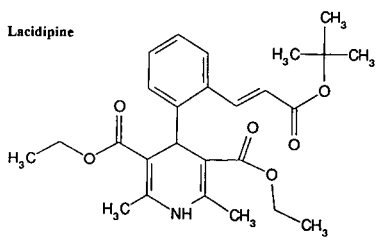

0021-9673/93/$06.00

excess of 0.5 ml/min with high aqueous content have resulted in the formation of liquid droplets inside the desolvation chamber. Therefore all experiments were performed at a flow-rate of 0.5 ml/min.

EXPERIMENTAL

Equipment

The HPLC–MS was performed using an LCC 2252 controller with two 2248 pumps (Pharmacia Biosystems, Milton Keynes, UK) with the flow set to 0.5 ml/min coupled to an HP59980B particle-beam interface and an HP5989A MS-ENGINE quadrupole mass spectrometer (Hewlett-Packard, Palo Alto, CA, USA) scanning 120–650 amu per 0.6 s. Chemical ionisation spectra were obtained using ammonia reagent gas and an electron energy of 230 eV. The fused silica used in the nebuliser assembly has an I.D. of 0.200 mm. These are available in pre-cut lengths (8.5 cm) (Hewlett-Packard).

Chemicals

Methanol (HPLC grade) was obtained from Rathburn (Walkerburn, UK), acetonitrile (HPLC solvent) and ammonium acetate (FSA laboratory supplies, Loughborough, UK). Distilled water was prepared in-house. Lacidipine, Ondansetron and Sumatriptan were obtained in-house and dissolved in acetonitrile, methanol and methanol–water (50:50) respectively.

Design

The reason for this evaluation was to determine performance trends, and thus identify an "optimum" set of parameters for day-to-day operation of the interface. Therefore the absolute responses obtained for the test compounds were of no interest. This made experimental design much easier.

Each experiment consisted of a series of flow injections (20 μl) of the test compounds with changes made in either the pressure of the nebulisation gas, the nebuliser position, the desolvation chamber temperature, the temperature of the nebulisation gas, or the temperature of the source in conjunction with changes in the solvent composition. Each data point was the average of three injections where the mass spectral response had been determined using the automated quantitation routine. The most intense response was taken as 100% and all others calculated as percentages of that.

Experiments were initially carried out on all three drugs with the solvent compositions methanol–water (25:75), (50:50) and (75:25) and then using only Ondansetron with the solvent compositions acetonitrile–water (25:75), (50:50) and (75:25).

RESULTS

The nebulisation gas pressure has a marked effect on the response obtained with solvent compositions methanol–water (25:75), (50:50) and (75:25) (Fig. 1). A 10-fold increase in response was obtained as the pressure is increased from 30–70 p.s.i. (1 p.s.i. = 6894.76 Pa). With solvent compositions acetonitrile–water (50:50) and (75:25) (Fig. 2) the improvement is less than 2-fold though at acetonitrile–water (25:75) the increase in response is 5-fold. These data clearly

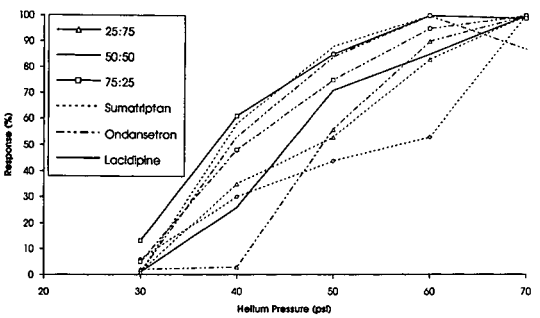

Fig. 1. Effect of helium pressure on response (methanol–water).

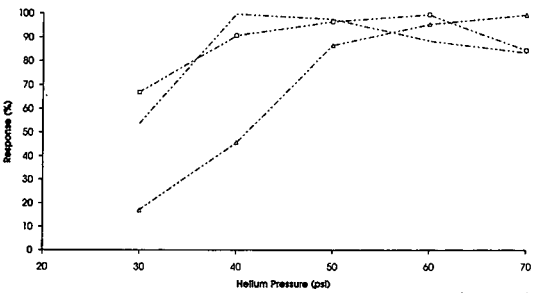

Fig. 2. Effect of helium pressure on response (acetonitrile–water). For symbols see Fig. 1.

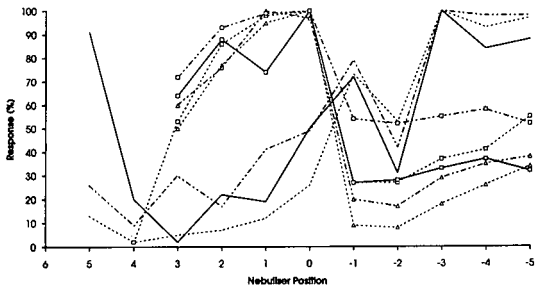

Fig. 3. Effect of nebuliser position at 40 p.s.i. (methanol–water). For symbols see Fig. 1.

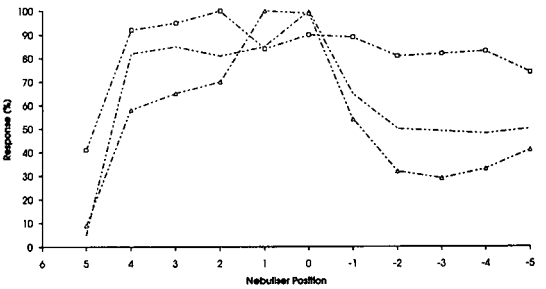

Fig. 6. Effect of nebuliser position on response at 60 p.s.i. (acetonitrile–water). For symbols see Fig. 1.

indicate that the nebulisation gas pressure has a most significant effect on the transmission of analyte molecules through the particle-beam interface.

The position of the fused-silica capillary inside the nebuliser body had a significant impact on the response obtained. It was observed that with a nebulisation gas pressure of 40 p.s.i. (Fig. 3) the position of the nebuliser could afford as much as a 10-fold increase in response. At 60 p.s.i. (Fig. 4) the variations in response were less severe but still significant. A similar response profile was obtained with Ondansetron using acetonitrile (Figs. 5 and 6) instead of methanol. It was observed that with a nebulisation gas pressure of 40 p.s.i. there appeared to be an optimum position when the fused-silica capillary was flush or protruding a little from the nebuliser body at all solvent compositions, except at methanol–water (50:50) when the optimum appeared to occur with the capillary retracted into the nebuliser body.

Increasing the desolvation chamber temperature afforded a variable improvement in response while using either methanol or acetonitrile (Figs. 7 and 8). Though it was quite clear

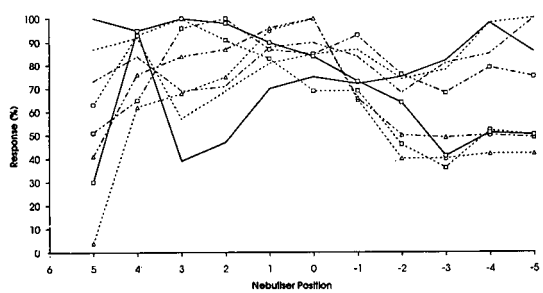

Fig. 4. Effect of nebuliser position at 60 p.s.i. (methanol–water). For symbols see Fig. 1.

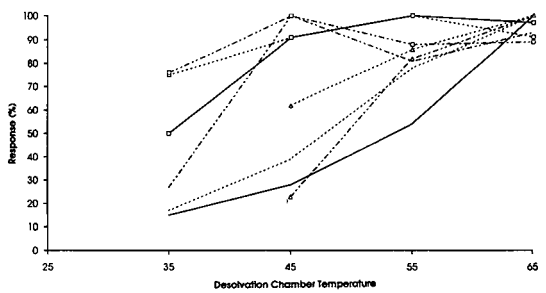

Fig. 7. Effect of desolvation chamber temperature (°C) on response (methanol–water). For symbols see Fig. 1.

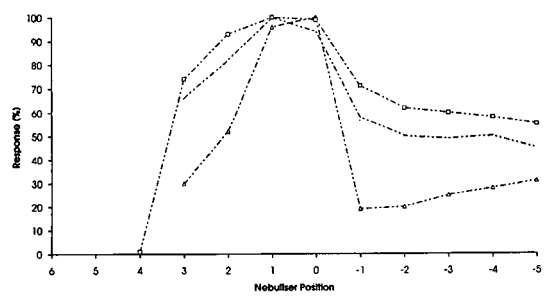

Fig. 5. Effect of nebuliser position on response at 40 p.s.i. (acetonitrile–water). For symbols see Fig. 1.

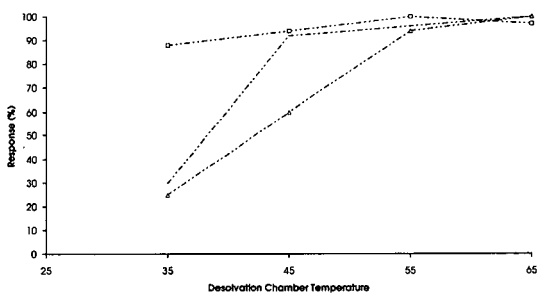

Fig. 8. Effect of desolvation chamber temperature (°C) on response (acetonitrile–water). For symbols see Fig. 1.

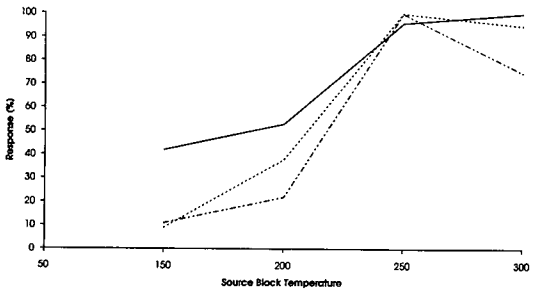

Fig. 9. Effect of source block temperature (°C) on response. Nebuliser gas pressure, 60 p.s.i.; desolvation chamber temperature, 55°C; solvent composition, methanol–water (50:50).

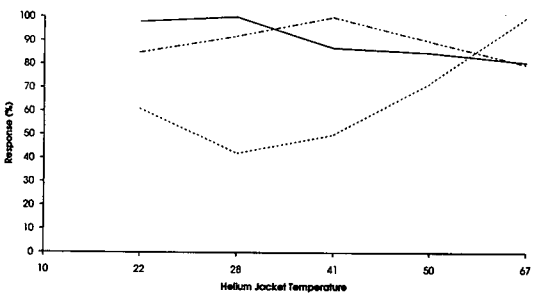

Fig. 11. Effect of heating helium on response at 60 p.s.i. Nebuliser gas pressure, 60 p.s.i.; desolvation chamber temperature, 55°C; solvent composition, methanol–water (50:50). Helium jacket temperature in °C.

that an improvement in response was obtained at higher temperatures. This must reflect both the mass of the analyte and the susceptibility of the various solvent compositions to desolvation.

The remaining experiments were carried out with a nebuliser gas pressure of 60 p.s.i., a desolvation chamber temperature of 55°C and with a solvent composition of methanol–water (50:50).

Changing the source block temperature from 150–300°C (Fig. 9) resulted in as much as a 10-fold increase in response for Sumatriptan and Ondansetron, but only a 2.5-fold increase for Lacidipine. This is likely to reflect the chemical properties of the anlayte as well as the degree of desolvation already achieved during passage through the interface.

Heating the helium nebulisation gas afforded, if anything, a decrease in response with a nebulisation gas pressure of 40 p.s.i. (Fig. 10). There was no apparent trend with a nebulisation gas pressure of 60 p.s.i. (Fig. 11). Possibly the nebulisation gas pressure and the desolvation chamber temperature masked any increase in response. If that were the case the increases in response could only have been very minor.

Addition of 0.1 *M* ammonium acetate to the solvent system resulted in a 2.5-fold increase in response for both Sumatriptan and Ondansetron with a 1.5-fold increase for Lacidipine. Increasing the concentration of the ammonium acetate did not appear to afford any further increase in response, such "carrier effects" have been previously reported [5]. Lacidipine affords less of an increase probably due to its greater mass than either Ondansetron or Sumatriptan, such that the "carrier effect" is reduced.

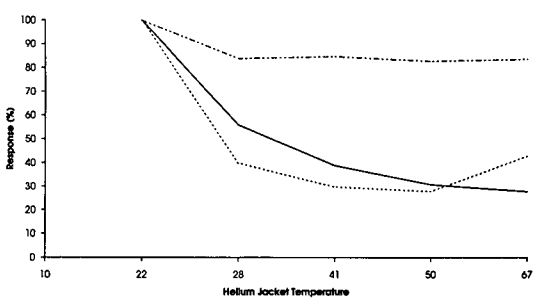

Fig. 10. Effect of heating helium on response at 40 p.s.i. Nebuliser gas pressure, 60 p.s.i.; desolvation chamber temperature, 55°C; solvent composition, methanol–water (50:50). Helium jacket temperature in °C.

CONCLUSION

Examination of the results obtained indicate that the nebulisation gas pressure, nebuliser position, desolvation chamber temperature and source temperature all have a significant impact on sensitivity. It was also observed that the optimum settings at one solvent composition were often close to optimum for most other solvent compositions. Heating the helium nebulisation gas appeared to offer no improvement in sensitivity.

Following this study the particle-beam interface is routinely operated in this laboratory using the following conditions: (i) helium nebulisation gas pressure 60 p.s.i.,(ii) nebuliser position 0–1

(so the silica capillary protrudes a little), (iii) desolvation chamber temperature 55°C, (iv) source block temperature 250°C, (v) 0.2 *M* aqueous ammonium acetate.

REFERENCES

1 R.D. Voyksner, C.S. Smith and P.C. Knox, *Biomed. Environ. Mass Spectrom.*, 19 (1990) 523–534.
2 A. Apffel and M.L. Perry , *J. Chromatogr.*, 554 (1991) 103–118.
3 A.P. Tinke, R.A.M. van der Hoeven, M.A. Niessen, U.R. Tjaden and J. van der Greef , *J. Chromatogr.*, 554 (1991) 119–124.
4 F.R. Brown and W.M. Draper, *Biol. Mass. Spectrom.* 20 (1991) 515–521.
5 T.A. Bellar, T.D. Behymer and W.L. Budde, *J. Am. Soc. Mass Spectrom.*, 1 (1990) 92–98.

Journal of Chromatography, 647 (1993) 107–119
Elsevier Science Publishers B.V., Amsterdam

CHROMSYMP. 2793

Liquid chromatography–mass spectrometry for the identification of minor components in benzothiazole derivatives

W.M.A. Niessen*

Division of Analytical Chemistry, Leiden/Amsterdam Center for Drug Research, P.O. Box 9502, 2300 RA Leiden (Netherlands)

C.C. McCarney and P.E.G. Moult

Technical Centre, Monsanto Europe SA, Rue Laid Burniat, B-1348 Louvain-la-Neuve (Belgium)

U.R. Tjaden

Division of Analytical Chemistry, Leiden/Amsterdam Center for Drug Research, P.O. Box 9502, 2300 RA Leiden (Netherlands)

J. van der Greef

Division of Analytical Chemistry, Leiden/Amsterdam Center for Drug Research, P.O. Box 9502, 2300 RA Leiden (Netherlands) and TNO-CIVO Institutes, P.O. Box 360, 3700 AJ Zeist (Netherlands)

ABSTRACT

Various mass spectrometric techniques were explored for their ability to detect and identify minor components in benzothiazole-derived compounds, namely gas chromatography–mass spectrometry, liquid chromatography–mass spectrometry using a moving-belt, a thermospray and a particle-beam interface and liquid chromatography–tandem mass spectrometry in combination with a thermospray interface. The necessary changes in the liquid chromatographic solvent systems were accomplished by translation of gradient runs into a series of isocratic runs, and a UV photodiode-array detector was used to trace the peaks. The methodology developed and the advantages and limitations of the different techniques employed are discussed.

INTRODUCTION

The use of high-performance liquid chromatography (HPLC) has become invaluable in defining the composition of benzothiazole derivatives, which are used as vulcanization accelerators [1]. The identification of minor components in these products by comparison of the retention times with those of known compounds has always been questionable, as it assumes that compounds with different structures will have different retention times under a particular set of chromatographic conditions, an assumption that has been found to be misleading in our laboratories, especially when the mixtures are complex.

During the last decade, new techniques have become available that can remove the uncertainty when using this method of peak identification, and their application to benzothiazole derivatives has been explored. In this study, various interfaces for combined liquid chromatography–mass spectrometry (LC–MS) [2] were evaluated for

* Corresponding author.

0021-9673/93/$06.00

their potential in the identification of minor components found in laboratory samples of 2(3*H*)-benzothiazolethione and its derived products. The procedure followed can be summarized as follows: the HPLC gradient elution programmes, initially developed for the analysis of the products using UV detection, were translated into a series of isocratic runs; a UV photodiode-array (PDA) detector was used to correlate the various peaks in the chromatogram. LC–MS was then performed under isocratic conditions using various interfaces, *i.e.*, the moving-belt interface (MBI) in both electron impact (EI) and positive-ion chemical ionization (CI) modes [2,3], the thermospray (TSP) interface in both buffer ionization and discharge-on modes [2,4] and the particle beam interface (PBI) in the EI mode [2,5]. For further structure elucidation, tandem mass spectrometry (MS–MS) was performed in combination with the TSP interface and GC–MS data were also acquired.

In this paper the procedures used and some of the results are outlined and discussed with some typical examples. Lastly, the abilities of the different LC–MS interfaces to characterize successfully the benzothiazole derivatives are compared.

(1)

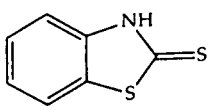

(2)

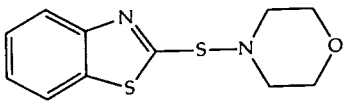

(3)

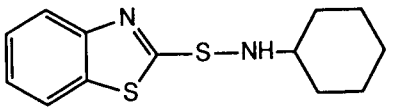

(4)

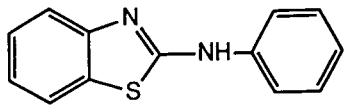

(10)

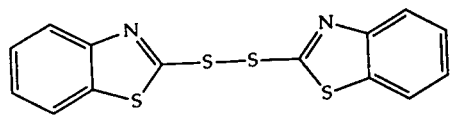

Fig. 1. Structures of the major components studied. **1** = 2(3*H*)-benzothiazolethione; **2** = 4-(2-benzothiazolylthio)morpholine; **3** = N-cyclohexyl-2-benzothiazolesulphenamide; **4** = N-phenyl-2-benzothiazolamine; **10** = 2,2′-dithiobisbenzothiazole.

EXPERIMENTAL

Materials

Acetonitrile was of HPLC quality (Rathburn Chemicals, Walkerburn, UK). Water was purified with a Milli-Q water purification system (Millipore). All other chemicals were of analytical-reagent grade.

Sample solutions containing *ca.* 5 mg/ml were prepared in either acetonitrile or dioxane. Generally, the solutions were centrifuged before use. Samples A and B contained 2(3*H*)-benzothiazolethione (**1** in Fig. 1) as its major constituent, sample C primarily consisted of 4-(2-benzothiazolylthio)morpholine (**2** in Fig. 1) and sample D of N-cyclohexyl-2-benzothiazolesulphenamide (**3** in Fig. 1).

Liquid chromatography

Gradient elution was performed using a Beckman (Anaheim, CA, USA) System Gold injection and solvent-delivery system, a 250 mm × 4.6 mm I.D. Beckman Ultrasphere ODS column and a Hewlett-Packard (Palo Alto, CA, USA) Type 1040-A photodiode-array detector, equipped with a Hewlett-Packard Model 85B computer and operated in the range 200–400 nm.

Three different gradient programmes were applied, using mixtures of solvent A [20% (v/v) acetonitrile in water] and solvent B (acetonitrile). For samples A and B a linear gradient programme was used from 16% to 94% solvent B in 30 min, followed by washing the column with solvent B for 20 min. The flow-rate was 1.6 ml/min. For sample C a gradient programme was applied, in which both the solvent composition and the flow-rate were changed with time (see Fig. 2). For sample D a linear gradient programme was used from 5% to 94% solvent B in 33 min, starting 10 min after injection and followed by washing the column with solvent B

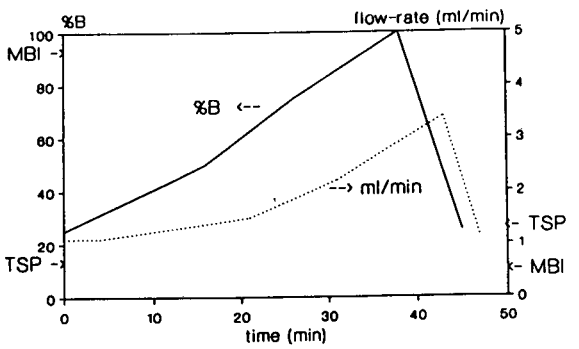

Fig. 2. Gradient elution and flow-rate programme used for the analysis of sample C. Optimum flow-rate and solvent composition conditions for the moving-belt interface (MBI) and the thermospray (TSP) interface are indicated on the abscissae.

for 12 min. The flow-rate was kept at 1.6 ml/min.

For the translation of the gradient runs to a set of isocratic runs, the same instrumentation was used. In an isocratic run either pure solvent B or a fixed percentage of solvent B (*e.g.*, 75%, 50% or 25%) was added to solvent A. The mobile phases used in the LC–MS experiments were made in the same way. The flow-rate used was 1.0 ml/min with mobile phases containing ≥50% of solvent B and 0.5 ml/min with mobile phases containing <50% of solvent B. The column was washed with pure acetonitrile after each run.

Gas chromatography–mass spectrometry

GC–MS was performed on a combination of a Chrompack Packard (Middelburg, Netherlands) Model 438A gas chromatograph and a Finnigan MAT (San José, CA, USA) Model 700 ion trap detector. A 10 m × 0.25 mm I.D. Chrompack CP-Sil-5 capillary column was coupled to the mass spectrometer by means of an open split coupling. A temperature-programmed GC separation was performed with a linear temperature ramp of 15°C/min from 70 to 280°C.

LC–MS using a moving-belt interface

LC–MS experiments with a Finnigan MAT moving-belt interface were performed with a Finnigan MAT HSQ-30 hybrid MS–MS instrument. It was operated in the EI or CI mode (ammonia as reagent gas). The moving-belt interface was operated with a solvent evaporator temperature of 200–220°C, a belt speed of 35 mm/s and the vaporizer at position 7–8.

The LC system consisted of an LKB (Bromma, Sweden) Model 2150 high-pressure pump, a Rheodyne (Cotati, CA, USA) Model 7125 injection valve with a 20-μl loop, a Beckman 250 mm × 4.6 mm I.D. Ultrasphere ODS column and a Kratos (Manchester, UK) Model 757 variable-wavelength detector, operated at either 254 or 275 nm.

LC–MS experiments with a thermospray interface

LC–MS was performed with a Finnigan MAT thermospray interface on a Finnigan MAT TSQ-70 triple quadrupole mass spectrometer. The thermospray interface was operated with a vaporizer temperature of 100–120°C, a block temperature of 200°C and a repeller potential of 0–50 V. LC–thermospray MS was performed either in the thermospray buffer ionization mode, by using 0.1 mol/l ammonium acetate in water in solvent A instead of water, or in the discharge-on mode (discharge potential 1 kV) with the regular solvent system. No influence on the chromatographic retention time was observed as a result of the addition of ammonium acetate to the solvent system.

The LC system consisted of an LKB Model 2150 high-pressure pump, a Rheodyne Model 7125 injection valve with a 20-μl loop, a Beckman 250 mm × 4.6 mm I.D. Ultrasphere ODS column and a Waters (Rochester, MN, USA) Model 440 fixed-wavelength detector, operated at 254 nm.

LC–MS with a particle-beam interface

LC–MS was performed with a Hewlett-Packard Model 59980A particle-beam interface, fitted on a Finnigan MAT TSQ-70 triple quadrupole mass spectrometer [6]. The mass spectrometer was operated in the EI mode.

The LC system was similar to that used with the thermospray interface. The column (150 mm × 4.6 mm I.D.) was laboratory-packed with 10-μm C_{18} material. A mobile phase of acetonitrile–water (75:25) was used at a flow-rate of 0.5 ml/min.

MS–MS experiments

MS–MS experiments were performed on a Finnigan MAT TSQ-70 triple quadrupole mass spectrometer equipped with a Finnigan MAT thermospray interface. Samples subjected to collision-induced dissociation (CID) were introduced either in the column by-pass or in the LC mode. The collision pressure and energy were optimized for a particular application, and were typically set at 0.05–0.15 Pa of air and 10–50 eV, respectively.

RESULTS AND DISCUSSION

General strategy

The objectives of this study were the assessment of the potential of current LC–MS techniques for the unequivocal characterization of minor components in benzothiazole compounds.

The samples of interest generally have a purity exceeding 95% for the major component, with the remainder consisting of a number (usually up to 10) minor components. The low concentration and number of the minor components practically exclude fraction collection and off-line mass spectrometric analysis. Further, in some fraction collection experiments, unwanted modification of the components in a fraction was observed, with the UV chromatogram of the fraction differing considerably from the original part of the chromatogram. For these reasons, on-line LC–MS was considered to be the method of choice. At first, the MBI was selected because of its ability to be used with both EI and CI, which is most favourable for structure elucidation. For reasons outlined below, the MBI was replaced with the TSP interface; preliminary studies were also performed with a PBI when it became available in our laboratory.

Unfortunately, the LC conditions that were developed for optimum resolution of the minor components and UV detection were not compatible with direct on-line LC–MS analysis with the MBI or TSP interface (*cf.*, Fig. 2), principally because of the gradient elution conditions employed. Considering the facts that the moving belt interface with a direct contact deposition device, as used in this project, does not perform well under gradient elution conditions [2,3], and that the ionization conditions in LC–TSP-MS depend strongly on the mobile phase composition [2,4], it was decided to perform the LC–MS experiments with isocratic elution. Further, the applied flow-rates are generally too high for the MBI, while the range of flow-rate programming is not compatible with the TSP interface (*cf.*,

TABLE I

PEAK CORRELATION FOR 2(3*H*)-BENZOTHIAZOLETHIONE, SAMPLE A

Gradient (min)		UV max. (nm)	100%B	75% B	50% B
254 nm[a]	PDA				
	4.88	243,282		2.77	3.42
7.27	6.87[b]	321			
8.33	–				
	14.16	324			8.24
	15.88	328			10.83
17.10	16.20	237,303			11.35
23.15	22.38	264,301,330		9.02	
26.24	25.33	270		13.70	
33.94	33.00	260–280	6.75		
	33.70	306	8.12		
35.22	35.94	289,370	11.41		

[a] The data for 254 nm were obtained using a different apparatus with a fixed-wavelength UV detector and a different column.
[b] Major component.

Fig. 2). Therefore, it was decided to translate each gradient run into a series of isocratic runs. For the MBI, an additional advantage of this procedure is that the analysis is performed at the highest possible acetonitrile content of the mobile phase. In order to ensure the correlation between the peaks in the chromatograms obtained under gradient conditions and those under isocratic conditions, a PDA detector was used. Following this, the LC–MS analysis was performed under isocratic conditions.

UV photodiode-array detection; peak correlation

The samples of interest were first analysed with the appropriate gradient programme using a PDA detector. The peak purity was checked by comparing UV spectra at the front end, the back end and the top of the chromatographic peak. In this way, a collection of UV spectra and retention time data was obtained for each sample. As an example, these data are summarized for sample A in Table I and for sample C in Table II.

Subsequently, the samples were analysed in a series of isocratic runs using the PDA detector. The peaks detected were checked for peak purity and the UV spectra obtained were compared with the UV spectra obtained under gradient conditions. Corresponding peaks in gradient and isocratic runs could be found in this way (see Tables I and II for the results with samples A and C, respectively). Careful comparison of the UV spectra is obligatory; a conclusion cannot be based on comparing the wavelengths of absorbance maxima only. Although this procedure was cumbersome with the old version of the PDA detector and accompanying software that was available, it worked fairly well provided that the samples were not too complex. It can be considered as a general method of keeping track of UV-absorbing chromatographic peaks when the mobile phase composition must be changed, *e.g.*, for on-line LC–MS analysis. Further, the use of the PDA detector allows the detection of components that show low absorbance at the one fixed wavelength selected with a conventional UV detector for LC (see, for instance, the peaks at retention times 14.16 and 15.88 in Table I).

The availability of UV spectra of the various components in the samples also allowed the generation of cross-correlation tables, based on retention times and UV spectra. For instance, the peaks at 6.87 and 25.33 in the gradient run with sample A correspond to the peaks at 7.12 and 27.90, respectively, in the gradient run with sample C (using a different gradient programme); the second peak is also found in the 75% isocratic runs with both samples, *i.e.*, at 13.70 for sample A and at 13.94 for sample C. By studying the data from a wider variety of

TABLE II

PEAK CORRELATION FOR 4-(2-BENZOTHIAZOLYLTHIO)-MORPHOLINE, SAMPLE A

Gradient (min)		UV max. (nm)	100%B	75% B	50% B	37.5% B
275 nm[a]	PDA					
6.66	5.87	239,278	3.08	3.02	3.78	9.61
	7.12	321			4.07	
10.94	9.33	273			5.34	15.33
	10.91	238,276			5.62	18.11
16.03	14.44[b]	272				
	20.16	279				
	25.54	276–315		10.23		
27.29	26.13	290		10.90		
28.51	27.90	270	5.68	13.94		

[a] The data for 275 nm were obtained using a different apparatus with a fixed-wavelength UV detector and a different column.
[b] Major component.

samples, more extensive cross-correlation tables could be made, which substantially helped in the identification of the compounds in the various samples.

In some instances, the PDA was also helpful in discriminating between isomers. In samples A and sample C a component with a molecular mass of 300 was observed. From the respective UV spectra, shown in Fig. 3, it could be concluded that these components were not identical, but in fact isomers (**8** and **24**). The identity of one of the isomers (**24**) was checked with a standard, while literature data on the UV spectrum of the other (**8**) were available [7].

Obviously, the isocratic conditions that were needed to detect certain components in the mixture with the PDA detector do not necessarily correspond to the conditions required in LC–MS.

LC–MS using a moving-belt interface

The primary reason for selecting the MBI was its ability to generate EI mass spectra that would be easily interpretable from the broad knowledge of EI fragmentation and with the use of on-line library searching. Some typical EI mass spectra obtained in on-line LC–MS with the MBI are given in Fig. 4. An additional feature of the MBI-MS system was the ability to perform exact mass determination via high-resolution measurements.

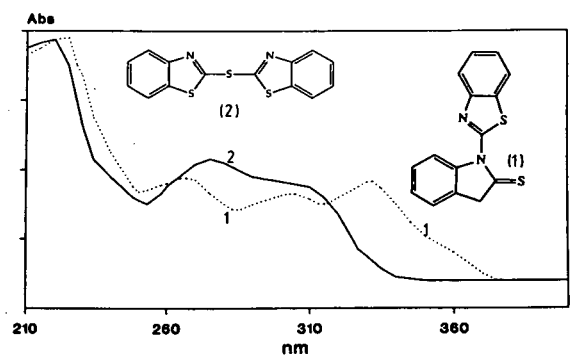

Fig. 3. UV spectra of the two components with molecular mass 300. 1 = [2,3′(2′*H*)-bibenzothiazole]-2′-thione (**8**); 2 = 2,2′-thiobisbenzothiazole (**24**).

In practice, some severe problems were experienced, which seriously limited the potential of the MBI. Although it was possible to obtain EI spectra for some of the minor components (see, *e.g.*, Fig. 4a), the combination of peak tailing in the isocratic runs and the common belt memory effects [2,3,8] led to the inability to obtain clean EI spectra for those components at very low levels, or for ones eluting close to the major compound (see, *e.g.*, Fig. 4b). As a result, it was impossible to obtain interpretable EI spectra in many cases. Generally, the mass region below *m/z* 170 was hardly useful with respect to spectral interpretation. With the use of reconstructed mass chromatograms in the region of a chromatographic peak it can be decided which peaks in a spectrum were actually due to the compound, and which were due to the interferences from belt memory effects. For the peak the spectrum of which is given in Fig. 4b, the peaks at *m/z* 167 and 86 are fragment peaks due to the major component of the sample. Various background subtraction procedures failed to produce relatively reproducible spectra, as a result of which it remains unclear which peaks should be considered during the interpretation. Attempts to solve these problems by using isocratic runs with mobile phases with a higher water content were discontinued because, for some components, thermal degradation was observed as a result of the higher solvent evaporator temperature needed with higher water contents of the mobile phase.

Another difficulty that was experienced is related to the amount of structural information that could be derived from the mass spectra. In the spectrum of N-phenyl-2-benzothiazolamine (**4**), a known constituent of sample A, in Fig. 4c, a loss of 45 u is observed, which basically can only be explained by a loss of CSH, resulting from a major rearrangement of the ion.

The two spectra in Fig. 4d and e are due to components that surprisingly do not show up in the UV chromatograms. The tentative structures assigned to the probable molecular ions at *m/z* 524 and 391 resulted from the following considerations. High-resolution peak matching on *m/z* 391 results in an elemental composition of $C_{20}H_{13}N_3S_3$. Loss of 33 u (SH) results in *m/z*

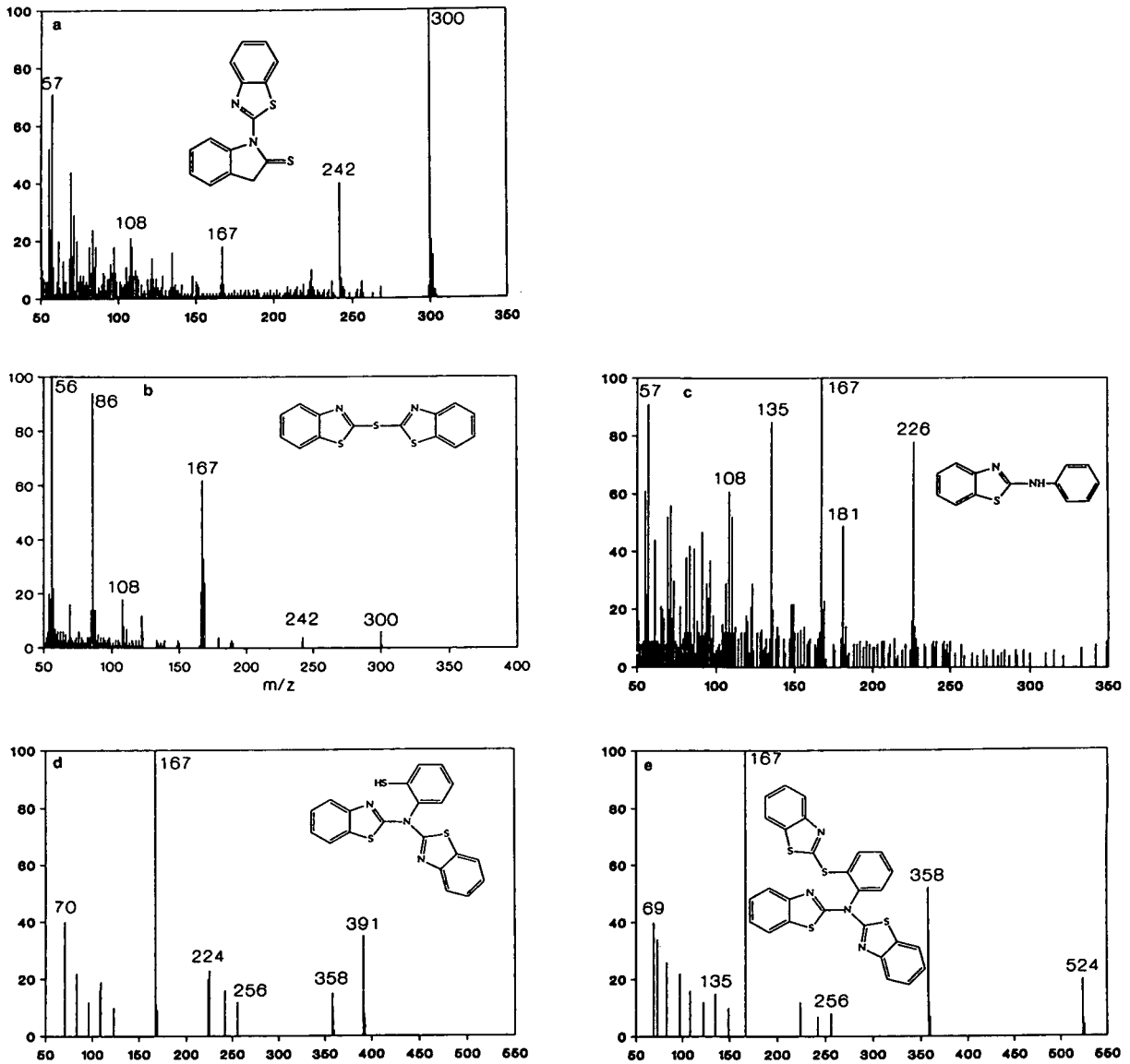

Fig. 4. EI mass spectra for some minor components in sample A or C obtained with LC–MS using a moving-belt interface. (a) Spectrum of [2,3′(2′*H*)-bibenzothiazole]-2′-thione (**8**) (gradient 22.38 min) obtained from sample A with a 75% B in A isocratic run. (b) Spectrum of 2,2′-thiobisbenzothiazole (**24**) (gradient 25.54 min) obtained from sample C with a 100% B isocratic run. (c) Spectrum of N-phenyl-2-benzothiazolamine (**4**) (gradient 16.20 min) obtained from sample A with a 50% B in A isocratic run. (d) Spectrum of **9** (not observed in gradient) obtained from sample A with a 100% B isocratic run. (e) Spectrum of **11** (not observed in gradient) obtained from sample A with a 100% B isocratic run.

358, which fragments to *m/z* 256, 242 and 224. The latter can be explained by the loss of a benzothiazole group. Loss of 166 u (a mercaptobenzothiazole group) from the *m/z* 524 molecular ion also resulted in *m/z* 358, with a similar fragmentation pattern. Other isomers are also possible.

In Tables IV and VI a summary is given of the

compounds that could be identified in the samples A and C, respectively, using the MBI system. The compounds identified are indicated by a number, referring to Table III, in which the names of all compounds found are collected.

LC–MS with a thermospray interface

Considering the difficulties in obtaining sufficient information with the MBI, it was decided to investigate the potential of the TSP interface, which was also available in our laboratory, for this identification problem. Some feasibility tests showed that generally identical spectra are obtained with buffer ionization and discharge-on modes (with only some differences with respect to the observed solvent adduct ions), and that generally no fragmentation is observed. Obviously, some compounds are not amenable to the type of ionization obtained with the TSP interface, *e.g.*, sulphur (S_8) is not detected in TSP whereas it is detected by EI. Further, the response is highly compound dependent, as is demonstrated, *e.g.*, by the fact that the major component in sample A, 2(3*H*)-benzothiazolethione (**1**), yields a signal in buffer ionization that is only three times higher than that of minor component N-phenyl-2-benzothiazolamine (**4**). This may lead to difficulties in detecting and identifying the less polar compounds, an effect that is further enhanced by the fact that these components elute in the final part of the chromatograms.

Another problem met in the experiments with the TSP interface was the difficulty of detecting the peaks of minor compounds in the total ion chromatogram (TIC), as instability of the TSP vaporization process sometimes yielded unstable TIC traces. By systematic searching through the data files using mass chromatography, it was possible to extract the various peaks from the data, but in searching for unknowns such a procedure can be cumbersome.

Nevertheless, with the TSP interface a significant number of peaks in the various samples could be detected and the molecular mass could be determined. In some instances the molecular mass confirmed the presence of expected compounds. This is the case, for instance, with the sulphinamide **20** and the sulphonamide **22** found in sample C, which could be identified from their molecular masses and chromatographic retention times, as standards were available.

However, as fragmentation was lacking, other means must be used for structure elucidation and identification. Some experiments applying repeller-induced fragmentation [9,10] gave some results, especially when the peak intensity was sufficiently large. In many instances, however, a significant decrease in signal intensity was observed, which is partly due to the fragmentation, but which restricted the ability to detect the peak and to produce the accompanying spectrum. Therefore, the potential of tandem mass spectrometry was investigated.

TABLE III

IDENTIFICATION OF THE COMPOUNDS STUDIED

1	2(3*H*)-Benzothiazolethione
2	4-(2-Benzothiazolylthio)morpholine
3	N-Cyclohexyl-2-benzothiazolesulphenamide
4	N-Phenyl-2-benzothiazolamine
5	2(3*H*)-Benzothiazolone
6	Benzothiazole
7-2	2-(Methylthio)benzothiazole
7-3	3-Methyl-2(3*H*)-benzothiazolethione
7-6	6-Methyl-2(3*H*)-benzothiazolethione
8	[2,3′(2′*H*)-Bibenzothiazole]-2′-thione
9	N,N-Di(2-benzothiazolyl)-2-aminobenzenethiol
10	2,2′-Dithiobisbenzothiazole
11	N,N-Di(2-benzothiazolyl)-S-(2-benzothiazolyl)-2-aminobenzenethiol
12	Sulphur
13	Benzenamine
14	N,N′-Diphenylthiourea
15	N-Phenylbenzenamine
16	2-(Phenylthio)benzothiazole
17	10*H*-Phenothiazine
18	2-Phenylbenzothiazole
19	2,2′-Bisbenzothiazole
20	4-(2-Benzothiazolylsulphinyl)morpholine
21	2-(4-Morpholinyl)benzothiazole
22	4-(2-Benzothiazolylsulphonyl)morpholine
23	2-(4-Morpholinyldithio)benzothiazole
24	2,2′-Thiobisbenzothiazole
25	N-Cyclohexyl-2-benzothiazolesulphinamide
26	N-Cyclohexyl-2-benzothiazolesulphonamide
27	N-Cyclohexyl-2-benzothiazolamine

LC–MS–MS with a thermospray interface

MS–MS was applied to this problem in a number of ways, using either product ion or precursor ion scans. In the product ion mode, an ion with a particular m/z value is selected in the first mass analyser and transferred to a collision chamber. The fragment ions generated on collision are mass analysed in the second mass analyser. In the precursor ion mode, the procedure is reversed: an ion with a particular m/z value is selected in the second mass analyser. A signal is only detected when the ions mass analysed in the first mass analyser generate that particular ion on collision. The m/z value of the precursor ion leading to the product ion detected is recorded [11]. Product ion spectra were obtained for selected chromatographic peaks during LC–TSP-MS operation. In this way a considerable number of unknowns could be identified; for others identification was not possible based on the information obtained from the MS–MS data. However, considering the type of products and expected minor components involved, precursor ion scans can be used to trace existing minor components. Precursor ion scans that were applied included the product ions of m/z 134, 166, 168, 87 (for the morpholine derivatives) and 99 (for the cyclohexyl derivatives). Precursor ion scans were performed in combination with LC and also with column-bypass injection of the samples. Subsequently, product ion spectra were acquired from all new precursor ions detected in this way. A number of unknowns could be identified in this way. Unfortunately, a considerable number of product ion spectra contained little information on the identity of the compound. In one of the samples three unknown precursors were detected in a precursor m/z 168 experiment, *i.e.*, at m/z 254, 238 and 252. The product ion spectra of the precursor contained product ions at m/z 168, 87, 71 and 43 for the precursor ion at m/z 254, and at m/z 168, 85 and 57 for the precursor ions at m/z 238 and 252. No identification of the groups attached to mercaptobenzothiazole is possible from these data.

The compounds identified in samples A, B, C and D using LC–MS and LC–MS–MS with the TSP interface are indicated in the Tables IV, V, VI and VII, respectively. It can be concluded that most of the components of these four samples could be identified.

Intermolecular reactivity in thermospray

An interesting aspect of the TSP experiments is the observation of considerable intermolecular

TABLE IV

PEAK IDENTIFICATIONS IN 2(3*H*)-BENZOTHIAZOLETHIONE, SAMPLE A[a]

Gradient (min)	UV max. (nm)	M_r	Identification[b]	MBI	TSP	GC–MS
4.88	243,282	151	**5**	–	×	–
6.87	321	167	**1 + 6**	×	×	×
14.16	324	181	**7**	–	×	×
15.88	328	181	**7**	–	×	×
16.20	237,303	226	**4**	×	×	–
22.38	264,301,330	300	**8**	×	×	×
		391	**9**	×	×	–
25.33	270	332	**10**	×	×	×
		524	**11**	×	×	–
33.00	260–280	256	**12**	×	–	×
33.70	306	?	–	–	–	–
35.94	289,370	?	–	–	–	–

[a] × = –Identified; – = not detected.

[b] See Table III.

TABLE V

PEAK IDENTIFICATIONS IN 2(3*H*)-BENZOTHIAZOLETHIONE, SAMPLE B[a]

Gradient (min)	UV max. (nm)	M_r	Identification[b]	TSP	BPI	GC–MS
	241	93	**13**	×	–	×
7.02	216,248	135	**6**	×	–	×
7.02	321	167	**1**	×	×	×
10.34	272	228	**14**	×	–	×
12.32	324	181	**7-3**	×	×	×
14.56	275	181	**7-2**	×	×	×
17.20	237,303	226	**4**	×	×	×
		169	**15**	×	–	×
		243	**16**	×	×	–
17.69	328	181	**7-6**	×	–	–
18.31	250	199	**17**	×	–	×
20.78	217,295	211	**18**	×	×	×
21.17	250,285	–	–	–	–	–
23.67	300	–	–	–	–	–
		300	**8**	×	–	×
24.24	242,343	268	**19**	×	×	×
34.35	260–280	256	**12**	–	–	×

[a,b] See Table IV.

reactivity. As the samples contained over 95% of the major component, large amounts of this material were generally introduced into the ion source. Spectra acquired during the elution of the major components indicate intermolecular reactions in the ion source. Although these reactions were not studied in detail, some typical results are briefly discussed here.

In the TSP mass spectrum of 2(3*H*)-benzothiazolethione shown in Fig. 5a, a strong

TABLE VI

PEAK IDENTIFICATIONS IN 4-(2-BENZOTHIAZOLETHIO)MORPHOLINE, SAMPLE C[a]

Gradient (min)	UV max. (nm)	M_r	Identification[b]	MBI	TSP	GC–MS
5.87	239,278	268	**20**	–	×	–
7.12	321	167	**1**	–	×	–
9.33	273	220	**21**	×	×	×
10.91	238,276	284	**22**	–	×	–
14.44	272	252	**2**	×	×	×
20.16	279	284	**23**	–	×	–
25.54	276–315	300	**24**	×	×	×
26.13	290	?	–	–	–	–
27.90	270	332	**10**	×	×	×

[a,b] See Table IV.

TABLE VII

PEAK IDENTIFICATIONS IN N-CYCLOHEXYL-2-BENZOTHIAZOLESULPHENAMIDE, SAMPLE D[a]

Gradient (min)	UV max. (nm)	M_r	Identification[b]	TSP	GC–MS
4.77	321	167	**1**	×	×
5.17	250–281	135	**6**	×	×
8.66	277	280	**25**	×	–
11.61	273	296	**26**	×	–
		232	**27**[c]	×	?
19.64	278	264	**3**	×	–
22.82	270	332	**10**	×	×
30.67	297	?	–	–	–

[a,b] See Table IV.
[c] Not detected in LC–UV.

protonated molecule is observed at m/z 168. In addition, peaks are observed at m/z 209, which is an acetonitrile adduct of the protonated molecule, m/z 248 and 262. The latter two peaks, resulting from the addition of 80 and 94 μ, respectively, to the protonated molecule could not be identified by MS–MS. The product ion spectra of m/z 248 and 262 show m/z 168 in both spectra and fragments at m/z 81 and 95, respectively. The same peaks are present in the TSP mass spectrum of 2,2′-dithiobisbenzothiazole shown in Fig. 5b, in which considerable fragmentation is observed. Addition of 80 and 94 u to the major constituent is frequently observed, *e.g.*, also in the analysis of 4-(2-benzothiazolethio)morpholine, resulting in ions at m/z 333 and 347. To prevent the reactions and to avoid severe source contamination in many of the experiments the major component was directed to waste.

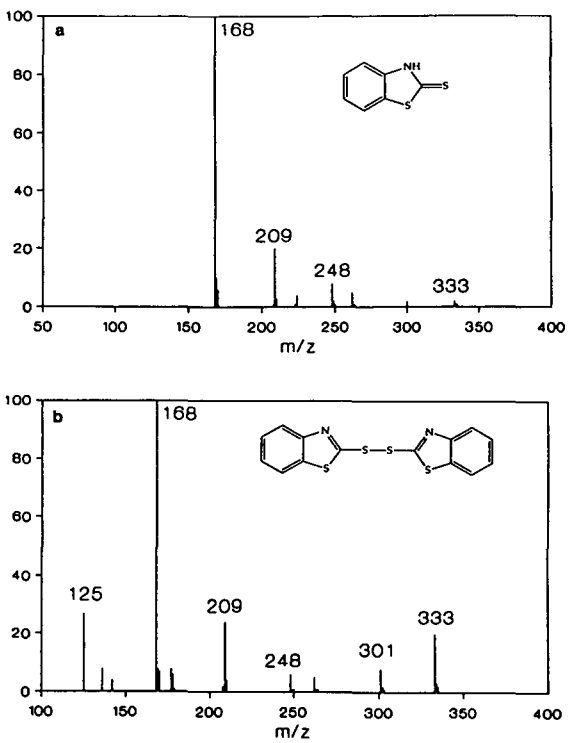

Fig. 5. Thermospray mass spectra obtained with high concentrations of (a) 2(3*H*)-benzothiazolethione (**1**) and (b) 2,2′-dithiobisbenzothiazole (**10**).

GC–MS

In samples A and B, a variety of low-molecular-mass and low-polarity compounds appears to be present. Some of these compounds might not be easily protonated in the TSP ionization applied in LC–MS. Therefore, additional information on the compounds present in the samples may be obtained from GC–MS. Care must be taken with the results as some compounds, such as those in samples C and D, may lack sufficient thermal stability for GC–MS analysis. Further, direct correlation of the identified compounds with the LC retention times is impossible. In

practice, GC–MS helped in and/or confirmed the identification of some of the compounds in samples A and B. The components in samples A–D detected and identified by GC–MS are indicated in Tables IV–VII.

LC–MS with a particle-beam interface

In the final stage of this project, a PBI system became available in our laboratory. Considering the initial strategy developed, in which the MBI was used for its ability to obtain EI spectra, and the results from GC–MS experiments, it was decided to analyse sample B with the PBI. The total ion chromatogram obtained is shown in Fig. 6. The components in sample B that were identified using the PBI are indicated in Table V. These preliminary data confirmed the usefulness of our initial strategy. However, the use of PBI appears to be more appropriate than that of MBI. Some warning must be given here. From both GC–MS and LC–PBI-MS data, it became clear that several components present in the investigated samples do not give clearly interpretable EI spectra. The spectrum of 2,2′-bisbenzothiazole (**19**), shown in Fig. 7, may serve as an example of this. Apart form a strong molecular ion, very few informative fragment peaks are present that would allow the identification of this compound. In this particular instance, the spectrum is available in the NBS library, but with other similar compounds identification will be difficult.

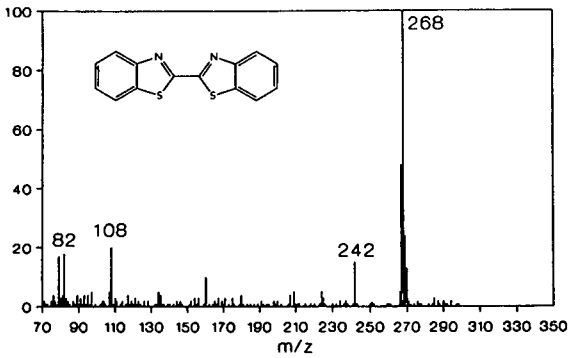

Fig. 7. EI mass spectrum of 2,2′-bisbenzothiazole (**19**).

CONCLUSIONS

The methodology developed, especially TSP in combination with LC–MS and LC–MS–MS and PBI, is capable of characterizing most of the minor components in the benzothiazole-derived compounds. However, greater difficulties would be experienced with components that are below a concentration of 0.1%.

The use of various LC–MS interfaces for these types of compounds allows a comparison of their potential. For identification purposes the availability of EI spectra is most helpful. Therefore, MBI and PBI are the first choice. However, the MBI is a mechanical device that is not easy to operate routinely and suffers from severe memory problems. PBI is simple and reliable, results in useful total ion chromatograms and is capable of EI and solvent-independent CI. It is considered to be the interface of choice for the identifi-

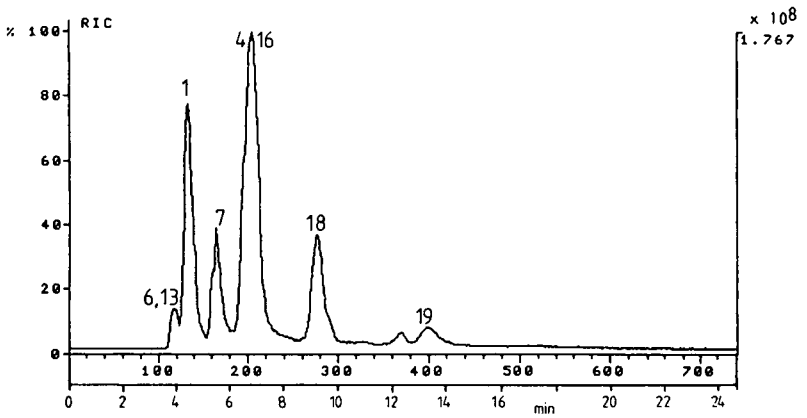

Fig. 6. Total ion current chromatogram of an LC–particle-beam-MS analysis of sample B. For conditions, see Experimental.

TABLE VIII

COMPARISON OF TECHNIQUES USED[a]

Technique	**1** (polar stable)	**22** (polar labile)	**12** (non-polar stable)	**10** (non-polar labile)
Moving-belt	+	−	+	±
Particle-beam	+	−	+	±
Thermospray	+	+	−[b]	+
GC–MS	+	−	+	+

[a] + = Good signal; ± = resonable; − = poor or no signal.
[b] Sulphur is not sensitive to TSP ionization owing to insufficient proton affinity.

cation problems with these relatively non-polar and thermally stable compounds. The TSP interface used in combination with MS–MS is also capable of producing useful spectra for the identification of the components in the mixtures. The techniques used in this study are compared in Table VIII. The ability of the various techniques to achieve molecular mass information and structure information from fragmentation is compared for four compounds differing in polarity and stability. It can be concluded that more than one MS technique should be used in identification problems such as this.

ACKNOWLEDGEMENTS

Several workers in our groups were involved in this project and we express our appreciation to them for their practical assistance. H.J.E.M. Reeuwijk (LACDR) is thanked for her extensive work on gradient and isocratic HPLC and the photodiode-array UV spectra, and her help in constructing the peak correlation tables, E.R. Verheij (LACDR and TNO) and G.F. LaVos (TNO) for their experiments with the moving belt, C.E.M. Heeremans (LACDR) for her thermospray work and R.A.M. van der Hoeven (LACDR) for his many hours working with the thermospray, particle-beam and GC–MS systems.

REFERENCES

1 F. Smejkal, M. Popl and A. Cihova, *J. Polym. Sci.*, 68 (1981) 145.
2 W.M.A. Niessen and J. van der Greef, *Liquid Chromatography–Mass Spectrometry*, Marcel Dekker, New York, 1992.
3 P.J. Arpino, *Mass Spectrom. Rev.*, 8 (1989) 35.
4 P.J. Arpino, *Mass Spectrom. Rev.*, 9 (1990) 631.
5 P.C. Winkler, D.D. Perkins, W.K. Williams and R.F. Browner, *Anal. Chem.*, 60 (1988) 489.
6 A.P. Tinke, R.A.M. van der Hoeven, W.M.A. Niessen, U.R. Tjaden and J. van der Greef, *J. Chromatogr.*, 554 (1991) 119.
7 S. Sagawa, H. Kunihiro, O. Kimura and M. Inoue, *Ger. Offen.*, 2 258 484 (1973).
8 J. van der Greef, A.C. Tas, M.C. ten Noever de Brauw, M. Höhn, G. Meyerhoff and U. Rapp, *J. Chromatogr.*, 323 (1985) 81.
9 W.M.A. Niessen, R.A.M. van der Hoeven, M.A.G. de Kraa, C.E.M. Heeremans, U.R. Tjaden and J. van der Greef, *J. Chromatogr.*, 474 (1989) 113.
10 W.M.A. Niessen, R.A.M. van der Hoeven, M.A.G. de Kraa, C.E.M. Heeremans, U.R. Tjaden and J. van der Greef, *J. Chromatogr.*, 478 (1989) 325.
11 K.L. Busch, G.L. Glish and S.A. McLuckey, *Mass Spectrometry/Mass Spectrometry*, VCH, New York, 1988.

Journal of Chromatography, 647 (1993) 121–129
Elsevier Science Publishers B.V., Amsterdam

CHROMSYMP. 2858

On-line low-level screening of polar pesticides in drinking and surface waters by liquid chromatography–thermospray mass spectrometry

H. Bagheri*, E.R. Brouwer, R.T. Ghijsen and U.A.Th. Brinkman

Department of Analytical Chemistry, Free University, De Boelelaan 1083, 1081 HV Amsterdam (Netherlands)

ABSTRACT

Mass spectra of 39 carbamate, triazine, phenylurea and organophosphorus polar pesticides were obtained by liquid chromatography–mass spectrometry with a thermospray interface. The analytes generated $[M + H]^+$ or $[M + NH_4]^+$ as the base peak with methanol–0.1 *M* ammonium acetate as the mobile phase in the discharge positive-ion mode. Chlorophenols showed much better sensitivity in the negative-ion mode; their spectra were dominated by the deprotonated molecular ion. Trace enrichment of these pesticides on a 10 mm × 3.0 mm I.D. precolumn packed with C_{18}-bonded silica was coupled on-line with reversed-phase column liquid chromatography–thermospray mass spectrometry (LC–TSP-MS). The LC separation was carried out on a 250 × 4.6 mm I.D. C_{18}-bonded silica column using a linear methanol–aqueous ammonium acetate gradient [10:90 to 90:10 (v/v) in 45 min]. When optimized TSP-MS conditions and 50-ml water samples were used, the detection limits for the pollutants tested typically were in the 2–90 ng/l range with time-scheduled selected-ion monitoring; the repeatability was good and the LC–TSP-MS system was robust. Several surface and drinking water samples were analysed and low levels of simazine, atrazine, isoproturon and diuron were detected.

INTRODUCTION

Polar pollutants are of major interest in environmental water studies. In our laboratory, preliminary results on the determination of these pollutants using an on-line trace enrichment–column liquid chromatography (LC)–diode-array detection (DAD) system have been reported [1]. In order to establish whether or not the concentrations of polar pesticides exceed tolerance levels in surface water (1–3 μg/l) and drinking water (0.1 μg/l) samples, it is necessary to have a robust system that meets these low detection limit requirements.

In most instances, the determination of toxic organic compounds is still carried out by means of gas chromatography (GC) coupled with selective and/or mass spectrometric (MS) detection. However, for polar pollutants LC and especially reversed-phase LC (RPLC) is nowadays regarded as the separation technique of choice. RPLC has been used for the determination of organic pollutants with a variety of detectors [2–6]; however, the use of (RP)LC in conjunction with MS detection is becoming increasingly important. In the last decade, a variety of interfaces such as the direct liquid introduction [7], thermospray (TSP) [8] and particle beam [9,10] types have been designed and developed to solve the incompatibility of these two powerful analytical techniques. Whereas a particle beam interface provides electron impact (EI) spectra (suitable for identification), TSP, the most commonly used interface, offers better sensitivity. However, the limits of detection obtained by conventional LC–TSP-MS do not meet the tolerance levels for environmental pollutants (0.1 μg/l for drinking water and 1–3 μg/l for surface water) [8,11,12]. Trace enrich-

* Corresponding author.

0021-9673/93/$06.00

ment prior to LC is therefore a necessary step. Trace enrichment is still mainly carried out by means of liquid–liquid extraction. These methods, however, are laborious and time consuming, large volumes of (toxic) organic solvents are used and sample losses can hardly be avoided. The use of off-line [13,14] or on-line [15–18] precolumn techniques is therefore to be preferred to obtain trace enrichment. In the on-line mode the compounds of interest are trapped on small (5–10 mm × 2.0–4.6 mm I.D.) precolumns packed with a suitable stationary phase (*e.g.*, alkyl-bonded silica, polymer-based materials, ion exchangers) or on so-called membrane extraction discs, which contain up to 90 mass% of such stationary phases in a PTFE mesh, and transferred to the analytical column. It is obvious that compared with off-line techniques, in which only part of the total sample is injected, the analyte detectability will be much better and the speed of analysis, of course, much higher in the on-line mode.

LC–TSP-MS coupled off-line with sample treatment has been used for the determination of different polar pesticides [19–23]. In a recent paper, the on-line trace enrichment of several phenylurea herbicides on a polymer-based precolumn and on membrane extraction discs (C_{18}-bonded silica) combined with this coupled set-up was reported [24]. Some of these compounds were identified in environmental samples at the low ng/l level. In this study, an attempt was made to extend this work and to develop a method that will allow the analysis of drinking and surface water for the simultaneous determination of several groups of pesticides, *e.g.*, carbamates, triazines, organophosphorus and phenylureas pesticides, in a single procedure.

EXPERIMENTAL

Chemicals

HPLC-grade water was prepared by purifying demineralized water in a Mili-Q filtration system (Millipore, Bedford, MA, USA). HPLC-grade methanol was obtained from J.T. Baker (Deventer, Netherlands) and ammonium acetate (99%) from Merck (Darmstadt, Germany). All pesticides were of 96–99% purity and were purchased from Riedel-de Haën (Seelze, Germany). Stock solutions (200 μg/ml) of the analytes were made by weighing and dissolution in methanol. Drinking and surface water samples were spiked with a standard mixture of 21 pesticides at levels ranging from 0.1 to 10 μg/l.

Instrumentation

The LC system consisted of a Kipp & Zonen (Delft, Netherlands) Model 4140 LC pump for delivering the aqueous sample (5 ml/min) and wetting of the precolumn, a Hewlett-Packard (Waldbronn, Germany) Model 1090 gradient pump for delivering the mobile phase (1 ml/min) and a six-port switching valve (Rheodyne, Berkeley, CA, USA). The analytical column was a 250 mm × 4.6 mm I.D. stainless-steel column packed with 5-μm base-deactivated C_{18} material (Supelchem, Leusden, Netherlands). The precolumn was a 10 × 3.0 mm I.D. stainless-steel column packed with 40-μm Bondesil-C_{18} (Analytichem, Harbor City, CA, USA).

A Hewlett-Packard (Palo Alto, CA, USA) Model 5989 A MS Engine was connected to the LC column outlet via a Hewlett-Packard TSP interface. All data were acquired on a Hewlett-Packard UX 98578 X data system. A solution of polypropylene glycol (PPG) (16.7 mg/ml) in methanol–0.1 *M* ammonium acetate (1:3, v/v), was used to calibrate the mass spectrometer for *m/z* 268.2, 442.3 and 558.4 ($[M + NH_4]^+$ ions of PPG oligomers with relatively equal intensity over the mass range 150–800 u) in the discharge positive-ion (PI) mode and for *m/z* 367.3, 715.3 and 889.6 ($[M + CH_3COO]^-$ ions of PPG oligomers) in the negative-ion (NI) mode using discharge ionization. The source block temperature was set at 200°C and that of the quadrupole analyser at 100°C.

The vaporization temperature of the TSP cartridge was optimized by a probe survey facility programme. A plot of stem temperature *vs.* tip temperature was made and the stem temperature required for complete vaporization of the mobile phase was determined by finding the inflection point and taking a *ca.* 5% lower temperature for the actual LC–TSP-MS operation [25]. Changing the composition of the mobile phase can affect the stem temperature. In

this study, the stem temperature was programmed from 120 to 110°C when altering the methanol–water composition from 10:90 to 90:10 (v/v) in 45 min.

Analytical procedures

The C_{18} precolumn was flushed at 5 ml/min with 5 ml of methanol and then 5 ml of HPLC-grade water prior to preconcentration. Subsequently, a 50-ml sample was preconcentrated (5 ml/min) on the precolumn. The analytes trapped on the precolumn were desorbed in the backflush mode with methanol–0.1 *M* ammonium acetate (10:90, v/v) and transferred on-line to the C_{18} analytical column. The actual separation of the analytes was carried out using a 45-min linear gradient to methanol–0.1 *M* ammonium acetate (90:10, v/v).

For all compounds calibration graphs were constructed over the range 0.1–10 μg/l; the analyses were done in duplicate (six data points). These calibration graphs were used as external standards for the analysis of real samples.

RESULTS AND DISCUSSION

Recently, we reported on the use of RPLC–TSP-MS for the determination of phenylurea herbicides in drinking and surface waters [24]. In order to test the general usefulness of the method, a large number of polar pollutants representing different classes of compounds were studied using essentially the same conditions as before, *viz.*, gradient elution with methanol–0.1 *M* ammonium acetate and TSP-MS in the discharge PI and, occasionally, the NI mode. Preliminary studies revealed that N-methylcarbamates, organophosphorus pesticides and triazines can be included in the chromatographic procedure developed for the phenylureas. Chlorophenols showed much better analyte detectability in the NI than in the PI mode. With the nitrophenols studied the breakthrough volumes generally were much smaller than the 50 ml recommended for the other classes of pesticides. Phenoxyacetic acids did not show a good TSP-MS response under the conditions used. The latter two classes of analytes were therefore not included in the present study.

Mass spectra

Table I shows that the TSP mass spectra (PI mode) of all but four of the pesticides selected are dominated by the protonated molecular ions. Aldicarb-sulphone, carbaryl and malation have $[M + NH_4]^+$ as the base peak and paration-ethyl ($M_r = 291$) has a base peak at *m/z* 262, which may be due to the formation of an $[M + H - NO]^+$ fragment ion [26]. Some further comments are as follows. Among the carbamates tested, aldicarb-sulphone showed fragment ions at *m/z* 165 and 183, corresponding to the loss of isocyanate from the protonated molecular ion, and the ammonia adduct ions, respectively (Fig. 1). The ammonia chemical ionization (CI) mass spectrum of this carbamate was also reported to show an ion at *m/z* 165 in capillary supercritical fluid chromatography–MS [27]. All phenylureas generated $[M + H]^+$ as the base peak; $[M + NH_4]^+$ was observed as adduct ion in some instances [28]. These results are in good agreement with literature data [29–31], although for, *e.g.*, monuron and diuron, $[M + NH_4]^+$ has sometimes been reported to be the base peak [29]. In LC–MS using a direct liquid introduction interface, the mass spectra of some phenylureas have been found to be dominated by quasi-molecular ions [32,33]. The mass spectra of the triazine herbicides were relatively simple and they all showed the protonated molecular ion as the base peak. A protonated methanol adduct ion was observed for both simazine and atrazine. Fragment ions at *m/z* 168 and 182 generated by simazine and atrazine, respectively, may well be due to the replacement of a chlorine by a hydrogen atom, taking place in the spray (see Fig. 7). Actually, with the phenylurea diuron the same phenomenum is observed, but as a two-step process for both chlorine atoms. For all organophosphorus compounds except parathion-ethyl and diazinon the ammonia adduct ions were either very intense fragments or the base peak, which is in agreement with previously reported results [29].

In contrast to the pesticides discussed above, chlorophenols show distinctly stronger signals in

TABLE I

RETENTION TIMES, MAJOR IONS AND LIMITS OF DETECTION OF 39 POLAR PESTICIDES IN LC–TSP-MS

No.	t_R (min)	Compound	Class[a]	M_r	Major ions, m/z (relative abundance, %)[b]	LOD[c] (ng/l)
1	10.6	Aldicarb-sulphone	CA	222	240(100), 165(51), 183(30), 223(10)	65
2	16.8	1-(3-Chloro-4-hydroxy-phenyl)-3,3-dimethylurea	PU	214	215(100), 217(22), 232(17), 181(15)	50
3	19.3	Dimethoate	OP	229	230(100), 247(50)	10
4	20.5	Desmethylmetoxuron	PU	200	201(100), 218(57), 203(32), 220(16)	25
5	21.8	Isocarbamid	CA	185	186(100), 203(20)	–
6	22.3	Carbendazim	CA	191	192(100)	–
7	23.1	Monomethylmetoxuron	PU	214	215(100), 217(33), 232(25)	10
8	24.5	Metoxuron	PU	228	229(100), 231(33), 201(18)	10
9	26.4	Cyanazine	TZ	240	241(100), 243(33), 207(13)	10
10	27.1	Monuron	PU	198	199(100), 201(32), 216(15)	10
11	28.5	Simazine	TZ	201	202(100), 204(40), 168(32)	2
12	29.9	Carbaryl	CA	201	219(100), 202(35), 220(13)	–
13	30.5	Monolinuron	PU	214	215(100), 232(50), 217(32)	–
14	31.3	Fluormeturon	PU	232	233(100), 250(30)	–
15	31.7	Atraton	TZ	211	212(100), 213(14)	10
16	32.0	Chlortoluron	PU	212	213(100), 215(25), 230(10)	–
17	32.0	Metobromuron	PU	258	259(100), 261(90), 276(53), 278(53)	–
18	32.2	Atrazine	TZ	215	216(100), 218(32), 182(22)	5
19	33.3	Isoproturon	PU	206	207(100), 208(15)	5
20	33.9	Diuron	PU	232	233(100), 235(65), 250(22), 165(17), 252(15), 199(15)	15
21	34.0	Difenoxuron	PU	286	287(100), 288(15)	–
22	35.1	Azinphos-methyl	OP	317	318(100), 335(78)	25
23	35.2	Terbutylazine	TZ	225	226(100), 227(14)	–
24	35.5	Promethon	TZ	225	226(100), 227(16)	–
25	35.7	Propazine	TZ	229	230(100), 232(50), 231(32)	5
26	36.0	Secbutylazine	TZ	229	230(100), 232(35), 231(12)	–
27	36.3	Linuron	PU	248	249(100), 266(76), 251(70), 268(50)	–
28	36.7	Terbutylazine	TZ	229	230(100), 232(35), 231(12)	–
29	36.7	Secbumeton	TZ	225	226(100), 201(2)	–
30	37.2	Chlorobromuron	PU	292	295[d](100), 312(80), 293(76), 310(53)	–
31	37.8	Malathion	OP	330	348(100), 331(50), 175(20), 192(20)	35
32	39.2	Terbutryne	TZ	241	242(100), 243(12)	–
33	39.3	Trietazine	TZ	229	230(100), 232(26)	15
34	39.8	Prometryn	TZ	241	242(100), 243(14)	15
35	41.2	Neburon	PU	274	275(100), 277(66)	–
36	41.2	Parathion-ethyl	OP	291	262(24), 263(11)	90
37	42.2	Diazinon	OP	304	305(100), 306(15)	30
38	43.8	Disulfoton	OP	274	275(100), 292(50)	30
39	47.8	Carbotuthion	OP	342	343(100), 345(35)	–

[a] CA = Carbamates; OP = organophosphorus pesticides; PU = phenylureas; TZ = triazines.
[b] LC eluent: methanol–0.1 *M* ammonium acetate [10:90 to 90:10 (v/v) in 45 min].
[c] Limits of detection (signal-to-noise ratio = 3:1) under time-scheduled SIM conditions.
[d] Highest peak of cluster starting at m/z 293.

TSP-MS in the NI mode [34,35]. As an example, Fig. 2 shows the mass spectra of 3,4-dichlorophenol, 2,3,4-trichlorophenol and 2,3,5,6-tetrachlorophenol. $[M-H]^-$ is the base peak in all instances; the adduct ion $[M+CH_3COO]^-$ for 3,4-dichlorophenol (m/z 221) is much more

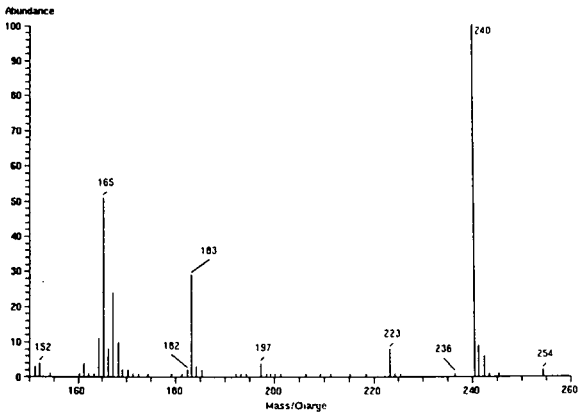

Fig. 1. TSP mass spectrum of aldicarb-sulphone in the discharge PI mode. For details, see text.

pronounced than the corresponding adducts of 2,3,4-trichlorophenol and 2,3,5,6-tetrachlorophenol at m/z 255 and 289, respectively. The cluster ions beginning at m/z 161 (Fig. 2B) and 195 (Fig. 2C) are due to the presence of $[M-Cl]^-$. The predominance of the deprotonated molecular ions in the mass spectra can be attributed to the lower gas-phase acidity of the chlorophenols compared with acetate.

RPLC–TSP-MS

In order to achieve good chromatographic resolution and efficient trace enrichment from 50–100-ml aqueous samples, it is necessary to use the same type of bonded-phase material, *i.e.*, C_{18}-bonded silica, in the precolumn and the analytical column, to select a sufficiently long, *i.e.*, 25 cm, analytical column, and to use a fairly large diameter, *i.e.*, 3.0–4.6 mm I.D., pre- and main columns. Under these conditions, the sample capacity will be high and the separation power of the analytical column will not be affected by band broadening caused during analyte transfer from the precolumn. Fig. 3 shows a full-scan RPLC–TSP-MS trace for a mixture of 21 pesticides (N-methylcarbamates, phenylureas, organophosphorus compounds and triazines) using a 45-min linear gradient of methanol–0.1 *M* ammonium acetate (10:90 to 90:10, v/v). All analytes except malathion and trietazine are well resolved. The last two pesticides can easily be distinguished on the basis of their base peaks, which are at m/z 348 and 230, respectively. The peak at 45.2 min is probably phthalate esters.

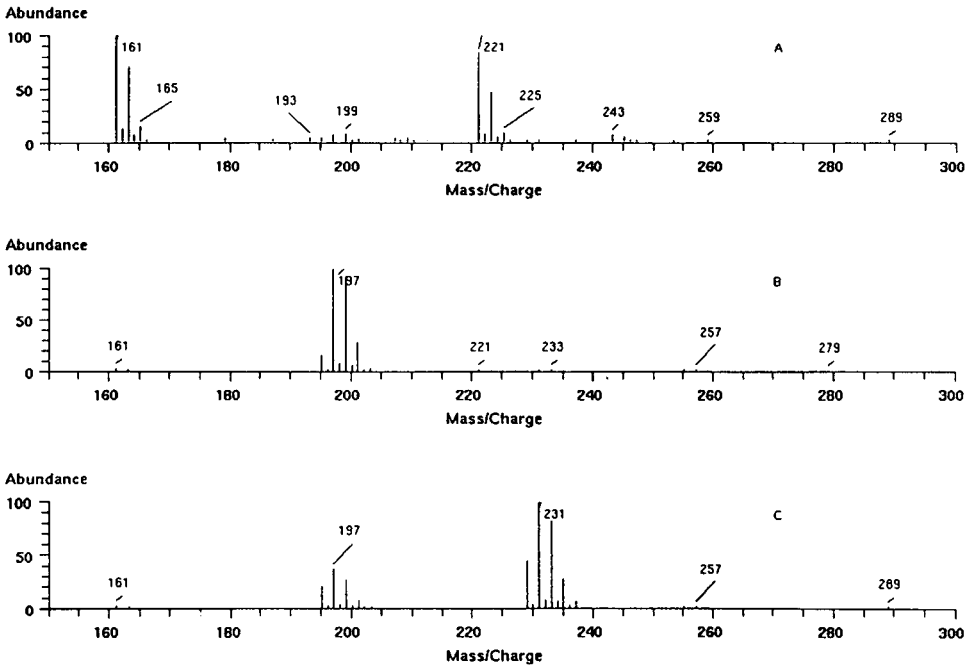

Fig. 2. TSP mass spectra of (A) 3,4-dichlorophenol, (B) 2,3,4-trichlorophenol and (C) 2,3,5,6-tetrachlorophenol in the discharge NI mode. For details, see text.

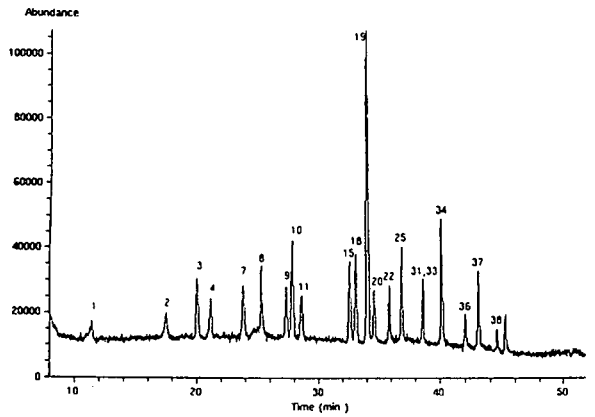

Fig. 3. RPLC–TSP-MS full-scan trace for 21 polar pesticides (150–350 u). Column, 250 mm × 4.6 mm I.D. stainless-steel containing 5-μm C_{18}-bonded silica; eluent, linear methanol–0.1 *M* ammonium acetate gradient [10:90 to 90:10 (v/v) in 45 min]; 25-μl loop injection. For peak designation, see Table I.

Fig. 4 shows on-line trace enrichment–RPLC–TSP-MS traces obtained after preconcentration of 50 ml of river Rhine water and 50 ml of river Rhine water spiked with the mixture of 21 pesticides at the 1 μg/l level. The chromatograms were recorded under time-scheduled selected-ion monitoring (SIM) conditions using the base peaks listed in Table I. As C_{18}-bonded silica rather than a more hydrophobic polymer is used as the packing material in the precolumn, the peak broadening is less than in our previous study [24]. On-line trace enrichment–RPLC–TSP-MS traces (NI mode) obtained after preconcentration of 50 ml of river Meuse water and 50 ml of the river water spiked with four chlorophenols at the 1 μg/l level are shown in Fig. 5.

The performance of the total trace enrichment–RPLC–TSP-MS system was tested by analysing river Rhine water spiked with the mixture of 21 pesticides at various levels ranging from 0.1 to 10 μg/l. Each experiment was carried out by preconcentrating 50 ml of water and using time-scheduled SIM. Over the concentration range tested, the correlation coefficients (R^2) were 0.97–0.998 for all analytes. The relative standard deviation (R.S.D.) was typically 5–15% ($n = 6$) using a river Rhine water sample spiked at the 1 μg/l level. The limits of detection for the 21 pesticides in the mixture were in the range 2–90 ng/l (signal-to-noise ratio = 3:1); they are included in Table I. The analytical data can be considered satisfactory.

Applications

Preliminary experiments indicated that at least three of the pesticides tested, *viz.*, simazine, atrazine and isoproturon, are present at low levels in the river Rhine water. In order to improve further both the sensitivity and selectivi-

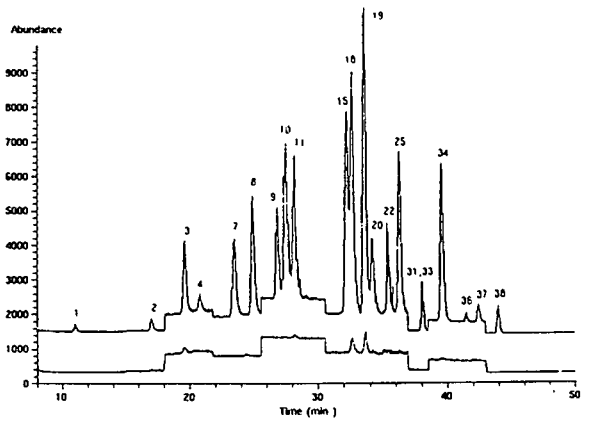

Fig. 4. On-line trace-enrichment RPLC–TSP-MS trace for 50 ml of (bottom) river Rhine water and (top) river Rhine water spiked with a mixture of 21 polar pesticides at 1 μg/l. Column, 250 mm × 4.6 mm I.D. stainless-steel containing 5-μm C_{18}-bonded silica; eluent, linear methanol–0.1 *M* ammonium acetate gradient [10:90 to 90:10 (v/v) in 45 min]; MS, discharge PI mode. For peak designation, see Table I.

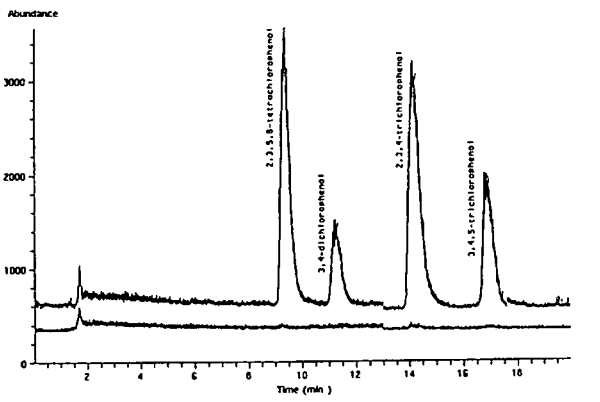

Fig. 5. On-line trace-enrichment RPLC–TSP-MS trace for 50 ml of (bottom) river Meuse water and (top) river Meuse water spiked with a mixture of four chlorophenols at 1 μg/l. Column, 150 mm × 4.6 mm I.D. stainless-steel containing 5-μm Rosil C_{18}-bonded silica; eluent, linear methanol–0.1 *M* ammonium acetate gradient [10:90 to 90:10 (v/v) in 45 min]; MS, discharge NI mode, For details, see text.

ty, the sample volume was increased to 200 ml (which may cause breakthrough of some early eluting analytes, but not of these target compounds) and carefully time-scheduled SIM was used. Fig. 6 compares trace enrichment–RPLC–TSP-MS traces (PI mode) for river Rhine water, Amsterdam drinking water, HPLC-grade water (each 200 ml of sample) and a blank (no preconcentration) recorded using the following SIM schedule: 8–30.5 min, m/z 202; 30.5–33.2 min, m/z 216; 33.2–50 min, m/z 207. The presence of simazine, atrazine and isoproturon in the river Rhine and drinking water samples can be clearly seen. The small and distinct peaks in the chromatogram for HPLC-grade water (Fig. 6D) were not caused by memory effects, but were intrinsically present in this sample. This is demonstrated by the absence of these peaks in the chromatogram shown as trace C, and by the fact that no such peaks were observed in several mineral water samples (data not shown). The peak at $t_R = 31.6$ min in trace D, showing an ion at m/z 216, is not caused by any of the pesticides in our test set.

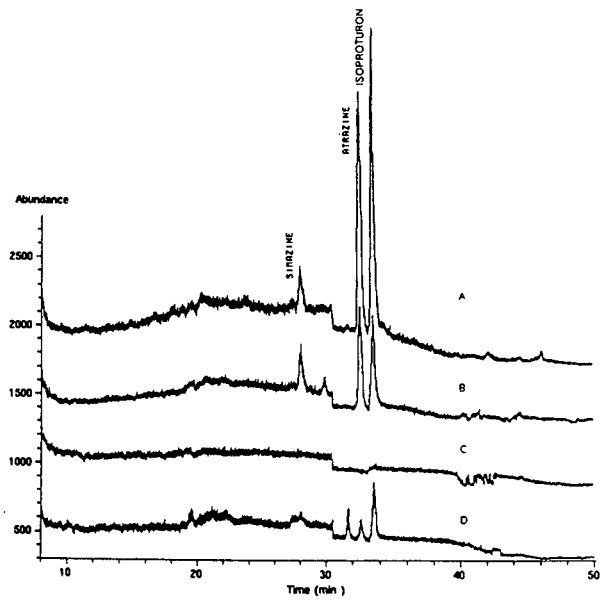

Fig. 6. On-line trace-enrichment RPLC–TSP-MS trace for 200 ml of (A) Rhine water, (B) Amsterdam drinking water, (C) blank without preconcentration and (D) HPLC-grade water. Column, 250 mm × 4.6 mm I.D. stainless-steel containing 5-μm C_{18}-bonded silica; eluent, linear methanol–0.1 M ammonium acetate gradient [10:90 to 90:10 (v/v) in 45 min]; MS, discharge PI mode. For details of time-scheduled SIM, see text.

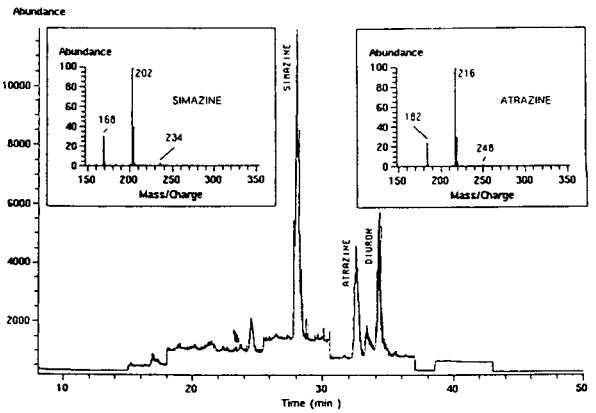

Fig. 7. On-line trace-enrichment RPLC–TSP-MS trace for river Mersey water (ions at m/z 202, 216, 207 and 233 monitored). Column, 250 mm × 4.6 mm I.D. stainless-steel containing 5-μm C_{18}-bonded silica; eluent, linear methanol–0.1 M ammonium acetate gradient [10:90 to 90:10 (v/v) in 45 min]; MS, discharge PI mode. For details, see text.

Analysis of 50 ml of water from the river Mersey (UK) and the river Meuse (Netherlands) gave the results shown in Figs. 7 and 8, respectively. As a further demonstration of the presence of the pesticides referred to above, mass spectra are included as insets. Table II summarizes the concentrations of simazine, atrazine,

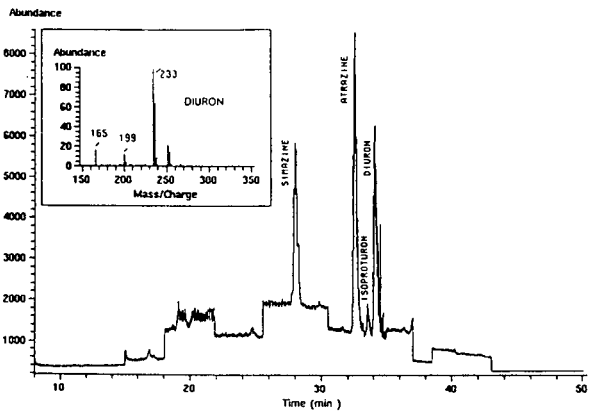

Fig. 8. On-line trace-enrichment RPLC–TSP-MS trace for river Meuse water (ions at m/z 202, 216, 207 and 233 monitored). Column, 250 mm × 4.6 mm I.D. stainless-steel containing 5-μm C_{18}-bonded silica; eluent, linear methanol–0.1 M ammonium acetate gradient [10:90 to 90:10 (v/v) in 45 min]; MS, discharge PI mode. For details, see text.

TABLE II

SURVEY OF SOME PESTICIDES DETECTED IN DRINKING AND SURFACE WATERS

Water source[a]	Concentration (μg/l)				Fig.
	Simazine	Atrazine	Isoproturon	Diuron	
Amsterdam drinking water	0.015	0.025	0.015	–	6A
River Rhine	0.030	0.070	0.065	0.030	–
River Mersey	3.2	0.9	–	2.1	7
River Meuse	1.2	1.0	0.070	2.0	8
HPLC-grade water	–	<0.006	<0.007	–	6D

[a] Sample size, 50 ml; for further details, see text.

isoproturon and diuron found in various water samples tested. With LC–TSP-MS under optimized conditions (PI mode) and 50-ml water samples, the detection limits for the four pollutants are in the 5–15 ng/l range for real samples. None of the other compounds listed in Table I was ever detected. In the drinking water samples tested, the observed levels for the polar pesticides in Table II invariably were below those permitted for drinking water (0.1 μg/l). As regards the surface water samples, high values (alert-alarm level, 1 and 3 μg/l, respectively) were occasionally found. It is interesting that the presence of 0.5–1.5 μg/l concentrations of diuron has recently been reported by another group from our laboratory using on-line trace enrichment–RPLC with diode-array UV detection [36].

As regards simazine and atrazine, the present results regarding Amsterdam drinking water and river Rhine water are consistent with our previous work using an off-line combination of LC and GC–MS [37]. Finally, the two chloro-*s*-triazines have also been detected at similar levels in drinking water from Paris using trace enrichment on a cation exchanger and LC with UV detection [38].

CONCLUSIONS

The mass spectra of 39 polar pesticides have been recorded in RPLC–TSP-MS using a C_{18} analytical column and a linear methanol–0.1 *M* ammonium acetate gradient under discharge PI conditions. The protonated molecular ion or an ammonia adduct ion appeared as the base peak for all N-methylcarbamates, triazines, organophosphorus pesticides and phenylureas tested except for parathion-ethyl. Proton abstraction was the dominant mechanism for a selected group of chlorophenols studied in the NI mode.

The on-line combination of trace enrichment of the pesticides from the four classes of compounds mentioned above from, typically, 50-ml water samples with RPLC–TSP-MS offers a fast, sensitive and selective method for the identification and determination of the target compounds down to the 5–100 ng/l level. This was demonstrated by analysing a series of surface and drinking water samples. Additional advantages are that the C_{18}-type precolumns can easily be reused for at least ten 50-ml runs, and that the consumption of organic solvents is extremely low. Current research is devoted to an extension of the programme to include an even larger number of environmental pollutants using both the PI and the NI modes, and to the use of a particle beam interface for the identification of unknown pollutants.

ACKNOWLEDGEMENTS

The authors thank Dr. B.L.M. Van Baar and Mr. R.J. Vreeken for useful comments. This study was carried out within the framework of the Rhine Basin Program (Amsterdam/Waldbronn).

REFERENCES

1 I. Liska, E.R. Brouwer, A.G.L. Ostheimer, H. Lingeman, U.A.Th. Brinkman, R.B. Geerdink and W.H. Mulder, *Int. J. Environ. Anal. Chem.*, 47 (1992) 267–291.
2 M.A. Brown, R.D. Stephens and I.S. Kim, *Trends Anal. Chem.*, 10 (1991) 330–336.
3 E.R. Brouwer, I. Liska, R.B. Geerdink, P.C.M. Frintrop, W.H. Mulder, H. Lingeman and U.A.Th. Brinkman, *Chromatographia*, 32 (1991) 445–452.
4 J. Slobodnik, E.R. Brouwer, R.B. Geerdink, W.H. Mulder, H. Lingeman and U.A.Th. Brinkman, *Anal. Chim. Acta*, 268 (1992) 55–65.
5 R. Reupert and G. Brausen, *GIT Fachz. Lab.*, 35 (1991) 1219–1221.
6 C. de Ruiter, J.C.H.F. Hefkens, U.A.Th. Brinkman, R.W. Frei, M. Evers, E. Mathijs and J.A. Meijer, *Int. J. Environ. Anal. Chem.*, 31 (1987) 325–339.
7 W.M.A. Niessen, *Chromatographia*, 21 (1986) 277–284.
8 P. Arpino, *Mass Spectrom. Rev.* 9 (1990) 631–669.
9 I.S. Kim, F.I. Sasinos, R.D. Stephens, J. Wang and M.A. Brown, *Anal. Chem.*, 63 (1991) 819–823.
10 D.R. Doerge and C.J. Miles, *Anal. Chem.*, 63 (1991) 1999–2001.
11 I. Hammond, K. Moore, H. James and C. Watts, *J. Chromatogr.*, 474 (1989) 175–180.
12 R.J. Vreeken, W.D. Van Dongen, R.T. Ghijsen and U.A.Th. Brinkman, in preparation.
13 H. Lingeman and U.R. Tjaden, in H. Lingeman and W.J.M. Underberg (Editors), *Detection Oriented Derivatization Techniques in Liquid Chromatography*, Marcel Dekker, New York, 1990.
14 M.W.F. Nielen, R.W. Frei and U.A.Th. Brinkman, in R.W. Frei and K. Zech (Editors), *Selective Sample Handling and Detection in High Performance Liquid Chromatography, Part A*, Elsevier, Amsterdam, 1988.
15 M.W.F. Nielen, U.A.Th. Brinkman and R.W. Frei, *Anal. Chem.*, 57 (1985) 806–810.
16 P. Subra, M.C. Hennion, R. Rosset and R.W. Frei, *Int. J. Environ. Anal. Chem.*, 37 (1989) 45–62.
17 E.R. Brouwer, H. Lingeman and U.A.Th. Brinkman, *Chromatographia*, 29 (1990) 415–418.
18 D.F. Hagen, C.G. Markell and G.A. Schmitt, *Anal. Chim. Acta*, 236 (1990) 157–164.
19 R.D. Voyksner and C.A. Haney, *Anal. Chem.*, 57 (1985) 991–996.
20 R.D. Voyksner, T. Pack, C. Smith, H. Swaisgood and D. Chen, in M.A. Brown (Editor), *Liquid Chromatography/Mass Spectrometry. Applications in Agricultural, Pharmaceutical and Environmental Chemistry*, American Chemical Society, Washington, DC, 1990, pp. 14–39.
21 D. Barcelo, G. Durand, R.J. Vreeken, G.J. de Jong, H. Lingeman and U.A.Th. Brinkman, *J. Chromatogr.*, 553 (1991) 311–328.
22 D. Barcelo, in M.A. Brown (Editor), *Liquid Chromatography/Mass Spectrometry. Applications in Agricultural, Pharmaceutical and Environmental Chemistry*, American Chemical Society, Washington, DC, 1990, pp. 48–61.
23 D. Barcelo and J. Albaiges, *J. Chromatogr.*, 474 (1989) 163–173.
24 H. Bagheri, E.R. Brouwer, R.T. Ghijsen and U.A.Th. Brinkman, *Analusis*, 20 (1992) 38–43.
25 *Hewlett-Packard 5989A MS Engine Hardware Manual*, Vol. 2, Hewlett-Packard, Avondale, PA, 1991, p. B10.
26 H. Budzikiewicz, C. Djerassi and D.H. Williams (Editors), *Mass Spectrometry of Organic Compounds*, Holden-Day, San Francisco, 1967, p. 515.
27 H.T. Kalonoski, R.W. Wright and R.D. Smith, *Biomed. Environ. Mass Spectrom.*, 13 (1986) 33–45.
28 H. Bagheri, R.J. Vreeken, R.T. Ghijsen and U.A.Th. Brinkman, in preparation.
29 D. Barcelo and J. Albaiges, *J. Chromatogr.*, 474 (1989) 163–173.
30 K. Levsen, K.H. Schafer and J. Freudenthal, *J. Chromatogr.*, 271 (1983) 51–60.
31 F.A. Maris, R.B. Geerdink, R.W. Frei and U.A.Th. Brinkman, *J. Chromatogr.*, 323 (1985) 113–120.
32 R.D. Voyksner, in J.D. Rosen (Editor), *Applications of Mass Spectrometry Techniques in Pesticide Chemistry*, Wiley, New York, 1987, pp. 146–160.
33 R.D. Voyksner, J.T. Bursey and E.D. Pellizari, *Anal. Chem.*, 56 (1984) 1507–1514.
34 D. Barcelo, *Chromatographia*, 25 (1988) 295–299.
35 R.J. Vreeken, U.A.Th. Brinkman and G.J. de Jong, *Biomed. Environ. Mass Spectrom.*, 19 (1988) 481–492.
36 J. Slobodnik, M.G.M. Groenewegen, E.R. Brouwer, H. Lingeman and U.A.Th. Brinkman, *J. Chromatogr.*, 642 (1993) 359–370.
37 H. Bagheri, J.J. Vreuls, R.T. Ghijsen and U.A.Th. Brinkman, *Chromatographia*, 34 (1992) 5–13.
38 V. Coquart and M.C. Hennion, *J. Chromatogr.*, 585 (1991) 67–73.

Journal of Chromatography, 647 (1993) 131–136
Elsevier Science Publishers B.V., Amsterdam

CHROMSYMP. 2859

Volatile ion-pairing agents for liquid chromatographic–thermospray mass spectrometric determination of amino acids and amino acid amides

R.G.J. van Leuken*, G.T.C. Kwakkenbos and A.L.L. Duchateau

DSM Research, P.O. Box 18, 6160 MD Geleen (Netherlands)

ABSTRACT

The behaviour of volatile ion-pairing agents in terms of performance of the combined liquid chromatography–mass spectrometry is described. The applicability of heptafluorobutanoic acid, tridecafluoroheptanoic acid and nonadecafluorodecanoic acid as volatile ion-pairing agents is demonstrated by the analysis of mixtures of amino acids and the corresponding amino acid amides. Translation of a non-volatile to a volatile ion-pair system that is suitable for thermospray mass spectrometry is described. Using nonadecafluorodecanoic acid, the retention times of the compounds studied were comparable to those obtained with *n*-dodecylsulphonic acid. Further, with nonadecafluorodecanoic acid, the repeatability of the tests and the calibration graphs of the compounds investigated were good. The sensitivity of the mass spectrometer towards the compounds of interest was greatly improved by postcolumn addition of trifluoroacetic acid and ionization with gaseous ammonia. Using nonadecafluorodecanoic acid, the method was applied to the analysis of samples from bio-organic synthesis.

INTRODUCTION

Reversed-phase high-performance liquid chromatography (HPLC) is one of the most commonly used techniques for the separation of both polar and ionic compounds, with or without using non-volatile ion-pairing agents. In liquid chromatography–thermospray mass spectrometry (LC–TSP-MS), volatile buffers and ion-pairing agents are required for the mass spectrometer. Hence, either replacement of non-volatile substances by volatile equivalents or post-column suppressor techniques [1–3] are necessary.

The use and selectivity of volatile buffers for LC–TSP-MS have been evaluated by several workers [4–6]. Applications of volatile ion-pairing agents with LC–UV and amperometric detection have been reported [6–10]. In these studies short-chain perfluorinated carboxylic acids are used instead of strong non-volatile ion-pairing agents. Compared with alkylsulphonates, perfluorinated carboxylic acids have lower boiling points and are therefore suitable for preparative chromatography [8,9]. So far, only a short-chain perfluorinated carboxylic acid has been reported as a volatile ion-pairing agent for LC–TSP-MS analysis [6].

The aim of this study was to replace the non-volatile additives used in a LC reaction detection system for the determination of amino compounds [11] by volatile additives which are suitable for LC–TSP-MS. To this end, the behaviour of a series of perfluorinated carboxylic acids as volatile ion-pairing agents for LC–TSP-MS was investigated. In the mobile phase, sodium phosphate was replaced with triethylammonium (TEA) formate. The selection of this type of buffer and ion-pairing agent still allowed the use of the reaction detection system [11] for routine analysis, while the LC–TSP-MS system

* Corresponding author.

0021-9673/93/$06.00

could be applied for identification and/or confirmation purposes.

The influence of heptafluorobutanoic acid (HFBA), tridecafluoroheptanoic acid (TDFA) and nonadecafluorodecanoic acid (NDFA) on the retention of several amino acids and amino acid amides was investigated and compared with *n*-dodecylsulphonic acid.

In order to increase the mass spectrometric sensitivity, both postcolumn addition of trifluoroacetic acid (TFA) and chemical ionization with gaseous ammonia [12] were applied. After optimization of the mass spectrometric parameters, spectra of the amino acids and amides were recorded in the full-scan mode. Determination of the compounds was performed in the multiple-ion detection (MID) mode.

The sensitivity, linearity and repeatability of the LC–TSP-MS system were investigated.

EXPERIMENTAL

Chemicals

α-Methylalaninamide (α-Me-Ala-NH_2) was obtained from DSM Research. Other amino acid amides and amino acids were obtained from Sigma (St. Louis, MO, USA). The pairing ions *n*-dodecylsulphonic acid, TDFA and NDFA were supplied by Aldrich (Milwaukee, WI, USA), TFA and HFBA by Janssen Chimica (Beerse, Belgium) and 2-propanol (IPA), ethanol, 2-mercaptoethanol (MCE) and *o*-phthalaldehyde (OPA) by Merck (Darmstadt, Germany). All other chemicals were of analytical-reagent grade. Water was purified with a Milli-Q system (Millipore). Samples from bio-organic synthesis were supplied by DSM Research.

Buffer, eluent, reagent and sample preparation

Sodium phosphate and triethylammonium (TEA) formate buffers were prepared by dissolving the corresponding bases (0.1 *M*) in water and, after adding the required amount of ion-pairing agent, adjusted the pH to 3.0 with phosphoric acid and formic acid, respectively. The eluents were mixtures of buffer containing different amounts (0.5–8 m*M*) of ion-pairing agent and 20% (v/v) 2-propanol. Potassium borate buffer (0.4 *M*, pH 10.0) was prepared by dissolving boric acid in water and adjusting the pH to 10.0 with potassium hydroxide solution. OPA–MCE reagent was a mixture of potassium borate buffer (0.4 *M*, pH 10.0), OPA (6 m*M*), MCE (0.1%) and ethanol (1.0%). Standard solutions of the amino acids and the amino acid amides were dissolved in the appropriate eluent. Samples were diluted with 0.1 *M* formic acid to pH 3.0.

Instrumentation

A Gilson (Villiers-le-Bel, France) Model 305 pump was used for solvent delivery; injection was performed with a Rheodyne (Cotati, CA, USA) Model 7125 injection valve with a 20-μl loop. The column used was a Nucleosil-120-C_{18} (250 × 4.0 mm I.D., 5 μm) from Macherey–Nagel (Düren, Germany). The flow-rate was 1.0 ml/min. The separations were carried out at ambient temperature.

For reaction detection, the OPA–MCE reagent was added to the column effluent by a mixing T-piece. This was effected with a Gilson Model 305 pump at a flow-rate of 1.0 ml/min. The reaction was carried out in a coiled capillary stainless-steel tube (12 m × 0.35 mm I.D., coil diameter 12 mm) at ambient temperature. The fluorescence detector was a Waters Model 420, equipped with a 338-nm band-pass filter for excitation and a 415-nm long-pass filter for emission. Peak integration and quantitative analysis were performed with a Hewlett-Packard Model 3350 laboratory data system.

For MS detection, a Finnigan MAT TSQ-70 triple quadrupole mass spectrometer equipped with a thermospray interface was used. To maintain optimum ionization conditions, postcolumn addition of 2% (v/v) aqueous TFA solution at a flow-rate of 0.1 ml/min was effected with a Gilson Model 302 pump. The solution was added to the column effluent using a Lee (Frankfurt, Germany) visco-jet micromixer. Gaseous ammonia, obtained from Hoek Loos (Amsterdam, Netherlands), was added at an optimum source pressure of 120 Pa (0.9 Torr). After optimization, the vaporizer temperature, the repeller voltage and the source temperature were kept at 85°C, 20 V and 190°C, respectively. The electron multiplier was operated at 2 kV. Scanning was performed from mass 80 to 310 with a scan time

of 2 s. MID with a scan time of 0.24 s per m/z (*ca.* 2 s) was used for quantitative analysis on the $[M + TEA + H]^+$ ions at m/z 191 and 190 (Ala and Ala-NH_2), m/z 205 and 204 (α-Me-Ala and α-Me-Ala-NH_2), m/z 219 and 218 (Val and Val-NH_2) and m/z 233 and 232 (Leu and Leu-NH_2).

RESULTS AND DISCUSSION

Influence of the pairing ion on retention and separation of amino compounds

For the separation of a mixture of four amino acids and the corresponding acid amides, the influence of four types of perfluorinated ion-pairing agents was investigated. Fig. 1 shows the separation of the mixture using HFBA, TDFA and NDFA. The concentration of the pairing agent was 4 m*M*. For comparison, the chromatogram obtained using *n*-dodecylsulphonate (0.5 m*M*) is also given in Fig. 1. With increasing chain length of the perfluorinated pairing agent, an increase in retention was noted for all amino acids and amino acid amides. The best separation of the compounds was obtained using NDFA as ion-pairing agent (Fig. 1d). Seven out of eight amino compounds could be separated using this type of pairing agent. With *n*-dodecylsulphonate (0.5 m*M*), six out of eight compounds were separated (Fig. 1e). Regarding the chromatographic performance of NDFA, it can be stated that this ion-pairing agent is a good substitute for *n*-dodecylsulphonate in the separation of amino acids and acid amides.

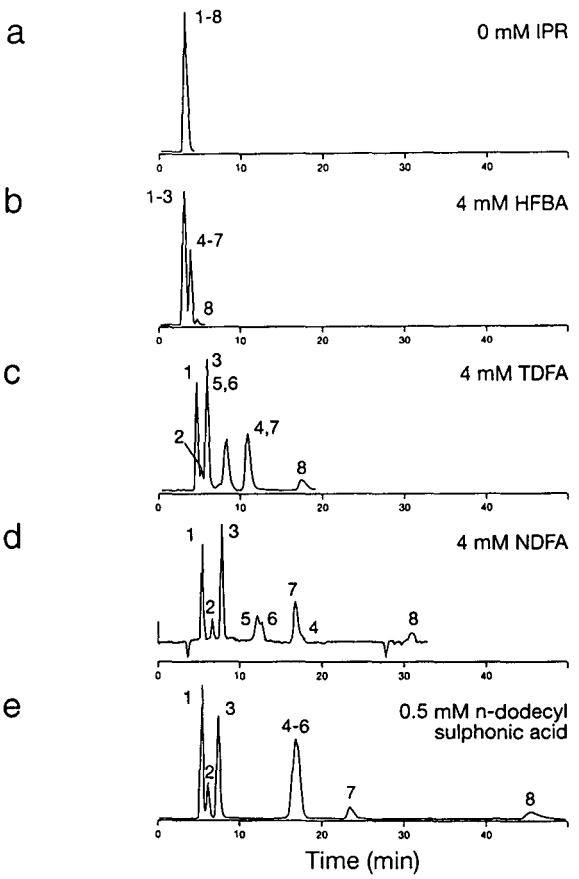

Fig. 1. Chromatograms of amino acids and amino acid amides. Buffer: (a–d) 0.1 *M* triethylammonium formate; (e) 0.1 *M* sodium phosphate. Peaks: 1 = Ala; 2 = α-Me-Ala; 3 = Val; 4 = Leu; 5 = Ala-NH_2; 6 = α-Me-Ala-NH_2; 7 = Val-NH_2; 8 = Leu-NH_2. Detection, fluorescence. For other conditions, see Experimental.

The dependence of the retention times of the amino compounds on the concentration of TDFA and NDFA is shown in Fig. 2. An increase in the retention times of all compounds was noted with an increase in the concentration of TDFA.

For NDFA, a substantial increase in retention was seen up to 1 m*M*. At higher concentrations of NDFA, only a slight effect of the ion-pairing agent concentration on the retention could be observed.

Mass spectrometric data

Postcolumn addition of TFA to the column effluent resulted in an effluent pH of less than 2, which facilitated the ionization of the amino acids, resulting in an increase in sensitivity. Addition of gaseous ammonia also increased the sensitivity to both amino acids and amino acid amides. The sensitivity to the amino acids and amino acid amides was enhanced overall by a factor 3 and 5, respectively.

The base peak in all the mass spectra was the $[M + TEA + H]^+$ ion (M + 102). The $[M + H]^+$ ion (M + 1) and the $[M + IPA + H]^+$ ion (M + 61) were also present as abundant ions in the mass spectra of the compounds investigated. As an example, the mass spectra of Val and Val-NH_2 are shown in Fig. 3.

In Table I, the intensities of the most abundant ions in the mass spectra of the compounds studied are shown. For the amino acids, the intensity of the $[M + 61]^+$ ion was higher than

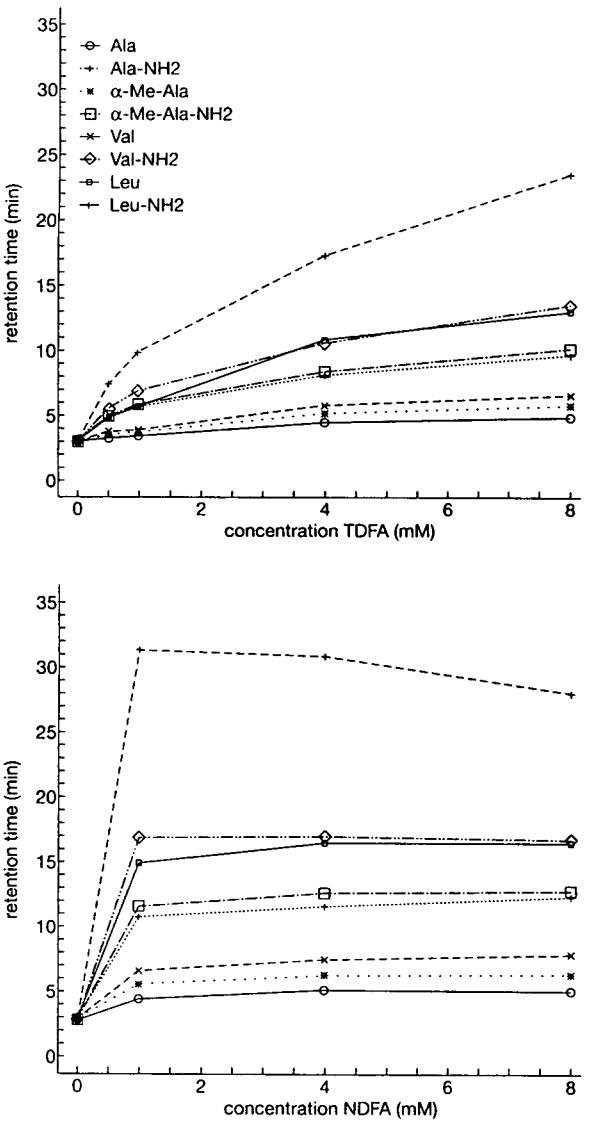

Fig. 2. Dependence of retention times on the concentration of TDFA and NDFA. Mobile phase, 0.1 *M* triethylammonium formate; detection, fluorescence. For other conditions, see Experimental.

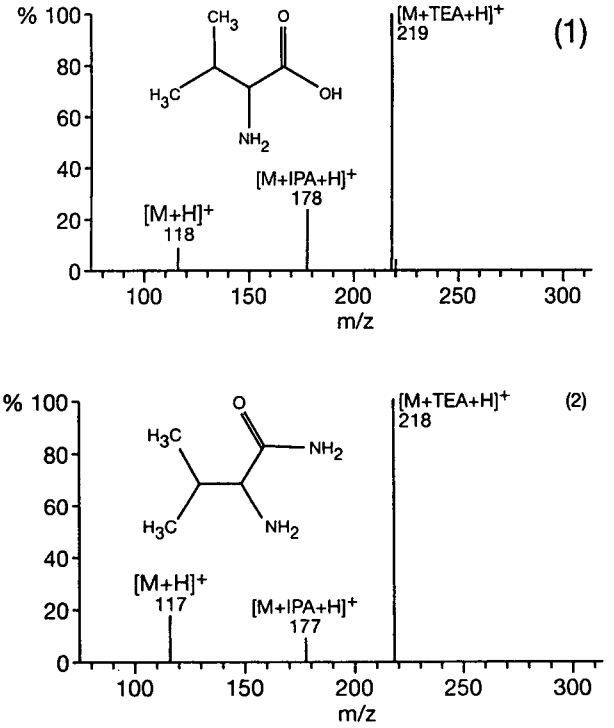

Fig. 3. Mass spectra of (1) Val and (2) Val-NH_2.

that of the $[M + 1]^+$ ion, whereas for the amino acid amides the opposite was observed. This difference may be explained by the difference in proton affinity of the α-amino group of the acid and the acid amide. As the $[M + TEA + H]^+$ ion was the most intense ion in the mass spectra (Table I), this ion was selected for MS detection.

Linearity, precision and sensitivity of the LC–TSP-MS method

The linearity of the amount *versus* MID response relationship was established over the range 200 ng–20 μg for each of the compounds studied. Linear regression analysis from calibration graphs indicated that the correlation co-

TABLE I

INTENSITIES (%) OF THE MOST ABUNDANT IONS IN THE MASS SPECTRA OF THE AMINO COMPOUNDS STUDIED

Compound	M + 102	M + 61	M + 1
Ala (M_r 89)	100	80.3	16.6
Ala-NH_2 (M_r 88)	100	<1	12.9
α-Me-Ala (M_r 103)	100	3.0	<1
α-Me-Ala-NH_2 (M_r 102)	100	<1	<1
Val (M_r 117)	100	24.4	9.3
Val-NH_2 (M_r 116)	100	4.8	13.9
Leu (M_r 131)	100	19.6	12.3
Leu-NH_2 (M_r 130)	100	<1	9.5

TABLE II

MINIMUM DETECTABLE AMOUNTS (MDA) WITH MID DETECTION

Compound	MDA (μg)	Compound	MDA (μg)
Ala	0.5	Val	0.3
Ala-NH_2	0.2	Val-NH_2	0.2
α-Me-Ala	0.1	Leu	0.9
α-Me-Ala-NH_2	0.2	Leu-NH_2	0.1

efficients were >0.9995, except for Ala (0.994), Ala-NH_2 (0.998) and Val (0.998). The within-run precision of the assay gave a relative standard derivation (R.S.D.) of <5% ($n = 3$; 1–3 μg level) for Val-NH_2, α-Me-Ala, α-Me-Ala-NH_2, Leu and Leu-NH_2. For Ala, Ala-NH_2 and Val, an R.S.D. of >5% ($n = 3$, 1–3 μg level) was found.

The detection limits for the compounds studied using MID, based on a signal-to-noise ratio of 3, are given in Table II.

As an application, a representative chromatogram of a Val-NH_2 sample from a chemo-enzymatic reaction performed on the laboratory scale is shown in Fig. 4. Using MID at m/z 218 and 219, selective detection of Val-NH_2 and Val, respectively, could be achieved. At m/z 219, the isotope peak of Val-NH_2 is clearly visible.

In this manner, LC–TSP-MS analysis was used for confirmation of the results obtained by means of the LC reaction detection system.

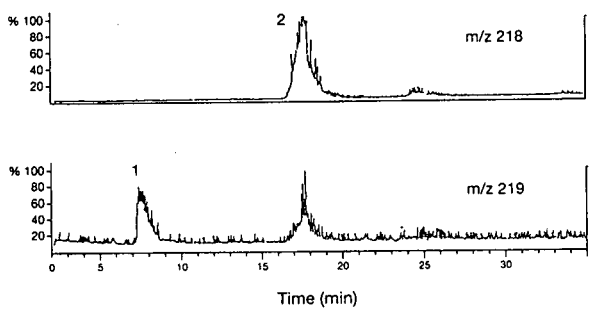

Fig. 4. Mass chromatograms of a Val-NH_2 sample from an enzymatic hydrolysis experiment. Peaks: 1 = Val; 2 = Val-NH_2. Mobile phase, 0.1 *M* triethylammonium formate and 8 m*M* NDFA. For other conditions, see Experimental.

CONCLUSIONS

For the determination of amino acids and amino acid amides, a non-volatile mobile phase consisting of sodium phosphate buffer and *n*-dodecylsulphonic acid has been successfully translated to a volatile system containing triethylammonium formate and nonadecafluorodecanoic acid, which is suitable for LC–TSP-MS analysis. The predominant ions in the mass spectra of the amino compounds are $[M + TEA + H]^+$, $[M + IPA + H]^+$ and $[M + H]^+$ Target LC–TSP-MS determination of amino acids and amino acid amides is possible with these ions, even when LC separation is not optimum. Increased MS sensitivity was achieved by postcolumn addition of TFA and chemical ionization with gaseous ammonia. Calibration graphs with good linearity were obtained and the repeatability was satisfactory. The method was suitable for the analysis of samples from bio-organic synthesis.

ACKNOWLEDGEMENT

The authors thank Mr. E. Claessen, Katholieke Industriële Hogeschool Limburg (Diepenbeek, Belgium), for technical assistance.

REFERENCES

1 R.C. Simpson, C.C. Fenselau, M.R. Hardy, R.R. Townsend, Y.C. Lee and R.J. Cotter, *Anal. Chem.*, 62 (1990) 248.
2 J.J. Conboy, J.D. Henion, M.W. Martin and J.A. Zweigenbaum, *Anal. Chem.*, 62 (1990) 800.
3 R.J. Vreeken, W.D. van Dongen, R.T. Ghijsen, G.J. de Jong, H. Lingeman, U.A.Th. Brinkman, R.G.J. van Leuken, G.T.C. Kwakkenbos and R.S. Deelder, *Biol. Environ. Mass Spectrom.*, 21 (1992) 305.
4 R.D. Voyksner and C.A. Haney, *Anal. Chem.*, 57 (1985) 991.
5 D. Barcelo, *Org. Mass Spectrom.*, 24 (1989) 219.
6 A.L.L. Duchateau, B.H.M. Munsters, G.T.C. Kwakkenbos and R.G.J. van Leuken, *J. Chromatogr.*, 552 (1991) 605.
7 M. Patthy and R. Gyenge, *J. Chromatogr.*, 449 (1988) 191.
8 I. De Miguel, E. Puech-Costes and D. Samain, *J. Chromatogr.*, 407 (1987) 109.

9 G. Inchauspe, P. Delrieu, P. Dupin, M. Laurant and D. Samain, *J. Chromatogr.*, 404 (1987) 53.
10 D. Guo, C.T. Mant and R.S. Hodges, *J. Chromatogr.*, 386 (1987) 205.
11 A.L.L. Duchateau and M.G. Crombach, *Chromatographia*, 24 (1987) 339.
12 R.G.J. van Leuken and G.T.C. Kwakkenbos, *J. Chromatogr.*, 626 (1992) 81.

Journal of Chromatography, 647 (1993) 137–146
Elsevier Science Publishers B.V., Amsterdam

CHROMSYMP. 2797

Determination of saponins in crude plant extracts by liquid chromatography–thermospray mass spectrometry

Marc P. Maillard and Kurt Hostettmann*

Institut de Pharmacognosie et Phytochimie, École de Pharmacie, Université de Lausanne, CH-1015 Lausanne (Switzerland)

ABSTRACT

The determination of saponins in crude plant extracts by liquid chromatography–thermospray mass spectrometry is described. The method is shown to be suitable for the separation, identification and determination of saponins carrying up to three sugars. The mass spectra recorded on-line provide information on the molecular mass, the nature of the sugars and their sequence. Selected applications for saponins from the molluscicidal plant *Tetrapleura tetraptera* are described.

INTRODUCTION

The inability of high-performance liquid chromatography (HPLC) to detect substances that lack a good chromophore poses several problems to phytochemists for the identification of these compounds in crude plant extracts. This is particularly true with saponins, which generally occur together with phenolic glycosides such as flavonoids and xanthones and/or pigments in plant extracts of high polarity.

Saponins are glycosides that commonly occur in higher plants. They are biosynthesized by more than 500 species belonging to almost 80 different families [1]. This class of natural compounds is also found in marine organisms [2]. They are classified into two groups according to the structure of their aglycone moiety (sapogenin): the triterpene group, in which the aglycone is usually an oleanane, ursane or dammarane skeleton, and the steroid group. The latter also includes the steroid alkaloids. The most common sugars encountered in saponins are hexoses (glucose, galactose, mannose), 6-deoxyhexoses (rhamnose), pentoses (arabinose, xylose), uronic acids (glucuronic acid, galacturonic acid) or amino sugars (glucosamine, galactosamine). Sugars may be linked to the sapogenin at one or two glycosylation sites (through an ether or/and an ester linkage), giving the corresponding monodesmosidic or bidesmosidic saponins, respectively.

Analyses of saponins are often performed by HPLC using an ultraviolet (UV) detector at short wavelength. Separations are achieved on reversed-phase columns with detection at 206 nm as there is only poor absorption by saponins at higher wavelengths [3]. Consequently, there are limitations concerning the solvents and gradients that can be used. When a gradient solvent system is used, refractive index measurement is not practicable. Thus, an alternative is to derivatize the saponins, in order to attach a chromophore that facilitates UV detection at higher wavelength (254 nm). Encouraging results have been obtained by derivatization of the saponins with 4-bromophenacyl bromide in the presence of a crown ether. This method has previously been employed for the analysis of fatty acids and prostaglandins. Details of the procedure have been published [4].

However, with all these methods, the identities of peaks can be confirmed only by their

* Corresponding author.

0021-9673/93/$06.00

retention times and comparison with authentic samples. Application of mass spectrometry (MS) as a tool for identification of the peaks is therefore a useful alternative.

The combination of HPLC and MS has been attempted since the early 1980s and systems with several types of interface for direct and indirect introduction of the column effluent have been described [5].

Different systems capable of coupling micro HPLC directly with fast atom bombardment (FAB) have been developed [6–8]. These techniques, which, depending on the interface, are termed Frit FAB and continuous flow (CF)-FAB types, have been successfully applied to the separation, identification and determination of saponins [9–12]. Using these methods, the HPLC elution profiles of saponins were well traced by total ion current (TIC) and MS, and the positive- and negative-ion FAB mass spectra allowed the identification of each peak. However, operation with this kind of interface is troublesome, and flow-rates of the LC effluent have to be around 5 μl/min in the ion source of the mass spectrometer. This requires the splitting of the effluent after the column separation. Further, there are problems such as poor peak sharpness, peak tailing and lack of sensitivity.

For the problem under investigation, one of the main disadvantages of CF-FAB and Frit-FAB was the very low flow-rates. We tried to operate with an interface capable of introducing aqueous phase into the mass spectrometer at a flow-rate that is compatible with that usually used in phytochemical analysis. The thermospray (TSP) interface was chosen for this purpose, owing to its simplicity, its ability to handle a variety of difficult samples and its operating flow-rate of about 1–2 ml/min.

Thermospray interface (TSP)

Since its invention by Blackley and Vestal [13], the TSP interface has proved to be ideal for on-line LC–MS. Its mechanically simple inmentation means that it is now widely used for the routine application of LC–TSP-MS to the direct identification of organic compounds in complex mixtures. This interface is now available for nearly all mass spectrometers on the market [14].

In the TSP interface, the analyte is ionized either by the use of additives (volatile salt solutions) or by the use of electron beams or electrical discharge. The ions pass through an orifice in a cone and are mass analysed. For saponins, which are very polar compounds, their analysis needs a postcolumn addition of a 0.5 *M* solution of ammonium acetate, giving a final concentration of *ca.* 80 m*M* after dilution with the column effluent, in order to provide the volatile buffer for ion evaporation ionization. Hence, the mass spectra recorded by this method look like chemical ionization (CI) mass spectra.

EXPERIMENTAL

Plant material

Fruits of *Tetrapleura teraptera* Taub. (Leguninosae) were collected near Ile-Ife, Nigeria. A voucher specimen is retained at the University of Ife. The dried powdered pulp of the fruits was extracted with methanol. The crude methanolic extract (30 mg/ml) was analysed on a Waters μ-Bondapak C_{18} column (10 mm, 300 × 3.9 mm I.D.), with a 30–80% gradient of aqueous acetonitrile within 30 min. The flow-rate was maintained at 1 ml/min.

Saponins **G** and **H** were previously isolated in our laboratory from the leaves of *Swartzia simplex* Spreng. collected in Panama (for isolation and purification procedures see the original reference [15]). Samples were injected directly into the loop (flow-injection mode).

Chemicals

HPLC-grade water was prepared by distillation on a Büchi (Flawil, Switzerland) Fontvapor 210 distillation instrument and passed through a 0.50-μm filter (Millipore, Bedford, MA, USA). HPLC-grade acetonitrile from Mächler (Reinach, Basle, Switzerland) was passed through a 0.45-μm Millipore filter. Ammonium acetate was obtained from Merck (Darmstadt, Germany).

LC–TSP-MS analysis

The LC–TSP-MS system used included a Waters 600 MS multi-solvent delivery LC system

and a Finnigan-MAT (San Jose, CA, USA) TSQ-700 triple quadrupole mass spectrometer equipped with a Finnigan-MAT TSP 2 interface. The electron multiplier voltage was 1800 V and the dynode voltage was kept at 15 kV, filament and discharge off. The repeller potential was optimized between 80 and 100 V, and the source temperature was kept at 270°C. The best results were recorded with temperatures of 100°C for the vaporizer and 310°C for the aerosol. Full-scan spectra from m/z 400 to 1000 (scan time 1.2 s) were obtained. Postcolumn addition of 0.2 ml/min of a 0.5 *M* solution of ammonium acetate was used to provide the volatile buffer for ion evaporation ionization. The TSP mass spectra were recorded by injecting 10 μl of a 1 mg/ml solution of crude extracts or 2 μg of pure compounds.

RESULTS AND DISCUSSION

LC–TSP-MS has been applied to the analysis of the molluscicidal saponins from the methanolic extract of fruits of *Tetrapleura tetraptera* (Leguminosae–Mimosoideae). This West African tree, locally known as Aridan, is mainly used by traditional healers in the management of convulsions, inflammation and rheumatic pains [16]. Previous reports have dealt with the strong molluscicidal activity of this plant [17,18] and *T. tetraptera* is now considered to be one of the most promising plants in the local control of the parasitic disease schistosomiasis in Africa [19]. We recently reported the isolation and identification of the five principal molluscicidal constituents of Aridan, which proved to be saponins. These compounds (**A–E**) are among the most powerful natural molluscicides and have very similar potencies to those of synthetic compounds [20,21].

Reversed-phase HPLC analysis with an acetonitrile–water gradient of the crude methanolic extract of the fruits of *T. tetraptera* showed a series of compounds whose UV spectra recorded with a diode-array detector indicated an absorption maximum at 200 nm. The same extract was analysed by LC–TSP-MS using a μBondapak C_{18} column for separation. Mass spectral detection was operated in the scan mode (m/z 450–1000). The LC–MS total ion current corresponded well with the UV trace at 206 nm. Six major peaks were visible, corresponding to the five known compounds (**A–E**) and to a sixth saponin (**F**), not yet identified. Plots of selected ion traces (*e.g.*, the $[M+H]^+$ ion) allow the location of each compound in the chromatogram (Fig. 1).

The TSP mass spectra acquired for saponins **A**, **B**, **D** and **E** in the extract displayed strong $[M+H]^+$ quasi-molecular peaks, together with adduct species such as $[M+CH_3CN+NH_4]^+$, confirming the molecular mass. In addition, an important $[A+H]^+$ peak for the aglycone was visible in these spectra (see also Table I for other fragments of importance).

Optimization of the experimental parameters (temperatures of the TSP vaporizer and ion source block) permitted "soft" ionization under sufficiently mild conditions to provide information on fragmentation of the osidic chain of the saponin. Thus, it was possible to observe peaks corresponding to the loss of one (mono- and diglycosides) and then two sugars (diglycosides) in all spectra. Additional losses of 18 and 42 u fragments accounted for the elimination of water (H_2O) and the acetamide moiety ($COCH_2$) from the inner sugar (Figs. 2–5 and Table I).

The mass spectrum obtained for saponin **C** showed a different pattern. Small quasi-molecular peaks at m/z 855 ($[M+CH_3CN+NH_4]^+$), 814 ($[M+NH_4]^+$) and 797 ($[M+H]^+$) confirmed the molecular mass. The base peak in this spectrum appeared at m/z 784 $\{[(M+NH_4)-30]^+\}$, resulting from the rapid elimination of a CHOH fragment. This phenomenon was also observed in the desorption chemical ionization (D/CI) mass spectrum of this saponin [21] and in those of other saponins containing a 14α-CH_2OH moiety [22]. A small peak resulting from the loss of one sugar was present at m/z 622 ($[784-\text{hexose}]^+$). In addition, important aglycone peaks at m/z 473 ($[A+H]^+$) and 490 ($[A+NH_4]^+$) were visible in this spectrum (Fig. 6).

Examination of the spectrum of the unknown compound **F** (Fig. 7) gave some information about its structure. In the first instance, the molecular mass was established as 837 {quasi-

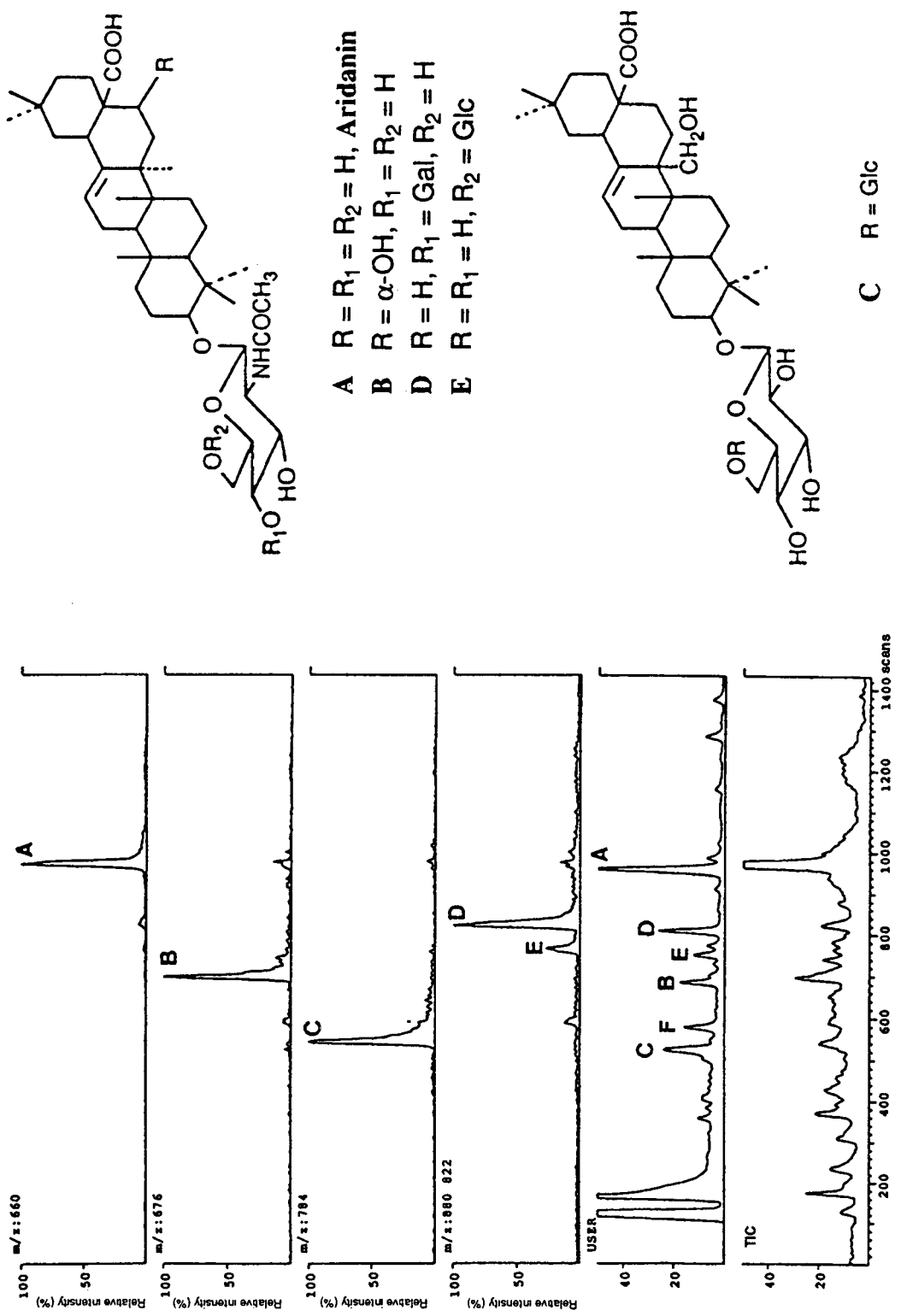

Fig. 1. LC–TSP-MS of the methanolic extract of the fruits of *T. tetraptera* and selected-ion current profiles of five known saponins. HPLC conditions: column, μBondapak C_{18}; eluent, CH_3CN–H_2O, 30:70→80:20 over 30 min flow-rate; 1 ml/min. TSP conditions: vaporizer temperature, 100°C; source temperature, 270°C; buffer, 0.5 *M* ammonium acetate; flow-rate, 0.2 ml/min; 1.5 s per scan; detection, UV at 206 nm.

TABLE I

MAJOR IONS OBSERVED IN THE TSP MASS SPECTRA (m/z) TOGETHER WITH THEIR RELATIVE INTENSITIES (%)

Ion[a]	Saponin					
	A	**B**	**D**	**E**	**F**	**C**
$[A + H]^+$	457 (46)	473 (95)	457 (78)	457 (100)	473 (66)	473 (49)
$[A + NH_4]^+$	474 (22)	490 (57)	474 (39)	474 (46)	490 (47)	490 (39)
$[(M + H) - hex - 42]^+$	–	–	618 (23)	618 (16)	–	–
$[(M + H) - hex - H_2O]^+$	–	–	642 (36)	642 (36)	–	–
$[(M + H) - hex]^+$	–	–	660 (76)	660 (17)	676 (39)	–
$[(M + CH_3CN + NH_4) - hex]^+$	–	–	718 (42)	718 (15)	734 (35)	–
$[(M + H) - 42]^+$	618 (22)	634 (19)	780 (23)	780 (15)	–	–
$[(M + H) - H_2O]^+$	642 (38)	658 (38)	–	–	–	–
$[M + H]^+$	660 (100)	676 (95)	822 (42)	822 (25)	838 (37)	797 (3)
$[(M + NH_4) - CHOH - hex]^+$	–	–	–	–	–	622 (8)-
$[(M + NH_4) - CHOH]^+$	–	–	–	–	–	784 (100)
$[M + NH_4]^+$	–	–	–	–	–	814 (17)
$[M + CH_3CN + NH_4]^+$	718 (85)	734 (80)	880 (100)	880 (42)	896 (55)	855 (4)

[a] hex = Hexose.

molecular peaks at m/z 838 ($[M + H]^+$) and 896 ($[M + CH_3CN + NH_4]^+$)}. In a second step, elimination of a terminal hexosyl moiety was observed, generating peaks at m/z 676 {$[(M + H) - hexose]^+$} and 734 {$[(M + CH_3CN + NH_4) - hexose]^+$}, followed by the loss of an N-acetylglucosyl unit. Hence this compound should be a glycoside of saponin **B**. The base peak in this spectrum was recorded at m/z 784. It could represent a residual presence of saponin **C** in this spectrum. Isolation of compound **F** is in progress.

In the first example described in this paper, LC–TSP-MS of mono- and diglycosides is

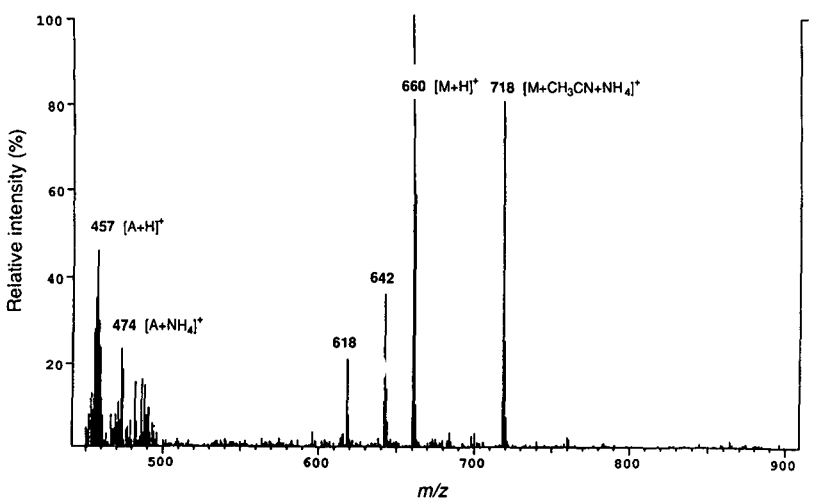

Fig. 2. LC–TSP-MS of aridanin (**A**) obtained after on-column analysis of the methanolic extract of *T. tetraptera*. For conditions, see Fig. 1.

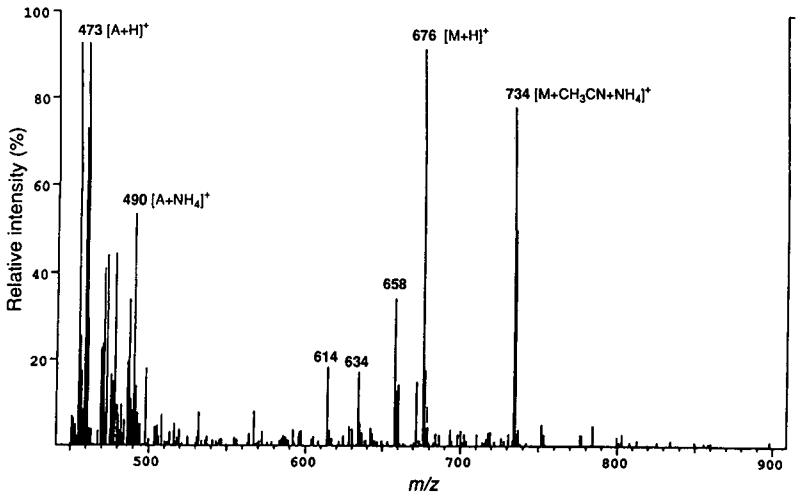

Fig. 3. LC–TSP-MS of saponin (**B**) obtained after on-column analysis of the methanolic extract of *T. tetraptera*. For conditions, see Fig. 1.

shown. However, after optimization of the experimental parameters, it was also possible to analyse triglycosides. The mass spectrum recorded on-line provided information on the molecular mass, the nature of the sugars and their sequence.

Two saponins (**G** and **H**), previously isolated from a methanolic extract of the leaves of *Swartzia simplex* [15] (Leguminosae–Caesalpinaceae), were used to demonstrate the ability of TSP to perform such analyses. With post-column addition of ammonium acetate to provide the volatile buffer for ion evaporation ionization, the TSP mass spectra acquired for both saponins showed $[M + NH_4]^+$ quasi-molecular peaks. Subsequent losses of sugars were observed.

For saponin **G**, simultaneous cleavage of a

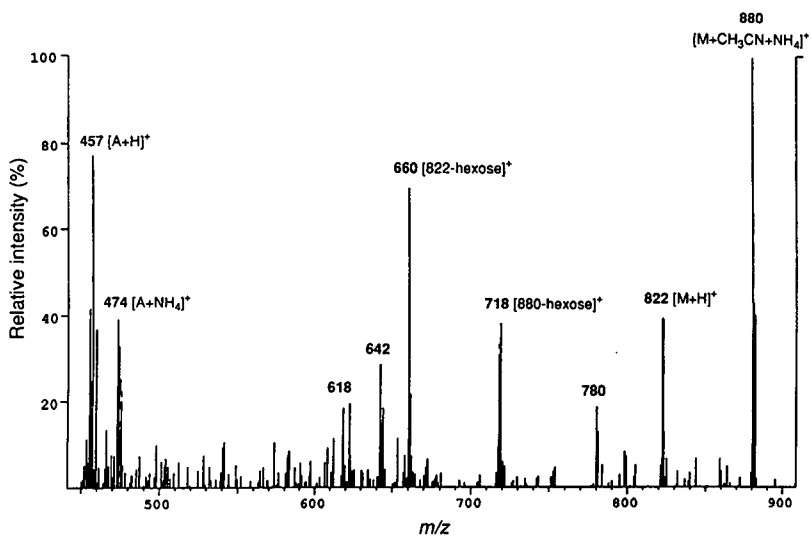

Fig. 4. LC–TSP-MS of saponin (**D**) obtained after on-column analysis of the methanolic extract of *T. tetraptera*. For conditions, see Fig. 1.

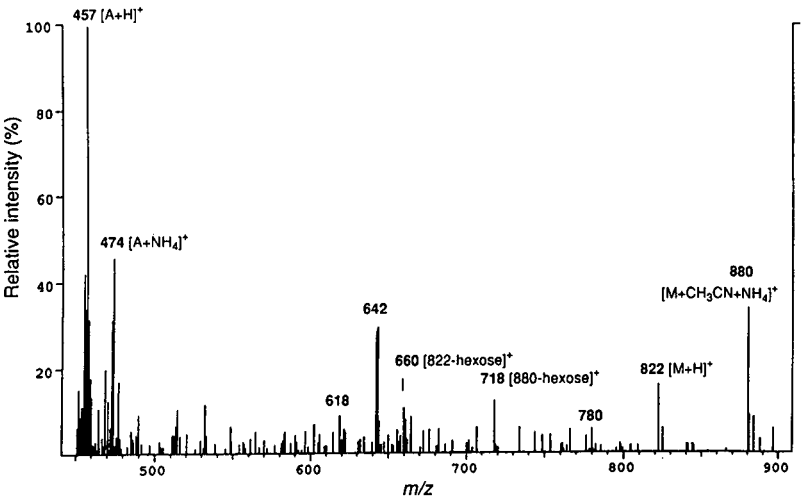

Fig. 5. LC–TSP-MS of saponin (**E**) obtained after on-column analysis of the methanolic extract of *T. tetraptera*. For conditions, see Fig. 1.

rhamnosyl $[(M + NH_4) - 146]^+$ moiety and a glucosyl $[(M + NH_4)-162]^+$ moiety indicated that both sugars were in terminal positions. Additional signals could be observed at *m/z* 650, 636 and 474, which corresponded to the elimination of both sugar moieties together with an additional inner glucuronic acid residue. The fragmentation patterns indicated clearly that rhamnose was attached to the glucuronic acid and that glucose belonged to a second chain (Fig. 8).

In the mass spectrum of saponin **H**, the signals at *m/z* 796 $\{[(M + NH_4)-132]^+\}$ and 765 $\{[(M + NH_4)-146]^+\}$ corresponded to the simultaneous elimination from the quasi-molecular ion of a xylosyl moiety and of a rhamnosyl moiety. Addi-

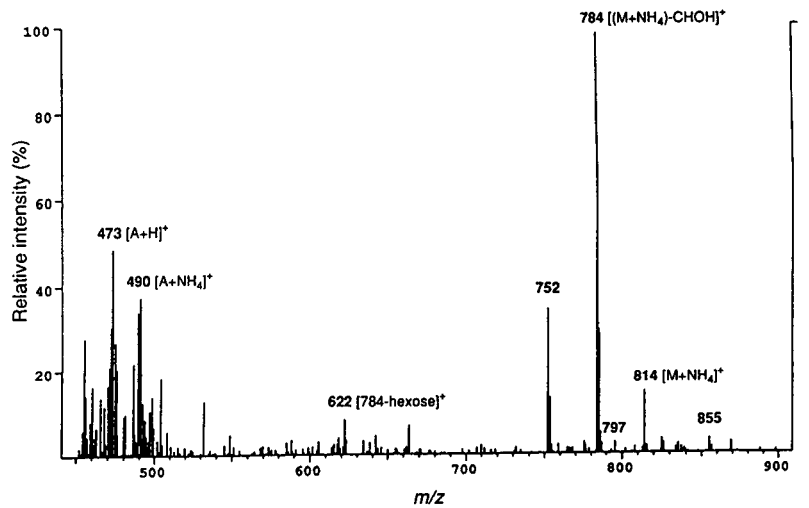

Fig. 6. LC–TSP-MS of saponin (**C**) obtained after on-column analysis of the methanolic extract of *T. tetraptera*. For conditions, see Fig. 1.

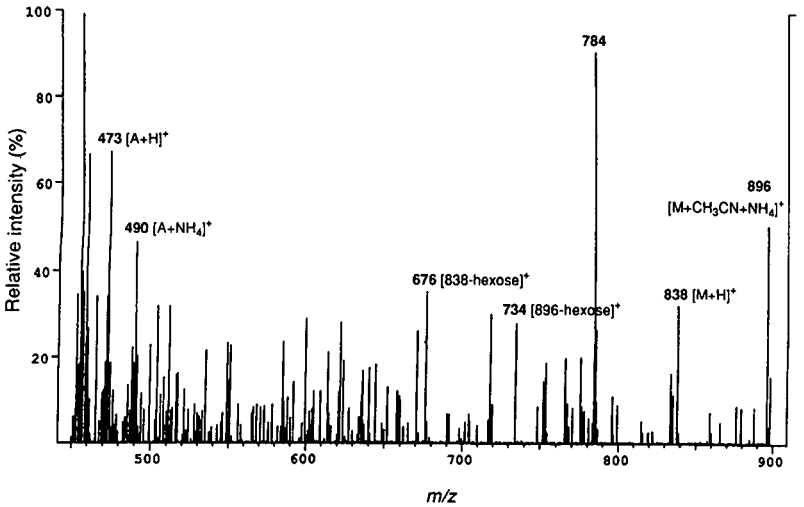

Fig. 7. LC–TSP-MS of the unknown saponin (**F**) obtained after on-column analysis of the methanolic extract of *T. tetraptera*. For conditions, see Fig. 1

tional signals for the glucuronic acid–oleanolic acid moiety and the oleanolic acid moiety were observed at m/z 650 $\{[(M + NH_4) - 278]^+\}$ and 474 $\{[(M + NH_4) - 454]^+\}$, respectively. From this fragmentation pattern, it could be deduced that rhamnose and xylose were both terminal sugars and that they were linked to a glucuronic acid (Fig. 9).

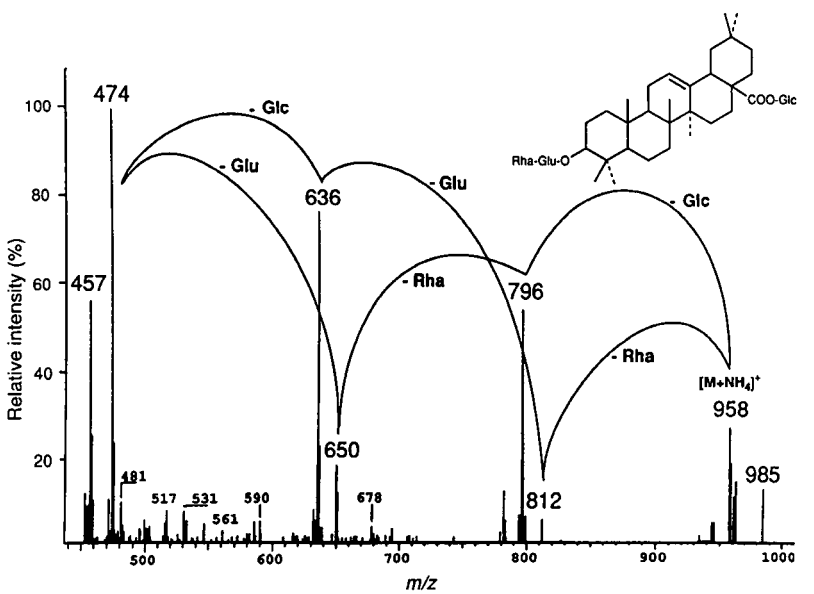

Fig. 8. TSP mass spectrum of saponin (**G**) obtained in the flow-injection mode. HPLC conditions: eluent, CH_3CN–H_2O (50:50); flow-rate, 1 ml/min. TSP conditions: vaporizer temperature 100°C; source temperature, 270°C; buffer, 0.5 *M* ammonium acetate; flow-rate, 0.2 ml/min; detection, UV at 206 nm.

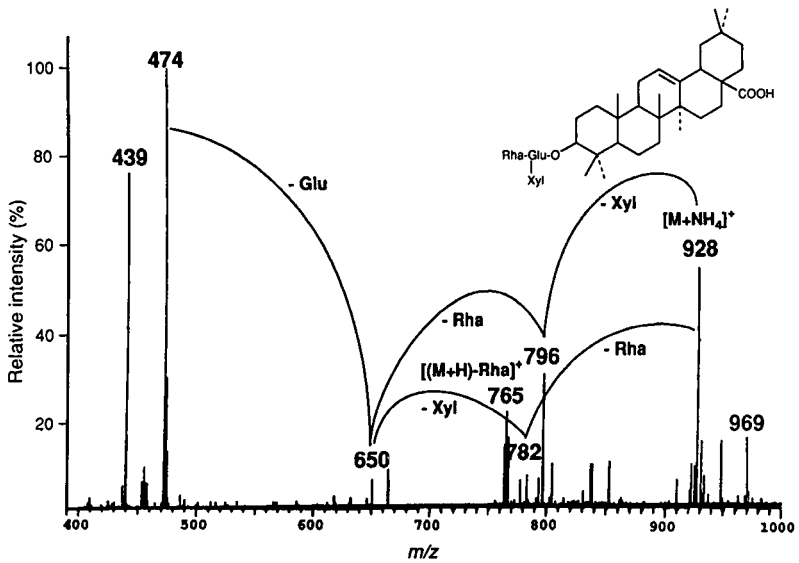

Fig. 9. TSP mass spectrum of saponin (**H**) obtained in the flow-injection mode. For conditions, see Fig. 8.

CONCLUSIONS

LC–TSP-MS is a suitable method for the detection of saponins in crude plant extracts, even in presence of other products such as phenolic compounds.

Addition of ammonium acetate as buffer provides an ionization similar to that obtained with D/CI (NH_3, positive-ion mode), and the same information can be recorded on-line. After optimization of the experimental parameters, different results such as molecular mass, the nature of the sugars and their sequence can be obtained.

Under the conditions described in this paper, it has not yet been possible to obtain molecular mass data for saponins carrying more than three sugars. However, experiments are in progress to increase the sensitivity of this method for polar glycosides of higher mass.

ACKNOWLEDGEMENT

Financial support from the Swiss National Science Foundation is gratefully aknowledged.

REFERENCES

1 K. Hostettmann, M. Hostettmann and A. Marston, *Methods Plant Biochem.*, 7 (1991) 435.
2 R. Tschesche and G. Wulff, *Biochem. Biophys. Res. Commun.*, 30 (1973) 462.
3 B. Domon, A.-C. Dorsaz and K. Hostettmann, *J. Chromatogr.*, 315 (1984) 441.
4 I. Slacanin, A. Marston and K. Hostettmann, *J. Chromatogr.*, 448 (1988) 265.
5 P. Arpino, *Fresenius' J. Anal. Chem.*, 337 (1990) 667.
6 Y. Ito, T. Takeuchi, D. Ishii and M. Goto, *J. Chromatogr.*, 346 (1985) 161.
7 Y. Ito, T. Takeuchi, D. Ishii, M. Goto and T. Mizuno, *J. Chromatogr.*, 358 (1986) 201.
8 R.M. Caprioli, in R.M. Caprioli (Editor), *Continuous-Flow Fast Atom Bombardment Mass Spectrometry*, Wiley, Chichester, 1990, p. 1.
9 M. Hattori and T. Namba, *Jeol News*, 23A (1987) 2.
10 M. Hattori, Y. Kawata, N. Kakiuchi, K. Matsuura, T. Tomimori and T. Namba, *Shoyakugaku Zasshi*, 42 (1988) 228.
11 M. Hattori, Y. Kawata, N. Kakiuchi, K. Matsuura, T. Tomimori and T. Namba, *Chem. Pharm. Bull.*, 36 (1988) 4467.
12 H.-S. Young, J.C. Park and J.S. Choi, *Korean J. Pharmacogn. (Saeng'yakhak Joeji)*, 19 (1988) 248.
13 C.R. Blackley and M.L. Vestal, *Anal. Chem.*, 55 (1983) 750.
14 A.P. Bruins, *Methodol. Surv. Biochem. Anal.*, 18 (1988) 339.

15 C. Borel, M.P. Gupta and K. Hostettmann, *Phytochemistry*, 26 (1987) 2685.
16 *J.A. Ojewole and S.K. Adesina, Planta Med.*, 49 (1983) 99.
17 C.O. Adewunmi and V.O. Marquis, *J. Parasitol.*, 67 (1981) 67.
18 C.O. Adewunmi and V.O. Marquis, *Phytother. Res.*, 1 (1987) 69.
19 K. Hostettmann, in H. Wagner, H. Hikino and N.R. Farnsworth (Editors), *Economic and Medicinal Plant Research*, Vol. 3, Academic Press, London, 1989, p. 73.
20 M.P. Maillard, C.O. Adewunmi and K. Hostettmann, *Helv. Chim. Acta*, 72 (1989) 668.
21 M.P. Maillard, C.O. Adewunmi and K. Hostettmann, *Phytochemistry*, 31 (1992) 1321.
22 M.O. Hamburger and K. Hostettmann, *Helv. Chim. Acta*, 69 (1986) 221.

Journal of Chromatography, 647 (1993) 147–154
Elsevier Science Publishers B.V., Amsterdam

CHROMSYMP. 2798

Use of liquid chromatography–thermospray mass spectrometry in phytochemical analysis of crude plant extracts

Marc P. Maillard, Jean-Luc Wolfender and Kurt Hostettmann*

Institut de Pharmacognosie et Phytochimie, École de Pharmacie, Université de Lausanne, CH-1015 Lausanne (Switzerland)

ABSTRACT

Qualitative analyses of selected compounds by high-performance liquid chromatography of crude plant extracts are not always straightforward owing to the lack of a suitable chromophore for UV detection or because insufficient material is present. In both instances, however, coupling liquid chromatography with thermospray mass spectrometry has proved to be ideal for the direct detection of these compounds. Different examples of analyses of bioactive constituents (including ginkgolides, sesquiterpene lactones, acetogenins and saponins) in crude plant extracts are described. Total ion current traces and mass chromatograms allow the easy detection of these compounds in the extracts. Depending on the ionization pattern, $[M + H]^+$ or $[M + NH_4]^+$ ions are used for selected ion monitoring studies.

INTRODUCTION

Analyses of natural products of plant origin are generally problematic. These substances usually occur in complex mixtures, containing up to several thousand different constituents. Sometimes only one compound is responsible for the pharmacological and/or toxic properties of the plant. Hence the phytochemist needs very efficient methods to analyse such extracts and identify their active principles.

Two points have to be noted. First, the method for separating the different constituents of the extract has to be as selective as possible. Chromatographic techniques are the main tools for analyses of drug extracts, and different methods have been developed (thin-layer chromatography, gas chromatography and liquid chromatography), with different ranges of application, depending on the substances being analysed [1]. Second, optimum detection of the separated peaks is required. Normally, an ultraviolet (UV) detector is used.

However, different problems can arise. In some instances, where the extract is very complex, it may be difficult to identify a specific peak. Insufficient resolution of the separation and peak overlapping can perturb the analysis. In other instances, the substances of interest do not possess suitable chromophores for easy detection by conventional methods, or the amount of compounds to be detected is too small for the sensitivity of the detector. All these problems require the development of new types of detector, more universal and more versatile.

The aims of qualitative analyses in phytochemistry are numerous. Some of them are as follows. Chromatographic analyses are used to "pilot" the preparative isolation of natural products (optimization of the experimental conditions, checking of the different fractions throughout the separation) and to control the final purity of the isolated compounds. For chemotaxonomic purposes, the botanical relationships between different species can be indicated by chromato-

* Corresponding author.

0021-9673/93/$06.00

graphic comparisons of the chemical composition. Finally, comparison of chromatographic "fingerprints" between authentic samples and unknowns permits the identification of drugs and/or the detection of adulterants.

However, in many applications it may be necessary not only to detect but also to identify compounds in extracts. With conventional detection, the identities of peaks can be confirmed only from their retention times and by comparison with authentic samples. Hence, the development of new techniques has been necessary.

Interesting results have been obtained by coupled techniques, such as gas chromatography–mass spectrometry (GC–MS) [2], gas chromatography–Fourier transform infrared spectrometry (GC–FT-IR) [3], liquid chromatography–UV spectrometry with diode-array detection (LC–UV) [4] and liquid chromatography–mass spectrometry (LC–MS) [5].

The main advantage of these techniques is their ability to provide qualitative information on the detected peaks. The use of a diode array UV detector allows, for example, the whole UV spectrum of a specific product in a crude extract to be obtained on-line. This technique has been particularly useful for the identification of polyphenolic compounds [6] and bitter principles [7].

LC–MS techniques are more recent and are still generally regarded as pure research tools, without any major routine uses [8]. The principal consequence is that this technique does not yet appear to have gained the popularity that it merits and is still relatively little used in analytical work.

However, some less sophisticated interfaces have recently been developed, and are now widely available in laboratories, *e.g.*, the thermospray (TSP) interface [9].

This interface is capable of introducing an aqueous phase into the MS system at a flow-rate compatible with that usually used in phytochemical analysis (about 1–2 ml/min). From this point of view, the TSP interface is particularly well suited for this kind of analysis, and in fact TSP has already proved valuable, especially in the detection of alkaloids [10, 11]. More recently, LC–TSP-MS of flavonoids has also been reported [12]. However, so far, routine applications of LC–TSP-MS in phytochemistry are still rare.

In this paper, the ability of this method to detect and identify biologically active compounds in crude plant extracts is reported; special emphasis is placed on the detection of substances that lack a strong chromophore and are thus unsuitable for conventional UV detection.

EXPERIMENTAL

Plant material

Commercially available leaves of *Ginkgo biloba* L. (Ginkgoaceae) (Dixa, St. Gallen, Switzerland) were extracted with methanol–water (1:1). The methanolic extract was then partitioned between ethyl acetate and water. The organic phase was analysed on a Nucleosil C_{18} (5 μm) column (125 × 4.0 mm I.D.) (Macherey–Nagel, Düren, Germany) with methanol–water (40:60) as eluent at a flow-rate of 1 ml/min.

Artemisia annua L. (Asteraceae) was grown in Switzerland (Mediplant, Conthey, Switzerland). Its aerial parts (2.0 g) were extracted by maceration at room temperature in 200 ml of dichloromethane for 24 h. The extract was analysed on a Nucleosil C_{18} (7 μm) column (250 × 4.0 mm I.D.) (Macherey–Nagel), with a gradient of aqueous methanol from 50 to 75% in 30 min. Trifluoroacetic acid (0.1%) was added to the solvents. The flow-rate was maintained at 1 ml/min.

Annona purpurea L. (Annonaceae) was collected at Cierro Jefe, Panama, and a voucher specimen is retained at the University of Panama, Panama City. Extraction was achieved at room temperature with dichloromethane. The crude dichloromethane extract was analysed on a Nucleosil C_{18} (7 μm) column (250 × 4.0 mm I.D.) (Macherey–Nagel), with isocratic elution with acetonitrile–water (85:15) or with a gradient of acetonitrile–water from 60:40 to 85:15 in 30 min. The flow-rates were 1 ml/min.

Fruits of *Tetrapleura teraptera* Taub. (Leguminosae) were collected near Ile-Ife, Nigeria. A voucher specimen is retained at the University of Ife. The dried powdered pulp of the fruits was extracted with methanol. The crude methanolic extract (30 mg/ml) was ana-

lysed on a μBondapak C_{18} (10 μm) column (300 × 3.9 mm I.D.) (Waters, Bedford, MA, USA) with a gradient of aqueous acetonitrile from 30–80% in 30 min. The flow-rate was maintained at 1 ml/min.

The retention times of the identified products in these extracts were all confirmed by injection of authentic samples under the same conditions.

Chemicals

HPLC-grade water was prepared by distillation on a Büchi (Flawil, Switzerland) Fontavapor 210 distillation instrument and passed through a Millipore (Bedford, MA, USA) 0.50-μm filter. HPLC-grade acetonitrile and methanol from Mächler (Reinach, Basle, Switzerland) were passed through a Millipore 0.45-μm filter. Ammonium acetate and trifluoroacetic acid were obtained from Merck (Darmstadt, Germany).

LC–TSP-MS analysis

The LC–TSP-MS system included a Waters 600 MS multi-solvent delivery LC system and a Finnigan-MAT (San Jose, CA, USA) TSQ-700 triple quadrupole mass spectrometer equipped with a Finnigan-MAT TSP 2 interface. The electron multiplier voltage was 1800 V and the dynode voltage kept at 15 kV. Unless specified otherwise, the filament and discharge were off. The repeller potential was optimized between 80 and 100 V. The block source temperature and temperature for the vaporizer were optimized to maximize the intensities of the quasi-molecular peaks. Full-scan spectra from *m/z* 400 to 1000 (scan time 1.2 s per scan) were obtained. A postcolumn addition of 0.2 ml/min of a 0.5 *M* solution of ammonium acetate (giving a final concentration of about 80 m*M* after dilution with the column effluent) was used to provide the volatile buffer for ion evaporation ionization. The thermospray spectra were recorded by injecting 10 μl of a 1 mg/ml solution of crude extracts or 2 μg of pure compounds.

RESULTS AND DISCUSSION

Ginkgo biloba

Preparations containing *Ginkgo biloba* L. (Ginkgoaceae) leaf extracts have become a major market, with estimated annual sales of US$ 500 million world-wide [13]. The antagonistic activity of *G. biloba* on platelet aggregation induced by platelet aggregation factor (PAF) is associated with the non-flavonoid fraction, composed of ginkgolides, which are diterpenes [14]. Owing to the difficulty of identifying these compounds among other substances in crude leaf extracts (low concentrations, weak chromophores), analysis and standardization of *Ginkgo biloba* preparations have previously been carried out by HPLC of their phenolic constituents, which do not contribute to the inhibition of PAF [15]. Hence methods for the determination of ginkgolides in such preparations are urgently needed.

The TSP mass spectrum of ginkgolides revealed only a strong quasi-molecular ion $[M + NH_4]^+$ peak, without other adduct species, as is the case with desorption/chemical ionization (D/CI, NH_3 positive-ion mode). No subsequent fragmentation was shown (Fig. 1). However, as ginkgolides are easily ionized by TSP, on-line LC–TSP-MS was demonstrated to be a very efficient method to detect these diterpenes in a *Ginkgo biloba* leaf extract (Fig. 1). Ginkgolides were not visible in the UV trace, but the total ion current (TIC) trace showed the presence of these compounds. Further, the specific display of ion traces for masses corresponding to the respective quasi-molecular ion $[M + NH_4]^+$ peaks allowed the identification of all ginkgolides in the extract.

Repetitive quantitative analyses of the same *Ginkgo biloba* leaf extract showed that the reproducibility of detection (*i.e.*, the area under the curve) was good (standard deviation of about 10%), as long as all the parameters of ionization (source block temperature, vaporizer temperature, aerosol temperature, pressure in the source) were well stabilized. Different temperatures for the source and aerosol were tried, and the best results were obtained with the block source temperature kept at 225°C and the vaporizer temperature fixed at 62°C. Ionization was induced by the use of ammonium acetate and the filament was operated at 600 V with a 0.200 mA emission current.

Using these parameters for ionization and isocratic elution with methanol–water (40:60), it was possible to analyse different

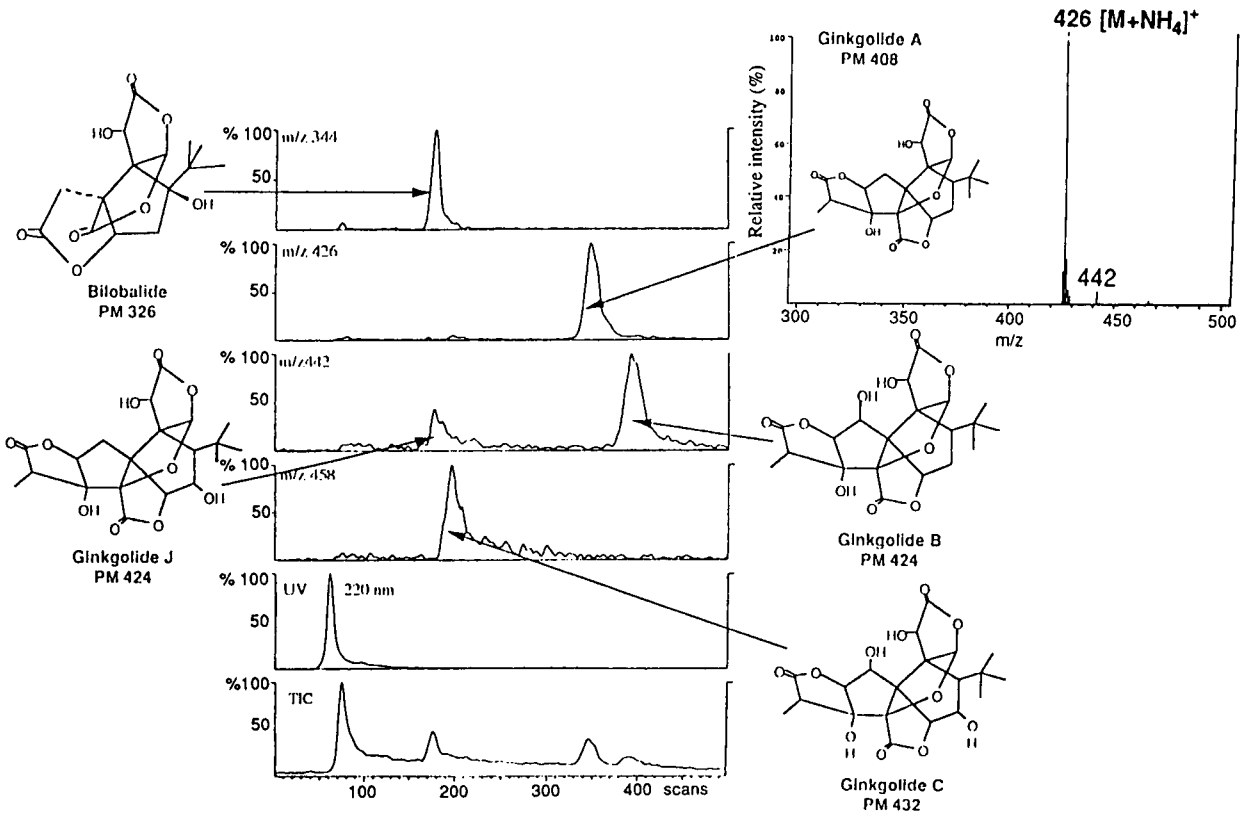

Fig. 1. LC–TSP-MS analysis of *Ginkgo biloba* extract and TSP mass spectrum of ginkgolide A. Column, Nucleosil C_{18}; eluent, MeOH–H_2O (40:60), 1 ml/min; detection: UV 220 nm. TSP: vaporizer 62°C; source 225°C; filament on, 600 V and 200 mA; buffer, 0.5 *M* CH_3COONH_4 at 0.2 ml/min; 1.2 s per scan.

phytotherapeutic preparations containing *Ginkgo biloba* extracts. Low levels of detection, in the range of 1 ng (*ca.* 0.3 pmol/μl) were obtained, and even homeopathic preparations could be analysed by this technique. Thus, the sensitivity of the LC–TSP-MS analysis of ginkgolides is comparable to those obtained with GC-MS, as the latter technique permits the detection of gingkolides at concentrations as low as 0.1 pmol/μl of injected purified material [16].

Artemisia annua

The antimalarial compound artemisinin is found in extracts of *Artemisia annua* L. (Asteraceae), a Chinese plant, locally known as Qinghao [17]. Artemisinin represents one of the most remarkable success stories of antimalarial compounds from plants. This metabolite is a sesquiterpene lactone, too complex to be synthesized on a large scale. Hence, the only way to obtain this active principle remains its isolation from dried plant material. In order to increase the efficiency of the method, cultures of different strains of *A. annua* have been performed for the optimization of their artemisinin content. In addition, suitable analytical methods for its determination have had to be developed.

HPLC–UV determination of this compound in a crude plant extract is not straightforward because it lacks a suitable chromophore for detection with conventional UV detectors. It also occurs with phenolic components which interfere in the analysis. LC–TSP-MS can provide a solution to this detection problem, because the TSP mass spectrum of artemisinin shows different quasi-molecular peaks *i.e.*, at *m/z* 283 [M +

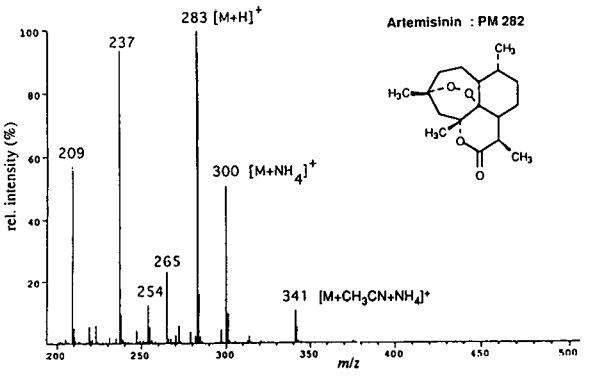

Fig. 2. TSP mass spectrum of artemisinin. Column, Nucleosil C_{18}, eluent CH_3CN–H_2O gradient from 50:50 to 75:25 in 30 min; flow-rate, 1 ml/min; detection UV at 208 nm; TSP vaporizer, 90°C; source, 280°C; filament on, 600 V and 200 mA; buffer, 0.5 *M* at CH_3COONH_4 0.2 ml/min; 1.2 s per scan.

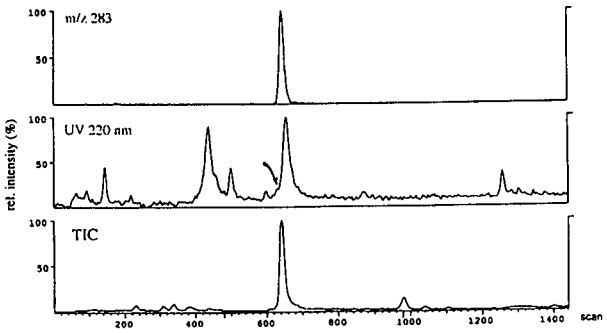

Fig. 3. LC–TSP-MS analysis of a dichloromethane extract of the aerial parts of *Artemisia annua*. Conditions as in Fig. 2. Artemisinin is indicated by an arrow in the UV trace.

$H]^+$, 300 $[M + NH_4]^+$ and 341 $[M + CH_3CN + NH_4]^+$ (Fig. 2). The base peak in this spectrum is the $[M + H]^+$ ion, as is the case for the D/CI spectrum (NH_3 or other reagent gas, positive-ion mode) [18]. Peaks resulting from the subsequent elimination of water (*m/z* 265) and HCOOH (*m/z* 237) were also visble in the TSP spectrum.

Chromatographic analysis of the dichloromethane extract of the aerial parts of *A. annua* showed, even at lower wavelengths, a UV trace that was not suitable for artemisinin detection. Phenolic components are present, co-migrate with artemisinin and interfere with the analysis. However, observation of the TIC trace, together with selective display of the *m/z* 283 $[M + H]^+$ ion trace permits a very efficient detection of the sesquiterpene lactone (Fig. 3).

Annona purpurea

The third example shown here is the identification of acetogenins in the leaves of *Annona purpurea* L. (Annonaceae). Acetogenins are fatty acid derivatives that possess tetrahydrofuran rings and a methylated γ-lactone with various substituents along the hydrocarbon chain. They exhibit a broad range of potent biological activities (cytotoxicity, antitumour activity, antimalarial, antimicrobial and immunosuppressant potencies and antifeedant and pesticidal actions) [19]. This kind of metabolite seems to occur only in the Annonaceae family, and so far more than 80 different products have been isolated from different *Annona* species and four other genera [20].

The 208-nm trace of an HPLC-UV analysis of a dichloromethane extract of *A. purpurea* shows some small peaks which can be related, after observation of their whole UV spectra, to the acetogenin group.

As is the case with D/CI (NH_3, positive-ion mode) [21], acetogenins are easily ionized in TSP, displaying strong quasi-molecular peaks with $[M + H]^+$ ions as the base peak, together with adduct species $[M + NH_4]^+$ (relative intensity *ca.* 70%) and $[M + CH_3CN + NH_4]^+$ (*ca.* 50%). Further, LC–TSP-MS analysis of the dichloromethane extract is straightforward (Fig. 4).

In the mass range 600–750 (in which the molecular masses of the acetogenins can be found), it was possible to see a series of different compounds under the HPLC conditions used [isocratic, acetonitrile–water (85:15)].

Modification of the chromatographic conditions with a gradient of acetonitrile from 60% to 85% within 30 min led to an improvement in the resolution and allowed the separation of eight compounds (**1–8**) (Figs. 5 and 6) [22].

Compounds **3–6** are known substances, whereas **1**, with a new type of skeleton for an acetogenin, and **2**, a stereoisomer of cherimoline (**3**), are new natural products. Structure determinations of acetogenins **7** and **8** are in progress.

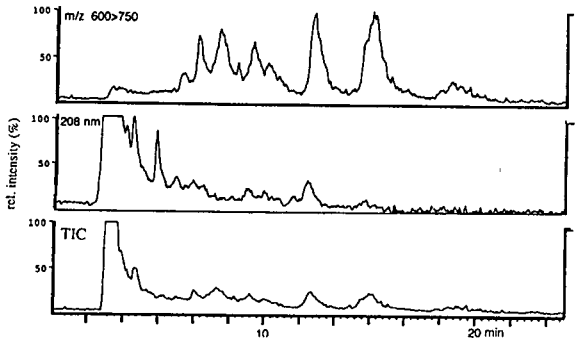

Fig. 4. LC–TSP-MS analysis of the crude dichloromethane extract of *Annona purpurea* leaves. Column, Nucleosil C_{18}, eluent, CH_3CN–H_2O (85:15), at 1 ml/min; detection, UV at 208 nm; TSP: vaporizer, 90°C; source, 250°C; filament off; buffer, 0.5 *M* CH_3COONH_4, at 0.2 ml/min; 1.2 s per scan.

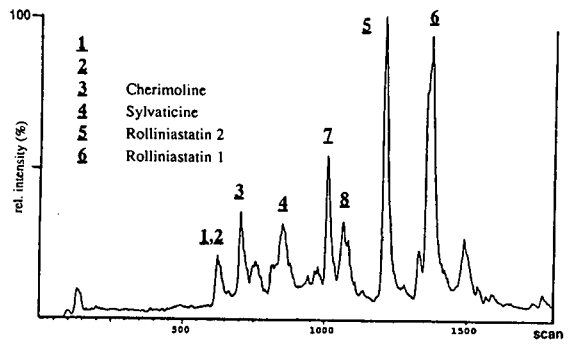

Fig. 5. LC–TSP-MS analysis of acetogenins from *Annona purpurea*. Column, Nucleosil C_{18}, eluent CH_3CN–H_2O gradient from 60:40 to 85:15, flow-rate, 1 ml/min; detection UV at 208 nm, TSP vaporizer, 90°C; source, 250°C; filament off; buffer, 0.5 *M* CH_3COONH_4 at 0.2 ml/min.

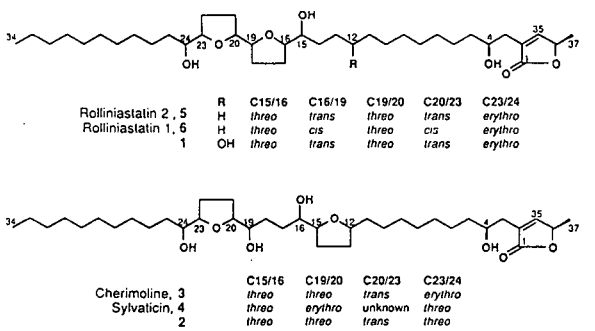

Fig. 6. Structures of the acetogenins isolated from the leaves of *Annona purpurea*.

Tetrapleura tetraptera

The above-mentioned applications of TSP in the analysis of crude drug extracts of plant origin all involve the detection of known compounds in complex mixtures. However, LC–TSP-MS can also be used in the detection and on-line identification of unknown products in vegetable extracts. In order to illustrate this potential, results of the LC–TSP-MS analysis of the methanolic extract of the fruits of the African tree *Tetrapleura tetraptera* Taub (Leguminosae) are described (see also the paper by Maillard and Hostettmann [23], elsewhere in this volume).

T. tetraptera is considered to be one of the most promising plants for the local control of the parasitic disease schistosomiasis in Africa [24]. Its fruits contain a large amount of molluscicidal saponins which kill the intermediate snails at concentrations similar to those of synthetic compounds [25].

Analysis of the methanolic extract of these fruits by LC–TSP-MS was also performed with postcolumn addition of ammonium acetate.

The TSP total ion current trace (mass range 450–900 u) coincided well with the UV trace at 208 nm (Fig. 7). Each peak on these chromatograms corresponded to a saponin. Retention times were confirmed by injection of pure material. The TSP spectra acquired on-line for each saponin (*e.g.*, saponins **A** and **D** in Fig. 8) displayed strong $[M+H]^+$ quasi-molecular peaks, together with adduct species such as $[M+CH_3CN+NH_4]^+$, confirming their molecular masses.

Fragmentation of the sugar moiety was observed and peaks corresponding to the loss of one (mono- and diglycosides) and then two sugars (diglycosides) were present. For example, in the spectrum of saponin **D** (Fig. 8), the peaks at m/z 718 $[(M+CH_3CN+NH_4)-162]^+$ and *m/z* 660 $[(M+H)-162]^+$ accounted for the elimination of the terminal galactosyl moiety. In addition, an important peak $[A+H]^+$ {or $[(M+H)-162-203]^+$} for the aglycone was visible in these spectra.

All the structural information provided on-line by the LC–TSP-MS technique, *i.e.*, molecular

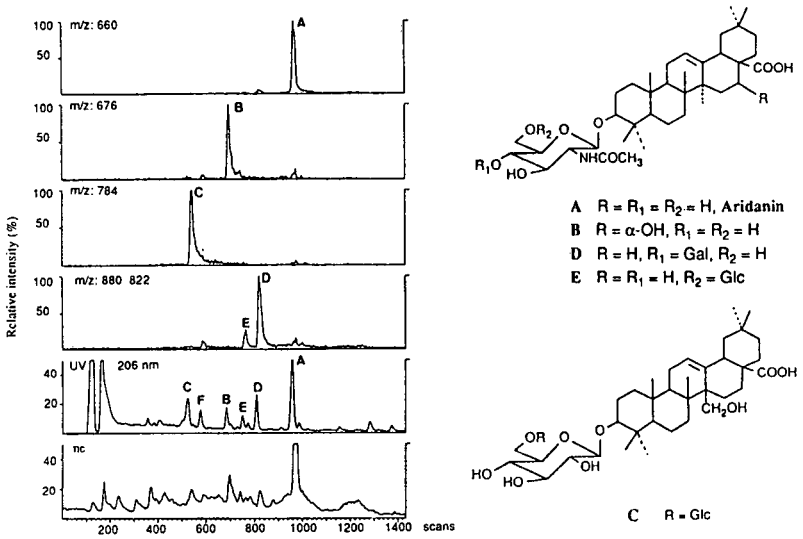

Fig. 7. LC–TSP-MS analysis of the methanolic extract from the fruits of *Tetrapleura tetraptera*. Column, μBondapak C_{18}; eluent, CH_3CN–H_2O gradient from 30:70 to 80:20 in 30 min; flow-rate 1 ml/min; detection, UV at 206 nm; TSP vaporizer, 100°C; source, 270°C; filament off; buffer, 0.5 *M* CH_3COONH_4, at 0.2 ml/min, 1.5 s per scan.

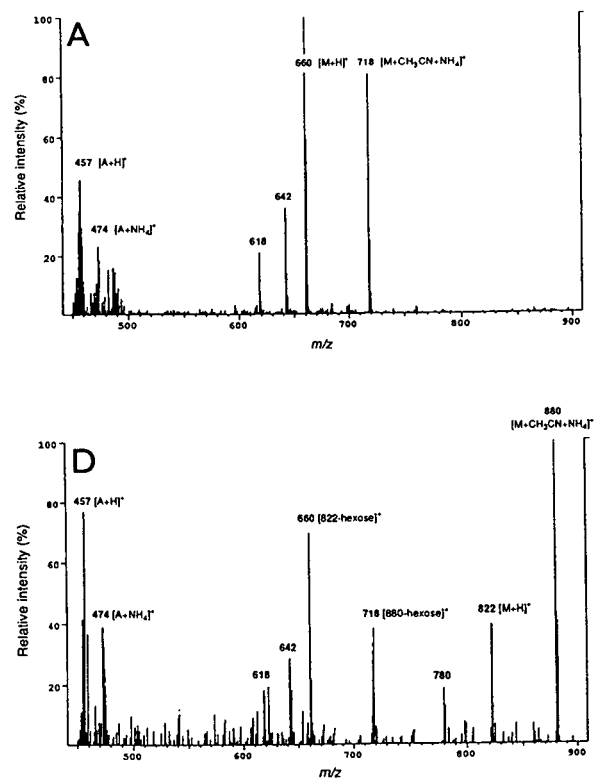

Fig. 8. TSP mass spectra of saponins **A** and **D** obtained after on-column analysis of the methanolic extract of *Tetrapleura tetraptera*. Conditions as in Fig.6.

mass, number, nature and sequence of the sugars and molecular mass of the aglycone, are of great help in structure elucidation processes.

CONCLUSIONS

The coupling of LC and MS has not yet been widely used in phytochemical analysis. However, some encouraging results have already been obtained with the TSP interface. Qualitative information (including molecular mass and fragmentation pattern) on the detected peak are provided by this technique. In addition, when all the ionization parameters are optimized and well stabilized, semi-quantitative analyses can be performed, and low limits of detection, comparable to those obtained by GC–MS, for example, are obtained.

For all these reasons, LC–TSP-MS is very useful for different applications, such as the detection of known compounds in crude plant extracts, the determination of trace compounds in complex mixtures and the identification of unknown products in extracts.

The LC–TSP-MS offers an additional instrumental technique to the modern phytochemi-

cal laboratory. It is relatively simple to use, and therefore will find many applications in routine analysis.

ACKNOWLEDGEMENTS

Financial support was provided by the Swiss National Science Foundation, the Association of Swiss Pharmacy and the Mediplant Foundation.

REFERENCES

1 M. Hamburger and K. Hostettmann, *J. Pharm. Biomed. Anal.*, 7 (1989) 1337.
2 B.Y. Taillez, *Trends Anal. Chem.*, 3 (1984) 6.
3 K.-H. Kubeczka and W. Herres, *GIT Fachz. Lab., Suppl.*, 4 (1984) 33.
4 S.A. George and A. Mante, *Chromatographia*, 15 (1982) 419.
5 W.M. Niessen and J. Van der Greef, *Liquid Chromatography–Mass Spectrometry* (*Chromatographic Series*, Vol. 58), Marcel Dekker, New York, 1992, pp. 3–57.
6 K. Hostettmann, B. Domon, D. Schaufelberger and M. Hostettmann, *J. Chromatogr.*, 283 (1984) 137.
7 J.-L. Wolfender, M. Hamburger, K. Hostettmann, J.O. Msonthi and S. Mavi, *J. Nat. Prod.*, 56 (1993) 682.
8 P. Arpino, *Fresenius' J. Anal. Chem.*, 337 (1990) 667.
9 A.P. Bruins, *Methodol. Surv. Biochem. Anal.*, 18 (1988) 339.
10 T.-M Chen, R.C. George, J.L. Weir and T. Leapheart, *J. Nat. Prod.*, 53 (1990) 359.
11 C. Giroud, T. Van des Leer, R. Van der Heijden, R. Verpoorte, C.E. Heeremans, W.M. Niessen and J. Van der Greef, *Planta Med.*, 57 (1991) 142.
12 E. Schroeder and I. Merfort, *Mass Spectrom.*, 20 (1991) 11.
13 E.J. Corey, M.-C. Kang, M.C. Desai, A.K. Ghosh and I.N. Houpis, *J. Am. Chem. Soc.*, 110 (1988) 649.
14 P. Braquet, L. Touqui, T.-S. Shen and B.B Vargaftig, *Pharmacol. Rev.*, 39 (1987) 97.
15 B. Meier, A. Hasler and B. Keller, *Planta Med.*, 55 (1989) 639.
16 N. Chauret, J. Carrier, M. Mancini, R. Neufeld, M. Weber and J. Archambault, *J. Chromatogr.*, 588 (1991) 281.
17 D.L. Klayman, *Science*, 228 (1985) 1049.
18 H.M. Fales, E.A. Sokoloski, L.K. Pannel, Q.-L. Pu, D.L. Klayman, A.J. Li, A. Brossi and J.A. Kelley, *Anal. Chem.*, 62 (1990) 2494.
19 J.K. Rupprecht, Y.-H. Hui and J. McLaughlin, *J. Nat. Prod.*, 53 (1990) 237.
20 X.-P. Fang, M.J. Rieser, Z.-M. Gu, G.-X. Zhao and J.L. McLaughlin, *Phytochem. Anal.*, 4 (1993) 27.
21 A. Alkofahi, J.K. Rupprecht, Y.-M. Liu, C.-J. Chang, D.L. Smith and J.L. McLaughlin, *Experientia*, 46 (1990) 539.
22 F. Cepleanu, K. Ohtani, M. Hamburger, M.P. Gupta, P. Solis and K. Hostettmann, *Helv. Chim. Acta*, 76 (1993) 1379.
23 M. Maillard and K. Hostettmann, *J. Chromatogr.*, 647 (1993) 137.
24 K. Hostettmann and A. Marston, in K.E Mott (Editor), *Plant Molluscicides*, Wiley, Chichester, 1987, pp. 299–321.
25 M. Maillard, C.O. Adewunmi and K. Hostettmann, *Helv. Chim. Acta*, 72 (1989) 668.

Journal of Chromatography, 647 (1993) 155–166
Elsevier Science Publishers B.V., Amsterdam

CHROMSYMP. 2795

Investigation into lacidipine and related metabolites by high-performance liquid chromatography–mass spectrometry

Paolo Rossato, Marina Scandola* and Pietro Grossi

Drug Metabolism Department, Research Laboratories, Glaxo S.p.A., Via Fleming 4, 37135 Verona (Italy)

ABSTRACT

HPLC–MS methods were developed in order to characterize the main biotransformation products of lacidipine, a new antihypertensive drug. Thermospray and particle beam interfaces were used because of their complementary information. In fact, the former provided molecular mass indication, while PB allowed the acquisition of typical electron impact and chemical ionization spectra. Chemical ionization was performed with methane and isobutane as reagent gases. This paper describes the application of these techniques for the analysis of lacidipine and standard metabolites and their identification in biological fluids.

INTRODUCTION

Lacidipine (Fig. 1) is a dihydropyridine derivative [1] that has been developed as an antihypertensive drug [2]. As shown in Fig. 1, the main phase I metabolic routes consist of the oxidation of the dihydropyridine ring to pyridine (compounds **B**, **D**, **F**, **G** and **H**) and the hydrolysis of the ester moieties (compounds **C**, **D**, **E** and **F**). Further phase I metabolic pathways involve the hydroxylation of the methyl groups (compound **G**) and the formation of lactones (compound **H**).

Lacidipine is administered orally in relatively low doses (2–6 mg/day) [3] and, in order to study its metabolic profile, it has been necessary to develop a sensitive and specific method for the assay of the parent drug and its metabolites in biological fluids. Mass spectrometry plays an important role in the structural elucidation and determination of substituted dihydropyridines at a low level. Electron impact (EI) [4], chemical ionization (CI) [5] and fast atom bombardment (FAB) [6] were previously used to investigate lacidipine and related compounds. For other dihydropyridines, combined techniques (GC–MS [7–14] and LC–MS [15,16]) have also been used to analyse biological fluids. For lacidipine and its metabolites, HPLC–MS methods were developed by using thermospray (TSP) and particle beam (PB) interfaces. The characterization of the metabolites by TSP-MS and PB-MS is described, including an example of the application of TSP-MS for the identification of the main metabolite in rat plasma.

EXPERIMENTAL

The HPLC–MS system comprised a Model 1090A solvent-delivery system (Hewlett Packard, USA), a Model Uvidec-100 UV detector (Jasco, Japan) and a Model 5988A single quadrupole mass spectrometer (Hewlett-Packard), equipped with a thermospray or a Model 59980A particle beam interface (Hewlett-Packard).

Lacidipine and its standard metabolites were synthesized by Chemical Development, Glaxo Research Laboratories (Verona, Italy) [1]. Stock solutions of standard compounds in methanol were prepared at a concentration of about 1

* Corresponding author.

0021-9673/93/$06.00

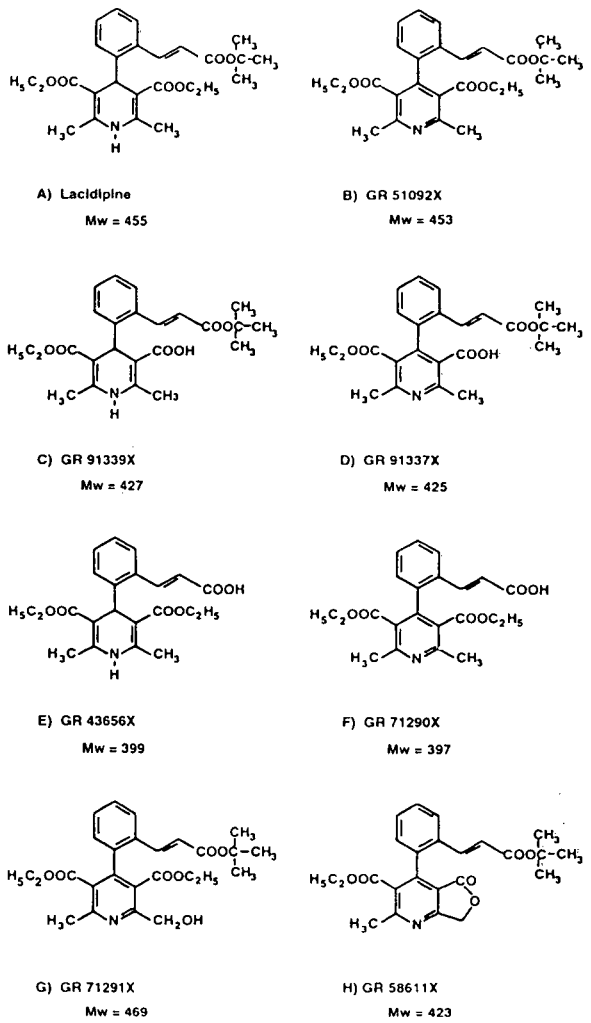

Fig. 1. Structures of lacidipine and investigated metabolites. Mw = Molecular mass.

mg/ml. They were diluted with the mobile phase just before injection.

HPLC–TSP-MS conditions for standard metabolites

Mobile phase for thermospray HPLC–MS consisted of 0.05 *M* ammonium acetate (pH 6.2)–methanol–acetonitrile (55:35:10, v/v/v). The flow-rate was 1.2 ml/min and the injection volume was 100 μl.

The thermospray interface was operated with probe temperatures set at 100°C (stem) and 162–164°C (tip). The source was maintained at 275°C, with the analyser manifold pressure of $2.6 \cdot 10^{-6}$ Torr (1 Torr = 133.322 Pa). The measurements were performed in the "filament-on" acquisition mode, in both positive- and negative-ion conditions. The electron multiplier was set at 2800 V and the scan range was 300–600 mass units.

HPLC–PB-MS conditions for standard metabolites

Mobile phase (flow-rate 0.4 ml/min) consisted of acetonitrile–water (75:25, v/v). The sample volume injected was 100 μl.

The particle beam interface was operated with the desolvation chamber temperature set at 70°C, the second momentum separator pressure at 0.6 Torr and the helium inlet pressure at 30 p.s.i. (1 p.s.i. = 6894.76 Pa).

For EI measurements the source temperature was maintained at 250°C, and for CI at 200°C. The reagent gases used for CI were methane and isobutane. Mass spectra were obtained in both positive- and negative-ion mode with source pressure of 0.3 Torr and manifold pressure of $1.1 \cdot 10^{-4}$ Torr when methane was used, while for isobutane the two pressures were 0.45 and $1.6 \cdot 10^{-4}$ Torr, respectively.

HPLC–TSP-MS conditions for plasma samples

A column-switching technique was used for the direct injections of rat plasma samples.

The loop of a Model 7125 manual injection valve (Rheodyne) was substituted by a 30 × 4.6 mm precolumn packed with Spherisorb RP-18 30–40 μm silica (Merck), which was conditioned with 3 ml of methanol and 3 ml of water before each injection.

Rat plasma (0.5–1.0 ml) was diluted before injection with an equal volume of 20% acetonitrile in water and 100 μl of concentrated formic acid. After each injection the precolumn was washed with 3 ml of water, then backflushed by valve switching into a 100 × 4.6 mm Novapack analytical column (Waters) maintained at 50°C.

Gradient elution was performed at 1.2 ml/min flow-rate with a mobile phase consisting of methanol, acetonitrile and aqueous ammonium acetate (0.05 *M*, pH 5), the compositon of which varied according to Table I.

The thermospray interface was operated with

TABLE I

CHROMATOGRAPHIC CONDITIONS FOR HPLC–MS ANALYSIS OF RAT PLASMA SAMPLES

Column, 100 × 4.6 mm Novapack (Waters); precolumn, 30 × 4.6 mm, Perisorb RP-18, 30–40 μm (Merck); mobile phase, Ammonium acetate (0.05 *M*, pH 5.0) in a mixture of methanol, acetonitrile and water; flow-rate, 1.2 ml/min; temperature, 50°C; UV detector wavelength, 282 nm; injection volume, 100 μl.

Time (min)	Methanol (%)	Acetonitrile (%)	Water (%)
0	35	10	55
7	35	10	55
30	60	10	30
35	80	10	10
45	80	10	10
70	35	10	55

the probe temperatures initially set at 102°C (stem) and 162–164°C (tip) for 7 min, then gradually changed according to a linear gradient up to 98°C (stem) and 150–152°C (tip) at 30 min. The mass spectrometer source was maintained at 275°C with the filament on and the measurements were performed in positive-ion conditions. The other MS conditions were the same as reported in the previous section.

RESULTS AND DISCUSSION

Thermospray

Positive and negative thermospray mass spectra of lacidipine are reported in Fig. 2. The base peak was assigned as the adduct ion $[M + NH_4]^+$, *m/z* 473, whereas a low-intensity peak was observed for the protonated molecular ion, *m/z* 456. The presence in the mobile phase of acetonitrile and ammonium acetate led to the formation of an adduct ion at *m/z* 514, ascribed to $[M + CH_3CN + NH_4]^+$, [17]. In the negative-ion spectra, molecular ion, *m/z* 455, and deprotonated $[M - H]^-$ ion, *m/z* 454, were both present. These ionic species are originated by two mechanisms —electron attachment and deprotonation— both present in thermospray ionization.

The molecular ions and the related adducts of metabolites in positive- and negative-ion spectra are reported in Table I. The base peak in the positive-ion TSP spectra of three pyridine derivatives was the protonated molecular ion, $[MH]^+$, whereas for the dihydropyridine it was the adduct ion $[M + NH_4]^+$. In negative-ion TSP mass spectra, the ionic species $[M + OAc]^-$ were assigned as the adducts with the acetate of the mobile phase.

The positive-ion TSP mass spectra of compounds **G** and **H**, the hydroxylated and the lactone metabolite, respectively, are reported in Fig. 3. For metabolite **H** the protonated molecular ion (*m/z* 424) and two adduct ions ($[M + NH_4]^+$ and $[M + CH_3CN + NH_4]^+$) were observed. The two fragment ions at *m/z* 368 and 385 can be ascribed to the cleavage of the *tert.*-butyl ester moiety (*m/z* 368 = $[MH - C(CH_3)_3 + H]^+$ and its ammonium adduct ion (*m/z* 385 = $[MH - C(CH_3)_3 + NH_4]^+$).

For metabolite **G**, the protonated molecular ion (*m/z* 470) and the adduct $[M + CH_3CN + NH_4]^+$ (*m/z* 528) were present. The other fragments corresponded to the ionic species previously described for the lactone metabolite **H** (*m/z* 368, 385, 424, 441 and 482). This was probably due to the condensation of side chains ($-COOC_2H_5$ and $-CH_2OH$) of metabolite **G** with loss of ethanol caused by the operating high temperatures.

Particle beam

Electron impact. Additional structural information was obtained from particle beam mass spectra. The electron impact mass spectrum of lacidipine is shown in Fig. 4(a). The molecular ion abundancy was very low (*m/z* 455, 2%), while the fragment ions related to cleavages of the side chains were observed. Radical losses of $\cdot C(CH_3)_3$, $\cdot OC(CH_3)_3$ and $\cdot COOC(CH_3)_3$ produced the ionic species at *m/z* 398, 382 and 354 already described [4]. The base peak, at *m/z* 252, is generated by elimination of *tert.*-butyl cinnamate (see structure in Fig. 4a).

The other compounds showed a similar behaviour and the mass spectra were in agreement with those previously obtained by direct probe introduction [4]. The base peaks included the

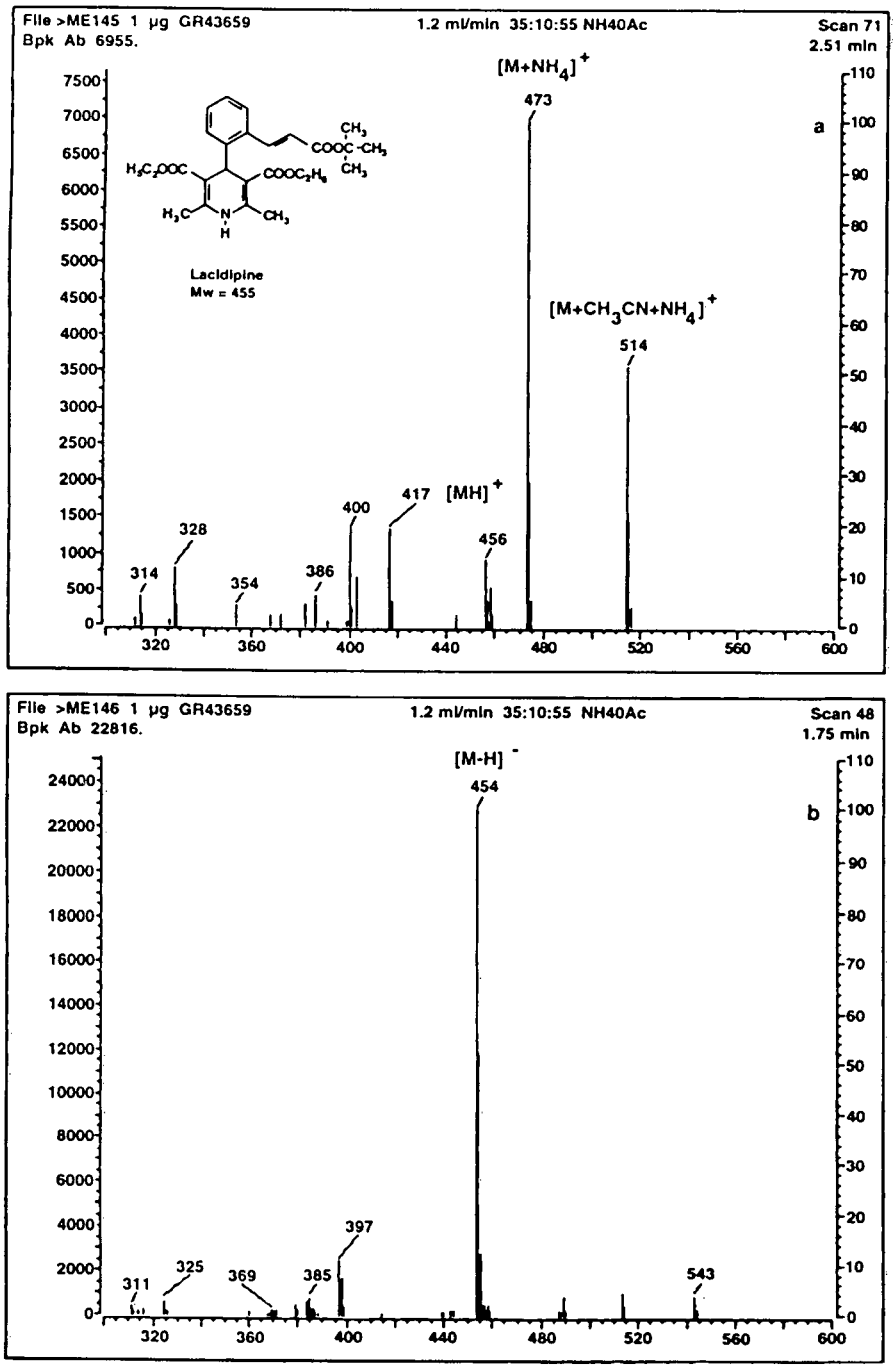

Fig. 2. Thermospray mass spectra of lacidipine: (a) positive-ion mode; (b) negative-ion mode.

pyridine ring but they were generated by different fragment ions.

It is noteworthy that the EI mass spectra of compounds **G** and **H** (Fig. 4b and c) were almost superimposable. For compound **G** the neutral loss of CH_3CH_2OH and the condensation to lactone was the primary reaction, followed by a fragmentation pathway similar to compound **H**. By PB-EI it was not possible to distinguish these two metabolites.

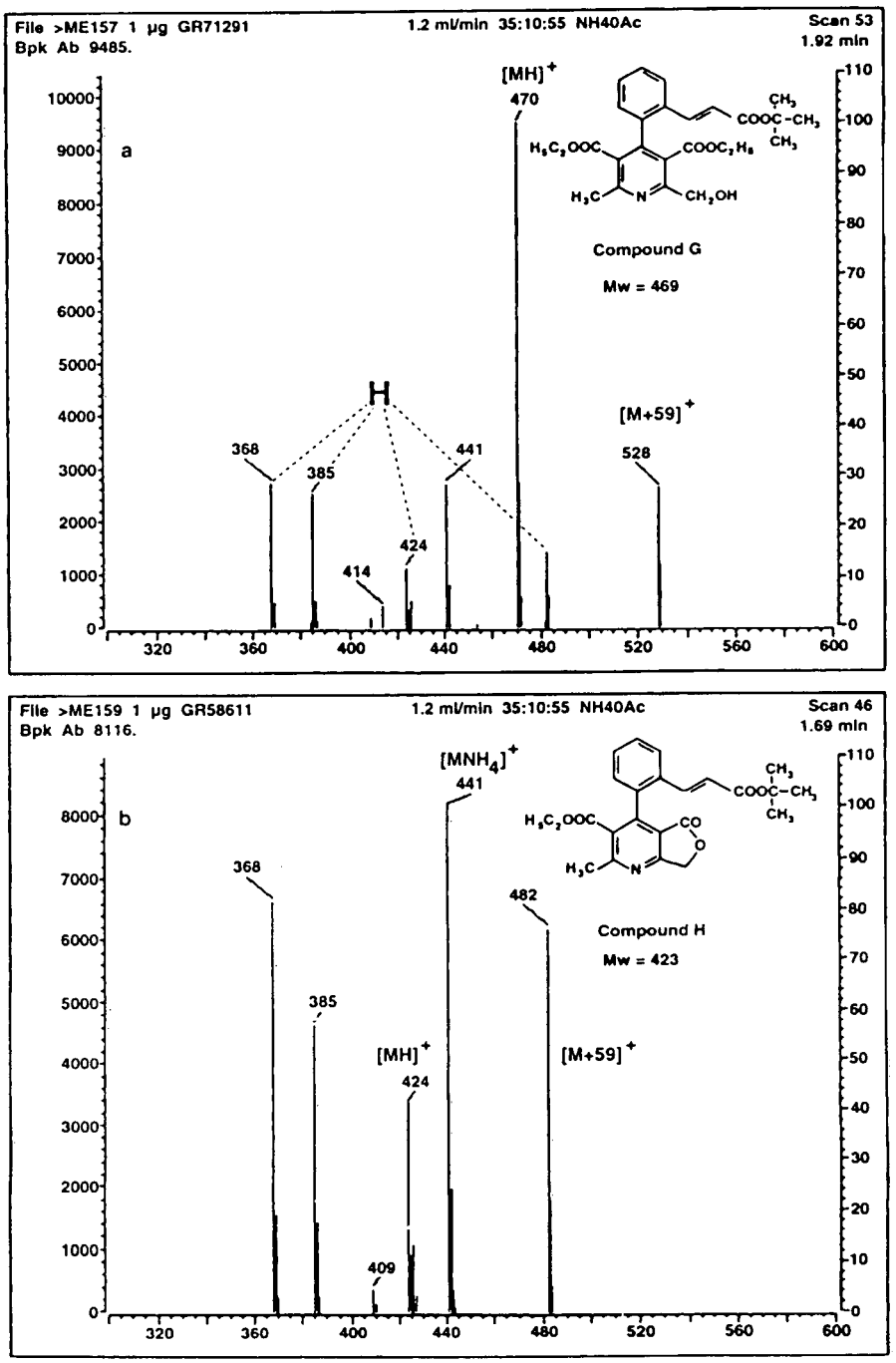

Fig. 3. Thermospray positive-ion mass spectra of metabolites **G** and **H**.

Chemical ionization. PB-CI-MS-measurements were performed using two reagent gases: methane and isobutane. The *methane* CI^+ mass spectra of lacidipine and metabolites **G** and **H** are shown in Fig. 5a, b and c. An intense fragmentation was observed for all the analysed compounds. In the lacidipine spectrum (Fig. 5a) the base peak was the fragment ion at *m/z* 354, which was assigned as $[MH - CH_2{=}C(CH_3)_2, -C_2H_5OH]^+$ and $[MH - HCOOC(CH_3)_3]^+$ ions.

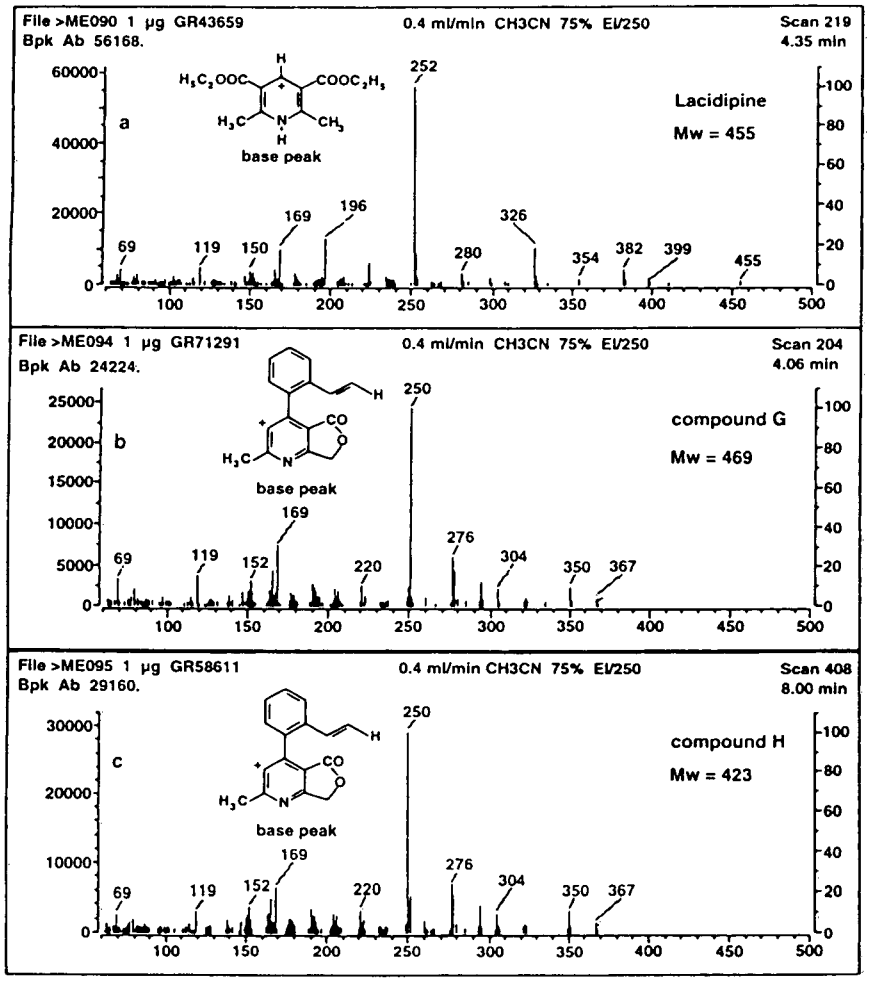

Fig. 4. PB-EI mass spectra of: (a) lacidipine; (b) compound **G**; (c) compound **H**.

Both processes were confirmed by exact mass measurements performed on a ZAB-2F double-focusing instrument [5]. The protonated molecular ion was observed at m/z 456 and the product of addition with reagent gas, $[M + C_2H_5]^+$, was at m/z 484.

For compound **G** (Fig. 5b) the protonated molecular ion was not detectable and, as already observed in the PB-EI mass spectrum, its cyclization to lactone was the preferred reaction. The mass spectra of the two compounds, **G** and **H**, were similar. The base peak at m/z 350 was attributed to $[MH - HOC(CH_3)_3]^+$ and/or $[MH - HCOOC_2H_5]^+$. The second most intense peak in both spectra at m/z 368 was assigned as the $[MH - C(CH_3)_3 + H]^+$ ion.

Methane negative-ion CI mass spectra of these compounds are shown in Fig. 6. The molecular ions of lacidipine and compound **H**, generated by electron attachment, were observed as base peaks at m/z 455 and 423, respectively. For compound **G** the molecular ion was observed at m/z 469, although at a very low relative abundance (1%). The other signals in the mass spectrum (Fig. 6b) were the same as for the lactone (Fig. 6c).

Isobutane positive-ion CI mass spectra of compounds **G** and **H** are reported in Fig. 7b and 7c.

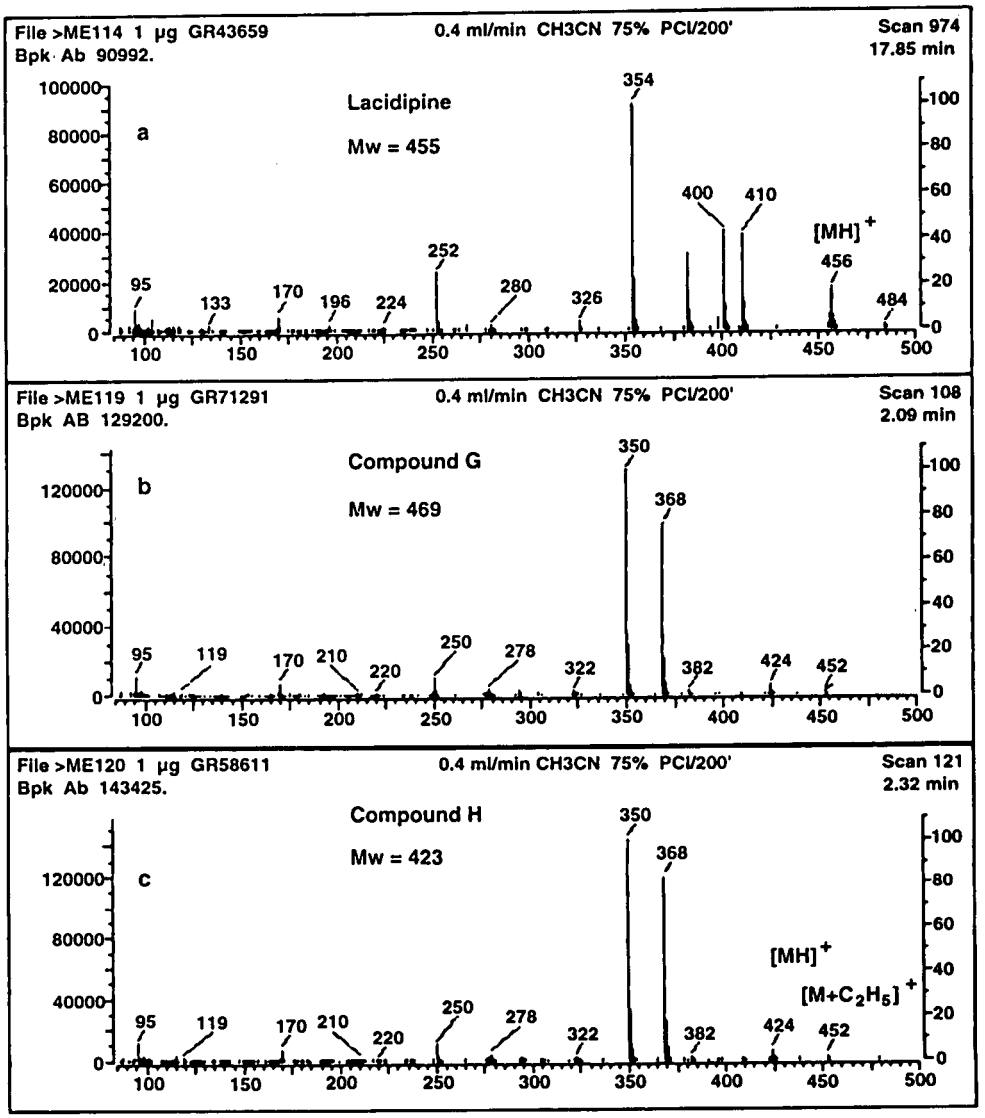

Fig. 5. PB-CI in methane, positive-ion mode, mass spectra: (a) lacidipine; (b) compound G; (c) compound H.

A very weak protonated molecular ion was present for compound **H** and the two more abundant peaks at m/z 350 and 368 were the same as PB-CI$^+$ spectra with methane (Fig. 5c). Also, for lacidipine (Fig. 7a) a close resemblance with the mass spectrum in methane was observed.

A similar behaviour as with methane was observed in the negative-ion mode CI with isobutane.

Identification of lacidipine metabolite in rat plasma

HPLC–TSP-MS was also used for the identification of a lacidipine metabolite in rat plasma. The profile of metabolites in the plasma of rats administered a 2.5 mg/kg oral dose of [2,6-^{14}C] lacidipine has already been described [18]. The metabolic pathways involve as a preliminary step the hydrolysis of ethyl and *tert.*-butyl ester moieties or, alternatively, the oxidation of the

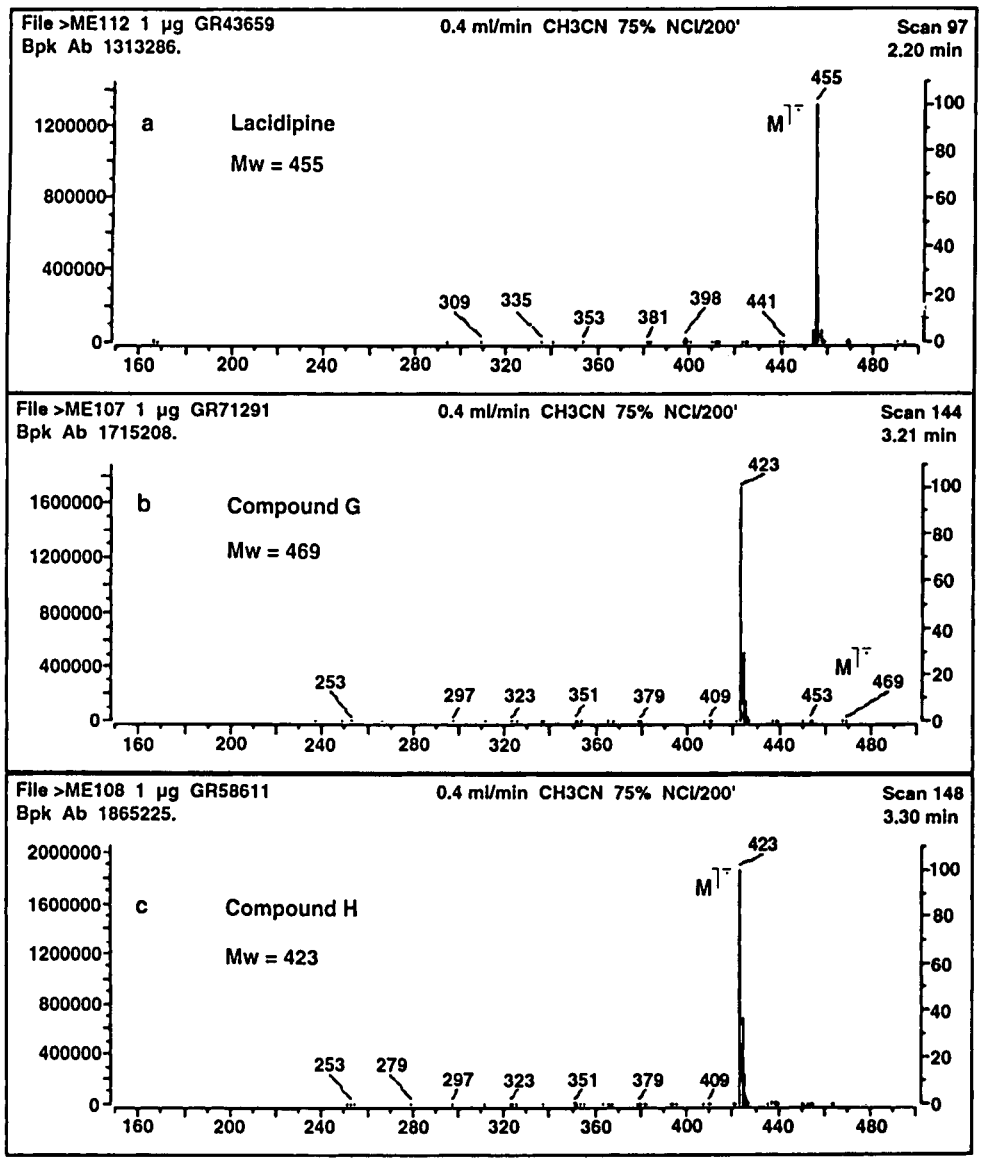

Fig. 6. PB-CI in methane, negative-ion mode, mass spectra: (a) lacidipine; (b) compound **G**; (c) compound **H**.

heterocyclic ring to pyridine. A full thermospray mass spectrum was obtained only for the main metabolite, which is formed by hydrolysis of the ethyl ester moiety and maintains an intact dihydropyridine ring. In Fig. 8 TSP-MS measurements of a rat plasma sample are reported. The total ion chromatogram (Fig. 8a) shows, in addition to the main metabolite peak, several other peaks related to plasma matrix compounds. The mass spectrum of the metabolite, reported in Fig. 8b, was in agreement with that of standard compound **C** (the relative abundances of its $[MH]^+$ species and the adducts ions are reported in Table II). The base peak at m/z 384 was ascribed to the decarboxylation reaction $[MH - CO_2]^+$. The main peaks in the spectra showed

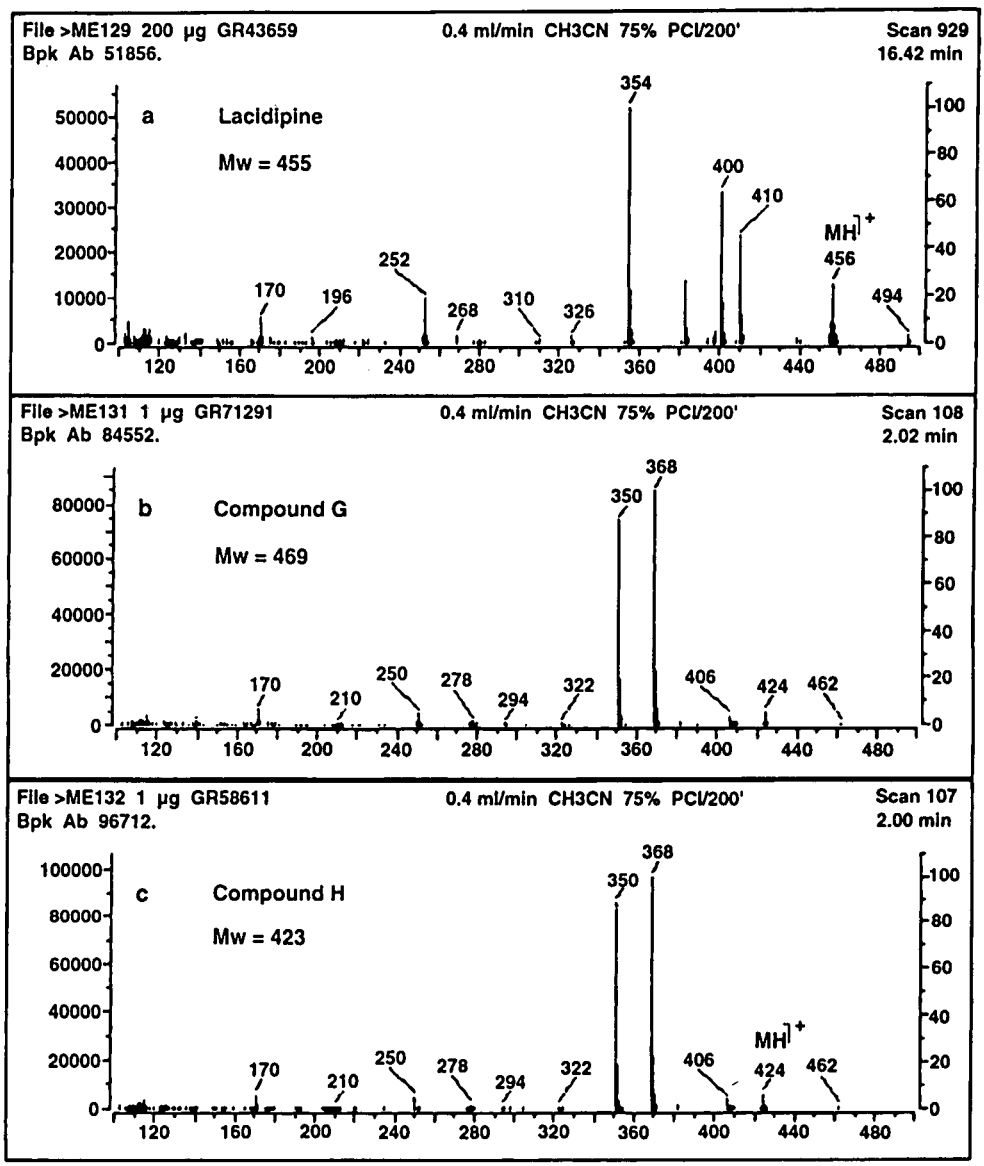

Fig. 7. PB-CI in isobutane, positive-ion mode, mass spectra: (a) lacidipine; (b) compound **G**; (c) compound **H**.

the isotopic cluster, due to ^{14}C-labelled lacidipine.

CONCLUSIONS

Mass spectra obtained by HPLC–MS with thermospray and particle beam interfaces and different ionization techniques (EI and CI) were compared to determine a system suitable for the analysis of lacidipine and its metabolites. This was performed by thermospray HPLC–MS, in fact particle beam mass spectra in either electron impact or chemical ionization mode of two metabolites (compounds **G** and **H**) were not distinguishable.

The thermospray interface was used for the

TABLE II

RELATIVE INTENSITIES OF (PSEUDO)MOLECULAR IONS AND ADDUCT IONS IN TSP (POSITIVE AND NEGATIVE ION MODE)

Ionic species (rel.ab.%)		Compound							
		A (lacidipine)	**B**	**C**	**D**	**E**	**F**	**G**	**H**
TSP^+	$[MH]^+$	456 (12%)	454 (100%)	428 (10%)[a]	426 (100%)	400 (28%)	398 (100%)	470 (100%)	424 (40%)
	$[M + NH_4]^+$	473 (100%)	–	445 (45%)	–	417 (100%)	–	–	441 (100%)
	$[M + CH_3CN + NH_4]^+$	514 (50%)	512 (30%)	486 (20%)	484 (30%)	458 (48%)	456 (16%)	528 (30%)	482 (78%)
TSP^-	$[M]^{-\cdot}$	455 (50%)	453 (100%)	427 (60%)	425 (100%)	399 (88%)	397 (80%)	469 (100%)	423 (100%)
	$[M - H]^-$	454 (100%)	–	426 (100%)	424 (78%)	398 (100%)	396 (100%)	–	–
	$[M + CH_3COO]^-$	–	–	486 (10%)	–	458 (22%)	456 (50%)	–	–

[a] Base peak in TSP^+ is the fragment ion at m/z 384, $[M - CO_2]^+$.

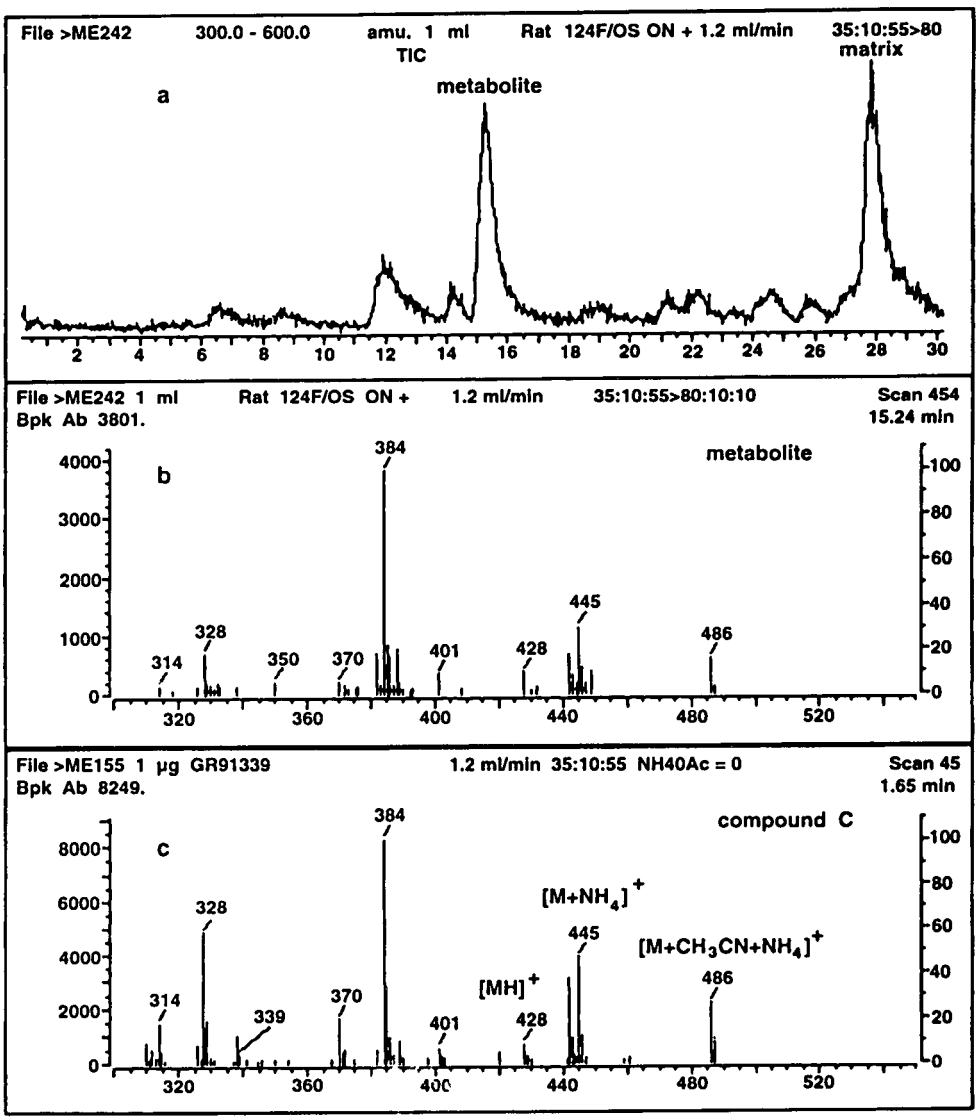

Fig. 8. HPLC–TSP-MS measurements of a rat plasma sample. (a) Total ion current (TIC) chromatogram. (b) Mass spectrum of the peak eluting at 15.2 min. (c) Mass spectrum of compound C standard.

identification of lacidipine metabolites in biological fluids as shown by the HPLC–TSP-MS analysis performed to elucidate the structure of the main metabolite in rat plasma.

REFERENCES

1 C. Semeraro, D. Micheli, D. Pieraccioli, G. Gaviraghi and A.D. Borthwick, *UK Pat.*, GB 2 164 336 B (March 19, 1986).
2 D. Micheli, A. Collodel, C. Semeraro, G. Gaviraghi and C. Carpi, *J. Cardiovasc. Pharmacol.*, 15 (1990) 666.
3 M. Perelman, *J. Cardiovasc. Pharmacol.*, 17, Suppl. 4 (1991) 14.
4 M. Scandola, G. Tarzia and G. Gaviraghi, *Ann. Chim.*, 82 (1992) 193.
5 M. Hamdan, M. Scandola, D. Franchi, G. Gaviraghi and G. Tarzia, *Organic Mass Spectrom.*, 27 (1992) 240.
6 M. Hamdan, M. Scandola, D. Franchi, G. Gaviraghi and G. Tarzia, *Rapid Commun. Mass Spectrom.*, 5 (1991) 493
7 S. Higuchi and S. Kawamura, *J. Chromatogr.*, 223 (1981) 341.

8 Y. Umeno, E. Matsushima, M. Maniwa and T. Marunaka, *J. Chromatogr.*, 434 (1988) 123.
9 T. Takano and S. Hata, *Biomed. Environ. Mass Spectrom.*, 17 (1988) 477.
10 Y. Tokuma, T. Fujiwara and H. Noguchi, *Biomed. Environ. Mass Spectrom.*, 13 (1986) 251.
11 Y. Tokuma, T. Fujiwara and H. Noguchi, *Shitsuryo Bunsekii*, 33 (1985) 221.
12 Y. Tokuma, T. Fujiwara and H. Noguchi, *J. Chromatogr.*, 345 (1985) 51.
13 S. Higuchi and S. Kawamura, *J. Chromatogr.*, 223 (1991) 341.
14 O. Beck and T. Ryman, *J. Chromatogr.*, 337 (1985) 402.
15 A.P. Beresford, P.K. Macrae. D. Alker and R.J. Kobylecki, *Arzneim.-Forsch./ Drug Res.*, 39(2) (1989) 201.
16 L. Prokai, B.H. Hsu, H. Farag and N. Bodor, *Anal. Chem.*, 61(15) (1989) 1723.
17 P. Rossato, M. Scandola, F. Pugnaghi and P. Grossi, *Organic Mass Spectrom.*, 27 (1992) 1261.
18 P. Grossi and P. Rossato, in E. Reid and I. Wilson (Editors), *Methodological Surveys in Biochemistry and Analysis*, vol. 22, Royal Chemical Society, Cambridge, 1992.

Journal of Chromatography, 647 (1993) 167–181
Elsevier Science Publishers B.V., Amsterdam

CHROMSYMP. 2812

Determination of penicillin G, ampicillin, amoxicillin, cloxacillin and cephapirin by high-performance liquid chromatography–electrospray mass spectrometry

Rolf F. Straub and Robert D. Voyksner*

Analytical and Chemical Sciences, Research Triangle Institute, P.O. Box 12194, Research Triangle Park, NC 27709 (USA)

ABSTRACT

This report contributes to a preliminary investigation of high-performance liquid chromatographic (HPLC)–mass spectrometric (MS) methods for confirming β-lactam antibiotic residues in bovine milk. Initial work for each antibiotic evaluated the collisional activated dissociation (CAD) spectra that could be generated between the capillary and skimmer in the electrospray (ESP) interface. The drugs show various characteristic fragmentation, mostly within the β-lactam ring and the amide group. Response for a particular compound in a given solvent can vary drastically. Usually, the more organic component in the solvent, the higher the ESP response. In many cases use of acetonitrile also results in slightly better ion currents than for methanol when comparing equal percentages of either organic solvent in water. The ESP response of most of the tested antibiotics can be enhanced by the addition of formic acid or acetic acid to the mobile phase methanol–water (1:1). In general, the negative ion spectra are lower in intensity, exhibiting an $[M-H]^-$ ion and producing less fragmentation at higher CAD voltages as compared to positive ion spectra. An isocratic reversed-phase HPLC method for the separation of a mixture of five common β-lactam antibiotics was developed using acetic acid as a mobile phase additive and optimized for detection with a new ESP HPLC–MS interface. A post-column split ratio of 70:1 for the eluent from a 150 × 2 mm I.D. column was chosen to provide the required lower flow-rate (approximately 4 μl/min). The limit of detection for the simultaneous determination of these antibiotics was estimated to be 100 ppb. Electrospray HPLC–MS could be used to confirm these antibiotics for quantities down to about 100 pg entering the mass spectrometer. Multiresidue analysis with microbore HPLC–ESP-MS has the advantage that no post-column splitting of the eluent is required and all of the analyte (on-column injected) will be transferred into the ESP interface. Preliminary work showed good mass spectrometric sensitivity down to the level of regulatory interest, but chromatographic separation efficiency must be improved.

INTRODUCTION

Some penicillins and cephalosporins were produced semi-synthetically and represent an interesting class of β-lactam antibiotics because of their broad antimicrobial activity against both gram-positive and gram-negative organisms [1,2]. Penicillines contain bulky side-chains attached to a 6-aminopenicillanic acid nucleus (sulfur-containing thiazolidine ring fused to a β-lactam ring) and are degradable in presence of solvents [3] or by heat [4]. Acid labile penicillins are rapidly inactivated at an acid pH. Additionally, all penicillins are rapidly inactivated at an alkaline pH in the presence of carbohydrates. Cephalosporin structures are based on the 7-aminocephalosporinic acid nucleus (condensed dihydrotiazole ring in its skeleton) and are generally stable in acidic media as well as in presence of penicillinase [5]. Many efforts have been made to synthesize cephalosporins with different physico-chemical properties (mainly liposolubility) by variation of substituents [6]. Table I lists the chemical structures of β-lactam antibiotics discussed in this paper. They are commonly used as bacterial agents in excessive livestock farming and bovine milk production. The Food and Drug

* Corresponding author.

0021-9673/93/$06.00

TABLE I

IDENTITY OF CAD FRAGMENTS–POSITIVE ION MS OPERATION

M_r = Molecular mass of the free acid drug; CAD voltage = voltage measured at the end of the capillary (Analytica QBV 25-AL electrospray interface); m/z = mass-to-charge ratio (relative intensity of the peak in %, type of fragment); F_x, F_y, F_z, F_1, F_2, F_3, and F_4 = different collisional activated dissociation (CAD) fragments seen in the ESP spectra.

Drug (M_r)	CAD voltage	m/z (relative intensity and tentative identification of CAD fragments)
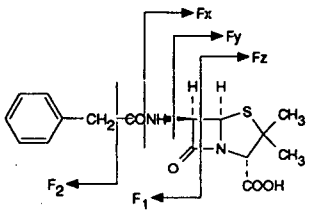	80	392 (54); 391 (51, $[M + K + H_2O]^+$); 367 (93, $[M + H + MeOH]^+$); 353 (41, $[M + H + H_2O]^+$); 335 (41, $[M + H]^+$); 309 (8); 279 (25); 176 (43, $[F_1 + H]^+$); 167 (33); 160 (49, $[F_z + H]^+$); 149 (14); 114 (25, $[F_z - COOH]^+$); 65 (43, $[2MeOH + H]^+$)
	160	367 (27, $[M + H + MeOH]^+$); 335 (7, $[M + H]^+$); 217 (4, $[F_x + H]^+$); 202 (3, $[F_y + H]^+$); 176 (21, $[F_1 + H]^+$); 160 (37, $[F_z + H]^+$); 149 (100); 121 (14); 114 (4, $[F_z - COOH]^+$); 93 (19); 91 (15, $[F_2]^+$); 70 (14); 57 (18)[a]; 52 (36)[a]
Penicillin G (334.4)		
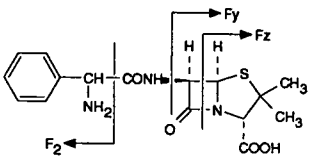	80	382 (18, $[M + H + MeOH]^+$); 350 (100, $[M + H]^+$); 65 (16, $[2MeOH + H]^+$)
	160	350 (89, $[M + H]^+$); 192 (24); 174 (20, $[F_y + H - CO]^+$); 160 (22, $[F_z + H]^+$); 114 (89, $[F_z - COOH]^+$); 108 (8); 106 (100, $[F_2]^+$)
Ampicillin (349.4)		
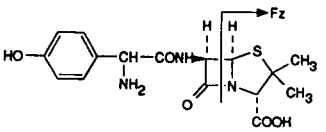	80	398 (12, $[M + H + MeOH]^+$); 367 (29); 366 (100, $[M + H])^+$; 349 (19, $[M + H - NH_3]^+$); 65 (19, $[2MeOH + H]^+$)
	160	366 (62, $[M + H]^+$); 349 (85, $[M + H - NH_3]^+$); 208 (41); 160 (6, $[F_z + H]^+$); 114 (100, $[F_z - COOH]^+$); 70 (14)
Amoxicillin (365.4)		
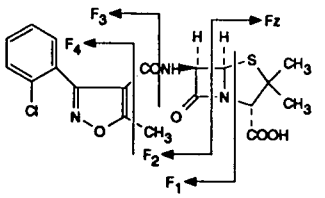	80	481 (28, $[M + 2Na]^+$); 437 (84, $[M + 2H]^+$); 436 (100, $[M + H]^+$); 148 (20); 74 (46); 65 (95, $[2MeOH + H]^+$)
	160	468 (56, $[M + H + MeOH]^+$); 454 (11, $[M + H_2O]^+$); 436 (36, $[M + H]^+$); 321 (<0.1, $[F_1 + H^+]^+$); 277 (64, $[F_2]^+$); 222 (19, $[F_3 + H]^+$); 220 (11); 178 (56, $[F_4 + H]^+$); 160 (100, $[F_z + H]^+$); 114 (68, $[F_z - COOH]^+$)
Cloxacillin (435.9)		
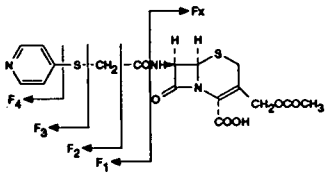	40	446 (63, $[M + Na]^+$); 424 (25, $[M + H]^+$); 413 (100, $[M - MeOH]^+$); 234 (32); 95 (8); 59 (33)[a]; 55 (36)[a]
	160	424 (45, $[M + H]^+$); 292 (41); 226 (15, $[F_x - COOH]^+$); 193 (21); 181 (26); 152 (62, $[F_1]^+$); 141 (23); 124 (59, $[F_2]^+$); 111 (62, $[F_3 + H]^+$); 79 (33, $[F_4 + H]^+$); 52 (100[a])
Cephapirin (423.4)		

[a] The indicated mass is outside the instrument's (Finnigan MAT 4500) calibration range and is probably inaccurate.

Administration (FDA) has recently indentified approximately 60 drugs which are likely residues in such animal-derived human foods and for which current analytical methodology is deficient in some way [7]. Analytical methods for β-lactam antibiotic residues provide a means of monitoring, controlling and measuring residues in animal food products.

Screening methods are often the most cost effective techniques because they use rapid sample analysis and are usually amenable to multiresidue analysis in field laboratory environments. For these reasons the detection of antibiotics in milk continues to be carried out by bioassay techniques such as microbiological tests [8], immunoassay [9,10], competitive binding [8,11,12] and enzyme inhibition [13]. With the possible exception of immunoassay, none of the screening procedures can distinguish β-lactam antibiotics from one another. Methods involving fluorescence [14] and thin-layer chromatography [15] were reported for analysis of penicillin G in milk. However, these procedures are not acceptable for current regulatory purposes. Therefore, specific chemical cleanup, separation and confirmation procedures for β-lactam antibiotics are needed for accurate identification and quantitation of suspect trace level residues in biological matrices.

Several methods using various extraction and deproteinization procedures [16] followed by high-performance liquid chromatography (HPLC) employing a variety of stationary and mobile phases for the separation have been investigated [17–23]. Ultraviolet and fluorescence detectors have been most routinely used but, where interferences have arisen, confirmation of analyte identity has been demonstrated through gas chromatography (GC)–mass spectrometry (MS) thus introducing problems associated with GC analysis [24,25]. Recently, Meetschen and Petz [26] described a method using GC for analysis of β-lactams with neutral side chains which required a time-consuming partitioning cleanup and derivatization. Confirmatory methods, whether they are a second independent quantitative analytical method based on a different methodology or highly definitive MS, ideally provide unequivocal proof of the suspected drug residue. Thermospray HPLC–MS has been successfully used to analyze non-volatile and thermally labile compounds [27–29] including several β-lactams [30–34]. Structurally different underivatived cephalosporins have been under extensive investigation by laser-induced vaporization, desorption chemical ionization, and fast atom bombardment mass spectrometry [35].

Another promising technique is atmospheric pressure ionization. Atmospheric pressure chemical ionization (APCI) forms ions in a discharge by means of chemical ionization [36–39] and electrospray (ESP) forms ions through ion evaporation in highly charged micron-size droplets [40,41]. The ESP ionization techniques is very mild and the obtained sensitivities are extremely good, although some restrictions are placed upon the conductivity and the flow rate of the mobile phase. Electrospray ion currents usually are maximized with solvents of low conductivities at flow-rates from 1 to 10 μl/min. These low flow-rates require liquid chromatography on the microbore scale to avoid post-column splitting. Recently, nanoscale capillary liquid chromatography and capillary zone electrophoresis have been successfully combined with quadrupole mass spectrometry via an ESP interface. These two microbore-scale methodologies have been applied to the separation and determination of sulfonamides commonly administered in subtherapeutic doses to promote growth in animals [42]. Very recently, the related "ion spray" technique was used for the investigation of veterinary drugs residues in bovine kidney. McLaughlin and Henion [43] applied reversed-phase ion-pair HPLC coupled with pulsed amperometry and ion spray MS to determine trace levels of four aminoglycosides.

Continuing our interest in developing new HPLC–MS methods for accurate determination of drug residues in biological matrices, we have studied the influence of different HPLC mobile phase and buffered solutions on the ionization process for β-lactam antibiotics. Both positive and negative ionization operational modes were applied to form characteristic ions. It was anticipated that several drugs requiring confirmatory procedures would exhibit only a single ion (most

commonly $[M + H]^+$ in positive and $[M - H]^-$ in negative ion operational mode) making identification difficult. Therefore, work enhancing the fragmentation through use of higher collisional activated dissociation (CAD) was used to aid in structural elucidation. For HPLC–ESP-MS analysis of a mixture of β-lactam antibiotics in milk, a post-column split ratio for 70:1 of the eluent from a 150 × 2 mm I.D. column was used to gain the required lower flow-rate for a successful ESP-MS operation.

EXPERIMENTAL

Material

Water was bidistilled and purified with a Milli-Q water system (Millipore, Bedford, MA, USA) prior to use. Methanol (MeOH), acetonitrile (MeCN) and 2-propanol (IPA) were of "HPLC/GC grade" quality (Baxter Healthcare, Muskegon, MI, USA). For mobile phase additives trifluoroacetic acid (TFA) (J. T. Baker, Marietta, GA, USA), formic acid (FOA), acetic acid (HOAc), ammonium acetate (NH_4OAc), heptafluorobutyric acid (HFBA), tetrabutylammonium hydroxide (TBAH) (Aldrich, Milwaukee, WI, USA) and ammonium hydroxide (NH_4OH) (Fisher Scientific, Rochester, NY, USA) were used. Arginine and gramicidin S from bacillus brevis (Sigma, St. Louis, MO, USA) were employed as tuning compounds in positive ion ESP-MS operation. The β-lactam antibiotic penicillin G (potassium salt), ampicillin (anhydrous), amoxicillin, cloxacillin (sodium salt) and cephapirin (sodium salt) were from Sigma. The drug standards were stored in a dry atmosphere at 4°C and were not dried or purified further before use.

Instrumentation

For flow infusion (FI) experiments a Sage 341B micro syringe pump (Sage Instruments, Division of Orion Research, Boston, MA, USA) and a 50-μl PS C-160 FN syringe for a Waters U6K injector (Dynatech Precision Sampling, Baton Rouge, LA, USA) were utilized.

The eluents used in the flow injection or separation of the drug mixture were delivered by an Isco (Lincoln, NE, USA) 100D syringe pump/pump controller Model 174262. The samples were injected with an Actuator, Model 732 with a 5-μl sample loop (Alcott Chromatography, Norcross, GA, USA) or with a Valco C14W.5 injector with a 0.5-μl sample loop (Isco) and separated on a 150 × 2 mm Ultremex 3, C_{18} column (Phenomenex, Torrance, CA, USA.) A Waters Model 484 MS tunable absorbance detector (Waters Assoc., Milford, MA, USA) was linked to the higher flow-rate port of an Acu-Rate IC-70 splitter (LC Packings International, San Francisco, CA, USA) and set to 230 nm. A Hewlett-Packard (Avondale, PA, USA) HP 3396A integrator was used to record the ultraviolet (UV) absorption chromatograms.

For small sample injections in micro-HPLC–ESP-MS determination a Valco C14W.5 injector with an internal 0.5-μl sample loop (Isco) and for larger injections a pheodyne 8125 injector with variable sample loop (Rheodyne, Cotati, CA, USA) was tested. The Rheodyne injector contributed to a larger void volume but was able to handle 1-, 5- and 30-μl injections of drug mixtures. A 15 cm × 320 μm I.D. Fusica C_{18} capillary column with a particle size of 3 μm protected by a μ-guard precolumn (LC Packings International) was connected through a 5-cm inlet capillary transfer line to the injector. The 35-cm column outlet capillary transfer line was linked to the Analytica electrospray needle. It is not recommended to directly interface the capillary column to the electrospray needle by removing the outlet capillary. This would damage the column and also increase the void volume.

An Analytica HPLC–ESP-MS interface Model QBV 25-AL (Analytica of Branford, Branford, CT, USA) was installed on a Finnigan MAT 4500 single quadrupole mass spectrometer (Finnigan MAT, San Jose, CA, USA) and used for the initial FI-CAD voltage experiments. For the FI-ESP-MS buffer studies and the negative ion ESP experiments a Analytica HPLC–ESP-MS interface, Model 100547-3, was connected to a Hewlett-Packard Engine, Model HP 5989A, single quadrupole mass spectrometer (Hewlett-Packard, Palo Alto, CA, USA). Two types of ESP needles were used with comparable results: The three layered original Analytica needle used a 50 μm I.D. stainless-steel tube to deliver

solvent, a 125 μm I.D. second layer tube to deliver an additional solvent to enhance ESP operation, especially when using high percentages of water. The third tube was used to add a gas to aid in nebulization of highly conducting or aqueous solvents. The 33-gauge Hamilton needle use a 110 μm I.D. SS-304 stainless-steel tube with a 210 μm O.D. and no second tube for additional solvent delivery (Hamilton, Reno, NV, USA). This needle was used in a cut length of 25 cm and with a 90° bevel at the tip. The same nebulization gas addition capability was maintained as with the original needle type. For all HPLC–ESP-MS determinations of the drugs a new computer controlled and more sensitive Analytica HPLC–ESP-MS interface, Model 101737 with autotune capability, was applied. For instrument control and data acquisition a Hewlett-Packard HP Vectra 80486-33 EISA personal computer/MS-DOS Chemstation software version M2.43 was utilized. Sample pH was measured with a Cole Parmer (Chicago, IL, USA) pH meter and an Orion Ross combination pH 81-15 electrode (Orion Research, Boston, MA, USA) as 20°C.

FI-ESP-MS Conditions

Mobile phases such as MeOH–water (8:2), (1:1) and (2:8) were tested for positive ion MS operation. A concentration of 100 ng/μl of the drug was dissolved in the appropriate mobile phase. The mobile phase additives were dissolved in MeOH–water (1:1) in the following concentration: 0.1% (v/v) TFA (pH 2.2), 0.1% (v/v) FOA (pH 3.1), 1% (v/v) HOAc (pH 3.4), 50 m*M* NH_4OH (pH 10.5), 10 m*M* HFBA (pH 2.2) and 10 m*M* TBAH (pH 12.1). For negative ion ESP operation the mobile phases IPA–water (8:2) and (1:1) were applied. The analytes were infused at a flow-rate of 1.2 μl/min and 2.4 μl/min. At both flow-rates similar signal responses were observed and other flow rates did not improve the signal intensity. To avoid a severe corona discharge in the ESP interface oxygen was coaxially mixed with the nebulized liquid.

For the flow injection-ESP-MS experiments on the Finnigan MAT 4500 instrument the ESP interface, Model QBV 25-AL, was operated at a needle voltage of 3.4 to 3.8 kV. Best results for positive ion operation was obtained with skimmer (S) and lens (L) voltages of $S_1 = 24$ V, $S_2 = 17$ V, $L_1 = -22$ V, $L_2 = -4$ V and $L_3 = -58$ V. The potential difference between the skimmer and the end of the capillary controlled the extend of fragmentation through CAD. The potential difference was varied between 40 and 240 V. The mass spectrometer scanned from a mass-to-charge ratio (m/z) 50–500 at a step size of 0.1 units and a rate of 0.33 scans/s. In the ESP interface, Model 100547-3, for the HP 5989A instrument, the needle is grounded and charging occurs by keeping the cylindrical electrode (V_1) at about 2.7 kV, the end plate (V_2) at 2.7 kV and the capillary (V_3) at 2.8 kV (positive ion operation required reverse polarity, and V_{1-3} operated about 1 kV higher than in negative ion operation). Best results for negative ions were obtained with $S_1 = -40$ V, $S_2 = -17$ V, $L_1 = 38$ V, $L_2 = 83$ V and $L_3 = 37$ V. Positive ion operation required reversed polarity and only slight adjustments of L_1, L_2 and L_3. The CAD voltage was varied between −40 to −400 V (40 to 400 V). The mass spectrometer scanned from m/z 40–500 at a step size of 0.1 units and a rate of 0.5 scans/s. The threshold value was set to 250. The system was checked by analyzing adenosine-5′-monophosphate in IPA–water (1:1) for negative ion and arginine/gramicidin S in MeOH–water (1:1) for positive ion operation.

Sample preparation procedure

Blank milk was collected from β-lactam free cows at North Carolina State University (Raleigh, NC, USA). A 0.5-ml aliquot of milk was diluted with a equal volume of a solution consisting of MeCN–water (1:1). The sample was vortex-mixed for 10–15 s, placed in a microseparation system with an M_r 10 000 cutoff filter and centrifuged for approximately 30 min at 3000 *g* with a 40° fixed-angle rotor. The five tested β-lactam antibiotics were spiked at different lens and skimmer concentration levels into the milk blank. A 0.5–5-μl aliquot of the colorless blank or spiked ultrafiltrate was injected into the HPLC system equipped with a UV and a MS detector. A synthetic mixture of the drugs was

made with the same solvent combination as used for the milk sample.

HPLC–ESP-MS conditions

HPLC separation was performed using a mobile phase consisting of 40% (v/v) MeCN and 1% (v/v) HOAC in water (pH 3.0). The mobile phase flow-rate into the 70:1 splitter was 300 μl/min. The splitting reduced the flow-rate of the eluent entering the ESP interface to 4.3 μl/min. Higher flow-rates decreased the sensitivity of the ESP-MS system and produced instable signals. To estimate the dead time (t_0) of the HPLC system, pure MeCN as an non-retained standard was injected. The measured values were in the range of $1.475 \leq t_0 \leq 1.480$ min. The resulting low flow-rate and the relative long transfer line to the MS detector gave a delay of about 10–15% in the total ion current (TIC) or extracted ion chromatogram compared to the retention time t_R measured from the UV chromatogram.

The Analytica HPLC–ESP-MS interface, Model 101737 has a different lens and skimmer arrangement compared to the former interface type used for flow injection or FI-ESP-MS experiments and was autotuned with a synthetic mixture of the five β-lactam antibiotics (100 ng/μl each). The mass spectrometer scanned from m/z 200–450 at a step size of 0.1 units and a rate of 0.33 scans/s. The threshold was 500 and the abundance of each mass was sampled six times during a scan. In single ion monitoring (SIM) data acquisition a dwell time of 200 ms resulted in 4.33 cycles/s.

Microbore HPLC–ESP-MS Conditions

Isocratic microbore HPLC separation was performed using a mobile phase consisting of 30% (v/v) MeCN and 1% (v/v) HOAc in water (pH 2.9). The mobile phase flow-rate through the column and into the ESP interface was 4 μl/min. For injection volumes over 0.5 μl the sample was concentrated on-column by using pure water as a weak eluent. The elution time was dependent from the injected sample volume and varied from 1 to 8 min.

The Analytica HPLC–ESP-MS interface, Model 101737, was equipped with a new fire polished gold plated glass capillary and autotuned with a synthetic mixture of the five β-lactam antibiotics (100 ng/μl each). In SIM data acquisition a dwell time of 200 ms resulted in 4.33 cycles s.

RESULTS AND DISCUSSION

Effect of CAD voltage of positive ion MS spectra

The initial work for β-lactam antibiotics evaluated the CAD spectra that could be generated between the capillary and skimmer in the ESP interface. The increase in potential different between the capillary and the skimmer transferred of more internal energy into the molecule through collisional activation, resulting in the formation of structurally relevant product ions.

Most of the CAD fragment ions detected for each antibiotic could be identified based on sample cleavages of various groups from the molecule. The mass spectra at two different CAD voltages are listed in Table I for all five tested antibiotics. Low CAD voltages (<+100V) generally form molecular adducts and only very few characteristic fragment ions. With CAD energies in the range of +100 V to +200 V more fragmentations occurred. Usually, the fragmentation followed a pattern with all tested penicillins showing a characteristic cleavage product of the β-lactam ring $[C_6H_9HSO_2 + H]^+$ at m/z 160 and a further loss of COOH at m/z 114. Fragments formed by the cleavage of the amide moiety are more specific for the different penicillins. Penicillin G formed a $[C_6H_5CH_2]^+$ ion at m/z 91, ampicillin exhibited a $[C_6H_5CHNH_2]^+$ ion at m/z 106 as the base peak, amoxicillin showed a loss of NH_3 at m/z 349, cloxacillin, that contains one chlorine, showed two fragments at m/z 321 and 178 assignable to its amide moiety. The ESP ionization of the cephalosporin, cephapirin, produced no fragments from a cleavage inside of the β-lactam ring. Instead, a loss of the carboxylic group (–COOH) was tentatively identified at m/z 220. Several ions with lower m/z ratios had their origin from a successive cleavage of the amide groups.

Electrospray response in various mobile phase combinations

Sometimes, ESP intensity in a given solvent can vary drastically. The signal intensity is usually dependent on the hydration of the analyte in a given solvent as well as if the analyte is charged in solution. Fig. 1 shows the trend of the relative ESP intensity of $[M+H]^+$ ion of penicillin G, amoxicillin and cephapirin in different MeOH–water mobile phase combinations at a capillary-skimmer potential of 80 V. To compensate for slightly different instrumental tuning parameters, an internal standard of 100 ng/μl arginine was used. Usually, the more organic in the solvent, the higher the ESP response. Acetonitrile also resulted in slightly better ion currents compared to methanol when equal percentages of either organic component in water were used. Different solvent ratios changed not only the intensity of the detected fragments but also affected adduct ions. Higher methanol content increased the intensity of the $[M+H+MeOH]^+$ ion. Higher water concentrations in the mixture increased the intensity of the $[M+Na+H_2O]^+$, $[M+K+H_2O]^+$ or $[M+H+H_2O]^+$ ions in the ESP mass spectrum. The mass spectrometer did not scan high enough to detect a dimer ion. Therefore, no valid evidence could be obtained to confirm dimer ion formations at a low capillary-skimmer potential depending on the mobile phase combination.

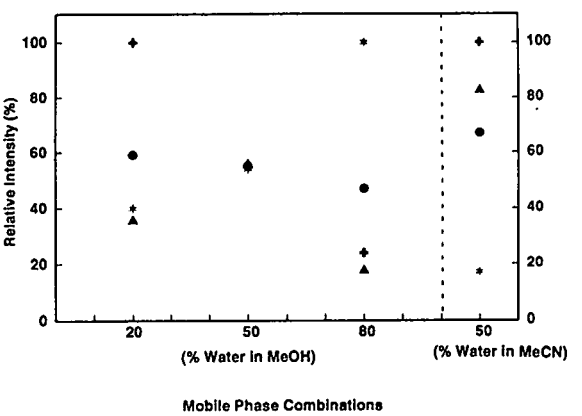

Fig. 1. Electrospray intensity for penicillin G (★) amoxicillin (+) and cephapirin (▲) in different mobile phase combinations at a capillary-skimmer potential of +160 V. ● = Average response.

Electrospray response using various mobile phase additives

A general approach to HPLC–ESP-MS includes minimization of eluent ion strength, use of as much organic modifier, such as methanol or acetonitrile, as practical and avoidance of buffer or other non-volatile mobile phase additives, unless they facilitate ionization. Mobile phase additives compete with sample ionization and result in a higher chemical background caused by adducts extending to a fairly high m/z ratio [44,45]. Therefore, it is necessary to compromise between ideal chromatographic conditions and conditions that support the ionization, desolvation and desorption processes of the HPLC–ESP-MS interface.

We used FI-ESP-MS experiments to assess the effect of various acids, bases and salts which change the pH of the mobile phase, and ion-pairing compounds on sensitivity. A lower pH of the eluent should favor the free acid form of the drugs, and thus increases the ESP response in positive ion mode. Suitable reversed-phase (RP) modifiers are volatile acids such as TFA, FAO, HOAc, volatile salts such as NH_4OAc, normally used in thermospray ionization to enhance ionization, and basic NH_4OH. There are an increasing number of reports using RP ion-pair HPLC methods to determine drug residues. Therefore, the effect of HFBA and TBAH addition to the eluent on ESP response of the five β-lactam antibiotics was tested. For this study, four different CAD voltages were applied for each drug infusion and the resulting mass spectra and the corresponding signal intensities were recorded. Fig. 2 presents bar graph plots of the relative ESP response of the $[M+H]^+$ ion (left column) and a characteristic $[fragment]^+$ ion (right column) of 100 ng/μl of each β-lactam antibiotic. The results obtained with the basic additive TBAH are not shown in Table II because the signals of all tested drugs were strongly suppressed in this eluent system. The only signal observed was the $[TBAH]^+$ ion at m/z 242.

In general, all five β-lactam antibiotics showed higher $[M+H]^+$ intensity at CAD voltages of +80 V and +160 V. An increase of the CAD voltage to +240 V or +320 V caused a severe drop in signal intensity. Therefore, the results at

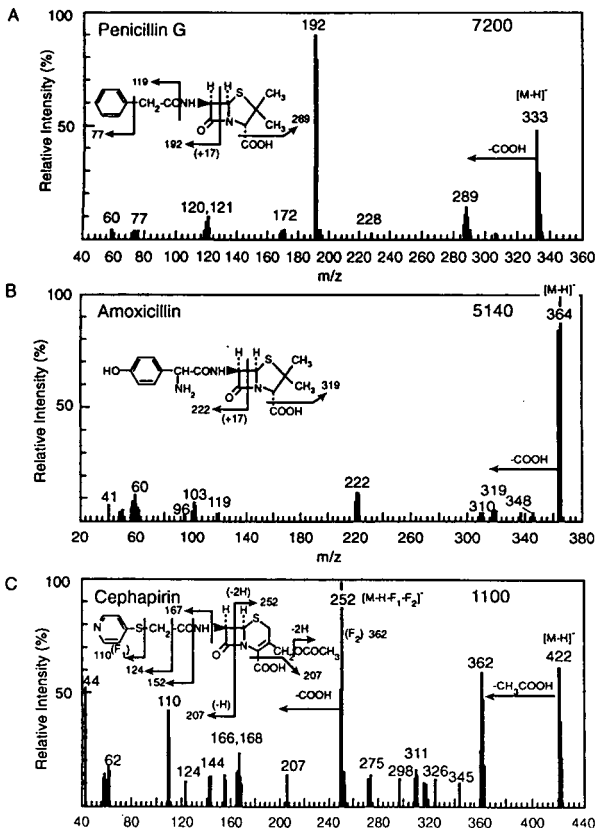

Fig. 2. Negative ion spectra of (A) penicillin G, (B) amoxicillin and (C) cephapirin at a CAD voltage of −120 V. Numbers at top right indicate ion counts.

higher CAD voltages were not listed in Table II. Comparing the intensity of characteristic fragment ions, a similar trend was observed throughout the whole palette of testing mobile phase systems. Using the mobile phase MeOH–water (1:1) without further additives gave poor ESP response. Addition of the strong acid TFA increased the ESP response of penicillin G and cloxacillin. For the other three drugs no significant increase or even distinct lower ESP responses are found. Addition of weaker acids such as FOA and HOAc drastically increased the ESP response of the $[M + H]^+$ ion as well as the fragment ions of all five drugs. A reasonable explanation for this increase may be a better droplet formation and nebulization capability due to the higher volatility and lower viscosity of these two acids. The near neutral pH of the eluent, achieved by the addition of NH_4OAc, weakened the ESP response of amoxicillin, ampicillin and cephapirin. Penicillin G and cloxacillin showed reasonably high ESP responses at lower CAD voltages. The use of the base NH_4OH as a mobile phase additive was well suited for penicillin G and cloxacillin. The addition of HFBA showed a reasonably good signal intensity for these two drugs. For the other three drugs no real advantage of using the two additives was found.

Table III shows the average ESP respond of all five tested compounds in the seven mobile phase system at four different CAD voltages. Over all, best ESP responses for drugs were achieved with 0.1% (v/v) FOA and 1% (v/v) HOAc in MeOH–water (1:1). The stronger acids TFA and HFBA did not facilitate ionization and are therefore not an ideal choice for future HPLC–ESP-MS work. The use of the volatile salts NH_4OAc and NH_4OH increased the ESP response in comparison to the unmodified eluent but the gain of signal intensity was rather limited. The use of FOA, HOAc or NH_4OAc to modify the mobile phase may be an interesting compromise between required chromatographic and electrospray conditions for a successful RP chromatographic separation and ESP-MS detection of β-lactam antibiotics.

Negative ion electrospray MS spectra

Penicillin contains a 6-aminopenicillanic acid nucleus and cephalosporins possess a 7-aminocephalosporinic acid nucleus. Due to their carboxylate group, the drugs are also suited to negative ion MS detection. A concentration of 100 ng/μl of each drug in IPA–water (8:2) was infused into the ESP interface at a flow-rate of 1.2 μl/min. In general, the negative ion spectra showed lower signal intensities, exhibiting all a $[M - H]^-$ ion and producing less fragmentations at higher capillary-skimmer voltages compared to positive ion spectra. The mass spectra at lower CAD voltages normally formed only the molecular ion and higher CAD voltages increased the background noise. The fragmentations seen in the mass spectra in Fig. 2 resulted mainly from a loss of COOH or HCO_2CH_3 and opening of the

TABLE II

COMPARISON BETWEEN DIFFERENT CAD VOLTAGES AND MOBILE PHASE ADDITIVES

CAD voltage = voltage measured at the end of the capillary (Analytica, Model 101737); relatvie intensity = relative signal intensity of the $[M+H]^+$ ion or $[fragment]^+$ ion; penicillin G, *m/z* 335 and *m/z* 160; ampicillin, *m/z* 350 and *m/z* 106; amoxicillin, *m/z* 366 and *m/z* 349; cloxacillin *m/z* 436 and *m/z* 277; cephapirin *m/z* 424 and *m/z* 111.

Drug	Mobile phase additive in MeOH–water (1:1)	Relative intensity (%) of $[M+H]^+$ ion at CAD = +80 V	Relative intensity (%) of $[fragment]^+$ ion at CAD = +160 V
Penicilin G	None, pH 8.4	30	5
	+0.1% (v/v) TFA, pH 2.2	44	21
	+0.1% (v/v) FOA, pH 3.1	44	15
	+1% (v/v) HOAC, pH 3.4	91	100
	+50 m*M* NH_4OAc, pH 7.1	55	61
	+50 m*M* NH_4OH, pH 10.5	100	50
	+10 m*M* HFBA, pH 2.2	68	41
Ampicillin	None, pH 8.4	4	16
	+0.1% (v/v) TFA, pH 2.2	5	6
	+0.1% (v/v) FOA, pH 3.1	100	100
	+1% (v/v) HOAc, pH 3.4	44	90
	+50 m*M* NH_4OAC, pH 7.1	9	10
	+50 m*M* NH_4OH, pH 10.5	14	10
	+10 m*M* HFBA, pH 2.2	2	0
Amoxicillin	None, pH 8.4	31	29
	+0.1% (v/v) TFA, pH 2.2	3	3
	+0.1% (v/v) FOA, pH 3.1	100	96
	+1% (v/v) HOAC, pH 3.4	73	100
	+50 m*M* NH_4OAC, pH 7.1	3	3
	+50 m*M* NH_4OH, pH 10.5	16	11
	+10 m*M* HFBA, pH 2.2	6	43
Cloxacillin	None, pH 8.4	3	0
	+0.1% (v/v) TFA, pH 2.2	63	67
	+0.1% (v/v) FOA, pH 3.1	31	100
	+1% (v/v) HOAC, pH 3.4	31	100
	+50 m*M* NH_4OAC, pH 7.1	56	93
	+50 m*M* NH_4OH, pH 10.5	100	93
	+10 m*M* HFBA, pH 2.2	34	63
Cephapirin	None, pH 8.4	2	4
	+0.1% (v/v) TFA, pH 2.2	9	5
	+0.1% (v/v) FOA, pH 3.1	100	100
	+1% (v/v) HOAC, pH 3.4	89	43
	+50 m*M* NH_4OH, pH 7.1	0.4	2
	+50 m*M* NH_4OH, pH 10.5	24	0.2
	+10 m*M* HFBA, pH 2.2	14	12

β-lactam ring, forming ions at *m/z* 289 and 192 for penicillin G, *m/z* 319 and 222 for amoxicillin, and *m/z* 207, 167, and 110 for cephapirin, respectively. It was found that at higher solvent pH, better ion currents were obtained from selected antibiotics such as β-lactams, amino-glycosides, tetracyclines, and sulfonamides [46]. Typically, pH 10 achieved through the addition of 50 m*M* NH_4OH resulted in highest ESP responses for $[M-H]^-$ ion for the three β-lactam antibiotics compared to the non-buffered solution (pH 7). This observation is consistent

TABLE III

COMPARISON BETWEEN DIFFERENT CAD VOLTAGES AND MOBILE PHASE ADDITIVES

Averaged data from all five drugs. CAD voltage = voltage measured at the end of the capillary (Analytica, Model 101737); relative intensity = relative signal intensity of the $[M + H]^+$ ion or $[fragment]^+$ ion; penicillin G, *m/z* 335 and *m/z* 160; ampillicin, *m/z* 350 and *m/z* 106; amoxicillin, *m/z* 366 and *m/z* 349; cloxacillin, *m/z* 436 and *m/z* 277; cephapirin *m/z* 424 and *m/z* 111.

Mobile phase additive in MeOH–Water (1:1)	Relative intensity (%) of $[M + H]^+$ ion at CAD =				Relative intensity (%) of $[fragment]^+$ ion at CAD =			
	+80 V	+160 V	+240 V	+320 V	+80 V	+160 V	+240 V	+320 V
None, pH 8.4	20	10	5	5	15	12	10	8
+0.1% (v/v) TFA, pH 2.2	35	28	5	2	30	28	3	1
+0.1% (v/v) FOA, pH 3.1	100	50	25	7	40	81	60	3
+1% (v/v) HOAc, pH 3.4	75	57	38	8	48	100	47	18
+50 m*M* NH_4OAc, pH 7.1	35	12	5	2	20	42	6	2
+50 m*M* NH_4OH, pH 10.5	70	35	10	5	30	40	21	14
+10 m*M* HFBA, pH 2.2	35	20	2	1	28	38	15	3

with the formation of anions in solution for the samples analyzed but these negative ion ESP signals were only one-fourth as sensitive as the $[M + H]^+$ peak in position ion ESP operation.

HPLC–UV chromatograms

Methodology was developed for the detection of the five β-lactam antibiotics directly from milk ultrafiltrate by RP chromatography using UV detection. Various elution systems consisting of MeCN, water, 1% (v/v) HOAc and 0.01 *M* NH_4OAc were investigated for separation of the individual drugs from milk ultrafiltrate. The addition of NH_4OAc to MeCN–water–HOAc mobile phase systems reduced the k' values of all five drugs to under 6 and no baseline separation could be achieved. Removing the salt increased the k' values and improved the peak symmetry. From the four tested mobile phase systems with 20%, 30%, 40% and 50% (v/v) MeCN and 1% (v/v) HOAC in water an addition of 40% (v/v) organic resulted in a baseline separation of all five drugs in a reasonable run time (about 15 min). Under these HPLC conditions the β-lactam antibiotics were retained, permitting their separation from most bovine milk extract interferences and providing a clean analytical window for their detection. Fig. 3A shows the UV chromatogram generated at 230 nm of a blank milk ultrafiltrate. Chromatograms of bovine milk ultrafiltrate spiked with a concentration of 80 ppm of each drug are given in Fig. 3B. The UV chromatogram of a synthetic mixture of 20 ppm of each drug reported in Fig. 3C showed a similar elution profile but a less intense solvent front at the beginning of the run. The average capacity factors of antibiotics in this mobile phase system were $k'_1 = 1.50$, $k'_2 = 3.53$, $k'_3 = 4.38$, $k'_4 = 5.26$ and $k'_5 = 8.17$.

HPLC–ESP-MS

Full-scan mass spectra (*m/z* 200–450) were obtained by HPLC–ESP-MS in 40% MeCN with 1% HOAc in water from injection of 500 ng per component. Fig. 4 displays the extracted ion current profiles of the five separated drugs (peaks 1–5). Due to the 70:1 post-column split ratio, a longer elution time and a slight tailing of the peaks occurred. The determination in the selected-ion monitoring (SIM) acquisition mode of a blank milk ultrafiltrate (A), 143 pg per

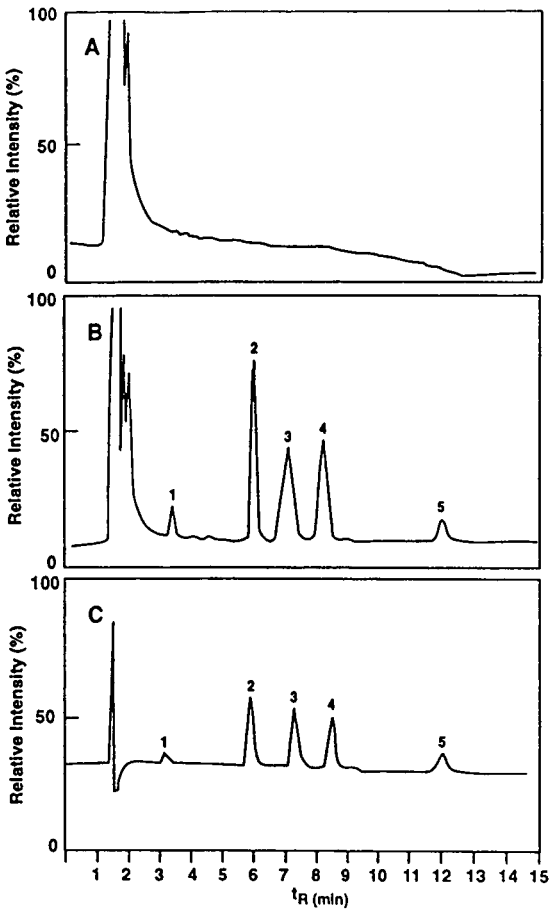

Fig. 3. HPLC–UV chromatograms of (A) blank milk ultrafiltrate, (B) 40 ng of each drug spiked into milk ultrafiltrate, (C) synthetic mixture of 10 ng of each drug. Peaks: 1 = penicillin G; 2 = cloxacillin; 3 = cephapirin; 4 = amoxicillin; 5 = ampicillin. Injection column 0.5 μl; flow-rate 0.3 ml/min; λ = 230 nm; AUFS = 1.0.

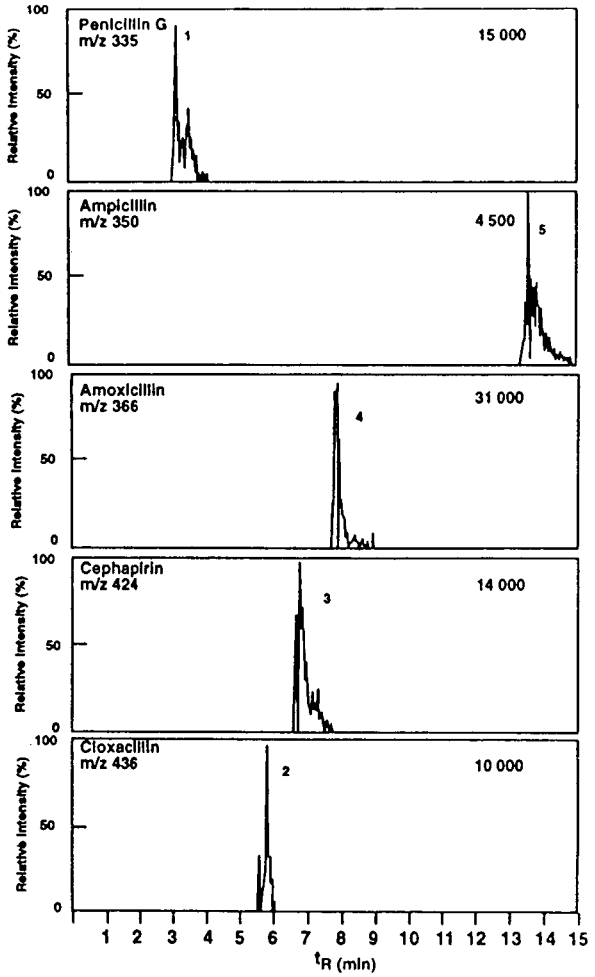

Fig. 4. Extracted ion current profiles of an HPLC–ESP-MS analysis of a synthetic mixture of the five analytes at a level of 7.1 ng per component corresponding to an on-column injection of 500 ng of each drug. Number at top right indicates ion counts. Peaks: 1 = penicillin G; 2 = cloxacillin; 3 = cephapirin; 4 = amoxicillin; 5 = ampicillin.

component spiked milk ultrafiltrate (B) and synthetic mixture (C) of the five analytes is shown in Fig. 5. The 143 pg level corresponds to 100% recovery from an injection of 0.5 μl of a 200 ppm sample. For this amount injected, signal-to-noise ratios ranged from 2 for penicillin G, 2 for cloxacillin, 4 for cephapirin, 6 for amoxicillin, to 10 for ampicillin. In the SIM acquisition mode the $[M + H]^+$ ion of each free drug was monitored and no interference from milk ultrafiltrate appeared.

Linearity of the HPLC–ESP-MS method was determined by spiking drug standards in a concentration of 20, 60, 80 and 200 ppm into blank milk ultrafiltrate corresponding to 143, 428, 571 and 1428 pg of each drug after splitting of the eluent from the HPLC system. Within this range r (n = 4) for penicillin G was 0.9997, for cloxacillin 0.9966, for cephapirin 0.9994, for amoxicillin 0.9979, and for ampicillin 0.9961 (Fig. 6).

Approaches to determine ppb levels in complex matrices —preliminary experiments

Determination at the levels of regulatory interest using this method would require on-column

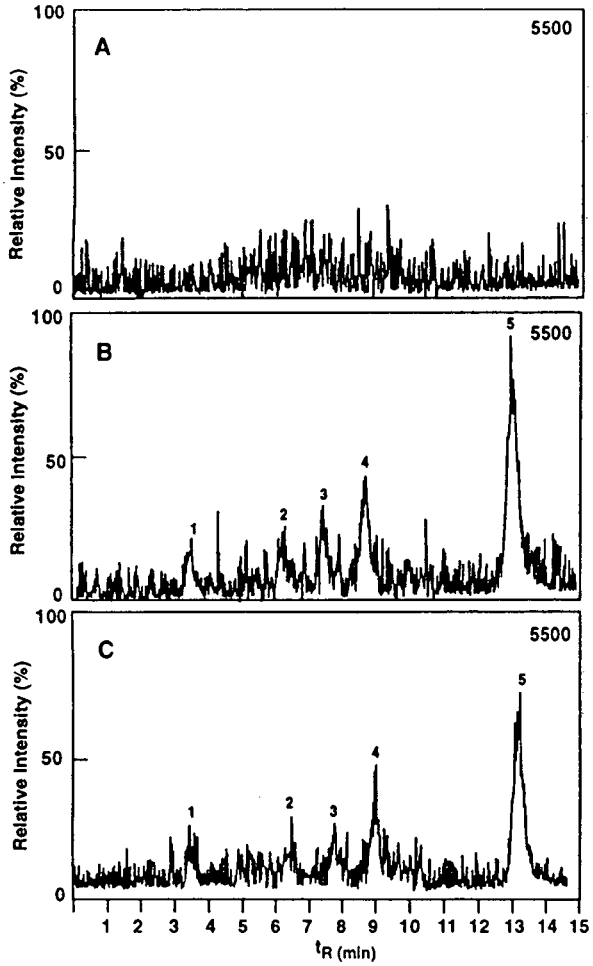

Fig. 5. HPLC–ESP-MS reconstructed total ion current profiles of (A) blank milk ultrafiltrate, (B) 143 pg of each drug in milk ultrafiltrate, and (C) synthetic mixture of 143 pg of each drug in the SIM data acquisition mode. This corresponds to an on-column injection of 10 ng of each drug. Number at top right indicates ion counts. Peaks: 1 = penicillin G; 2 = cloxacillin; 3 = cephapirin; 4 = amoxicillin; 5 = ampicillin.

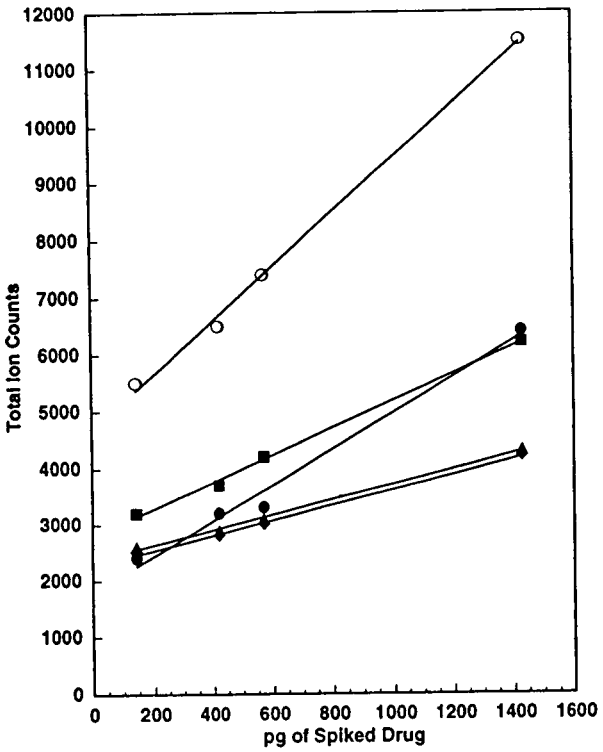

Fig. 6. Heights of peaks in total ion current profile *versus* amount for β-lactam antibiotics introduced into the mass spectrometer. ● = Penicillin G; ◆ = cloxacillin; ▲ = cephapirin; ■ = amoxicillin; ○ = ampicillin.

detection of 5 pg/μl penicillin G, 10 pg/μl of cloxacillin, amoxicillin, ampicillin, and 20 pg/μl of cephapirin according to the known tolerance levels for the particular drug used on dairy cows [47]. All of these amounts are currently below the instrument detection limits discussed above. To detect 5 ppb levels of these drugs, an injection of about 30 μl is required to achieve a mass loading suitable for ESP-MS detection. Usually, an on-column concentration step is needed prior to elution at this higher injection volume [48].

Preliminary studies have demonstrated that β-lactam antibiotics can be concentrated directly on an analytical column from filtrates with a weak solvent such as water and eluted under isocratic conditions or with a solvent gradient. Similar approaches were already used successfully for determination of novobiocin [49], virginiamycin [50] and tetracyclines [51]. Samples with high matrix interference can be treated under a procedure sometimes termed "heart-cutting" [17], and rechromatographed under different conditions. This approach has been successfully used for determination of penicillin G and lincomycin resides in milk and tissue [19].

Another possibility would be the utilization of a recently introduced mechanical vibration-assisted ESP source [52]. This ultrasonic mechani-

cal vibration nebulization-assisted electrospray (ultraspray) allows consistent charged droplet production less affected by solution flow rate, conductivity and solution chemistry than with a conventional ESP interface. The initial charged droplet size produced is primarily a function of the frequency of mechanical vibration. This new interface type has the advantage that it can directly operate at flow-rates up to 400 μl/min and the disadvantages stemming from a post-column splitting of the eluent would be omitted without loosing the ability to work with well suited and efficient 150 × 2 mm columns. The signal intensity of the $[M+H]^+$ peak of 100 ng/μl penicillin G in MeOH–water (1:1) with addition of 1% (v/v) HOAc within the flow-rate range of 2–50 μl/min was nearly constant.

To further investigate the feasibility of a direct HPLC–ESP-MS separation at flow-rates under 10 μl/min, we also tested a packed RP capillary column system operating at a flow-rate of 2–10 μl/min [53] and, therefore, more favorable operation without splitting of the solvent flows. A synthetic mixture of 5 pg/μl of each drug was eluted with the mobile phase containing 30% (v/v) MeCN and 1% (v/v) HOAc in water. The separation was performed on a 15 cm × 320 μm I.D. Fusica C_{18} capillary column. The void volumes of various parts (*e.g.*, injector, transfer lines, connections, conventional stainless-steel electrospray needle and large injection volume) caused band broadening which reduced resolution. Fig. 7 presents the ion trace of all five β-lactam drugs acquired under the SIM mode. Also, remarkable is the change in elution order of penicillin G and cloxacillin on the microbore column compared to the 2.1 mm I.D. column. To effectively pursue this promising small scale separation technique we are currently working on the reduction of void volumes which will improve spray formation and ESP ionization efficiency.

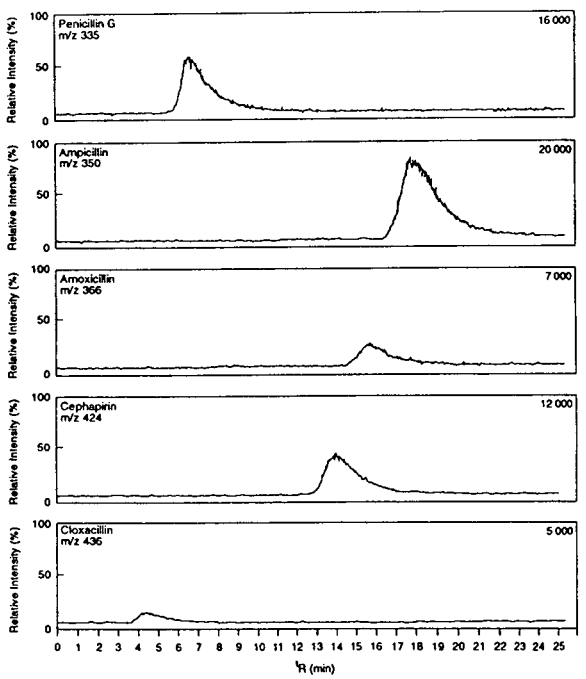

Fig. 7. Extracted ion current profiles of an microbore HPLC–ESP-MS analysis of a synthetic mixture of the five analytes at a level of 5 pg/μl per component. Number at top right indicates ion counts of the particular mass peak seen in the ion trace. Peaks: 1 = cloxacillin; 2 = penicillin G; 3 = cephapirin; 4 = amoxicillin; 5 = ampicillin.

CONCLUSIONS

The HPLC–ESP-MS method described for a multiresidue analysis of β-lactam antibiotics was developed based on preliminary flow injection and infusion experiments clarifying CAD and solvent dependence of the analysis. Due to the low flow-rate limitation required for successful ESP ionization, a post-column splitting of the eluent from the column was necessary. The lower amount of analytes entering the ESP interface also produced a necessary sacrifice of overall detection sensitivity. Therefore, the 5 ppb level of regulatory interest was not reached with this method despite good chromatographic resolution of the analytes.

Further improvements are suggested by discussing on-column concentration techniques and possibilities for an elimination of the eluent splitting prior to ESP ionization and MS detection. So far, the use of a RP microbore HPLC column shows promising results if the chromatographic separation can be improved and void volumes reduced to reasonable levels.

Future work will focus on the optimization of

instrumental parameters, improvement of apparatus performance, and evaluation of other chromatographic modes to multiresidue analysis.

ACKNOWLEDGEMENTS

We thank Mr. D. Heller from FDA, Center for Veterinary Medicine, Beltsville MD, USA, for helpful discussions concerning the project, Dr. K.L. Tyczkowska of the College of Veterinary, North Carolina State University, Raleigh, NC, USA, for the blank milk ultrafiltrate, and Analytica of Branford Inc., Branford, CT, USA, for the flow injection experiment with the mechanical vibration-assisted ESP interface.

This research was supported by US Food and Drug Administration Cooperative Agreement No. FD-U-000581.

REFERENCES

1 E.H. Flynn, *Cephalosporins and Penicillins, Chemistry and Biology*, Academic Press, New York, 1872.
2 D.F. Wishart, *J. Am. Vet. Med. Assoc.*, 185 (1984) 1106.
3 K.L. Tyczkowska, R.D. Voyksner and A.L. Aronson, *J. Chromatogr.*, 594 (1991) 195, and references cited therein.
4 M.M. Siegel, R.K. Isensee and D.J. Beck, *Anal. Chem.*, 59 (1987) 989.
5 A. Goodman-Gilman, L.S. Goodman, T.W. Rau and F. Murad (Editors), *The Pharmacological Basis of Therapeutics*, MacMillan, New York, 7th ed., 1979.
6 M.E. Wolff, *Medical Chemistry*, Wiley, New York, 4th ed., 1979.
7 *Fed. Reg.*, 52 (1987) 165, 196; 54 (1989) 196; US Government Printing Office Superintendent of Documents, Washington, DC.
8 D.M. Mac Cauley and V.S. Packard, *J. Food Prot.*, 44 (1981) 696.
9 J.J. Ryan, E.E. Wildman, A.H. Duthie, H.V. Atherton and J.J. Aleong, *J. Dairy Sci.*, 69 (1986) 1510.
10 P. Rohrer, M. Schaellibaum and J. Nicolet, *J. Assoc. Off. Anal. Chem.*, 48 (1985) 59.
11 S.E. Charm and R. Chi, *J. Assoc. Off. Anal. Chem.*, 71 (1988) 304.
12 D.L. Collins-Thompson, D.S. Wood and I.Q. Thompson, *J. Food Prot.*, 51 (1988) 632.,
13 S.A. Thorogood and A. Ray, *J. Soc. Dairy Technol.*, 37 (1984) 38.
14 R.D. Munns, W. Shimoda, J.E. Roybal and C. Vieira, *J. Assoc. Off. Anal. Chem.*, 68 (1985) 968.
15 W.A. Moats, *J. Agric. Food Chem.*, 31 (1983) 1348.
16 W.A. Moats, *J. Assoc. Off. Anal. Chem.*, 3 (1990) 343; and references cited therein.
17 J. Carlquist and D. Westerlund, *J. Chromatogr.*, 344 (1985) 285.
18 K. Tyczkowska and A.L. Aronson, *J. Assoc. Off. Anal. Chem.*, 71 (1988) 773.
19 W.A. Moats, *J. Chromatogr.*, 507 (1990) 177.
20 A.I. MacIntosh, *J. Assoc. Off. Anal. Chem.*, 73 (1990) 880.
21 W.A. Moats and R. Malisch, *J. Assoc. Off. Anal. Chem. Int.*, 75 (1992) 257.
22 W.A. Moats, *J. Chromatogr.*, 593 (1992) 15.
23 K.L. Tyczkowska, R.D. Voyksner, R. Straub and A.L. Aronson, *J. Assoc. Off. Anal. Chem.*, submitted for publication.
24 R.M. Simpson, F.B. Suhre and J.W. Shafter, *J. Assoc. Off. Anal. Chem.*, 68 (1985) 23.
25 M.A. Hayes, *J. Chromatogr. Sci.*, 26 (1988) 146.
26 U. Meetschen and M. Petz, *J. Assoc. Off. Chem.*, 73 (1990) 373.
27 M.L. Vestal, *Science*, 226 (1984) 275.
28 C.R. Blackey, J.J. Carmody and M.L. Vestal, *J. Am. Chem. Soc.*, 102 (1980) 5931.
29 D. Pilosof, Kim H. Yong, D.F. Dyckes and M.L. Vestal, *Anal. Chem.*, 56 (1984) 1236.
30 S.E. Unger and B.M. Wanach, *Spectroscopy*, 1 (1986) 33.
31 S. Suwnrumpha and R.B. Freas, *Biomed. Environ. Mass Spectrom.*, 18 (1989) 983.
32 K. Tyczkowska, R.D. Voyksner and A.L. Aronson, *J. Chromatogr.*, 490 (1989) 101.
33 R.D. Voyksner, K. Tyczkowska and A.L. Aronson, *J. Chromatogr.*, 567 (1991) 389.
34 K.L. Tyczkowska, R.D. Voyksner and A.L. Aronson, *J. Vet. Pharmacol. Therap.*, 14 (1991) 51.
35 M. Scandola, G. Tarzia, G. Gaviraghi, D. Chiarello and P. Traldi, *Biomed. Environ. Mass Spectrom.*, 18 (1989) 851.
36 G.W. Griffin, I. Dzidic, D.I. Caroll, R.N. Stillwell and E.C. Horning, *Anal. Chem.*, 45 (1973) 1204.
37 E.C. Horning, M.G. Horning, D.I. Caroll, I. Dzidic and R.N. Stillwell, *Anal. Chem.*, 45 (1973) 936.
38 E.C. Horning, M.G. Horning, D.I. Caroll, I. Dzidic and R.N. Stillwell, *Adv. Biochem. Psychopharmacol.*, 7 (1973) 15.
39 M.W. Siegel and W.L. Fite, *J. Phys. Chem.*, 80 (1976) 2871.
40 C.M. Whitehouse, R.N. Dreyer, M. Yamashita and J.B. Fenn, *Anal. Chem.*, 57 (1985) 675.
41 J.B. Fenn, M. Mann, C.K. Meng, S.F. Wong and C.M. Whitehouse, *Mass Spectrom. Rev.*, 9 (1990) 37.
42 J.R. Perkins, C.E. Parker and K.B. Tomer, *J. Am. Soc. Mass Spectrom.*, 3 (1992) 139; and references cited therein.
43 L.G. McLaughlin and J.D. Henion, *J. Chromatogr.*, 591 (1992) 195.
44 A.P. Bruins, T.R. Covey and J.D. Henion, *Anal. Chem.*, 59 (1987) 2642.
45 M.G. Ikonomou, A.T. Blades and P. Kebarle, *Anal. Chem.*, 62 (1990) 957.

46 R. Straub and R.D. Voyksner, *Proceedings of the 40th Annual Conference on Mass Spectrometry and Allied Topics, Washington, DC, May 31–June 5, 1992*, p. 1879.
47 J.W. Harman, *Food Safety and Quality –FDA Strategy Needed to Address Animal Drug Residues in Milk, Report to the Chairman*, Human Resources and Intergovernmental Relations Subcommittee, Committee on Government Operations, House of Representatives, Washington, DC, 1992, pp. 60–62.
48 W.A. Moats, *J. Assoc. Off. Anal. Chem.*, 73 (1990) 343.
49 W.A. Moats and L. Leskinen, *J. Assoc. Off. Anal. Chem.*, 71 (1988) 776.
50 W.A. Moats and L. Leskinen, *J. Agric. Food Chem.*, 36 (1988) 1297.
51 W.A. Moats, *J. Chromatogr.*, 358 (1986) 253.
52 C.M. Whitehouse, S. Shen, and J.B. Fenn, presented at the *40th Annual Conference on Mass Spectrometry and Allied Topics, Washington, DC, May 31–June 5, 1992*; paper TOA 1:15.
53 M.T. Davis and T.D. Lee, *Protein Sci.*, 1 (1992) 935.

Announcement from the Publisher

ELSEVIER SCIENCE PUBLISHERS

prefers the submission of electronic manuscripts

Electronic manuscripts have the advantage that there is no need for the rekeying of text, thereby avoiding the possibility of introducing errors and resulting in reliable and fast delivery of proofs.

The preferred storage medium is a $5\frac{1}{4}$ or $3\frac{1}{2}$ inch disk in MS-DOS format, although other systems are welcome, e.g. Macintosh.

Your disk and (**exactly matching**) printed version (printout, hardcopy) should be submitted together to the accepting editor. In case of revision, the same procedure should be followed such that, on acceptance of the article, the file on disk and the printout are **identical**. Both will then be forwarded by the editor to Elsevier.

Please follow the general instructions on style/arrangement and, in particular, the reference style of this journal as given in 'Instructions to Authors'.

Please label the disk with your name, the software & hardware used and the name of the file to be processed.

Further information can be found under 'Instructions to Authors - Electronic manuscripts'.

Contact the Publisher for further information.

ELSEVIER SCIENCE PUBLISHERS B.V.
P.O. Box 330, 1000 AH Amsterdam
Netherlands
Fax: (+31-20) 5862-304

Synthesis and Applications of Isotopically Labelled Compounds 1991

Proceedings of the Fourth International Symposium, Toronto, Canada, 3-7 September 1991

edited by **E. Buncel**, *Queen's University, Kingston, Ont., Canada and* **G.W. Kabalka**, *University of Tennessee, Knoxville, TN, USA*

The Fourth International Symposium on the Synthesis and Applications of Isotopes and Isotopically Labelled Compounds attracted some 400 scientists from over 20 countries. The scientific program consisted of three plenary lectures, 97 invited and contributed talks presented in 15 sessions on diverse topics, and 85 poster presentations.
This proceedings volume covers the full texts of all the contributions, providing comprehensive, state-of-the-art information of interest to readers in chemistry, pharmacology, biochemistry and the medical sciences.

Contents:

1992 xxxiv + 788 pages
Price: US$ 320.00 / Dfl. 560.00
ISBN 0-444-89280-X

ELSEVIER
SCIENCE PUBLISHERS

TO ORDER
Contact your regular supplier or:
ELSEVIER SCIENCE PUBLISHERS
P.O. Box 211
1000 AE Amsterdam
The Netherlands
Customers in the USA & Canada:
ELSEVIER SCIENCE PUBLISHERS
Attn. Judy Weislogel
P.O. Box 945
Madison Square Station
New York, NY 10160-0757, USA
No postage will be added to prepaid book orders. US $ book prices are valid only in the USA and Canada. In all other countries the Dutch guilder (Dfl.) price is definitive. Customers in The Netherlands please add 6% BTW. In New York State please add applicable sales tax. All prices are subject to change without prior notice.

PUBLICATION SCHEDULE FOR THE 1993 SUBSCRIPTION

Journal of Chromatography and *Journal of Chromatography, Biomedical Applications*

MONTH	1992	J–A	M	J	J	A	S	O	N	D	1994
Journal of Chromatography	Vols. 623–627	Vols. 628–636	637/1 637/2 638/1 638/2	639/1 639/2 640/1 + 2	641/1 641/2 642/1 + 2 643/1 + 2 644/1	644/2 645/1 645/2 646/1	646/2 647/1 647/2	648/1 648/2			
Cumulative Indexes, Vols. 601–650											651/1 + 2
Bibliography Section		649/1		649/2			650/1			650/2	
Biomedical Applications		Vols. 612, 613 and 614/1	614/2 615/1	615/2 616/1	616/2 617/1	617/2 618/1 + 2	619/1 619/2	620/1 620/2	621/1 621/2	622/1 622/2	

INFORMATION FOR AUTHORS

(Detailed *Instructions to Authors* were published in Vol. 609, pp. 437–443. A free reprint can be obtained by application to the publisher, Elsevier Science Publishers B.V., P.O. Box 330, 1000 AH Amsterdam, Netherlands.)

Types of Contributions. The following types of papers are published in the *Journal of Chromatography* and the section on *Biomedical Applications:* Regular research papers (Full-length papers), Review articles, Short Communications and Discussions. Short Communications are usually descriptions of short investigations, or they can report minor technical improvements of previously published procedures; they reflect the same quality of research as Full-length papers, but should preferably not exceed five printed pages. Discussions (one or two pages) should explain, amplify, correct or otherwise comment substantively upon an article recently published in the journal. For Review articles, see inside front cover under Submission of Papers.

Submission. Every paper must be accompanied by a letter from the senior author, stating that he/she is submitting the paper for publication in the *Journal of Chromatography.*

Manuscripts. Manuscripts should be typed in **double spacing** on consecutively numbered pages of uniform size. The manuscript should be preceded by a sheet of manuscript paper carrying the title of the paper and the name and full postal address of the person to whom the proofs are to be sent. As a rule, papers should be divided into sections, headed by a caption (*e.g.*, Abstract, Introduction, Experimental, Results, Discussion, etc.) All illustrations, photographs, tables, etc., should be on separate sheets.

Abstract. All articles should have an abstract of 50–100 words which clearly and briefly indicates what is new, different and significant. No references should be given.

Introduction. Every paper must have a concise introduction mentioning what has been done before on the topic described, and stating clearly what is new in the paper now submitted.

Illustrations. The figures should be submitted in a form suitable for reproduction, drawn in Indian ink on drawing or tracing paper. Each illustration should have a legend, all the *legends* being typed (with double spacing) together on a *separate sheet.* If structures are given in the text, the original drawings should be supplied. Coloured illustrations are reproduced at the author's expense, the cost being determined by the number of pages and by the number of colours needed. The written permission of the author and publisher must be obtained for the use of any figure already published. Its source must be indicated in the legend.

References. References should be numbered in the order in which they are cited in the text, and listed in numerical sequence on a separate sheet at the end of the article. Please check a recent issue for the layout of the reference list. Abbreviations for the titles of journals should follow the system used by *Chemical Abstracts.* Articles not yet published should be given as "in press" (journal should be specified), "submitted for publication" (journal should be specified), "in preparation" or "personal communication".

Dispatch. Before sending the manuscript to the Editor please check that the envelope contains four copies of the paper complete with references, legends and figures. One of the sets of figures must be the originals suitable for direct reproduction. Please also ensure that permission to publish has been obtained from your institute.

Proofs. One set of proofs will be sent to the author to be carefully checked for printer's errors. Corrections must be restricted to instances in which the proof is at variance with the manuscript. "Extra corrections" will be inserted at the author's expense.

Reprints. Fifty reprints will be supplied free of charge. Additional reprints can be ordered by the authors. An order form containing price quotations will be sent to the authors together with the proofs of their article.

Ovomucoid Bonded Column for Direct Chiral Separation

ULTRON ES-OVM

Narrow-Bore Column (2.0 I.D. x 150 mm) for Trace Analyses
Analytical Column (4.6 I.D. , 6.0 I.D. x 150 mm) for Regular Analyses
Semi-Preparative Column (20.0 I.D. x 250 mm) for Preparative Separation

Analysis of Trace FLURBIPROFEN in Metabolite with NARROW-BORE COLUMN

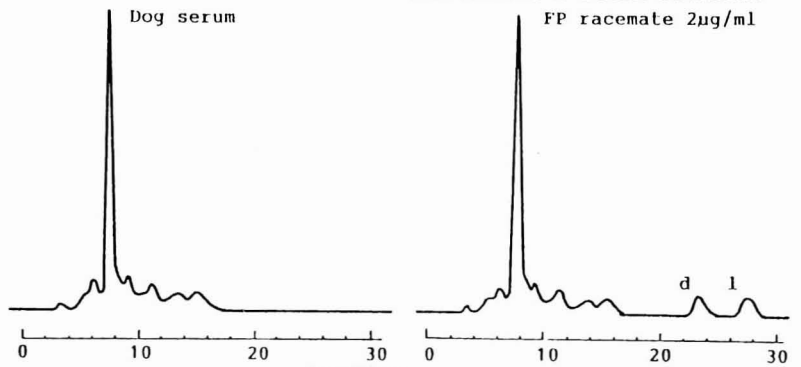

Conditions

Column: ULTRON ES-OVM(2.0I.D. x 150mm)
Mobile Phase: 20mMPhosphate Buffer(pH=3.0)/CH3CN =100/15
Flow Rate: 0.1ml/min
Temperature: 25°C
Injection: 5μl
Detection: UV- 247nm(0.05AUFS)

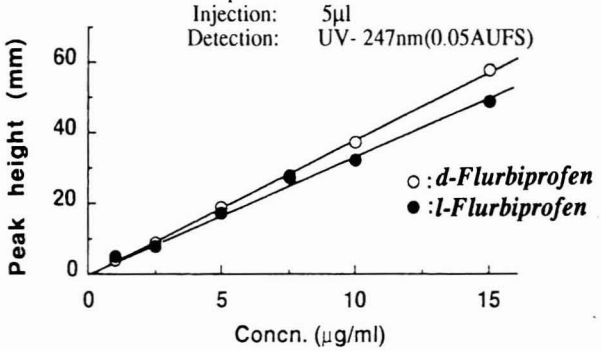

Calibration Curve for Each Enantiomer of Flurbiprofen

SHINWA CHEMICAL INDUSTRIES, LTD.

50 Kagekatsu-cho, Fushimi-ku, Kyoto 612, JAPAN
Phone:+81-75-621-2360 Fax:+81-75-602-2660

In the United States and Europe, please contact:

Rockland Technologies, Inc.

538 First State Boulevard, Newport, DE 19804, U.S.A.
Phone: 302-633-5880 Fax: 302-633-5893